

Consortium



for

Small-Scale Modelling

Technical Report No. 28

***RADAR_MIE_LM and RADAR_MIELIB
Calculation of Radar Reflectivity
from Model Output***

January 2016

DOI: 10.5676/DWD_pub/nwv/cosmo-tr_28

Deutscher Wetterdienst

MeteoSwiss

Aeronautica Militare - Reparto per la Meteorologia

ΕΘΝΙΚΗ ΜΕΤΕΩΡΟΛΟΓΙΚΗ ΤΠΗΡΕΣΙΑ

Instytucie Meteorologii i Gospodarki Wodnej

Administratia Nationala de Meteorologie

ROSHYDROMET

Agenzia Regionale per la Protezione Ambientale del Piemonte

Agenzia Regionale per la Protezione Ambientale dell'Emilia-Romagna

Centro Italiano Ricerche Aerospaziali

Amt für GeoInformationswesen der Bundeswehr



www.cosmo-model.org

Editor: Massimo Milelli, ARPA Piemonte

RADAR_MIE_LM and RADAR_MIELIB

***Calculation of Radar Reflectivity
from Model Output***

*Ulrich Blahak**

* Ulrich Blahak
Deutscher Wetterdienst
Frankfurter Str. 135
63067 Offenbach am Main
Germany

Contents

Contents	2
1 Preface	5
2 Introduction	6
3 Factors contributing to the radar "bright band"	7
4 Theoretical basis	7
4.1 Equivalent radar reflectivity factor	7
4.2 Extinction	8
4.3 Backscattering and extinction by spheres	8
4.4 Backscattering and extinction by two-layered spheres	10
4.5 Refractive index of hydrometeors	10
4.5.1 Water	12
4.5.2 Ice	13
4.5.3 Mixtures of ice, air and water	14
4.5.4 Mixtures of ice, air and water — Wieners formula	14
4.5.5 Mixtures of ice, air and water — Maxwell-Garnetts formula	16
4.5.6 Mixtures of ice, air and water — Bruggemann formula	17
5 Routines in radar_mielib	18
5.1 Refractive index of pure ice and water	18
5.1.1 FUNCTION m_complex_water_ray	18
5.1.2 FUNCTION m_complex_water_liebe	19
5.1.3 FUNCTION m_complex_ice_ray	20
5.1.4 FUNCTION m_complex_ice_warren	21
5.1.5 FUNCTION m_complex_ice_maetzler	22
5.2 Refractive index of mixture materials	23
5.2.1 FUNCTION m_complex_oguchi	23
5.2.2 FUNCTION m_complex_maxwellgarnett	24
5.2.3 FUNCTION m_complex_bruggemann	25
5.2.4 FUNCTION get_m_mix	26
5.2.5 FUNCTION get_m_mix_nested	28
5.3 Backscattering cross section for single precipitation particles	31
5.3.1 SUBROUTINE MIE_DRY_GRAUPEL	31
5.3.2 SUBROUTINE RAYLEIGH_DRY_GRAUPEL	33
5.3.3 SUBROUTINE MIE_DRYHAIL	35
5.3.4 SUBROUTINE MIE_DRYSNOW	36
5.3.5 SUBROUTINE MIE_DRYSNOW_TWOSPH	38
5.3.6 SUBROUTINE MIE_WATERSPH_WETHAIL	40
5.3.7 SUBROUTINE MIE_SPONGY_WETHAIL	41
5.3.8 SUBROUTINE MIE_WATERSPH_WETGR	43
5.3.9 SUBROUTINE MIE_SOAK_TWOSPH_WETGR	45
5.3.10 SUBROUTINE MIE_MEAN_WETGR	47
5.3.11 SUBROUTINE MIE_SOAK_WETGR	48
5.3.12 SUBROUTINE RAYLEIGH_SOAK_WETGR	50
5.3.13 SUBROUTINE MIE_WETSNOW_TWOSPH	51

6	radar_mie_lm: Interface functions for the LM	54
6.1	An approximation for the degree of melting applicable for bulk microphysical schemes	54
6.2	An efficient Rayleigh-Approximation for melting hydrometeors with Oguchis refractive index formulation	59
6.3	Controlling reflectivity calculations in LM — relevant namelist parameters and their setting	60
6.4	Tables of namelist parameter settings for the EMA choice	64
6.5	Additions to LM-runscreens to enable reflectivity calculations	67
7	Backscattering cross sections of dry ice particles	68
7.1	One-layered sphere	68
7.2	Two-layered sphere	71
8	Backscattering cross sections for melting ice particles relative to the mass-equivalent water drop	73
8.1	Rayleigh: soaked wet graupel, LM-scheme	74
8.2	Rayleigh: soaked wet graupel, Seifert/Beheng-scheme	77
8.3	Rayleigh: soaked wet snow, LM-scheme	80
8.4	Rayleigh: soaked wet snow, Seifert/Beheng-scheme	82
8.5	Mie: soaked twosphere wet graupel, LM-scheme	84
8.6	Mie: soaked twosphere wet graupel, Seifert/Beheng-scheme	86
8.7	Mie: soaked twosphere wet snow, LM-scheme	88
8.8	Mie: soaked twosphere wet snow, Seifert/Beheng-scheme	90
8.9	Mie: soaked wet graupel, LM-scheme	92
8.10	Mie: soaked wet graupel, Seifert/Beheng-scheme	95
8.11	Mie: soaked wet snow, LM-scheme	98
8.12	Mie: soaked wet snow, Seifert/Beheng-scheme	100
8.13	Mie: watersphere wet graupel, LM-scheme	102
8.14	Mie: watersphere wet graupel, Seifert/Beheng-scheme	103
8.15	Mie: watersphere wet snow, LM-scheme	104
8.16	Mie: watersphere wet snow, Seifert/Beheng-scheme	105
8.17	Mie: spongy wet hail, Seifert/Beheng-scheme	106
8.18	Mie: watersphere wet hail, Seifert/Beheng-scheme	107
8.19	Mie: twosphere soaked wet snow, LM-scheme	108
8.20	Mie: twosphere soaked wet snow, Seifert/Beheng-scheme	138

9	Index of the Figures of Section 8	168
9.1	Rayleigh: soaked wet graupel, LM-scheme	168
9.2	Rayleigh: soaked wet graupel, Seifert/Beheng-scheme	168
9.3	Rayleigh: soaked wet snow, LM-scheme	168
9.4	Rayleigh: soaked wet snow, Seifert/Beheng-scheme	168
9.5	Mie: soaked twosphere wet graupel, LM-scheme	168
9.6	Mie: soaked twosphere wet graupel, Seifert/Beheng-scheme	169
9.7	Mie: soaked twosphere wet snow, LM-scheme	169
9.8	Mie: soaked twosphere wet snow, Seifert/Beheng-scheme	169
9.9	Mie: soaked wet graupel, LM-scheme	169
9.10	Mie: soaked wet graupel, Seifert/Beheng-scheme	169
9.11	Mie: soaked wet snow, LM-scheme	169
9.12	Mie: soaked wet snow, Seifert/Beheng-scheme	170
9.13	Mie: watersphere wet graupel, LM-scheme	170
9.14	Mie: watersphere wet graupel, Seifert/Beheng-scheme	170
9.15	Mie: watersphere wet snow, LM-scheme	170
9.16	Mie: watersphere wet snow, Seifert/Beheng-scheme	170
9.17	Mie: spongy wet hail, Seifert/Beheng-scheme	170
9.18	Mie: watersphere wet hail, Seifert/Beheng-scheme	171
9.19	Mie: twosphere soaked wet snow, LM-scheme	171
9.20	Mie: twosphere soaked wet snow, Seifert/Beheng-scheme	173
	References	176

1 Preface

This Technical Report describes a new implementation of the computation of radar reflectivity values on the native model grid points, which will soon become available in the COSMO-Model together with the new Efficient Modular VOlume scanning RADar forward Operator (EMVORADO).

While the abovementioned computation of grid point reflectivities is one of several processing steps within the EMVORADO, it can also be used on its own, without the “full” EMVORADO-simulation of polar volumetric radar data. In that sense, it is a replacement for the presently very simple Rayleigh-type ‘DBZ’ computation available in the COSMO module `pp_utilities.f90`, which is currently used for output diagnosis in the COSMO `GRIBOUT-namelist(s)`. Well, “replacement” is not entirely correct, because the present method will still be available as one of several options. The new options are the more accurate (and more expensive) Mie-scattering, but also two new variants of Rayleigh-type approximations of different complexity and cost, which differ from the current simple one mainly by a better treatment of partially melted particles (the famous radar “bright band”).

The present report is restricted to this “stand-alone” aspect. It covers the theoretical aspects of the unattenuated equivalent radar reflectivity factor (loosely called “reflectivity”), including the refractive index of hydrometeors, which is the basic material parameter, which determines the interaction with electromagnetic radiation. The latter possesses various possible and uncertain definitions for the ice-water-air-mixture of partially melted particles. Moreover, details of the implementation of these aspects into the new libraries `radar_mielib_vec.f90` and `radar_mie_lm_vec.f90` are described, before the report concludes with an exhaustive sensitivity study on the various (and uncertain!) choosable options for the backscattering cross section of partially melted particles.

Although developed in the framework of the COSMO-model, the new libraries can in principle be coupled to any other NWP model.

I have written most contents of this report alongside the code development during my Post-Doc time at the Institute of Meteorology and Climate Research, Tropospheric Branch (IMK-TRO), Karlsruhe Institute of Technology (KIT) in Germany. This work started in early 2005, when I first came into contact with numerical modeling and the COSMO-model, and was largely finished by 2010 when I started at Deutscher Wetterdienst. In 2005, the model still had its traditional name “Lokalmodell” LM, and I preserved this acronym at many places in the code in order to not forget the roots.

Later, together with Yuefei Zeng and Dorit Jerger (PhD-projects with financial support through DWD’s Extramural Reserach Programme) as well as our mentor Klaus-Dieter Beheng from IMK-TRO, we built the full EMVORADO-framework on top. But this is a different story.

Ulrich Blahak

2 Introduction

The program package `radar_mielib` provides Fortran-90 routines for the calculation of gridbox values of the equivalent radar reflectivity factor from model output based on Mie-scattering functions as well as Rayleigh approximation. Water drops and a variety of different kinds of dry and melting ice particles are considered (graupel, snow, cloud ice, hail).

Whereas `radar_mielib` contains quite general subroutines, the library `radar_mie_lm` provides the necessary interface routines to use them with the Lokalmmodell (LM) of the German Weather Service (DWD) together with the two-moment bulk microphysical scheme of Seifert and Beheng (2006) or the standard one-moment bulk microphysical schemes.

Note that in calculating gridbox values, propagation effects (extinction) and the spatial averaging properties (beam function) of radar systems are not considered. The neglect of attenuation confines the applicability of the calculated reflectivity values to quantitative comparisons at radar wavelengths with negligible attenuation only, e.g., S-band, or to situations or research questions where attenuation is not of primary importance. At shorter wavelengths (C-band, X-band) those effects have to be kept in mind when comparing with real radar data. The shorter the wavelength the stronger is attenuation. However, calculation of the extinction cross section is contained in the basic scattering routines in `radar_mielib`, but is not used further by routines in `radar_mielib` and `radar_mie_lm` which build upon them. Only a full radar forward operator, considering true ray paths from the antenna through the atmosphere, could make use of this information.

Special emphasis is given to the description of melting ice particles. It is well known, however, that this is a highly underdetermined problem, since, on one hand, the particles shapes are different from spherical and, on the other hand, the effective refractive index of the particle material (mixture of ice, water, and air) is very sensitive to the type and topology of mixture and the particles bulk density. Moreover, there is no absolutely precise theoretical description of the effective refractive index of such complex mixtures like in snow- and graupel particles — consequently, a large number of formulas for different applications are on the market.

In `radar_mielib`, the problem is tackled by providing routines for 3 different mixing formulas for the refractive index (Maxwell-Garnett, Wiener, Bruggemann), whereas only spherical shapes are considered. In case of Mie-scattering, also a concentric two-layer-sphere particle model is implemented, which can be used for, e.g., snowflakes and melting hail- and graupel particles. Moreover, different melting topologies are considered, e.g., accumulation of meltwater on the outside or fully soaked particles, melting taking place only on the outside or partly within the ice structure. Combining the tools leaves one with an infinite number of possibilities to describe a melting particle. Especially the Maxwell-Garnett mixing rule allows 15 different refractive index values for a single set of ice-water-air volume fractions. From this it can clearly be seen that there is a large natural variability, which has to be considered when comparing calculated with measured radar reflectivities. Sensitivity studies with the help of the tools from `radar_mielib` at least provide a lower bound for this high variability.

In the following sections, the tools of `radar_mielib` are described in detail. To facilitate their proper use, calculated backscatter coefficients for different types of melting particles (snow, graupel and hail) as a function of the degree of melting and particle mass are presented, considering about 800 different combinations of particle types and mixing rules. The different particle types are taken from the cloud microphysical schemes of the COSMO-model (formerly “Lokalmmodell” (LM) of the German Weather Service (DWD) — the standard 1-moment scheme as well as the 2-moment scheme of Seifert and Beheng (2006).

3 Factors contributing to the radar "bright band"

There are different (and sometimes competing) factors contributing to the observed radar bright band:

- Backscattering of single melting particles is enhanced in the presence of meltwater.
- Thinning of the number density (number of particles per volume of air) by increasing fall speed with increasing degree of melting reduces backscattering.
- Upper part of the melting layer: particle breakup is dominant.
Lower part: particle coalescence is dominant.

It should be emphasized that the backscattering enhancement of single melting particles treatable by the routines in `radar_mielib` is only one of several processes contributing to the observed radar bright band. Therefore, the results presented later in Section 8 about backscattering cross sections of single particles as function of the degree of melting attribute only to this part of the reflectivity maximum.

4 Theoretical basis

In this section formulas are collected to calculate the unattenuated equivalent radar reflectivity factor Z_e from model output which are implemented in `radar_mielib`. To simulate a real radar measurement, also attenuation, beam propagation and the beam smoothing function would have to be included, which is omitted here.

4.1 Equivalent radar reflectivity factor

Consider the assumption of incoherent single scattering being the dominant effect in radar backscattering. Then, the equivalent radar reflectivity factor is commonly defined as

$$Z_e = \frac{\lambda_0^4}{\pi^5 |K_{w,0}|^2} \int_0^\infty \sigma_b(D) N(D) dD \quad , \quad (1)$$

where λ_0 is the radar wavelength, $N(D)$ the particle size distribution as a function of the (spherical) particle diameter D , and σ_b denotes the backscattering cross section of a particle having diameter D . $|K_{w,0}|$ is a reference value of the dielectric factor used in the radar software, usually taken as 0.93 (water, $T = 0^\circ\text{C}$, $\lambda_{00} \approx 5 - 10$ cm). $N(D)$ depends also on time and location, but the explicit dependence is omitted for brevity.

Z_e would be output by a radar in case of a homogeneous spatial hydrometeor distribution across the range cell and no attenuation on the path to the cell. Written in the above notation, it is implicitly assumed that there is a unique relation between size (D) and $\sigma_b(D)$ as it is the case for water drops to a good degree of approximation. Taking into account also ice particles complicates the description, since then, this uniqueness breaks down and we have to extend the dependencies of N and σ to particle shape and particle effective refractive index ($\sigma_b(\text{shape}, D, \lambda_0, m)$).

As a compromise, one might define different types of ice hydrometeors (e.g., graupel, snow, hail) in a way that for these subtypes, a unique relation of σ and D exists. Then, Z_e is the sum of the contribution of each hydrometeor type. In fact, current microphysical descriptions in numerical weather prediction models classify ice hydrometeors in different types in a way to also let σ only depend on D .

As an example, the procedure to calculate Z_e from the output of a two-moment bulk microphysical scheme is as follows:

- $f(D)$: assume certain master function for $N(D)$, e.g., a four-parametric generalized gamma distribution. 2 free parameters are then deduced from the model predicted two moments (e.g., hydrometeor number- and mass density), and the other two parameters have to be fixed.
- Hydrometeors are a mixture of ice, air and water.
 - Choose appropriate formula to calculate m as a function of T , λ , material, density and the degree of melting f_{melt} . For this, several state-of-the-art effective medium approximations could be used, but this is always a delicate choice. A huge uncertainty and variability has to be expected there.
 - If the microphysics scheme does not predict f_{melt} , it has to be estimated from whatever information is available (temperature, particle size, etc.). This is a particularly difficult thing especially if there is no information about the particles history. Temperature and ventilation factors along backwards trajectories would be desirable for this task but are very costly to determine.
- σ_b : apply Mie-scattering (one- or twolayered sphere) or Rayleigh-Approximation to calculate σ_b .
- $Z_e = \sum$ (all hydrometeor categories)

For the LM, these tasks are accomplished by interface subroutines in the library `radar_mie_lm`, building on the more general tools provided by `radar_mielib`.

4.2 Extinction

For completeness, the formula for the twoway attenuation coefficient k_2 is given here:

$$k_2 = \frac{20}{\ln 10} \int_0^\infty \sigma_{ext}(D) N(D) dD \quad . \quad (2)$$

σ_{ext} is the extinction cross section, depending on D as well as λ_0 . Applying Lambert-Beer's extinction law, integration of k_2 along the radar beam yields the attenuation factor. Again, there are issues about beam smoothing and propagation path which render an accurate calculation from model data very difficult and costly (apart from considering different hydrometeor types).

The calculation of σ_{ext} is implemented in all basic scattering subroutines but is not used further up to now (2008). This could however be extended by users who wish to develop, e.g., a complete radar simulator including propagation effects.

4.3 Backscattering and extinction by spheres

Consider a plane parallel electromagnetic wave incident on a spherical object with refractive index m (complex) different to that of the surrounding medium, m_0 (real, no extinction). The Mie-solution of maxwells equations at a large distance from the scatterer leads to the formula for σ_b ,

$$\sigma_b = \frac{4\pi}{k^2} \left| \sum_{n=1}^{\infty} (-1)^n \left(n + \frac{1}{2} \right) (a_n - b_n) \right|^2 \quad . \quad (3)$$

a_n und b_n are the socalled Mie scattering coefficients of order n which depend only on the Mie-parameter $\alpha = \pi\lambda_0 m_0/D$ and the relative refractive index m/m_0 of the particle

material. They in turn involve spherical bessel functions of the arguments α and $\alpha m/m_0$ and are omitted here.

As an alternative, a_n and b_n can be efficiently calculated by recurrence formulas derived by, e.g., Deirmendjian (1969) or Bohren and Huffman (1983). These formulas themselves build on recurrence relations for the involved spherical bessel functions. The subroutine `SPHERE_SCATTER_BH()` of `radar_mielib` makes use of these relations.

A further simplification is the so called **Rayleigh-approximation** for particles having D small compared to λ_0 . Series expansions of a_n and b_n in equation (3) and retention of only the leading term yield the approximation

$$\sigma_b = \frac{\pi^5}{\lambda_0^4} \left| \frac{m^2 - 1}{m^2 + 2} \right|^2 D^6 = \frac{\pi^5}{\lambda_0^4} |K|^2 D^6 \quad \text{with} \quad \frac{m^2 - 1}{m^2 + 2} = K \quad (4)$$

where m_0 is set to 1 (air), so m/m_0 reduces to just m . K is called the dielectric factor. The Validity of the approximation depends on the Mie parameter and m/m_0 . Generally, larger m/m_0 yield a more restrictive size criterion. For water spheres a comparison of exact formula and approximation yields $D < \lambda_0/20$, for ice spheres $D < \lambda_0/5$. Bohren and Huffman (1983) formulate the condition as $|m/m_0| \pi D_k / \lambda_0 \ll 1$.

When the particles are very small compared with the wavelength, the Rayleigh-approximation is also valid for nonspherical particles. The smaller the particle the less important is its shape. D has then to be taken as the diameter of the volume equivalent sphere.

In case of $m = \text{const.}$ (e.g., for water drops or dry ice spheres) and application of the Rayleigh approximation for σ_b , Z_e is simply given by the 6. moment of the size distribution $N(D)$,

$$Z_e = \frac{|K_w|^2}{|K_{w,0}|^2} \int_0^\infty D^6 N(D) dD \quad , \quad (5)$$

where water drops have been assumed in the formula without loss of generality. Z_e is equivalent to the 6. Moment of the size distribution of (hypothetically) measured water drops, which explains the name "equivalent reflectivity factor". In cases of $N(D)$ being a certain type of function (e.g., a generalized gamma distribution), the integral in (5) can be solved analytically, involving gamma functions.

The extinction coefficient σ_{ext} for spherical particles is given by

$$\sigma_{ext} = \frac{4\pi}{k^2} \Re \left\{ \sum_{n=1}^{\infty} \left(n + \frac{1}{2} \right) (a_n + b_n) \right\} \quad . \quad (6)$$

A similar approximation as in equation (4) yields

$$\sigma_{ext} = \frac{\pi^2}{\lambda_0} \Im\{-K\} D^3 + \frac{2}{3} \frac{\pi^5}{\lambda_0^4} |K|^2 D^6 \quad , \quad (7)$$

with K having the same meaning as in equation (4). Two terms have been retained here since they might be of same order in certain situations. The first term describes the losses by absorption, second term the losses by scattering in all directions.

In case of a small water drop σ_{ext} is dominated by the absorption term (example with subscript w for water: $\lambda_0 = 1$ cm, $m_w = 4.97 - 2.79i$ (10°C) after Ray (1972), $|K_w|^2 = 0.91$, $\Im\{-K\} = 0.07$, $D = 0.1$ mm \Rightarrow absorption term = $7 \cdot 10^{-11}$ m², scattering term = $3 \cdot 10^{-14}$ m², geometrical cross section = $8 \cdot 10^{-9}$ m². In case of small ice particles both

Can't show picture #1 because `tr28_ub2-pics.pdf` not found. Create it from
`tr28_ub2.dvi` using `dvips` and `ps2pdf`!

Figure 1: Convention for the refractive indices m_0 , m_1 , m_2 and for the radii r_1 , r_2 in the calculation of the scattering functions for a two-layered sphere.

terms are important, since $\Im\{-K_i\} \ll |K_i|^2$ (subscript i for ice). Ice absorbs microwave radiation much less than water.

For water droplets in the microwave region, the approximation (7) is only valid for $D < \lambda_0/100$, whereas for ice spheres $D < \lambda_0/2$, which is by far less restrictive. The same rule of thumb as in the case of backscattering applies here as well: the larger $|m/m_0|$, the more restrictive is the size criterion on D . As soon as the particles contain water in any volume fraction, one should not calculate σ_{ext} by the above approximation, but with the exact formula (6).

4.4 Backscattering and extinction by two-layered spheres

Today, exact solutions to the scattering problem of N-layered spheres are available which reduce to the classical Mie-formula for a simple sphere. Since some hydrometeors like melting hail (ice core, spongy ice/water-shell) can be well approximated by a two-layered sphere, formulas for backscattering- and extinction cross sections for this configuration are included into `radar_mielib` as well.

As in the case of simple spheres, important parameters are the two Mie-parameters

$$\alpha_1 = \frac{2\pi r_1 m_0}{\lambda_0} \quad ; \quad \alpha_2 = \frac{2\pi r_2 m_0}{\lambda_0} \quad . \quad (8)$$

defined by the shell and core radii r_1 and r_2 , resp., as well as the corresponding relative refractive indices m_1 and m_2 (see Figure 1).

Depending on these parameters, the scattering coefficients a_n and b_n can be calculated analytically and then plugged into equation (3) and (6). To this end, formulas for a_n and b_n given by, e.g., Kerker (1969) are implemented into `radar_mielib` (subroutine `COATEDSPHERE_SCATTER()`) or, as a second alternative, an efficient subroutine making advantage of the recurrence relations for the spherical Bessel and Hankel functions given in the appendix of Bohren and Huffman (1983) is provided (subroutine `COATEDSPHERE_SCATTER_BH()`). The rather long and cumbersome formulas for a_n and b_n are omitted here. We refer the reader to the cited literature.

Note that numerical instabilities in calculating Bessel-functions by utilizing efficient recurrence relations (as is done here) are known to be problematic in case of large arguments to the Bessel functions. In the `radar_mielib`-subroutine `COATEDSPHERE_SCATTER()`, backward recurrence for the Bessel- and Hankel functions (programs taken from Zhang and Jin, 1996) are utilized, which is more stable than the forward recurrence implemented into subroutine `COATEDSPHERE_SCATTER_BH()`. However, `COATEDSPHERE_SCATTER()` is slower than `COATEDSPHERE_SCATTER_BH()`. Application of these routines to hydrometeor scattering in the microwave region should not be problematic, so both routines can be used.

4.5 Refractive index of hydrometeors

Up to this point, general formulas for the computation of the backscatter- and extinction cross section of spherical particles were given. An important parameter herein is the complex refractive index of the particle material $m = m' + im''$ (m_1 , m_2 for the two-layered

sphere), which will be presented in the next sections. m is connected to the relative dielectric constant $\epsilon = \epsilon' + i\epsilon''$ by the relation $\epsilon = m^2$. Note that in this paper the convention with negative imaginary part of m and ϵ is used which corresponds to a timefactor $\exp(i\omega t)$ in the description of electromagnetic waves. Under the assumption $\epsilon'' < 0$, $m'' < 0$ the following conversion formulas apply:

$$\epsilon' = m'^2 - m''^2 \quad (9)$$

$$\epsilon'' = 2m'm'' \quad (10)$$

$$m' = \sqrt{\frac{\sqrt{\epsilon'^2 + \epsilon''^2} + \epsilon'}{2}} \quad (11)$$

$$m'' = -\sqrt{\frac{\sqrt{\epsilon'^2 + \epsilon''^2} - \epsilon'}{2}} \quad (12)$$

The last two equations define the principal arm of the complex root function, as it is implemented also in most programming languages.

Hydrometeors consist of air, ice and/or water, so values of m for these materials are needed. For air, $m = 1$ is a very good approximation. For ice and water, m basically depends on wavelength and temperature. With these values, pure water and ice particles can be treated. These are given in subsubsection 4.5.1 and 4.5.2.

Things get by far more complicated in the case of dry snow particles (mixture of ice and air) or melting snow particles (mixture of ice, air and water). Here the task is to find an effective value m_{eff} , which leads to the same scattering functions when applied in the Mie-formulae that are observed for the mixture particle, whose scattering pattern highly depends on the topology of the mixture. This is a very difficult task, and consequently, there are a lot of mixing formulas on the market applicable to certain special situations. A general solution to the problem seems to be not existent. Moreover, mixing rules applicable for backscattering might not be applicable for extinction and vice versa (e.g., for granular mixtures with spatially inhomogeneous material distribution), since it is sometimes not possible to describe the directional scattering by a single value of m_{eff} .

In subsubsection 4.5.4 to subsubsection 4.5.6, some mixing formulas are presented which are currently used by the radar meteorological community for the mixture topologies encountered in dry and melting hydrometeors.

Can't show picture #2 because `tr28_ub2-pics.pdf` not found. Create it from
`tr28_ub2.dvi` using `dvips` and `ps2pdf`!

Figure 2: Complex refractive index of water after Ray (1972) as a function of wavelength λ_0 in m and temperature in °C (only his equations (5) and (6) are used). **Red:** real part, **blue:** negative imaginary part. Several curves are shown at constant temperatures of -10°C to 30°C in steps of 10°C.

Can't show picture #3 because `tr28_ub2-pics.pdf` not found. Create it from
`tr28_ub2.dvi` using `dvips` and `ps2pdf`!

Figure 3: Complex refractive index of water after Liebe et al. (1991) as a function of wavelength λ_0 in m and temperature in °C. **Red:** real part, **blue:** negative imaginary part. Several curves are shown at constant temperatures of -10°C to 30°C in steps of 10°C.

4.5.1 Water

Two models (formulas) for the complex index of refraction of water, m_w , are implemented into `radar_mielib` as functions. They give m_w as a function of wavelength λ_0 and temperature T . The first is the model of Ray (1972), which is applicable to the temperature range from -10°C to 30°C and to the wavelength range of about 1 mm to 1 m. Figure 2 depicts the real and imaginary parts of m_w for this model as a function of λ_0 and T . One clearly sees the anomalous dispersion signal connected to a classical Debye relaxation mode in the microwave region. With higher frequency (shorter wavelength) the real part drops down reflecting an increase in propagation phase speed, whereas in the same frequency range, the imaginary part has a distinct maximum, reflecting strong absorption. The complete formulas of Ray (1972) also contain several rotational and absorption bands in the infrared region, parameterized as gaussian peaks, but this is omitted in the `radar_mielib` function. Only the formulas (5) and (6) of Ray (1972) are used, which limits the applicability to the microwave region.

Another model is given by Liebe et al. (1991) with a slightly different application range, namely $300 \mu\text{m} < \lambda_0 < 0.3 \text{ m}$ and $-3^\circ\text{C} < T < 30^\circ\text{C}$. Figure 3 shows the real and imaginary parts of m_w for this model. The prominent Debye relaxation mode is also present here, as it should.

A comparison of both models can be found in Figure 4 for a temperature of 25°C, together with a model based on measurements of Segelstein (1981). The latter is only available for the temperature of 25°C. Nearly no differences between these descriptions are visible the wavelength range 5 mm to 20 cm, so all descriptions equally can be used in the microwave region, all giving similar results. Looking at other temperatures, nearly no differences between Rays and Liebes model can be found for the wavelength range 1 cm to 10 cm. At larger wavelength, the imaginary part is larger for Rays model, whereas at shorter wavelengths, the opposite is found. Liebes model should be used for $\lambda_0 < 1 \text{ cm}$, whereas both models are applicable from 1 cm to 10 cm, and Rays model is better from 10 cm to 1 m.

Can't show picture #4 because `tr28_ub2-pics.pdf` not found. Create it from
`tr28_ub2.dvi` using `dvips` and `ps2pdf`!

Figure 4: Comparison of the complex refractive index of water as function of wavelength in m at a temperature of 25°C for 3 different formulations. **Black:** Ray (1972), **blue:** Segelstein (1981), **red:** Liebe et al. (1991). **Solid lines:** real part, **Dashed lines:** imaginary part.

Can't show picture #5 because `tr28_ub2-pics.pdf` not found. Create it from
`tr28_ub2.dvi` using `dvips` and `ps2pdf`!

Figure 5: Complex refractive index of ice after Ray (1972) as a function of wavelength λ_0 in m and temperature in °C. **Red, right ordinate:** real part. **Blue, left ordinate (logarithmic scale):** negative imaginary part. Several curves are shown at constant temperatures of -20°C, -10°C and 0°C.

Can't show picture #6 because `tr28_ub2-pics.pdf` not found. Create it from
`tr28_ub2.dvi` using `dvips` and `ps2pdf`!

Figure 6: Complex refractive index of ice after Warren (1984) as a function of wavelength λ_0 in m and temperature in °C. **Red, right ordinate:** real part. **Blue, left ordinate (logarithmic scale):** negative imaginary part. Several curves are shown at constant temperatures from -60°C to 0°C in steps of 10°C.

Can't show picture #7 because `tr28_ub2-pics.pdf` not found. Create it from
`tr28_ub2.dvi` using `dvips` and `ps2pdf`!

Figure 7: Complex refractive index of ice after Mätzler (1998) as a function of wavelength λ_0 in m and temperature in °C. **Red, right ordinate:** real part. **Blue, left ordinate (logarithmic scale):** negative imaginary part. Several curves are shown at constant temperatures from -60°C to 0°C in steps of 10°C.

4.5.2 Ice

For the complex refractive index of ice, m_i , three models are available in `radar_mielib`. The first is again a model of Ray (1972), from the same paper as previously the model for water. The corresponding real and imaginary parts of m_i are depicted in Figure 5 as functions of λ_0 and T . The range of validity is given by the author to be $0.001 \text{ m} < \lambda_0 < 10^7 \text{ m}$ and $-20^\circ\text{C} < T < 0^\circ\text{C}$. Ray (1972) deduced it from then available measurements from the literature, but not fulfilling the Kramers-Kronig-relations (see, e.g., Bohren and Huffman, 1983), as criticized, e.g., by Warren (1984). The use of this model is therefore not recommended.

As a second and better model, the discrete m_i -tables given by Warren (1984) are implemented, as shown in Figure 6. The author critically and carefully reviewed the existing measurements in literature, combined with own measurements to deduce his lookup tables. Here the Kramers-Kronig-relations are fulfilled. Values of m_i at intermediate values of λ_0 and T are linearly interpolated. In the original paper, the range of validity is given as $45 \text{ nm} < \lambda_0 < 8.6 \text{ m}$ and $-60^\circ\text{C} < T < 0^\circ\text{C}$.

Third, the formula of Mätzler (1998) is available (see Figure 7). The author gives the range of validity as $0.1 \text{ mm} < \lambda_0 < 30 \text{ m}$ and $-250^\circ\text{C} < T < 0^\circ\text{C}$.

Can't show picture #8 because `tr28_ub2-pics.pdf` not found. Create it from
`tr28_ub2.dvi` using `dvips` and `ps2pdf`!

Can't show picture #9 because `tr28_ub2-pics.pdf` not found. Create it from
`tr28_ub2.dvi` using `dvips` and `ps2pdf`!

Figure 8: Comparison of the complex refractive index of ice as function of wavelength in m at temperatures of -2°C (solid lines) and -20°C (dashed lines) for 3 different formulations. **Upper panel:** real part. **Lower panel:** imaginary part. **Black:** Ray (1972), **blue:** Warren (1984), **red:** Mätzler (1998).

While very similar for the real part of m_i , it can be seen from Figure 8 that especially the model of Ray (1972) predicts a totally different behaviour of the imaginary part of m_i with wavelength than the other two models. Here, the models of Warren (1984) and Mätzler (1998) are in qualitative agreement, but Mätzler (1998) gives lower values of the imaginary part up to a factor of 8 compared to Warren (1984). The author of this document feels not to be in a position to recommend using one or the other, but using the model of Ray (1972) is not recommended because of the abovementioned reasons.

4.5.3 Mixtures of ice, air and water

In literature, many different formulations of the refractive index of a mixture material are presented termed "Effective Medium Approximations" (EMA). Mostly they have their origin in the field of physical chemistry. It is a very old concept dating back to the late 19th century but nevertheless still an actual topic in research. In the meteorological community dealing with radar measurements, mostly three formulations are used which are also part of `radar_mielib`. These will be introduced in the following subsections.

The general problem is to find an effective value for the refractive index m_{eff} of a mixture material leading to the same scattering pattern when replacing the actual mixture particle by a homogeneous particle and measuring/ calculating the scattering functions by some theory using m_{eff} . Many theoretical and experimental attempts can be found in literature, but we cannot go into detail here. A starting point for further study could be the book of Bohren and Huffman (1983) or the article of [shortciteNstroud1978](#).

It is immediately clear that such a technique inevitably gets complicated or leads to errors when applying it to particles which are not truly homogeneously mixed (mixture may have a macroscale topography) and/or when at least one of the mixture components is a strong dielectric like water. Some EMAs may be valid only for extinction or scattering in a certain direction depending on the method of their derivation.

4.5.4 Mixtures of ice, air and water — Wieners formula

Otto Wiener (1912) presented a quite general theory for a homogeneous mixture of inclusions (grains, fibres, layers, etc.) of N materials which are embedded in a homogeneous background medium with dielectric constant ϵ_0 . In case of spherical inclusions, he states

$$\frac{\epsilon_{eff} - \epsilon_0}{\epsilon_{eff} + f \epsilon_0} = \sum_{j=1}^N p_j \frac{\epsilon_j - \epsilon_0}{\epsilon_j + f \epsilon_0} \quad . \quad (13)$$

p_j denotes the relative volume fraction of the species j on the overall particle volume,

$$p_j = \frac{V_j}{V_m}, \quad \text{where } V_m = \text{Volume of mixture particle} \quad (14)$$

and ϵ_j is its dielectric constant. **Note that in fact $N+1$ materials are contained in the mixture!** The parameter f in general depends on the shape, orientation, mutual distance and alignment within the mixture body. Let us denote the partial volume fraction of the background medium with p_0 and the partial volume by V_0 , then it is

$$p_0 + \sum_{j=1}^N p_j = 1 \quad \text{and} \quad V_0 + \sum_{j=1}^N V_j = V_m \quad (15)$$

A good review of the original paper by Wiener is given by Lichtenecker (1926).

Formula (13) was derived under the assumption of a mixture of equally shaped and equally sized inclusions of N species into the background medium. In order to be applicable, one has to specify a value for the parameter f . Wiener (1912) showed that this can be accomplished under the following constraints:

- All inclusions have to be sufficiently separated so that the electromagnetic field inbetween can be regarded as homogeneous. This implies $p_0 > 0$ (in fact $p_0 \gg p_1, p_2$) so that the condition of large grain separation distances can be fulfilled.
- ϵ_0 has to be either the largest or the smallest value of all ϵ_x involved and it has to be significantly different to the adjacent ϵ_x .
- Isotropic distribution of the grains within the matrix medium.

Under these circumstances the parameter f depends largely only on the shape of the inclusions and attains the value 2 for spherical inclusions (Wiener then denotes f by "Formzahl" — shape number). A more detailed discussion of these constraints can be found in the original literature. However, since the classical derivations were done for real ϵ_x , it remains somehow unclear how to formulate these constraints for complex ϵ_x .

Often a seemingly similar formula is used by the radarmeteorological community in a way to set $\epsilon_0 = 1$ (vacuum, air) (see e.g., the review article by Oguchi (1983)) and at the same time assuming that there is no contribution of the background medium to the particles volume ($p_0 = 0$). The formula then reduces to an older formula (Lorenz-Lorentz, Clausius, Mosotti et others, see, e.g., Wiener, 1912 or Lichtenecker, 1926),

$$\frac{\epsilon_{eff} - 1}{\epsilon_{eff} + u} = \sum_{j=1}^N p_j \frac{\epsilon_j - 1}{\epsilon_j + u} \quad (16)$$

$$\sum_{j=1}^N p_j = 1 \quad .$$

In the following, formula (16) is referred to as Oguchi¹ formula. Oguchi (1983) designates the parameter u as shape parameter, similar to f in equation (13), and states that in case of spherical inclusions u attains the value 2.

The problem with this formula is that in neglecting the partial volume of the background medium, the assumption of mutual "large enough" distances between the inclusions is violated and the formula seems not to be applicable in general. Debye (1929) therefore restricts the formula to weak dielectrics and to the case of molecular mixtures which he regards as suspended spheres (single atoms) in vacuum (same argumentation in Bohren and Huffman (1983)). It is clearly not applicable to a melting ice particle with low air contribution since water is a strong dielectric. This was also found experimentally by Joss and Aufdermaur (1965).

However, when the background medium within the particle is air ($\epsilon_0 = 1$) with a considerable volume fraction and the particle is a mixture of ice and air (dry snow flake, graupel), the formula might be applicable since ice is a weak dielectric. The mixing term containing the air volume in (16) then vanishes and a "classical" formula used by radar meteorologists for many years (e.g., Battan, 1973) is recovered (also by appropriately using formula (13), which corroborates the validity of (16) for this special case).

¹Oguchi (1983) wrongly attributes equation (16) to Otto Wiener, whereas the latter showed in his 1912 paper, why and under what circumstances this formula is not applicable. Wiener derived equation (13) instead, among formulas for other mixing topologies.

4.5.5 Mixtures of ice, air and water — Maxwell-Garnetts formula

Maxwell-Garnetts formula (Maxwell Garnett, 1904) is a special case of a more general formulation, see Stroud (1975), in the limiting case of small spherical inclusions of random size suspended in a background medium ("matrix"), similar as is the Wiener-formula, except for the random size. (In fact, it will be shown later in this section to be exactly equal to Wieners formula in case of spherical inclusions.)

Bohren and Huffman (1983) derive the following formulation similar to the original paper of Maxwell Garnett (1904)

$$\epsilon_{eff} = \frac{p_1 \epsilon_1 + \sum_{j=2}^N p_j \beta_j \epsilon_j}{p_1 - \sum_{j=2}^N p_j \beta_j} \quad (17)$$

$$\beta_j = \frac{3 \epsilon_1}{\epsilon_j + 2 \epsilon_1} \quad , \quad (18)$$

where p_j denotes again the relative volume fraction of the species j on the overall particle volume,

$$p_j = \frac{V_j}{V_m}, \quad \text{where } V_m = \text{Volume of mixture particle} \quad (19)$$

and ϵ_j is its dielectric constant. It is

$$\sum_{j=1}^N p_j = 1 \quad .$$

in this case. Here, index 1 corresponds to the matrix medium and indices larger than 1 denote inclusion materials.

Bohren and Battan (1982) extended this model to spheroidal inclusions, which have random size, which are randomly oriented within the matrix medium and which have random principal axes ratios (shapes). For this, only the coefficients β_j have to be replaced by

$$\beta_j = \frac{2 \epsilon_1}{\epsilon_j - \epsilon_1} \left(\frac{\epsilon_j}{\epsilon_j - \epsilon_1} \ln \left(\frac{\epsilon_j}{\epsilon_1} \right) - 1 \right) \quad . \quad (20)$$

The complex logarithm denotes the principal arm. Note that this formulation is not invariant to a change in the matrix-species, but it is invariant to interchange the inclusions.

In case of a three-component mixture (as is the case with melting snow and graupel particles), formula (17) leads to numerous possibilities to specify matrix and inclusions. There are 3 possibilities to specify one material as matrix and the other two as inclusions. 12 additional possibilities arise by a two-fold application of a two-component mixture: one material is regarded as the matrix (3 possibilities), whereas the inclusion itself is regarded as a two-component mixture with 2 possibilities to specify matrix and inclusion. This leads to 6 possibilities. Changing further the roles of matrix and inclusion for the hosting material and the two-component sub-mixture, another 6 possibilities arise. Every possibility leads to different results. The degree of freedom (and the uncertainty about what to do) is therefore very large. In addition spherical and spheroidal inclusions can be discriminated, further doubling the number of possible choices.

An interesting comparison to the Wiener-formula can be made in rewriting equation (17) for spherical inclusions (β_j with equation (4.5.5)). After some manipulation,

$$\frac{\epsilon_{eff} - \epsilon_1}{\epsilon_{eff} + 2\epsilon_1} = \sum_{j=2}^N p_j \frac{\epsilon_j - \epsilon_1}{\epsilon_j + 2\epsilon_1} . \quad (21)$$

Changing the index convention to Wieners formula ($1 \rightarrow 0, N \rightarrow N - 1$) leads to the formula

$$\frac{\epsilon_{eff} - \epsilon_0}{\epsilon_{eff} + 2\epsilon_0} = \sum_{j=1}^N p_j \frac{\epsilon_j - \epsilon_0}{\epsilon_j + 2\epsilon_0} . \quad (22)$$

Now the species 1 to N are the inclusions and the species 0 is the matrix. Comparing to equation (13) with $f = 2$ (spherical inclusions), both formulas turn out to be exactly equal. Therefore, the same constraints concerning the applicability as for the Wiener-formula also apply to Maxwell-Garnetts formula. In particular, in the case of $p_1 \rightarrow 0$, the matrix material vanishes and the Maxwell-Garnett formula might no longer be applicable. In this case, another formula might be better suited, which will be described in subsubsection 4.5.6. On the other hand, Wieners formula with $f = 2$ does not require the spherical inclusions to be all of equal size.

In recent studies, mainly the Maxwell-Garnett formulation with the assumption of randomly oriented and randomly shaped small spheroidal inclusions is preferred in the literature, but with different assumptions about matrix and inclusions.

4.5.6 Mixtures of ice, air and water — Bruggemann formula

Another limiting case of the more general formulation of Stroud (1975) is the formula given by Bruggemann (1935),

$$\sum_{j=1}^N p_j \frac{\epsilon_j - \epsilon_{eff}}{\epsilon_j + 2\epsilon_{eff}} = 0 \quad (23)$$

$$p_j = \frac{V_j}{V_m}, \quad \text{where } V_m = \text{Volume of mixture particle}$$

$$\sum_{j=1}^N p_j = 1 .$$

It is applicable for a homogeneous mixture of subscale macroscopic granules of different materials (index j) in "dense packing" configuration without giving a special meaning to one of the component materials (Chýlek and Srivastava, 1983). In that sense, the mixing topology assumed for this formula might be regarded as the limiting case of vanishing matrix material (cf. end of subsubsection 4.5.5). It is based on an approximation of the Mie forward scattering function $S_1(0) = S_2(0)$ for the single granules in that only the leading term with coefficient a_1 in equation (3) is retained. The single granules therefore have to be very small compared to the wavelength. Formula (23) is invariant to interchanging the species, as is Oguchis formula (16).

The implicit equation (23) leads to the problem of finding the roots of a complex polynomial of order N in ϵ_{eff} . After the fundamental theorem of algebra there are exactly N complex roots. For $N \leq 3$ there exist analytical solutions ($N = 3$: Cardani's formula, e.g.), and for $N > 3$, these can be found, e.g., iteratively by Laguerre's method (Press et al., 2001).

However, only one of these roots has physical meaning and can be assigned to $m_{eff} = \sqrt{\epsilon_{eff}}$. Usually, the constraints of a negative imaginary part of ϵ_{eff} (by convention in `radar_mielib`) together with the real part of ϵ_{eff} being inbetween the range of real parts of the ϵ_j , the physical meaningful root ϵ_{eff} can be identified, at least for a three-component mixture of ice, air and water, as is needed for our purpose.

5 Routines in radar_mielib

To calculate Z_e by integration of equation (1) (Page 7), information about the particle size distribution and about the backscattering cross section σ_b as function of particle type, size and degree of melting is needed, which in turn requires information about the effective particle refractive index m_{eff} . The theoretical basics for σ_b (one- and two-layered Mie scattering, Rayleigh approximation) and m_{eff} were briefly discussed in earlier sections, and, in particular, different EMA approximations for m_{eff} were summarized. Up to now and in the remainder of this document, the particle size distributions itself are not treated in detail, since their proper treatment depends strongly on the application: for a bin microphysical scheme resolving explicitly the size distributions of different hydrometeor types, no assumptions have to be drawn about it, whereas for a bulk microphysical scheme, usually a parametric function prototype ("master function" approach) is chosen whose free parameters are diagnosed from model variables. Therefore, the main focus of this document is on the properties of single particles, whereas the integration over the entire size distribution is left for the user.

Before we turn to more detailed investigations of the differences caused by applying different combinations of EMA formulations and melting models for single particles (one-layered or two-layered spheres, different mixing material assumptions) in subsequent sections, a complete list of subroutines and functions from `radar_mielib` will be given in the following subsections providing tools for calculation of σ_b and m_{eff} of single particles.

Later in Section 6, the library `radar_mie_lm` is exemplified to show how these tools can be combined for reflectivity calculations in a mesoscale NWP-model. `radar_mie_lm` provides interface reflectivity calculation subroutines for the LM.

5.1 Refractive index of pure ice and water

5.1.1 FUNCTION `m_complex_water_ray` (lambda, T)

```
INTEGER, PARAMETER    :: kinddp = KIND(1.0d0)
COMPLEX(kind=kinddp)  :: m_complex_water_ray
DOUBLE PRECISION      :: T, lambda
```

Description:

Refractive index of water after Ray (1972), see subsubsection 4.5.1 on Page 12.
Valid for $-10^\circ\text{C} < T < 30^\circ\text{C}$, $0.001 \text{ m} < \lambda_0 < 1 \text{ m}$.

Input parameters:

<code>kinddp</code>	kind parameter for double precision
<code>lambda</code>	radar wavelength in m
<code>T</code>	temperature in $^\circ\text{C}$

Example:

```
mwater = m_complex_water_ray(0.055, 10.0)
```

5.1.2 FUNCTION m_complex_water_liebe (lambda, T)

```
INTEGER, PARAMETER :: kinddp = KIND(1.0d0)
COMPLEX(kind=kinddp) :: m_complex_water_liebe
DOUBLE PRECISION    :: T, lambda
```

Description:

Refractive index of water after Liebe et al. (1991), see subsection 4.5.1 on Page 12.
Valid for $-3^{\circ}\text{C} < T < 30^{\circ}\text{C}$, $0.0003\text{ m} < \lambda_0 < 0.3\text{ m}$.

Input parameters:

kinddp	kind parameter for double precision
lambda	radar wavelength in m
T	temperature in $^{\circ}\text{C}$

Example:

```
mwater = m_complex_water_liebe(0.055, 10.0)
```


5.1.3 FUNCTION m_complex_ice_ray (lambda, T)

```
INTEGER, PARAMETER :: kinddp = KIND(1.0d0)
COMPLEX(kind=kinddp) :: m_complex_ice_ray
DOUBLE PRECISION    :: T, lambda
```

Description:

Refractive index of ice after Ray (1972), see subsection 4.5.2 on Page 13.
Valid for $-20^{\circ}\text{C} < T < 0^{\circ}\text{C}$, $0.001\text{ m} < \lambda_0 < 10^7\text{m}$.

Input parameters:

kinddp	kind parameter for double precision
lambda	radar wavelength in m
T	temperature in $^{\circ}\text{C}$

Example:

```
mice = m_complex_ice_ray(0.055, -10.0)
```

5.1.4 FUNCTION m_complex_ice_warren (lambda, T)

```
INTEGER, PARAMETER :: kinddp = KIND(1.0d0)
COMPLEX(kind=kinddp) :: m_complex_ice_warren
DOUBLE PRECISION    :: T, lambda
```

Description:

Refractive index of ice after Warren (1984), see subsection 4.5.2 on Page 13.
Valid for $-60^{\circ}\text{C} < T < 0^{\circ}\text{C}$, $45 \cdot 10^{-9} \text{ m} < \lambda_0 < 8.6 \text{ m}$.

Input parameters:

kinddp	kind parameter for double precision
lambda	radar wavelength in m
T	temperature in $^{\circ}\text{C}$

Example:

```
mice = m_complex_ice_warren(0.055, -10.0)
```

5.1.5 FUNCTION `m_complex_ice_maetzler` (`lambda`, `T`)

```
INTEGER, PARAMETER :: kinddp = KIND(1.0d0)
COMPLEX(kind=kinddp) :: m_complex_ice_maetzler
DOUBLE PRECISION    :: T, lambda
```

Description:

Refractive index of ice after Mätzler (1998), see subsection 4.5.2 on Page 13.
Valid for $-250^{\circ}\text{C} < T < 0^{\circ}\text{C}$, $0.0001\text{ m} < \lambda_0 < 30\text{ m}$.

Input parameters:

<code>kinddp</code>	kind parameter for double precision
<code>lambda</code>	radar wavelength in m
<code>T</code>	temperature in $^{\circ}\text{C}$

Example:

```
mice = m_complex_ice_maetzler(0.055, -10.0)
```

5.2 Refractive index of mixture materials

5.2.1 FUNCTION `m_complex_oguchi`
 (`vol1`, `vol2`, `vol3`, `m1`, `m2`, `m3`, `fehler`)

```
INTEGER, PARAMETER :: kinddp = KIND(1.0d0)
COMPLEX(kind=kinddp) :: m_complex_oguchi
COMPLEX(kind=kinddp) :: m1, m2, m3
DOUBLE PRECISION    :: vol1, vol2, vol3
INTEGER, INTENT(out) :: fehler
```

Description:

Refractive index m_{eff} of a three-component mixture material after Oguchi (1983), see equation (16) in subsection 4.5.4 on Page 15.

Input parameters:

<code>kinddp</code>	kind parameter for double precision
<code>m1</code> , <code>m2</code> , <code>m3</code>	complex index of refraction for the three mixture components 1, 2 and 3
<code>vol1</code> , <code>vol2</code> , <code>vol3</code>	corresponding volume fractions (conform with p_1, p_2, p_3 from equation (16), $\sum p_j \stackrel{!}{=} 1$)

Output parameters:

<code>m_complex_oguchi</code>	complex refractive index m_{eff} of the mixture material, function result
<code>fehler</code>	error status (side effect): 0 = no error, 1 = error encountered

Example:

```
mmix = m_complex_oguchi(0.5, 0.3, 0.2, mwater, mice, mair, errorflag)
```

```

5.2.2 FUNCTION m_complex_maxwellgarnett
      (vol1, vol2, vol3, m1, m2, m3, inclusionstring, fehler)

INTEGER, PARAMETER    :: kinddp = KIND(1.0d0)
COMPLEX(kind=kinddp) :: m_complex_maxwellgarnett
COMPLEX(kind=kinddp) :: m1, m2, m3
DOUBLE PRECISION      :: vol1, vol2, vol3
CHARACTER(len=*)      :: inclusionstring
INTEGER, INTENT(out)  :: fehler

```

Description:

Refractive index of a three-component mixture material after Maxwell Garnett (1904), see subsubsection 4.5.5 on Page 16. Both formulas for spherical (equation (18)) and spheroidal (equation (20)) inclusions are implemented and can be chosen via a keyword parameter. The choice which material is the matrix and which are the inclusions is done via the order number of the material: No. 1 denotes the matrix, No. 2 and 3 represent the inclusions (see below).

Input parameters:

kinddp	kind parameter for double precision
m1, m2, m3	complex index of refraction for the three mixture components 1, 2 and 3. Index 1 denotes the matrix material and 2 and 3 represent the inclusions
vol1, vol2, vol3	corresponding volume fractions (conform with p_1, p_2, p_3 from equation (17), $\sum p_j \stackrel{!}{=} 1$)
inclusionstring	A string constant to choose if spherical or spheroidal inclusions should be assumed: 'spherical' — spherical inclusions 'spheroidal' — spheroidal inclusions

Output parameters:

m_complex_maxwellgarnett	complex refractive index m_{eff} of the mixture material, function result
fehler	error status (side effect): 0 = no error, 1 = error encountered

Example:

```
mmix = m_complex_maxwellgarnett(0.5, 0.3, 0.2, mwater, mice, mair, 'spheroidal', errorflag)
```

5.2.3 FUNCTION m_complex_bruggemann

(volair, volice, volwater, mair, mice, mwater, fehler)

```

INTEGER, PARAMETER  :: kinddp = KIND(1.0d0)
COMPLEX(kind=kinddp) :: m_complex_bruggemann
COMPLEX(kind=kinddp) :: mair, mice, mwater
DOUBLE PRECISION    :: volair, volice, volwater
INTEGER, INTENT(out) :: fehler

```

Description:

Refractive index of a three-component mixture of air, ice and water after Bruggemann (1935), see equation (23) in subsubsection 4.5.6 on Page 17.

Note: This routine is especially designed for mixtures of air, ice and water!

Input parameters:

kinddp	kind parameter for double precision
mair, mice, mwater	complex index of refraction for air, ice and water
volair, volice, volwater	corresponding volume fractions (conform with p_1, p_2, p_3 from equation (23), $\sum p_j \stackrel{!}{=} 1$)

Output parameters:

m_complex_bruggemann	complex refractive index m_{eff} of the mixture material, function result
fehler	error status (side effect): 0 = no error, 1 = error encountered

Example:

```
mmix = m_complex_bruggemann(0.5, 0.3, 0.2, mwater, mice, mair, errorflag)
```

5.2.4 FUNCTION get_m_mix

(m_a, m_i, m_w, volair, volice, volwater, mixingrulestring, matrixstring, inclusionstring, fehler)

```

INTEGER, PARAMETER          :: kinddp = KIND(1.0d0)
COMPLEX(kind=kinddp)        :: get_m_mix
COMPLEX(kind=kinddp), INTENT(in) :: m_a, m_i, m_w
DOUBLE PRECISION, INTENT(in)  :: volair, volice, volwater
CHARACTER(len=*), INTENT(in)  :: mixingrulestring
CHARACTER(len=*), INTENT(in)  :: matrixstring
CHARACTER(len=*), INTENT(in)  :: inclusionstring
INTEGER, INTENT(out)         :: fehler

```

Description:

Interface routine to the basic functions `m_complex_oguchi()`, `m_complex_maxwellgarnett()` and `m_complex_bruggemann()` for a three-component mixture. Three keyword parameter strings determine, which mixingrule and, if necessary, which matrix material should be chosen. **Note: This routine is especially designed for mixtures of air, ice and water!**

Input parameters:

<code>kinddp</code>	kind parameter for double precision
<code>m_a, m_i, m_w</code>	complex index of refraction for air, ice and water, resp.
<code>volair, volice, volwater</code>	corresponding volume fractions (conform with p_1, p_2, p_3 from equation (23), $\sum p_j \stackrel{!}{=} 1$)
<code>mixingrulestring</code>	A string constant to choose the mixing rule: 'oguchi' — <code>m_complex_oguchi()</code> , spherical inclusions 'maxwellgarnett' — <code>m_complex_maxwellgarnett()</code> 'bruggemann' — <code>m_complex_bruggemann()</code>
<code>matrixstring</code>	In case of <code>mixingrulestring = 'maxwellgarnett'</code> , choice of the matrix material: 'air' — air 'ice' — ice 'water' — water
<code>inclusionstring</code>	A string constant to choose if spherical or spheroidal inclusions should be assumed: 'spherical' — spherical inclusions 'spheroidal' — spheroidal inclusions

Output parameters:

<code>get_m_mix</code>	complex refractive index m_{eff} of the mixture material, function result
<code>fehler</code>	error status (side effect): 0 = no error, 1 = error encountered

Example:

```
mmix = get_m_mix(mair, mice, mwater, 0.2, 0.3, 0.5, 'maxwellgarnett', &  
                'ice', 'spheroidal', errorflag)
```


5.2.5 FUNCTION get_m_mix_nested

```
(m_a, m_i, m_w, volair, volice, volwater, mixingrulestring, hoststring,
matrixstring, inclusionstring, hostmatrixstring, hostinclusionstring,
kumfehler)
```

```
INTEGER, PARAMETER          :: kinddp = KIND(1.0d0)
COMPLEX(kind=kinddp)        :: get_m_mix_nested
COMPLEX(kind=kinddp), INTENT(in) :: m_a, m_i, m_w
DOUBLE PRECISION, INTENT(in)  :: volair, volice, volwater
CHARACTER(len=*), INTENT(in)  :: mixingrulestring
CHARACTER(len=*), INTENT(in)  :: hoststring
CHARACTER(len=*), INTENT(in)  :: matrixstring
CHARACTER(len=*), INTENT(in)  :: inclusionstring
CHARACTER(len=*), INTENT(in)  :: hostmatrixstring
CHARACTER(len=*), INTENT(in)  :: hostinclusionstring
INTEGER, INTENT(out)         :: kumfehler
```

Description:

Interface routine to the basic functions `m_complex_oguchi()`, `m_complex_maxwellgarnett()` and `m_complex_bruggemann()` for a three-component mixture. The difference to `get_m_mix()` (subsubsection 5.2.4) is that, once a particular mixing rule is chosen, additionally a twofold mixing of two two-component mixtures is possible. This offers for the Maxwell-Garnett rule 30 different choices in total. If this twofold mixing is specified, first m_{eff} of a mixture of two of the three components is calculated ("inner" mixing material), and later, this effective medium is mixed with the remaining third component ("outer" mixture). **Note that the twofold application of two two-component mixtures with different mixing rules is not implemented so far.** In case of Bruggemann- and Oguchi-rule, it does not make any difference if choosing the three-component or twofold two-component mixing.

Six keyword parameter strings determine, which mixingrule and (if necessary) if twofold two-component or three-component mixture with which matrix material(s) should be chosen (see below for details).

Note: This routine is especially designed for mixtures of air, ice and water!

Input parameters:

<code>kinddp</code>	kind parameter for double precision
<code>m_a, m_i, m_w</code>	complex index of refraction for air, ice and water, resp.
<code>volair, volice, volwater</code>	corresponding volume fractions (conform with p_1, p_2, p_3 from equation (23), $\sum p_j \stackrel{!}{=} 1$)
<code>mixingrulestring</code>	A string constant to choose the mixing rule: 'oguchi' — <code>m_complex_oguchi()</code> , spherical inclusions 'maxwellgarnett' — <code>m_complex_maxwellgarnett()</code> 'bruggemann' — <code>m_complex_bruggemann()</code>
<code>hoststring</code>	Determines which material should be the hosting ("outer") material in a twofold two-component mixture or if a three-component mixture should be chosen: 'none' — onefold three-component mixture 'air' — air 'ice' — ice 'water' — water

<code>matrixstring</code>	<p>In case of twofold two-component mixture (<code>hoststring</code> \neq 'none') and Maxwell-Garnett mixing rule, choice of the matrix material of the "inner" mixture:</p> <p>'air' — air 'ice' — ice 'water' — water (not equal to <code>hoststring</code>!)</p> <p>In case of three-component mixture (<code>hoststring</code> = 'none'), the usual choice of the matrix material:</p> <p>'air' — air 'ice' — ice 'water' — water</p>
<code>inclusionstring</code>	<p>A string constant to choose if spherical or spheroidal inclusions should be assumed (in case of twofold two-component mixture, for the "inner" mixture):</p> <p>'spherical' — spherical inclusions 'spheroidal' — spheroidal inclusions</p>
<code>hostmatrixstring</code>	<p>In case of <code>mixingrulestring</code> = 'maxwellgarnett' and twofold two-component mixture, choice of the matrix material of the "outer" mixture (no meaning in case of <code>hoststring</code> = 'none'):</p> <p>'air' — air 'ice' — ice 'water' — water 'airice' — air/ice-mixture 'airwater' — air/water-mixture 'icewater' — ice/water-mixture</p>
<code>hostinclusionstring</code>	<p>In case of twofold two-component mixture, for the "outer" mixture, a string constant to choose if spherical or spheroidal inclusions should be assumed:</p> <p>'spherical' — spherical inclusions 'spheroidal' — spheroidal inclusions</p>

Note that not all combinations of these six keyword parameter strings does make sense. Nonsense combinations will lead to an error ($m_{eff} = -999.99$), a corresponding error message and `kumfehler` \neq 0.

Output parameters:

<code>get_m_mix</code>	complex refractive index m_{eff} of the mixture material, function result
<code>kumfehler</code>	error status (side effect): 0 = no error, 1 = error encountered

Example:

5.3 Backscattering cross section for single precipitation particles

5.3.1 SUBROUTINE MIE_DRY_GRAUPEL

(x_g,a_geo,b_geo,m_i,lambda,C_back, mixingrulestring, matrixstring, inclusionstring)

```

INTEGER, PARAMETER          :: kinddp = KIND(1.0d0)
DOUBLE PRECISION, INTENT(in) :: x_g, lambda, a_geo, b_geo
COMPLEX(kind=kinddp), INTENT(in) :: m_i
CHARACTER(len=*), INTENT(in)  :: mixingrulestring
CHARACTER(len=*), INTENT(in)  :: matrixstring
CHARACTER(len=*), INTENT(in)  :: inclusionstring
DOUBLE PRECISION, INTENT(out) :: C_back

```

Description:

Backscattering cross section σ_b (Mie-scattering) of a dry graupel/snow/hail particle, assumed as a **sphere of homogeneous ice-air mixture material**. The particle bulk density is derived from the inverse mass-size-relation (40) with coefficients a_{geo} and b_{geo} assuming spherical shape. `mixingrulestring`, `matrixstring` and `inclusionstring` determine the effective medium approximation used to calculate the effective refractive index of the particles, which is done by function `get_m_mix` (Subsection 5.2).

For relatively small particles, the Rayleigh approximation can be applied instead by using subroutine `RAYLEIGH_DRY_GRAUPEL()` (subsubsection 5.3.2).

Input parameters:

<code>kinddp</code>	kind parameter for double precision
<code>x_g</code>	Mass of particle in kg (without air fraction)
<code>a_geo</code>	Coefficient a_{geo} of the inverse mass-size-relation (40)
<code>b_geo</code>	Coefficient b_{geo} of the inverse mass-size-relation (40)
<code>m_i</code>	Complex refractive index of ice
<code>lambda</code>	Radar wavelength in m
<code>mixingrulestring</code>	A string constant to choose the mixing rule: 'oguchi' — <code>m_complex_oguchi()</code> , spherical inclusions 'maxwellgarnett' — <code>m_complex_maxwellgarnett()</code> 'bruggemann' — <code>m_complex_bruggemann()</code>
<code>matrixstring</code>	In case of <code>mixingrulestring = 'maxwellgarnett'</code> , choice of the matrix material: 'air' — air 'ice' — ice 'water' — water (does not make sense here)
<code>inclusionstring</code>	A string constant to choose if spherical or spheroidal inclusions should be assumed: 'spherical' — spherical inclusions 'spheroidal' — spheroidal inclusions

Output parameters:

C_back Backscattering cross section σ_b in m^2

Example:

```
CALL MIE_DRY_GRAUPEL(2.3e-3, a_geo, b_geo, m_i, 0.055, C_back, &  
    'maxwellgarnett', 'ice', 'spheroidal')
```

5.3.2 SUBROUTINE RAYLEIGH_DRY_GRAUPEL

(x_g,a_geo,b_geo,m_i,lambda,C_back, mixingrulestring, matrixstring, inclusionstring)

```

INTEGER, PARAMETER          :: kinddp = KIND(1.0d0)
DOUBLE PRECISION, INTENT(in) :: x_g, lambda, a_geo, b_geo
COMPLEX(kind=kinddp), INTENT(in) :: m_i
CHARACTER(len=*), INTENT(in)  :: mixingrulestring
CHARACTER(len=*), INTENT(in)  :: matrixstring
CHARACTER(len=*), INTENT(in)  :: inclusionstring
DOUBLE PRECISION, INTENT(out)  :: C_back

```

Description:

Backscattering cross section σ_b (Rayleigh approximation) of a dry graupel/snow/hail particle, assumed as a **sphere of homogeneous ice-air mixture material**. The particle bulk density is derived from the inverse mass-size-relation (40) with coefficients a_{geo} and b_{geo} assuming spherical shape. `mixingrulestring`, `matrixstring` and `inclusionstring` determine the effective medium approximation used to calculate the effective refractive index of the particles, which is done by function `get_m_mix` (Subsection 5.2).

Input parameters:

<code>kinddp</code>	kind parameter for double precision
<code>x_g</code>	Mass of particle in kg (without air fraction)
<code>a_geo</code>	Coefficient a_{geo} of the inverse mass-size-relation (40)
<code>b_geo</code>	Coefficient b_{geo} of the inverse mass-size-relation (40)
<code>m_i</code>	Complex refractive index of ice
<code>lambda</code>	Radar wavelength in m
<code>mixingrulestring</code>	A string constant to choose the mixing rule: 'oguchi' — <code>m_complex_oguchi()</code> , spherical inclusions 'maxwellgarnett' — <code>m_complex_maxwellgarnett()</code> 'bruggemann' — <code>m_complex_bruggemann()</code>
<code>matrixstring</code>	In case of <code>mixingrulestring = 'maxwellgarnett'</code> , choice of the matrix material: 'air' — air 'ice' — ice 'water' — water (does not make sense here)
<code>inclusionstring</code>	A string constant to choose if spherical or spheroidal inclusions should be assumed: 'spherical' — spherical inclusions 'spheroidal' — spheroidal inclusions

Output parameters:

C_back Backscattering cross section σ_b in m^2

Example:

```
CALL RAYLEIGH_DRY_GRAUPEL(2.3e-3, a_geo, b_geo, m_i, 0.055, C_back, &  
    'maxwellgarnett', 'ice', 'spheroidal')
```

5.3.3 SUBROUTINE MIE_DRYHAIL

(x_h,a_geo,b_geo,m_i,lambda,C_back)

```

INTEGER, PARAMETER          :: kinddp = KIND(1.0d0)
DOUBLE PRECISION, INTENT(in) :: x_h, lambda, a_geo, b_geo
COMPLEX(kind=kinddp), INTENT(in) :: m_i
DOUBLE PRECISION, INTENT(out) :: C_back

```

Description:

Backscattering cross section σ_b (Mie-scattering) of a dry hail particle, assumed as a **homogeneous ice sphere**. It is an approximation to MIE_DRY_GRAUPEL() (subsubsection 5.3.1) in the sense that although the particle bulk density is permitted to deviate from pure ice, but solid ice is assumed for the particles refractive index (m_i). The purpose of this is to save computation time in case of high density ice particles. Therefore, this routine is only applicable to particle types whose coefficients a_{geo} and b_{geo} of the inverse mass-size-relation (40) represent nearly solid ice particles.

For smaller particles, the Rayleigh approximation can be applied by subroutine RAYLEIGH_DRY_GRAUPEL instead (subsubsection 5.3.2).

Input parameters:

kinddp	kind parameter for double precision
x_h	Mass of hail particle in kg
a_geo	Coefficient a_{geo} of the inverse mass-size-relation (40)
b_geo	Coefficient b_{geo} of the inverse mass-size-relation (40)
m_i	Complex refractive index of ice
lambda	Radar wavelength in m

Output parameters:

C_back	Backscattering cross section σ_b in m^2
--------	---

Example:

```
CALL MIE_DRYHAIL(2.3e-3, a_geo, b_geo, m_i, 0.055, C_back)
```


5.3.4 SUBROUTINE MIE_DRYSNOW

(x_s,a_geo,b_geo,m_i,lambda,C_back, mixingrulestring, matrixstring, inclusionstring)

```

INTEGER, PARAMETER          :: kinddp = KIND(1.0d0)
DOUBLE PRECISION, INTENT(in) :: x_s, lambda, a_geo, b_geo
COMPLEX(kind=kinddp), INTENT(in) :: m_i
CHARACTER(len=*), INTENT(in)  :: mixingrulestring
CHARACTER(len=*), INTENT(in)  :: matrixstring
CHARACTER(len=*), INTENT(in)  :: inclusionstring
DOUBLE PRECISION, INTENT(out)  :: C_back

```

Description:

Backscattering cross section σ_b (Mie-scattering) of a dry graupel/snow/hail particle, assumed as a **sphere of homogeneous ice-air mixture material**. The particle bulk density is derived from the inverse mass-size-relation (40) with coefficients a_{geo} and b_{geo} assuming spherical shape. `mixingrulestring`, `matrixstring` and `inclusionstring` determine the effective medium approximation used to calculate the effective refractive index of the particles, which is done by function `get_m_mix` (Subsection 5.2).

For smaller particles, the Rayleigh approximation can be applied by using subroutine `RAYLEIGH_DRY_GRAUPEL` instead (subsubsection 5.3.2).

The only difference to subroutine `MIE_DRY_GRAUPEL` (subsubsection 5.3.1) is that a equivalent spherical diameter threshold of 10^{-12} m is used instead of 10^{-6} m below which C_{back} is set to 0 to save computation time.

Input parameters:

<code>kinddp</code>	kind parameter for double precision
<code>x_s</code>	Mass of particle in kg (without air fraction)
<code>a_geo</code>	Coefficient a_{geo} of the inverse mass-size-relation (40)
<code>b_geo</code>	Coefficient b_{geo} of the inverse mass-size-relation (40)
<code>m_i</code>	Complex refractive index of ice
<code>lambda</code>	Radar wavelength in m
<code>mixingrulestring</code>	A string constant to choose the mixing rule: 'oguchi' — <code>m_complex_oguchi()</code> , spherical inclusions 'maxwellgarnett' — <code>m_complex_maxwellgarnett()</code> 'bruggemann' — <code>m_complex_bruggemann()</code>
<code>matrixstring</code>	In case of <code>mixingrulestring</code> = 'maxwellgarnett', choice of the matrix material: 'air' — air 'ice' — ice 'water' — water (does not make sense here)
<code>inclusionstring</code>	A string constant to choose if spherical or spheroidal inclusions should be assumed: 'spherical' — spherical inclusions 'spheroidal' — spheroidal inclusions

Output parameters:

C_back Backscattering cross section σ_b in m^2

Example:

```
CALL MIE_DRYSNOW(3.4e-5, a_geo, b_geo, m_i, 0.055, C_back, &  
    'maxwellgarnett', 'ice', 'spheroidal')
```

5.3.5 SUBROUTINE MIE_DRYSNOW_TWOSPH

```
(x_s,a_geo,b_geo,m_i,radienverh,lambda,C_back, mixingrulestring_shell,
matrixstring_shell, inclusionstring_shell, mixingrulestring_core,
matrixstring_core, inclusionstring_core)
```

```
INTEGER, PARAMETER          :: kinddp = KIND(1.0d0)
DOUBLE PRECISION, INTENT(in) :: x_s, lambda, a_geo, b_geo
DOUBLE PRECISION, INTENT(in) :: radienverh
COMPLEX(kind=kinddp), INTENT(in) :: m_i
CHARACTER(len=*), INTENT(in)  :: mixingrulestring_shell
CHARACTER(len=*), INTENT(in)  :: matrixstring_shell
CHARACTER(len=*), INTENT(in)  :: inclusionstring_shell
CHARACTER(len=*), INTENT(in)  :: mixingrulestring_core
CHARACTER(len=*), INTENT(in)  :: matrixstring_core
CHARACTER(len=*), INTENT(in)  :: inclusionstring_core
DOUBLE PRECISION, INTENT(out)  :: C_back
```

Description:

Backscattering cross section σ_b (Mie-scattering) of a dry snowflake, assumed as a **two-layered sphere of homogeneous ice-air mixture material in each layer, the core having higher bulk density than the shell (see Subsection 7.2)**. The overall particle bulk density is derived from the inverse mass-size-relation (40) with coefficients a_{geo} and b_{geo} assuming spherical shape. Note that b_{geo} has to represent a decreasing bulk density with size.

To model a snowflake by a two-layered sphere with a denser core and a less dense shell, additional information is necessary to assign the different bulk densities to core and shell, preserving overall particle mass. To this end, as additional parameter, the ratio of the inner to the outer sphere radius, **radienverh**, has to be specified with a value between 0 and 1. With this parameter, the procedure described later in Subsection 7.2 on Page 71 is applied to assign different bulk densities to core and shell.

Further, the input parameters **mixingrulestring_shell/ mixingrulestring_core**, **matrixstring_shell/ matrixstring_core** and **inclusionstring_shell/ inclusionstring_core** determine the effective medium approximation used to calculate the effective refractive index of the particles shell/ core, which is done by function **get_m_mix** (Subsection 5.2).

This routine uses the formulae of Bohren and Huffman (1983) for the backscattering cross section of a two-layered sphere (subroutine **COATEDSPHERE_SCATTER.BH()**), see Subsection 4.4.

Input parameters:

kinddp	kind parameter for double precision
x_s	Mass of particle in kg (without air fraction)
a_geo	Coefficient a_{geo} of the inverse mass-size-relation (40)
b_geo	Coefficient b_{geo} of the inverse mass-size-relation (40)
radienverh	Ratio of the inner to the outer sphere radius
m_i	Complex refractive index of ice
lambda	Radar wavelength in m

mixingrulestring_shell/ mixingrulestring_core	String constants to choose the mixing rule: 'oguchi' — <code>m_complex_oguchi()</code> , spherical inclusions 'maxwellgarnett' — <code>m_complex_maxwellgarnett()</code> 'bruggemann' — <code>m_complex_bruggemann()</code>
matrixstring_shell/ matrixstring_core	In case of <code>mixingrulestring = 'maxwellgarnett'</code> , choice of the matrix material: 'air' — air 'ice' — ice 'water' — water (does not make sense here)
inclusionstring_shell/ inclusionstring_core	String constants to choose if spherical or spheroidal in- clusions should be assumed: 'spherical' — spherical inclusions 'spheroidal' — spheroidal inclusions

Output parameters:

C_back	Backscattering cross section σ_b in m^2
--------	---

Example:

```
CALL MIE_DRYSNOW_TWOSPH(3.4e-5, a_geo, b_geo, m_i, 0.055, C_back, &
  'maxwellgarnett', 'air', 'spheroidal', &
  'maxwellgarnett', 'ice', 'spheroidal')
```

5.3.6 SUBROUTINE MIE_WATERSPH_WETHAIL (x_h, fmelt, m_i, m_w, lambda, C_back)

```

INTEGER, PARAMETER          :: kinddp = KIND(1.0d0)
DOUBLE PRECISION, INTENT(in) :: x_h, fmelt, lambda
DOUBLE PRECISION, INTENT(out) :: C_back
COMPLEX(kind=kinddp), INTENT(in) :: m_i, m_w

```

Description:

Backscattering cross section σ_b of a melting hail particle, assumed as a **solid spherical ice core with spherical water coating**, calculated by the two-sphere Mie-formulae. Here, the formulae of Kerker (1969) are applied (subroutine COATEDSPHERE_SCATTER()), see Subsection 4.4.

To speed up computation (but with some loss of stability), the **subroutine** MIE_WATERSPH_WETHAIL_BH() can be used instead with exactly the same input- and output parameters. This routine utilizes the formulae of Bohren and Huffman (1983) (subroutine COATEDSPHERE_SCATTER_BH()) instead of Kerker (1969), see Subsection 4.4.

Input parameters:

kinddp	kind parameter for double precision
x_h	Mass of hail particle in kg
fmelt	degree of melting, $f_{melt} = x_w/x_h$ (x_w = mass of water contained in the particle)
m_i	Complex refractive index of ice
m_w	Complex refractive index of water
lambda	Radar wavelength in m

Output parameters:

C_back	Backscattering cross section σ_b in m ²
--------	---

Example:

```
CALL MIE_WATERSPH_WETHAIL(2.3e-3, 0.7, m_i, m_w, 0.055, C_back)
```

Example sensitivity studies:

The dependence of σ_b on the degree of melting and on particle size for a specific temperature of $T = 5^\circ\text{C}$ is studied in detail in Subsection 8.18 on Page 107.

5.3.7 SUBROUTINE MIE_SPONGY_WETHAIL

```
(x_h, fmelt, f_water, m_i, m_w, lambda, C_back, mixingrulestring, matrixstring,
inclusionstring)
```

```
INTEGER, PARAMETER          :: kinddp = KIND(1.0d0)
DOUBLE PRECISION, INTENT(in) :: x_h, fmelt, f_water, lambda
COMPLEX(kind=kinddp), INTENT(in) :: m_i, m_w
CHARACTER(len=*), INTENT(in)  :: mixingrulestring
CHARACTER(len=*), INTENT(in)  :: matrixstring
CHARACTER(len=*), INTENT(in)  :: inclusionstring
DOUBLE PRECISION, INTENT(out)  :: C_back
```

Description:

Backscattering cross section σ_b of a melting hail particle, assumed as a **solid spherical ice core with a spherical coating of a "spongy" ice-water mixture**, calculated by the two-sphere Mie-formulae. Here, the formulae of Kerker (1969) are applied (subroutine COATEDSPHERE_SCATTER()), see Subsection 4.4. The mass fraction of water (**f_water**) in the outer spongy shell has to be preset and is held fixed throughout the melting process, as long as the inner ice core is not completely melted. After the inner core has completely vanished, **f_water** is increased automatically to represent now the melted fraction of the remaining homogeneous spherical particle.

It seems reasonable to assume larger values of **f_water** during later melting stages (larger **fmelt**) than for earlier melting stages (small **fmelt**).

To speed up computation (but with some loss of stability), the **subroutine** MIE_SPONGY_WETHAIL_BH() can be used instead with exactly the same input- and output parameters. This routine utilizes the formulae of Bohren and Huffman (1983) (subroutine COATEDSPHERE_SCATTER_BH()) instead of Kerker (1969), see Subsection 4.4.

Input parameters:

kinddp	kind parameter for double precision
x_h	Mass of hail particle in kg
fmelt	Degree of melting, $f_{melt} = x_w/x_h$ (x_w = mass of water contained in the particle)
f_water	Mass fraction of water in the outer spongy shell ($x_{water}/(x_{ice} + x_{water})$)
m_i	Complex refractive index of ice
m_w	Complex refractive index of water
lambda	Radar wavelength in m
mixingrulestring	A string constant to choose the mixing rule for the ice-water shell: 'oguchi' — m_complex_oguchi(), spherical inclusions 'maxwellgarnett' — m_complex_maxwellgarnett() 'bruggemann' — m_complex_bruggemann()

<code>matrixstring</code>	In case of <code>mixingrulestring = 'maxwellgarnett'</code> , choice of the matrix material for the ice-water shell: 'air' — air (does not make sense here) 'ice' — ice 'water' — water
<code>inclusionstring</code>	A string constant to choose if spherical or spheroidal inclusions should be assumed for the ice-water shell: 'spherical' — spherical inclusions 'spheroidal' — spheroidal inclusions

Output parameters:

<code>C_back</code>	Backscattering cross section σ_b in m^2
---------------------	---

Example:

```
CALL MIE_SPONGY_WETHAIL(2.3e-3, 0.7, 0.5, m_i, m_w, 0.055, C_back)
```

Example sensitivity studies:

The dependence of σ_b on the degree of melting and on particle size for a specific temperature of $T = 5^\circ\text{C}$ is studied in detail in Subsection 8.17 on Page 106.

5.3.8 SUBROUTINE MIE_WATERSPH_WETGR

(x_g,a_geo,b_geo,fmelt,m_w,m_i,lambda,C_back, mixingrulestring, matrixstring, inclusionstring)

```

INTEGER, PARAMETER          :: kinddp = KIND(1.0d0)
DOUBLE PRECISION, INTENT(in) :: x_g, lambda, a_geo, b_geo, fmelt
COMPLEX(kind=kinddp), INTENT(in) :: m_w, m_i
CHARACTER(len=*), INTENT(in)  :: mixingrulestring
CHARACTER(len=*), INTENT(in)  :: matrixstring
CHARACTER(len=*), INTENT(in)  :: inclusionstring
DOUBLE PRECISION, INTENT(out) :: C_back

```

Description:

Backscattering cross section σ_b (Mie-scattering, two-layered sphere) of a melting graupel particle, assumed as a **two-layered sphere composed of a homogeneous ice-air mixture core and a spherical water shell**. The bulk density (ice mass per particle volume) of the original unmelted particle is derived from the inverse mass-size-relation (40) with coefficients a_{geo} and b_{geo} assuming spherical shape. `fmelt` denotes the melted mass fraction or the degree of melting, f_{melt} , resp. It is assumed that the particle melts entirely at the outside of the ice-air core and that the meltwater is accumulated in a spherical shell. `mixingrulestring`, `matrixstring` and `inclusionstring` determine the effective medium approximation used to calculate the effective refractive index of the particle ice-air core, which is done by function `get_m_mix` (Subsection 5.2). Such a melting model should be applicable to relatively high-density graupel and/ or at later melting stages (`fmelt` > approx. 0.5).

For the calculation of the two-sphere backscattering cross section, the formulae of Kerker (1969) are applied (subroutine `COATEDSPHERE_SCATTER()`), see Subsection 4.4.

To speed up computation (but with some loss of stability), the **subroutine** `MIE_WATERSPH_WETGR_BH()` can be used instead with exactly the same input- and output parameters. This routine utilizes the formulae of Bohren and Huffman (1983) (subroutine `COATEDSPHERE_SCATTER_BH()`) instead of Kerker (1969), see Subsection 4.4.

Input parameters:

<code>kinddp</code>	kind parameter for double precision
<code>x_g</code>	Mass of particle in kg (without air fraction)
<code>a_geo</code>	Coefficient a_{geo} of the inverse mass-size-relation (40)
<code>b_geo</code>	Coefficient b_{geo} of the inverse mass-size-relation (40)
<code>fmelt</code>	Degree of melting, $f_{melt} = x_w/x_g$ (x_w = mass of water contained in the particle)
<code>m_w</code>	Complex refractive index of water
<code>m_i</code>	Complex refractive index of ice
<code>lambda</code>	Radar wavelength in m

<code>mixingrulestring</code>	<p>A string constant to choose the mixing rule for the ice-air core:</p> <p><code>'oguchi'</code> — <code>m_complex_oguchi()</code>, spherical inclusions</p> <p><code>'maxwellgarnett'</code> — <code>m_complex_maxwellgarnett()</code></p> <p><code>'bruggemann'</code> — <code>m_complex_bruggemann()</code></p>
<code>matrixstring</code>	<p>In case of <code>mixingrulestring = 'maxwellgarnett'</code>, choice of the matrix material for the ice-air core:</p> <p><code>'air'</code> — air</p> <p><code>'ice'</code> — ice</p> <p><code>'water'</code> — water (does not make sense here)</p>
<code>inclusionstring</code>	<p>A string constant to choose if spherical or spheroidal inclusions should be assumed for the ice-air core:</p> <p><code>'spherical'</code> — spherical inclusions</p> <p><code>'spheroidal'</code> — spheroidal inclusions</p>

Output parameters:

<code>C_back</code>	Backscattering cross section σ_b in m^2
---------------------	---

Example:

```
CALL MIE_WATERSPH_WETGR(2.3e-3, a_geo, b_geo, &
    0.45, m_w, m_i, 0.055, C_back, &
    'maxwellgarnett', 'ice', 'spheroidal')
```

Example sensitivity studies:

The dependence of σ_b on the degree of melting and on particle size for a specific temperature of $T = 5^\circ\text{C}$ is studied in detail in subsequent sections for the 4 different inverse mass-size-relations given in Subsection 7.1. These are:

- for inverse mass-size-relation (36) in Subsection 8.9 on Page 92,
- for inverse mass-size-relation (37) in Subsection 8.10 on Page 95,
- for inverse mass-size-relation (38) in Subsection 8.11 on Page 98,
- for inverse mass-size-relation (39) in Subsection 8.12 on Page 100.

5.3.9 SUBROUTINE MIE_SOAK_TWOSPH_WETGR

```
(x_g,a_geo,b_geo,fmelt,m_w,m_i,lambda,C_back, mixingrulestring_iceair,
matrixstring_iceair, inclusionstring_iceair, mixingrulestring_icewater,
matrixstring_icewater, inclusionstring_icewater)
```

```
INTEGER, PARAMETER           :: kinddp = KIND(1.0d0)
DOUBLE PRECISION, INTENT(in) :: x_g, lambda, a_geo, b_geo, fmelt
COMPLEX(kind=kinddp), INTENT(in) :: m_w, m_i
CHARACTER(len=*), INTENT(in)  :: mixingrulestring
CHARACTER(len=*), INTENT(in)  :: matrixstring
CHARACTER(len=*), INTENT(in)  :: inclusionstring
DOUBLE PRECISION, INTENT(out)  :: C_back
```

Description:

Backscattering cross section σ_b (Mie-scattering, two-layered sphere) of a melting graupel/snow particle, assumed as a **two-layered sphere composed of a homogeneous ice-air mixture core and a spherical ice-water mixture shell**. The bulk density (ice mass per particle volume) of the original unmelted particle is derived from the inverse mass-size-relation (40) with coefficients a_{geo} and b_{geo} assuming spherical shape. `fmelt` denotes the melted mass fraction or the degree of melting, f_{melt} , resp. It is assumed that the particle melts entirely on its outside and that the meltwater is soaked into the particle, displacing the air inclusions entirely from the outside. In this way, a spherical ice-water mixture shell forms around the ice-air core, growing to the inside with growing melt fraction, up to the melt fraction where the particle is completely soaked and the core has vanished. For a larger melt fraction, the particle is assumed as a sphere of homogeneous ice-water mixture.

Such a melting model should be applicable to graupel with intermediate density at all melting stages or to high-density graupel during an early melting stage (`fmelt` < approx. 0.5).

`mixingrulestring_iceair/` `mixingrulestring_icewater`, `matrixstring_iceair/` `matrixstring_icewater` and `inclusionstring_iceair/` `inclusionstring_icewater` determine the effective medium approximation used to calculate the effective refractive index of the particle ice-air core/ ice-water shell. Both calculations are performed using the function `get_m_mix` (Subsection 5.2).

For the calculation of the two-sphere backscattering cross section, the formulae of Kerker (1969) are applied (subroutine `COATEDSPHERE_SCATTER()`), see Subsection 4.4.

To speed up computation (but with some loss of stability), the **subroutine** `MIE_SOAK_TWOSPH_WETGR_BH()` can be used instead with exactly the same input- and output parameters. This routine utilizes the formulae of Bohren and Huffman (1983) (subroutine `COATEDSPHERE_SCATTER_BH()`) instead of Kerker (1969), see Subsection 4.4.

Input parameters:

<code>kinddp</code>	kind parameter for double precision
<code>x_g</code>	Mass of particle in kg (without air fraction)
<code>a_geo</code>	Coefficient a_{geo} of the inverse mass-size-relation (40)
<code>b_geo</code>	Coefficient b_{geo} of the inverse mass-size-relation (40)

<code>fmelt</code>	Degree of melting, $f_{melt} = x_w/x_g$ (x_w = mass of water contained in the particle)
<code>m_w</code>	Complex refractive index of water
<code>m_i</code>	Complex refractive index of ice
<code>lambda</code>	Radar wavelength in m
<code>mixingrulestring_iceair/ mixingrulestring_icewater</code>	String constants to choose the mixing rule for the ice-air core/ ice-water shell: 'oguchi' — <code>m_complex_oguchi()</code> , spherical inclusions 'maxwellgarnett' — <code>m_complex_maxwellgarnett()</code> 'bruggemann' — <code>m_complex_bruggemann()</code>
<code>matrixstring_iceair/ matrixstring_icewater</code>	In case of <code>mixingrulestring = 'maxwellgarnett'</code> , choice of the matrix material for the ice-air core/ ice-water shell: 'air' — air (not for <code>matrixstring_icewater</code>) 'ice' — ice 'water' — water (not for <code>matrixstring_iceair</code>)
<code>inclusionstring_iceair/ inclusionstring_icewater</code>	String constants to choose if spherical or spheroidal inclusions should be assumed for the ice-air core/ ice-water shell: 'spherical' — spherical inclusions 'spheroidal' — spheroidal inclusions

Output parameters:

<code>C_back</code>	Backscattering cross section σ_b in m^2
---------------------	---

Example:

```
CALL MIE_SOAK_TWOSPH_WETGR(2.3e-3, a_geo, b_geo, &
    0.45, m_w, m_i, 0.055, C_back, &
    'maxwellgarnett', 'ice', 'spheroidal', &
    'maxwellgarnett', 'water', 'spheroidal')
```

Example sensitivity studies:

The dependence of σ_b on the degree of melting and on particle size for a specific temperature of $T = 5^\circ\text{C}$ is studied in detail in subsequent sections for the 4 different inverse mass-size-relations given in Subsection 7.1. These are:

- for inverse mass-size-relation (36) in Subsection 8.5 on Page 84,
- for inverse mass-size-relation (37) in Subsection 8.6 on Page 86,
- for inverse mass-size-relation (38) in Subsection 8.7 on Page 88,
- for inverse mass-size-relation (39) in Subsection 8.8 on Page 90.

5.3.10 SUBROUTINE MIE_MEAN_WETGR

```
(x_g,a_geo,b_geo,fmelt,m_w,m_i,lambda,C_back, mixingrulestring_iceair,
matrixstring_iceair, inclusionstring_iceair, mixingrulestring_icewater,
matrixstring_icewater, inclusionstring_icewater)
```

```
INTEGER, PARAMETER          :: kinddp = KIND(1.0d0)
DOUBLE PRECISION, INTENT(in) :: x_g, lambda, a_geo, b_geo, fmelt
COMPLEX(kind=kinddp), INTENT(in) :: m_w, m_i
CHARACTER(len=*), INTENT(in)  :: mixingrulestring_iceair
CHARACTER(len=*), INTENT(in)  :: matrixstring_iceair
CHARACTER(len=*), INTENT(in)  :: inclusionstring_iceair
CHARACTER(len=*), INTENT(in)  :: mixingrulestring_icewater
CHARACTER(len=*), INTENT(in)  :: matrixstring_icewater
CHARACTER(len=*), INTENT(in)  :: inclusionstring_icewater
DOUBLE PRECISION, INTENT(out)  :: C_back
```

Description:

Backscattering cross section σ_b of a melting graupel particle (Mie-scattering, two-layered sphere model), assumed as melt fraction weighted mean of the backscattering coefficients calculated with the subroutines MIE_WATERSPH_WETGR() (subsubsection 5.3.8) and MIE_SOAK_TWOSPH_WETGR() (subsubsection 5.3.9):

$$C_{back} = f_{melt} C_{watersphere} + (1.0 - f_{melt}) C_{soak_{twosphere}} .$$

In this way, the melting particle is assumed to soak the meltwater during the early stage of melting and to accumulate more and more meltwater on the outside at later melting stages.

`mixingrulestring_iceair`, `matrixstring_iceair` and `inclusionstring_iceair` determine the choice of the effective medium approximation for the two-component ice-air core in subroutine MIE_WATERSPH_WETGR() as well as in subroutine MIE_SOAK_TWOSPH_WETGR(). `mixingrulestring_icewater`, `matrixstring_icewater` and `inclusionstring_icewater` do the same for the ice-water shell in MIE_SOAK_TWOSPH_WETGR().

Input- and output parameters are virtually the same as in subsubsection 5.3.9 on Page 45!

Example:

```
CALL MIE_MEAN_WETGR(2.3e-3, a_geo, b_geo, &
    0.45, m_w, m_i, 0.055, C_back, &
    'maxwellgarnett', 'ice', 'spheroidal', &
    'maxwellgarnett', 'water', 'spheroidal')
```

Example sensitivity studies:

Not shown in the present document.

5.3.11 SUBROUTINE MIE_SOAK_WETGR

```
(x_g,a_geo,b_geo,fmelt,meltratio_outside,m_w,m_i,lambda,C_back,
mixingrulestring, matrixstring, inclusionstring, hoststring,
hostmatrixstring, hostinclusionstring)
```

```
INTEGER, PARAMETER          :: kinddp = KIND(1.0d0)
DOUBLE PRECISION, INTENT(in) :: x_g, lambda, a_geo, b_geo, fmelt
DOUBLE PRECISION, INTENT(in) :: meltratio_outside
COMPLEX(kind=kinddp), INTENT(in) :: m_w, m_i
CHARACTER(len=*), INTENT(in)  :: mixingrulestring
CHARACTER(len=*), INTENT(in)  :: matrixstring
CHARACTER(len=*), INTENT(in)  :: inclusionstring
CHARACTER(len=*), INTENT(in)  :: hoststring
CHARACTER(len=*), INTENT(in)  :: hostmatrixstring
CHARACTER(len=*), INTENT(in)  :: hostinclusionstring
DOUBLE PRECISION, INTENT(out)  :: C_back
```

Description:

Backscatter cross section σ_b (Mie-scattering) of a melting graupel/snow particle, assumed as a **sphere composed of a homogeneous ice-water-air mixture material**. The bulk density (ice mass per particle volume) of the original unmelted particle is derived from the inverse mass-size-relation (40) with coefficients a_{geo} and b_{geo} assuming spherical shape. **fmelt** denotes the melted mass fraction or the degree of melting, f_{melt} , resp.

It is assumed that the particle melts partly on the outside and on the inside, within the ice structure, and that the meltwater is completely soaked and distributed homogeneously within the particle, displacing the air inclusions. The fraction of meltwater coming from the outside has to be preselected as input parameter **meltratio_outside** (between 0 and 1), which is the ratio when melting starts ($f_{melt} = 0$). Choosing **meltratio_outside** < 1 leads to larger particles compared to **meltratio_outside** = 1.

If f_{melt} is large enough (depending on bulk density and the actual **meltratio_outside**, see below), the meltwater completely fills the ice structure. Now the ice core melts homogeneously and the particle is assumed to be a homogeneous mixture of ice and water.

However, if **meltratio_outside** is sufficiently small, it could happen that the entire ice skeleton would be melted before all the air inclusions are filled with meltwater. Such particle would be unstable and splash into pieces sooner or later. To avoid this unrealistic asymptotic behaviour, the actual value of **meltratio_outside** increases linearly with growing f_{melt} from its value at $f_{melt} = 0$ (input parameter) to a value of 1 for $f_{melt} = 1$. In this way, the particle in any case converges to a water drop for $f_{melt} \rightarrow 1$.

Once the volume fractions of ice, water and air are derived based on the above assumptions, the effective refractive index of the particle is calculated by the function **get_m_mix_nested**, subsubsection 5.2.5. By proper choice of the input parameters **mixingrulestring**, **matrixstring**, **inclusionstring**, **hoststring**, **hostmatrixstring** and **hostinclusionstring**, the application of many different EMAs is possible, see subsubsection 5.2.5 on Page 28. Mie scattering is finally applied to calculate the backscattering cross section.

For small particles, the Rayleigh approximation can be applied instead to speed up the computation, by using subroutine **RAYLEIGH_SOAK_WETGR()** instead (subsubsection 5.3.12).

Input parameters:

<code>kinddp</code>	kind parameter for double precision
<code>x_g</code>	Mass of particle in kg (without air fraction)
<code>a_geo</code>	Coefficient a_{geo} of the inverse mass-size-relation (40)
<code>b_geo</code>	Coefficient b_{geo} of the inverse mass-size-relation (40)
<code>fmelt</code>	Degree of melting, $f_{melt} = x_w/x_g$ (x_w = mass of water contained in the particle)
<code>meltratio_outside</code>	Subpart ratio of the meltwater mass x_w which melts on the outside of the particle when melting starts ($f_{melt} = 0$). Value between 0 and 1. The complementary subpart of x_w is assumed to melt within the ice structure. The actual value depends on f_{melt} and increases linearly to 1 for $f_{melt} = 1$.
<code>m_w</code>	Complex refractive index of water
<code>m_i</code>	Complex refractive index of ice
<code>lambda</code>	Radar wavelength in m
<code>mixingrulestring,</code> <code>matrixstring, inclusionstring,</code> <code>hoststring, hostmatrixstring,</code> <code>hostinclusionstring</code>	see subroutine <code>get_m_mix_nested()</code> , subsubsection 5.2.5.

Output parameters:

<code>C_back</code>	Backscattering cross section σ_b in m^2
---------------------	---

Example:

```
CALL MIE_SOAK_WETGR(2.3e-3, a_geo, b_geo, &
    0.45, 0.7, m_w, m_i, 0.055, C_back, &
    'maxwellgarnett', 'water', 'spheroidal', &
    'air', 'icewater', 'spheroidal')
```

Example sensitivity studies:

The dependence of σ_b on the degree of melting and on particle size for a specific temperature of $T = 5^\circ\text{C}$ is studied in detail in subsequent sections for the 4 different inverse mass-size-relations given in Subsection 7.1. These are:

- for inverse mass-size-relation (36) in Subsection 8.13 on Page 102,
- for inverse mass-size-relation (37) in Subsection 8.14 on Page 103,
- for inverse mass-size-relation (38) in Subsection 8.15 on Page 104,
- for inverse mass-size-relation (39) in Subsection 8.16 on Page 105.

5.3.12 SUBROUTINE RAYLEIGH_SOAK_WETGR

```
(x_g,a_geo,b_geo,fmelt,meltratio_outside,m_w,m_i,lambda,C_back,
mixingrulestring, matrixstring, inclusionstring, hoststring,
hostmatrixstring, hostinclusionstring)
```

```
INTEGER, PARAMETER          :: kinddp = KIND(1.0d0)
DOUBLE PRECISION, INTENT(in) :: x_g, lambda, a_geo, b_geo, fmelt
DOUBLE PRECISION, INTENT(in) :: meltratio_outside
COMPLEX(kind=kinddp), INTENT(in) :: m_w, m_i
CHARACTER(len=*), INTENT(in)  :: mixingrulestring
CHARACTER(len=*), INTENT(in)  :: matrixstring
CHARACTER(len=*), INTENT(in)  :: inclusionstring
CHARACTER(len=*), INTENT(in)  :: hoststring
CHARACTER(len=*), INTENT(in)  :: hostmatrixstring
CHARACTER(len=*), INTENT(in)  :: hostinclusionstring
DOUBLE PRECISION, INTENT(out)  :: C_back
```

Description:

Backscatter cross section σ_b according to Rayleigh approximation of a melting graupel/snow particle, assumed as a **sphere composed of a homogeneous ice-water-air mixture material**. This subroutine uses the same principles to determine the effective refractive index of the melting particle as MIE_SOAK_WETGR() except that the backscattering cross section is calculated applying Rayleigh approximation instead of Mie-scattering. See subroutine MIE_SOAK_WETGR() in subsubsection 5.3.11 for further details.

Input- and output parameters the same as in subsubsection 5.3.11 on Page 48!

Example:

```
CALL MIE_SOAK_WETGR(2.3e-3, a_geo, b_geo, &
    0.45, 0.7, m_w, m_i, 0.055, C_back, &
    'maxwellgarnett', 'water', 'spheroidal', &
    'air', 'icewater', 'spheroidal')
```

Example sensitivity studies:

The dependence of σ_b on the degree of melting and on particle size for a specific temperature of $T = 5^\circ\text{C}$ is studied in detail in subsequent sections for the 4 different inverse mass-size-relations given in Subsection 7.1. These are:

- for inverse mass-size-relation (36) in Subsection 8.1 on Page 74,
- for inverse mass-size-relation (37) in Subsection 8.2 on Page 77,
- for inverse mass-size-relation (38) in Subsection 8.3 on Page 80,
- for inverse mass-size-relation (39) in Subsection 8.4 on Page 82.

5.3.13 SUBROUTINE MIE_WETSNOW_TWOSPH

```
(x_s,a_geo,b_geo,fmelt,meltingratio_outside,m_w,m_i,lambda,radienverh,C_back,
mixingrulestring_shell, matrixstring_shell, inclusionstring_shell,
mixingrulestring_core, matrixstring_core, inclusionstring_core,
hoststring_shell, hostmatrixstring_shell, hostinclusionstring_shell,
hoststring_core, hostmatrixstring_core, hostinclusionstring_core)
```

```
INTEGER, PARAMETER :: kinddp = KIND(1.0d0)
DOUBLE PRECISION, INTENT(in) :: x_g, lambda, a_geo, b_geo, fmelt
DOUBLE PRECISION, INTENT(in) :: meltingratio_outside
DOUBLE PRECISION, INTENT(in) :: radienverh
COMPLEX(kind=kinddp), INTENT(in) :: m_w, m_i
CHARACTER(len=*), INTENT(in) :: mixingrulestring_shell
CHARACTER(len=*), INTENT(in) :: matrixstring_shell
CHARACTER(len=*), INTENT(in) :: inclusionstring_shell
CHARACTER(len=*), INTENT(in) :: hoststring_shell
CHARACTER(len=*), INTENT(in) :: hostmatrixstring_shell
CHARACTER(len=*), INTENT(in) :: hostinclusionstring_shell
CHARACTER(len=*), INTENT(in) :: mixingrulestring_core
CHARACTER(len=*), INTENT(in) :: matrixstring_core
CHARACTER(len=*), INTENT(in) :: inclusionstring_core
CHARACTER(len=*), INTENT(in) :: hoststring_core
CHARACTER(len=*), INTENT(in) :: hostmatrixstring_core
CHARACTER(len=*), INTENT(in) :: hostinclusionstring_core
DOUBLE PRECISION, INTENT(out) :: C_back
```

Description:

Backscatter cross section σ_b (Mie-scattering, two-layered sphere) of a melting soaked graupel/snow particle, assumed as a **spherical core of a homogeneous ice-water-air mixture material and a shell of a similar ice-water-air mixture material but with lower bulk density**.

This subroutine uses the same principles to determine the effective refractive index of the melting particle as `MIE_SOAK_WETGR()`, applied to core and shell. A further input parameter is the ratio between the outer and inner sphere radii, `radienverh`. The initial masses of the unmelted core and shell are derived from the inverse mass-size-relation (40) with coefficients a_{geo} and b_{geo} assuming spherical shape, in a similar way as in subroutine `MIE_DRYSNOW_TWOSPH()`, subsection 5.3.5. See subroutine `MIE_SOAK_WETGR()` in subsection 5.3.11 for further details. Note that the input parameter `melratio_outside` from `MIE_SOAK_WETGR()` is termed `meltingratio_outside` here.

To calculate the backscattering coefficient of the two-layered spherical particle, the formulae of Bohren and Huffman (1983) are applied (subroutine `COATEDSPHERE_SCATTER_BH()`), see Subsection 4.4.

Input parameters:

<code>kinddp</code>	kind parameter for double precision
<code>x_s</code>	Mass of particle in kg (without air fraction)
<code>a_geo</code>	Coefficient a_{geo} of the inverse mass-size-relation (40)

<code>b_geo</code>	Coefficient b_{geo} of the inverse mass-size-relation (40)
<code>fmelt</code>	Degree of melting, $f_{melt} = x_w/x_s$ (x_w = mass of water contained in the particle). Same value for core and shell.
<code>meltingratio_outside</code>	Subpart ratio of the meltwater mass x_w which melts on the outside of the particle when melting starts ($f_{melt} = 0$). Value between 0 and 1. The complementary subpart of x_w is assumed to melt within the ice structure. The actual value depends on f_{melt} and increases linearly to 1 for $f_{melt} = 1$. Same value for core and shell.
<code>radienverh</code>	Ratio of the inner to the outer sphere radius
<code>m_w</code>	Complex refractive index of water
<code>m_i</code>	Complex refractive index of ice
<code>lambda</code>	Radar wavelength in m
<code>mixingrulestring_shell,</code> <code>matrixstring_shell,</code> <code>inclusionstring_shell,</code> <code>hoststring_shell,</code> <code>hostmatrixstring_shell,</code> <code>hostinclusionstring_shell</code>	Parameters determining the effective refractive index of the shell ice-water-air mixture material, see subroutine <code>get_m_mix_nested()</code> , subsection 5.2.5.
<code>mixingrulestring_core,</code> <code>matrixstring_core,</code> <code>inclusionstring_core,</code> <code>hoststring_core,</code> <code>hostmatrixstring_core,</code> <code>hostinclusionstring_core</code>	Parameters determining the effective refractive index of the core ice-water-air mixture material, see subroutine <code>get_m_mix_nested()</code> , subsection 5.2.5.

Output parameters:

<code>C_back</code>	Backscattering cross section σ_b in m^2
---------------------	---

Example:

```
CALL MIE_WETSNOW_TWOSPH(2.3e-3, a_geo, b_geo, &
    0.45, 0.7, m_w, m_i, 0.055, 0.5, C_back, &
    'maxwellgarnett', 'water', 'spheroidal', &
    'maxwellgarnett', 'ice', 'spheroidal', &
    'air', 'icewater', 'spheroidal', &
    'water', 'water', 'spheroidal')
```

Example sensitivity studies:

The dependence of σ_b on the degree of melting and on particle size for a specific temperature of $T = 5^\circ\text{C}$ is studied in detail in subsequent sections for the 2 different inverse mass-size-relations for snow given in Subsection 7.1. These are:

- for inverse mass-size-relation (38) in Subsection 8.19 on Page 108,
- for inverse mass-size-relation (39) in Subsection 8.20 on Page 138.

6 `radar_mie_lm`: Interface functions for the LM

As previously mentioned, the library `radar_mie_lm` provides interface routines for the LM to calculate Z_e as a sum of Integrals of the form equation (1) (Page 7) over the different hydrometeor types which are implemented into the LM microphysical schemes (cloud droplets, rain, cloud ice, snow, graupel and, depending on the scheme, hail). These interface functions call the subroutines for the basic particle properties m_{eff} and σ_b , which are provided by `radar_mielib` and were previously described in Section 5. For the particle size distributions, generalized gamma distributions are assumed for all hydrometeor types, which is consistent with the assumption in the bulk microphysical schemes of the LM. The parameters of these size distributions are derived from model variables (mass density, and in case of two-moment scheme, number density) consistent to the assumptions drawn for the applied microphysical scheme. Note that the exponential and gamma size distribution are a special case of the generalized gamma distribution.

For Mie-scattering as well as for Rayleigh approximation with general EMA approximation, the integration of Z_e is done over a finite size interval $[D_{min}; D_{max}]$ being prescribed in a reasonable way within the interface routines and being generally different for each hydrometeor category. There are also two much more efficient approaches implemented in `radar_mielib` utilizing Rayleigh approximation together with Oguchi's EMA approximation, which enables analytical solutions of the reflectivity integral (see Subsection 6.2).

The degree of melting f_{melt} (melted mass fraction) of the single particles is estimated as a function of size and ambient temperature by a parameterization which will be presented in Subsection 6.1. Two important parameters of this parameterization, T_{min} and $f_{meltbegin}$ (see Subsection 6.1), are also specified in the interface routines in a reasonable way, but can certainly be changed by the user. Note that the estimated degree of melting can only be regarded as a very simplified and uncertain approximation since important information is not available for a more thorough description, e.g., the temperature and riming rate along the particle backward trajectories (the "melting history"). See Subsection 6.1 for a more detailed description.

The user can choose by appropriate settings of certain namelist parameters (described in Subsection 6.3), if full Mie-scattering or Rayleigh approximation with one of 3 different levels of simplification for m_{eff} of snow, graupel and hail is applied (see also Subsection 6.5 for an example of the relevant namelist parameters added to namelist `GRIBOUT`). These different levels of simplification can lead to largely different results for Z_e in case of melting hydrometeors, whereas in case of dry ice particles no significant differences are observed. The physical reason for this behaviour is that ice is only a weak dielectric whereas water is a strong dielectric (permanently polar molecules) so that the choice of a certain EMA-formulation becomes important primarily in the presence of water within a mixture particle.

6.1 An approximation for the degree of melting applicable for bulk microphysical schemes

This section describes a simple parameterization of the degree of melting f_{melt} (melted mass fraction) of hydrometeors, which can be used with bulk microphysical models which in turn do not explicitly predict the degree of melting. First of all, let us recall the definition of f_{melt} ,

$$f_{melt} = \frac{x_w}{x_{i,0}} \quad , \quad (24)$$

where x_w is the mass of meltwater and $x_{i,0}$ is the unmelted mass of the particle, only counting the ice fraction, not the enclosed air. Values for f_{melt} are in the range of $[0, 1]$. 0 means unmelted and 1 means fully melted.

Generally, f_{melt} depends on the time a certain particle has spent in a certain environment (T , riming rate, rate of turbulent heat transfer towards the particle, determined by, e.g., Reynolds number and particle surface roughness, etc.). This means that for an accurate calculation, the exact trajectory of each single particle has to be known together with a detailed solution of the equation of heat exchange of particles with the environment, considering also the feedback on the environmental temperature. In a numerical weather prediction model, this can hardly be done.

Therefore, to construct a parameterization f_{melt} , some assumptions have to be made to simplify the problem. We draw the following assumptions:

- In the environment, T decreases with height and no intense vertical motions are present, so that particles found at a specific time and place originate from regions above, not below.
- Every hydrometeor category can be assigned its own parameterization of f_{melt} , following the same master function (see below), but with different parameters.
- Within each hydrometeor class, the rate of heat exchange with the environment is a function of particle size only.
- It follows from the previous assumptions, that the particles all begin to melt at a certain temperature level T_{min} , e.g., 0°C or slightly below,
- that f_{melt} only depends on the environmental temperature T and particle diameter D ,
- in particular that at a given temperature, f_{melt} is larger for smaller particles — we assume a simple dependence $f_{melt} \sim D^{-a}$ with $a > 0$.
- It is further assumed that below the height of a certain temperature level T_{max} , all particles are fully melted.

From these assumptions it follows that for a given environmental temperature there is a certain particle size D_{fm} at which the particles are just melted. Larger particles obey $f_{melt} < 1$. D_{fm} has to be 0 for $T = T_{min}$ and $D_{fm} \Rightarrow \infty$ for $T \Rightarrow T_{max}$. A simple *ansatz* for D_{fm} fulfilling these constraints is, for example, an inverse exponential formula with respect to temperature,

$$D_{fm}^a = D_{ref}^a \ln \left(\frac{T_{max} - T_{min}}{T_{max} - T} \right) \quad , \quad (25)$$

with $T_{min} \leq T < T_{max}$. The exponent a has been introduced here for later convenience. D_{ref} is a scaling parameter and has to be specified properly. D_{ref} represents the value of D_{fm} at a temperature $T = T_{1/e}$, where

$$T_{1/e} = T_{max} - \frac{1}{e} (T_{max} - T_{min}) \quad , \quad (26)$$

the e-folding value of T within the interval $[T_{min}, T_{max}]$.

Now, requiring that $f_{melt}(D_{fm}) = 1$ and $f_{melt} \sim D^{-a}$ immediately leads to

$$f_{melt} = \left(\frac{D_{fm}}{D} \right)^a = \left(\frac{D_{ref}}{D} \right)^a \ln \left(\frac{T_{max} - T_{min}}{T_{max} - T} \right) = \text{fct}(D, T) \quad (27)$$

again for $T_{min} \leq T < T_{max}$. This function has to be limited to the codomain $f_{melt} \in [0, 1]$ and extended to arbitrary temperatures by the constraints $f_{melt}(D_{fm}) = 0$ for $T < T_{min}$ and $f_{melt}(D_{fm}) = 0$ for $T < T_{max}$, which finally leads to the formulation

$$f_{melt}^* = \begin{cases} 0 & , T < T_{min} \\ \left(\frac{D_{ref}}{D}\right)^a \ln\left(\frac{T_{max} - T_{min}}{T_{max} - T}\right) & , T_{min} \leq T < T_{max} \\ 1 & , T \geq T_{max} \end{cases}$$

$$f_{melt} = \min[\max[f_{melt}^*, 0], 1] \quad . \quad (28)$$

This formulation is intended to describe f_{melt} in a temperature regime in which the sensible heat flux from the environment to the particle is an important mechanism in enhancing the temperature of the particle. The parameter T_{min} denotes the temperature where this melting process starts. In that regime, the abovementioned assumptions leading to formula (27) may be more or less reasonable.

However, it may be desirable to also include the effects of melting at lower temperatures $T < T_{min}$ caused by high riming rates and too small a transfer of latent heat of freezing away from the particle, as it is sometimes observed for, e.g., high density graupel particles. This effect may be active for large particles in the temperature range of $-10 < T < 0^\circ\text{C}$. To this end, a simple extension to formula (27) is proposed, based on the (maybe contradictory) assumption that the effect on f_{melt} does not depend on particle size. Without a more sound theoretical basis, we would not dare to go any further than a linear dependence on size or a stepfunction, and we limit ourselves to the even simpler constance assumption above. Concerning the temperature dependence at fixed size, a linear *ansatz* is used.

Introducing the two new parameters T_{mb} and f_{tmin} (T_{mb} = Temperature, at which riming induced melting starts, f_{tmin} = degree of melting reached at T_{min}), the following extended formula

$$f_{melt}^* = \begin{cases} 0 & , T < T_{mb} \\ \frac{f_{tmin}}{T_{min} - T_{mb}} (T - T_{mb}) & , T_{mb} \leq T < T_{min} \\ (1 - f_{tmin}) \left(\frac{D_{ref}}{D}\right)^a \ln\left(\frac{T_{max} - T_{min}}{T_{max} - T}\right) + f_{tmin} & , T_{min} \leq T < T_{max} \\ 1 & , T \geq T_{max} \end{cases}$$

$$f_{melt} = \min[\max[f_{melt}^*, 0], 1] \quad (29)$$

is implemented into `radar_mie_lm`.

Formula (29) is used if $T_{mb} < T_{min}$ whereas the extension is switched off choosing $T_{mb} \geq T_{min}$, which leads to application of formula (28).

Figure 9 shows f_{melt} as function of T and D after formula (29) for an exemplaric parameter set of T_{mb} , T_{min} , T_{max} , f_{tmin} and D_{ref} , suitable for high density graupel or hail particles. It can be seen that a distinct transition between the riming- and environmental temperature-induced melting processes can be modeled by appropriate parameter settings of the parameterization (29).

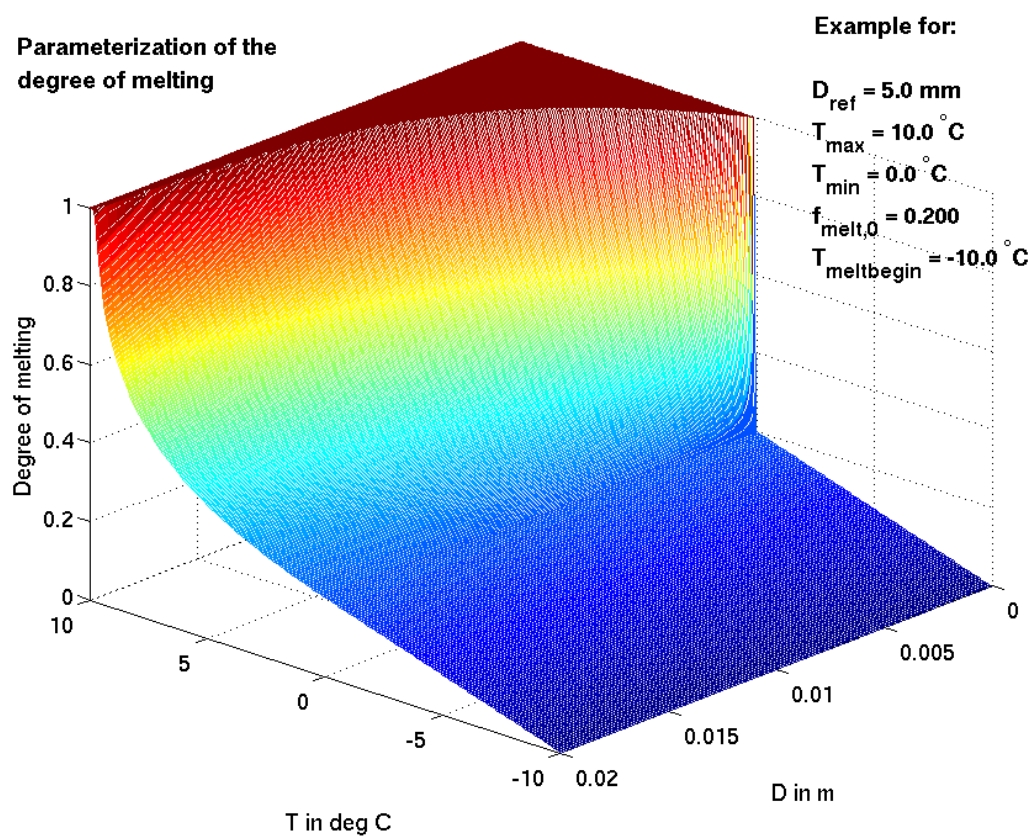


Figure 9: Parameterization function for the degree of melting f_{melt} as function of temperature in $^{\circ}\text{C}$ and particle diameter in mm for an exemplaric parameter set of formula (29), applicable to graupel or hail particles, see annotations. The exponent parameter a is 1.0.

The implementation into `radar_mie_lm` is as follows: for graupel- and hail particles, the parameters T_{mb} and f_{tmin} are set equal to the values annotated in Figure 9 by default. T_{min} is set to 0°C for all species. D_{ref} is chosen as $\min[6 \text{ mm}, \overline{D}(\bar{x})]$, with $\overline{D}(\bar{x})$ being the mean mass spherical equivalent diameter of the particle spectrum. For snow- and cloud ice particles, the riming-induced melting is switched off by choosing $T_{mb} > T_{min}$ by default, and D_{ref} is the same as for graupel and hail. Based on explicit simulations of melting particles carried out with a spectral bin microphysical model (Hebrew University Cloud Model HUCM), the exponent a is chosen as 0.5 for snow and cloud ice, 0.6 for graupel and 0.8 for hail particles.

To give the user some more control over the riming-induced melting degree parameterization at $T < 0^\circ\text{C}$, the parameters T_{mb} and f_{tmin} are available as namelist parameters for the snow-, graupel- and hail categories.

So far the parameter T_{max} remains to be discussed. This parameter denotes the temperature above which even the largest particles are assumed to be fully melted. From physical arguments it would seem reasonable to specify a fixed value (e.g., 10°C). However, there might be situations, e.g., strong convective downdrafts, in which the particles may "survive" longer. To account for this, a dynamic approach is chosen to make use of the information about the melting process and T_{max} which is provided by the melting parameterization of the cloud microphysical scheme itself: If there are particles of the specific type are present at locations with T exceeding the above fixed value, T_{max} is dynamically adjusted to the temperature of the lowest model height level where these melting hydrometeors are present. The fixed minimum value is presently chosen as 5°C for snow and cloud ice, 10°C for graupel and 20°C for hail. This is done every timestep at every horizontal gridpoint. This "precipitation-column"-approach should be reasonable in case of coarse numerical horizontal grid resolution and/or low windspeed. To prevent problems in case of high grid resolution and high windspeed, T_{max} is further set to its maximum value within a "search area" of $10 \times 10 \text{ km}^2$ centered around each gridpoint, providing a certain degree of smoothing.

The following subroutines in `radar_mie_lm` are connected to the f_{melt} -parameterization:

- `degree_of_melting_fun()`:
master function (29), input parameters are D , T_{mb} , T_{min} , T_{max} , f_{tmin} and D_{ref} . Output parameter is f_{melt} .
- `initialize_tmax()`:
Determination of T_{max} , separately for every hydrometeor category.
- Subroutines which itself call `degree_of_melting_fun()` with suitable input parameter sets for each hydrometeor type:
 - `degree_of_melting_ice()`, `degree_of_melting_ice_sb()`
 - `degree_of_melting_snow()`, `degree_of_snow_hail_sb()`
 - `degree_of_melting_graupel()`, `degree_of_graupel_hail_sb()`
 - `degree_of_melting_hail()`, `degree_of_melting_hail_sb()`

The results of the reflectivity calculations using the presented parameterization for f_{melt} look qualitatively promising for stratiform precipitation (radar "bright band"), but there will almost certainly be problems in case of deep convective events. It has to be mentioned, too, that up to now no attempt to verify or calibrate the formula (29) and its parameters has been undertaken aside the abovementioned tests using the HUCM bin microphysical model. Therefore, the above parameterization remains speculative to some degree. However, since almost no suitable measurements of the degree of melting in clouds are existing, the verification/calibration would have to rely on further simulations with HUCM or on a suitable detailed Lagrangian melting model. But even such a Lagrangian model would require

certain assumptions on the vertical and horizontal structure of precipitation and horizontal and vertical windspeed and therefore it is unclear whether the results of such a verification/calibration approach would be applicable in general.

6.2 An efficient Rayleigh-Approximation for melting hydrometeors with Oguchis refractive index formulation

There is a nice closed analytical solution for Z_e in Rayleigh approximation if a generalized gamma distribution is assumed for the particle mass distribution and Oguchis EMA formula for m_{eff} with shape factor $u = 2$ (equation (16) on Page 15) is applied. A further precondition is that the same degree of melting is assumed for all particles, regardless of their size. However, this EMA approximation is not valid in case of a mixture of strong and/or strongly differing dielectric materials, as is the case with melting hydrometeors.

Nevertheless, this approach is implemented into `radar_mie_lm` because of its computational efficiency. It has to be remembered that it can be safely applied for rain and for dry ice particles but may lead to much too small reflectivity values for melting hydrometeors.

Now, recalling that the dielectric factor K in the Rayleigh approximation equals $(\epsilon - 1)/(\epsilon + 2)$, Oguchis formula (16) with $u = 2$ for the effective refractive index of an ice-water-air mixture reads

$$\begin{aligned} \frac{\epsilon_{eff} - 1}{\epsilon_{eff} + 2} &= \frac{\epsilon_i - 1}{\epsilon_i + 2} p_i + \frac{\epsilon_w - 1}{\epsilon_w + 2} p_w + \frac{\epsilon_a - 1}{\epsilon_a + 2} p_a \\ K_{eff} &= K_i p_i + K_w p_w + K_a p_a \quad , \end{aligned} \quad (30)$$

where indices i, w, a and s denote ice, air, water and the mixture particle, and p_i, p_w, p_a are the respective volume fractions. Since

$$p_x = \frac{V_x}{V} = \frac{m_x}{\rho_x V} \quad x \in i, w, a \quad , \quad (31)$$

where V_x is partial volume of material x , V is total particle volume, m_x is partial mass of material x and ρ_x is the material's density, equation (30) can be rewritten to

$$K_{eff} = \frac{1}{V} \left(K_i \frac{m_i}{\rho_i} + K_w \frac{m_w}{\rho_w} + K_a \frac{m_a}{\rho_a} \right) \quad . \quad (32)$$

To a very good approximation, $K_a = 0$, and using the definition of partial densities $\rho_{p,s} = m_s/V$ and $\rho_{p,w} = m_w/V$,

$$K_{eff} = K_i \frac{\rho_{p,s}}{\rho_i} + K_w \frac{\rho_{p,w}}{\rho_w} \quad . \quad (33)$$

K_x are complex numbers, $K_x = K_{x,r} + i K_{x,i}$, so the square of the modulus of K_{eff} is

$$|K_{eff}|^2 = |K_i|^2 \left(\frac{\rho_{p,s}}{\rho_i} \right)^2 + |K_w|^2 \left(\frac{\rho_{p,w}}{\rho_w} \right)^2 + 2 \frac{\rho_{p,s} \rho_{p,w}}{\rho_i \rho_w} (K_{i,r} K_{w,r} + K_{i,i} K_{w,i}) \quad . \quad (34)$$

Defining $x = m_i + m_w$ as mass of a melting particle without its air contribution and f_{melt} as its degree of melting, so that $m_i = (1 - f_{melt})x$ and $m_w = f_{melt}x$, the Rayleigh reflectivity (equation (5)) for a population of melting particles is

$$\begin{aligned}
Z_e &= \frac{1}{|K_{w,0}|^2} \int_0^\infty |K_{eff}|^2 D^6 N(D) dD \\
&= \frac{1}{|K_{w,0}|^2} \int_0^\infty |K_{eff}|^2 D(x)^6 N(x) dx \\
&= \frac{1}{|K_{w,0}|^2} \left[\frac{|K_i|^2}{\rho_i^2} \int_0^\infty \left(\frac{6V}{\pi} \right)^2 \frac{m_i^2}{V^2} N(x) dx + \right. \\
&\quad \left. \frac{|K_w|^2}{\rho_w^2} \int_0^\infty \left(\frac{6V}{\pi} \right)^2 \frac{m_w^2}{V^2} N(x) dx + 2 \frac{K_{i,r}K_{w,r} + K_{i,i}K_{w,i}}{\rho_i\rho_w} \int_0^\infty \left(\frac{6V}{\pi} \right)^2 \frac{m_i m_w}{V^2} N(x) dx \right] \\
&= \frac{6^2}{\pi^2 |K_{w,0}|^2} \left[\frac{|K_i|^2}{\rho_i^2} \int_0^\infty (1 - f_{melt})^2 x^2 N(x) dx + \right. \\
&\quad \left. \frac{|K_w|^2}{\rho_w^2} \int_0^\infty f_{melt}^2 x^2 N(x) dx + 2 \frac{K_{i,r}K_{w,r} + K_{i,i}K_{w,i}}{\rho_i\rho_w} \int_0^\infty f_{melt} (1 - f_{melt}) x^2 N(x) dx \right] \\
&= \frac{6^2}{\pi^2 |K_{w,0}|^2} \left[\frac{|K_i|^2}{\rho_i^2} (1 - f_{melt})^2 + \frac{|K_w|^2}{\rho_w^2} f_{melt}^2 + 2 \frac{K_{i,r}K_{w,r} + K_{i,i}K_{w,i}}{\rho_i\rho_w} f_{melt} (1 - f_{melt}) \right] M_2, \tag{35}
\end{aligned}$$

where M_2 denotes the second moment of the particle mass distribution function. The last equality in equation (35) is only valid if all particles obey the same degree of melting, independent of their size. equation (35) is especially attractive since it only involves the calculation of the second moment with respect to mass, which in most cases is far more efficient since, for certain types of distribution functions $N(x)$ (e.g., generalized gamma distribution), M_2 can be written in closed analytical form.

Note, however, that a systematical underestimation of Z_e might possibly occur, since it is assumed here (as in all other routines of `radar_mie_lm`) that the mass of meltwater is contained in the particle mass x and the second moment M_2 , which contrasts the treatment of melting in most microphysical schemes, where the meltwater is (partially or completely) shedded to rainwater.

6.3 Controlling reflectivity calculations in LM — relevant namelist parameters and their setting

To enable output of radar reflectivity in LM, the user simply has to specify the output variable 'dBZ' within the list of output variables in the `GRIBOUT`-namelist. 'dBZ' is implemented for model level output as well as for pressure-level- or height-level interpolation. In case of interpolated output, the reflectivity is calculated first on model levels and subsequently interpolated to output pressure/height levels. In standard LM, the interpolation is done by cubic tension splines. However, reflectivity is a positive definite quantity and can vary over several orders of magnitude between adjacent grid points. In this case, cubic splines can lead to serious undershoots producing negative values. We therefore changed the interpolation in

our LM version to simple linear interpolation, but unfortunately this is not available in the operational LM version.

Once reflectivity output is chosen, the basic namelist parameter to control the kind of reflectivity calculation is

- `dbz%itype_refl`, namelist GRIBOUT (INTEGER: 1, 2, 3, or 4).

The radarwavelength can be specified by

- `dbz%lambda_radar`, namelist GRIBOUT (REAL).

To choose the parameters of the parameterization for the degree of melting in Subsection 6.1, which influence the riming-induced melting for $T < 0^\circ\text{C}$ (namelist GRIBOUT, REAL):

- `dbz%Tmeltbegin_s` (T_{mb} for snow)
- `dbz%meltddegTmin_s` (f_{tmin} for snow)
- `dbz%Tmeltbegin_g` (T_{mb} for graupel)
- `dbz%meltddegTmin_g` (f_{tmin} for graupel)
- `dbz%Tmeltbegin_h` (T_{mb} for hail; only for `itype_gscp` ≥ 2000)
- `dbz%meltddegTmin_h` (f_{tmin} for hail; only for `itype_gscp` ≥ 2000)

To further choose different EMA approximations of m_{eff} for different hydrometeor types, the following namelist parameters apply (namelist GRIBOUT, CHARACTER(len=12)):

- `dbz%ctype_drysnow_mie`
- `dbz%ctype_wetsnow_mie`
- `dbz%ctype_drygraupel_mie`
- `dbz%ctype_wetgraupel_mie`
- `dbz%ctype_dryhail_mie` (only for `itype_gscp` ≥ 2000)
- `dbz%ctype_wethail_mie` (only for `itype_gscp` ≥ 2000)
- `dbz%ctype_drysnow_ray`
- `dbz%ctype_wetsnow_ray`
- `dbz%ctype_drygraupel_ray`
- `dbz%ctype_wetgraupel_ray`
- `dbz%ctype_dryhail_ray` (only for `itype_gscp` ≥ 2000)
- `dbz%ctype_wethail_ray` (only for `itype_gscp` ≥ 2000)

Their setting depends in turn on `dbz%itype_refl`. The listing below and the subsequently linked tables show the different possible combinations of these parameters and the corresponding `radar_mielib` functions which are used to calculate radar reflectivity.

Further, in case of graupel particles and application of Mie-scattering (`dbz%itype_refl=1`), the namelist parameter `dbz%igraupel_type` (=1, 2, or 3) provides three possibilities for the melting model of graupel, see the listing below.

In case of melting hydrometeors, the degree of melting is derived from the parameterization described in Subsection 6.1 before calculating reflectivity according to the following listing.

The following listing shows combinations of the namelist parameter `dbz%itype_refl` with the other namelist parameters mentioned previously in this section. The links in the right column lead to the description of the corresponding `radar_mielib` subroutine and to subsequent tables which describe in detail the possible settings of the corresponding namelist parameter for the EMA approximation:

- `dbz%itype_refl = 1:`

Mie scattering, general EMA approximation

- **Cloud drops:**

Rayleigh approximation, analytical solution of (5)

- **Cloud ice:**

dry / melting: Rayleigh approximation (35) with EMA after Oguchi

- **Rain:**

Mie scattering, numerical solution using (3): `SPHERE_SCATTER_BH()`

- **Snow:**

dry ($T \leq 0^\circ\text{C}$):

`MIE_DRYSNOW_TWOSPH()` — `dbz%ctype_drysnow`: 6-character code, composed of two 3-character codes after Table 38 for core and shell, resp.

melting ($T > 0^\circ\text{C}$):

`MIE_WETSNOW_TWOSPH()` — `dbz%ctype_wetsnow`: 12-character code, composed of two 6-character codes after Table 40 for core and shell, resp.

`meltingratio_outside = 0.7`

`radienverh = 0.5`

- **Graupel:**

dry ($T \leq -10^\circ\text{C}$):

`MIE_DRY_GRAUPEL()` — `dbz%ctype_drygraupel`

melting ($T > -10^\circ\text{C}$):

depends on namelist parameter `dbz%igraupel_type`:

- `dbz%igraupel_type = 1:`

`MIE_SOAK_WETGR()` — `dbz%ctype_wetgraupel`

`melratio_outside = 0.7`

- `dbz%igraupel_type = 2:`

`MIE_SOAK_TWOSPH_WETGR()` — `dbz%ctype_wetgraupel`

- `dbz%igraupel_type = 3:`

`MIE_WATERSPH_WETGR()` — `dbz%ctype_wetgraupel`

- **Hail:**

dry ($T > 0^\circ\text{C}$): `MIE_DRY_GRAUPEL()` — `dbz%ctype_dryhail`

melting ($T \leq 0^\circ\text{C}$): `MIE_SPONGY_WETHAIL()` — `dbz%ctype_wethail_ray`

`fwater = 0.5`

- `dbz%itype_refl = 2:`

Rayleigh approximation with general EMA approximation

- **Cloud drops:**

Rayleigh approximation, analytical solution of (5)

- **Cloud ice:**
dry / melting: Rayleigh approximation with EMA after Oguchi
- **Rain:**
Rayleigh approximation, analytical solution of (5)

- **Snow:**
dry ($T > 0^{\circ}\text{C}$):
`RAYLEIGH_DRY_GRAUPEL()` — `dbz%ctype_drysnow_ray`
melting ($T \leq 0^{\circ}\text{C}$):
`RAYLEIGH_SOAK_WETGR()` — `dbz%ctype_wetsnow_ray`

- **Graupel:**
dry ($T \leq -10^{\circ}\text{C}$):
`RAYLEIGH_DRY_GRAUPEL()` — `dbz%ctype_drygraupel_ray`
melting ($T > -10^{\circ}\text{C}$):
`RAYLEIGH_SOAK_WETGR()` — `dbz%ctype_wetgraupel_ray`

- **Hail:**
dry ($T \leq 0^{\circ}\text{C}$):
`RAYLEIGH_DRY_GRAUPEL()` — `dbz%ctype_dryhail_ray`
melting ($T > 0^{\circ}\text{C}$):
`RAYLEIGH_SOAK_WETGR()` — `dbz%ctype_wethail_ray`

- `dbz%itype_refl = 3:`

Rayleigh approximation with EMA after Oguchi for cloud ice, snow, graupel and hail (analytical formula from Subsection 6.2), Rayleigh approximation (5) for cloud droplets and rain drops.

- `dbz%itype_refl = 4:`

Very simple and efficient Rayleigh approximation from `pp_utilities.f90` for all particles, crude description of melting particles

6.4 Tables of namelist parameter settings for the EMA choice

Table 38: 3-character Coding of the namelist-parameters `dbz%ctype_XXX` for two-component ice-air mixture materials and different EMA approximations, controlling the keywords of function `get_m_mix()`. Question marks denote wildcards for arbitrary characters.

mixingrulestring (1. character)	matrixstring (2. character)	inclusionstring (3. character)	ctype-Code
'bruggemann' -- 'b'	N/A	N/A	'b??'
'oguchi' -- 'o'	N/A	N/A	'o??'
'maxwellgarnett' -- 'm'	'ice' -- 'i'	'spherical' -- 'k'	'mik'
		'spheroidal' -- 's'	'mis'
	'air' -- 'a'	'spherical' -- 'k'	'mak'
		'spheroidal' -- 's'	'mas'

Table 39: Similar to Table 38: 3-character Coding of the namelist-parameters `dbz%ctype_XXX` for two-component ice-water mixture materials and different EMA approximations, controlling the keywords of function `get_m_mix()`. Question marks denote wildcards for arbitrary characters.

mixingrulestring (1. character)	matrixstring (2. character)	inclusionstring (3. character)	ctype-Code
'bruggemann' -- 'b'	N/A	N/A	'b??'
'oguchi' -- 'o'	N/A	N/A	'o??'
'maxwellgarnett' -- 'm'	'ice' -- 'i'	'spherical' -- 'k'	'mik'
		'spheroidal' -- 's'	'mis'
	'water' -- 'w'	'spherical' -- 'k'	'mwk'
		'spheroidal' -- 's'	'mws'

Table 40: 6-character Coding of the namelist-parameters `dbz%ctype_XXX` for three-component ice-water-air mixture materials and different EMA approximations, controlling the keywords of function `get_m_mix_nested()`. Question marks denote wildcards for arbitrary characters. Note that `inclusionstring` and `hostinclusionstring` are only displayed as representing spheroidal inclusions (i.e., character `'s'`), but both can also specify spherical inclusions by a character `'k'` instead, leading to 4 times more possibilities as laid out in the table below.

mixingrulestring (1. character)	hoststring (2. character)	matrixstring (3. character)	inclusionstring (4. character)	hostmatrixstring (5. character)	hostinclusionstring (6. character)	ctype-Code
'bruggemann' -- 'b'	N/A	N/A	N/A	N/A	N/A	'b????'
'oguchi' -- 'o'	N/A	N/A	N/A	N/A	N/A	'o????'
'maxwellgarnett' -- 'm'	'none' -- 'n'	'ice' -- 'i'	'spherical' -- 'k'	N/A	N/A	'mnik??'
		'water' -- 'w'	'spheroidal' -- 's'	N/A	N/A	'mnis??'
		'air' -- 'a'	'spherical' -- 'k'	N/A	N/A	'mnwk??'
			'spheroidal' -- 's'	N/A	N/A	'mnws??'
	'ice' -- 'i'	'air' -- 'a'	'spherical' -- 'k'	N/A	N/A	'mnak??'
			'spheroidal' -- 's'	N/A	N/A	'mnas??'
		'water' -- 'w'	'spherical' -- 's'	'ice' -- 'i'	'spheroidal' -- 's'	'miasis'
			'spheroidal' -- 's'	'airwater' -- 'r'	'spheroidal' -- 's'	'miasrs'
	'water' -- 'w'	'ice' -- 'i'	'spherical' -- 's'	'ice' -- 'i'	'spheroidal' -- 's'	'miwsis'
			'spheroidal' -- 's'	'airwater' -- 'r'	'spheroidal' -- 's'	'miwsrs'
		'ice' -- 'i'	'spherical' -- 's'	'water' -- 'w'	'spheroidal' -- 's'	'mwisws'
			'spheroidal' -- 's'	'airice' -- 's'	'spheroidal' -- 's'	'mwiwss'
	'air' -- 'a'	'water' -- 'w'	'spherical' -- 's'	'water' -- 'w'	'spheroidal' -- 's'	'mwassws'
			'spheroidal' -- 's'	'airice' -- 's'	'spheroidal' -- 's'	'mwasss'
		'ice' -- 'i'	'spherical' -- 's'	'air' -- 'a'	'spheroidal' -- 's'	'maisas'
			'spheroidal' -- 's'	'icewater' -- 'm'	'spheroidal' -- 's'	'maisms'
	'water' -- 'w'	'water' -- 'w'	'spherical' -- 's'	'air' -- 'a'	'spheroidal' -- 's'	'mawsas'
			'spheroidal' -- 's'	'icewater' -- 'm'	'spheroidal' -- 's'	'mawms'

Table 41: 6-character coding of the namelist-parameters `dbz%ctype_XXX` for a two-layered particle, composed of a two-component ice-air mixture core and a two-component ice-water shell, and for different EMA approximations, controlling the keywords of function `get_m_mix()`. Question marks denote wildcards for arbitrary characters. The code is a combination of two 3-character codes similar to Table 38 and Table 39. There are 36 possibilities altogether, namely all combinations of 3-character codes from part 1 (core material) and part 2 (shell material) of the table.

Part 1: 1.-3. character, ice-air mixture of particle core			
mixingrulestring (1. character)	matrixstring (2. character)	inclusionstring (3. character)	ctype-Code (1:3)
'bruggemann'	N/A	N/A	'b??'
'oguchi'	N/A	N/A	'o??'
'maxwellgarnett'	'ice'	'spherical'	'mik'
		'spheroidal'	'mis'
	'air'	'spherical'	'mak'
		'spheroidal'	'mas'
Part 2: 4.-6. character, ice-water mixture of particle shell			
mixingrulestring (4. character)	matrixstring (5. character)	inclusionstring (6. character)	ctype-Code (4:6)
'bruggemann'	N/A	N/A	'b??'
'oguchi'	N/A	N/A	'o??'
'maxwellgarnett'	'ice'	'spherical'	'mik'
		'spheroidal'	'mis'
	'water'	'spherical'	'mwk'
		'spheroidal'	'mws'

6.5 Additions to LM-runscripsts to enable reflectivity calculations

An example for the necessary additions to the namelist GRIBOUT to enable reflectivity calculation and output at each output timestep:

```

yvarml = ... , 'DBZ      ', ...
yvarzl = ... , 'DBZ      ', ...
yvarpl = ... , 'DBZ      ', ...

dbz%itype_refl = 1,

dbz%lambda_radar = 0.055,

dbz%Tmeltbegin_s  = 273.16,
dbz%meltdegTmin_s = 0.0,
dbz%Tmeltbegin_g  = 263.16,
dbz%meltdegTmin_g = 0.2,
dbz%Tmeltbegin_h  = 263.16,
dbz%meltdegTmin_h = 0.2,

! Settings for itype_refl=1
! (effektive refractive index for Mie-scattering):

dbz%ctype_drysnow_mie=   'masmas      ',
dbz%ctype_wetsnow_mie=   'mawsasmawsas',
dbz%ctype_drygraupel_mie= 'mis          ',

! Type of melting model for the Mie-calculations for
! partially melted graupel (1=soak, 2=twosphere, 3=watersphere):
! ( + corresponding ctype_wetgraupel_mie -- change accordingly!)

dbz%igraupel_type=1,
dbz%ctype_wetgraupel_mie= 'mawsms      ',

! Effective only for itype_gscp >= 2000:

dbz%ctype_dryhail_mie=   'mis          ',
dbz%ctype_wethail_mie=   'mws          ',

! Settings for itype_refl=2
! (effektive refractive index for Rayleigh-scattering):

dbz%ctype_drysnow_ray=   'mas          ',
dbz%ctype_wetsnow_ray=   'mawsas         ',
dbz%ctype_drygraupel_ray= 'mis          ',
dbz%ctype_wetgraupel_ray= 'mawsms         ',

! Nur bei itype_gscp >= 2000 wirksam:

dbz%ctype_dryhail_ray=   'mis          ',
dbz%ctype_wethail_ray=   'mawsms         ',

```

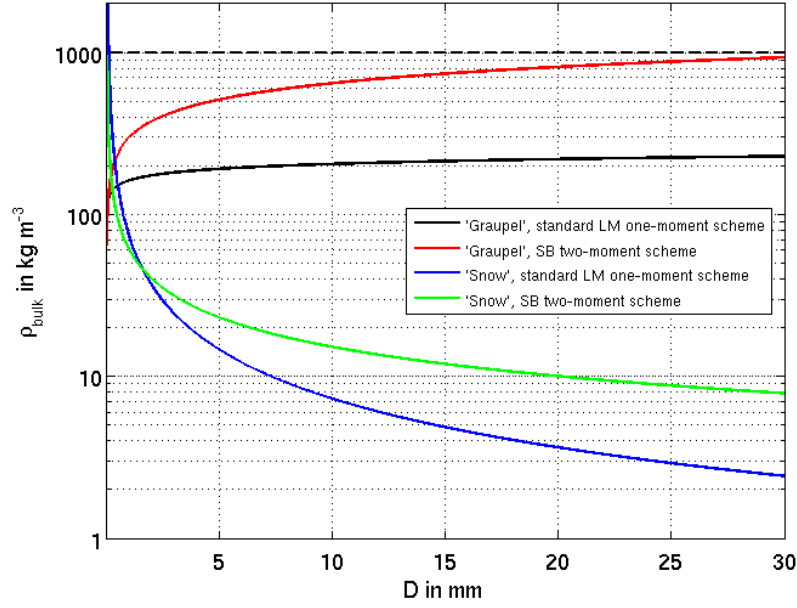



Figure 10: Bulk density of snow/graupel particles in kg m^{-3} as funktion of sphere equivalent diameter in mm, deduced from the 4 different inverse mass-size-relations presented in equations (36), (37), (38) and (39).

7 Backscattering cross sections of dry ice particles

We now turn to a more detailed investigation on the backscattering properties of single precipitation particles. In this section, the focus is on results for dry ice particles. In later sections, similar investigations will also be presented for melting ice particles.

For dry ice particles, basically two different particle models are available in `radar_mielib` if Mie-scattering is assumed. These are the one-layered ordinary sphere (suitable, e.g., for graupel and hail particles) and the two-layered sphere (e.g., for snow flakes). With Rayleigh scattering, only one-layered spheres are accounted for, since the Rayleigh approximation is an approximation to the Mie scattering functions for ordinary spheres.

In the following, the two different particle models are briefly described, together with a short examination of the differences in Z_e which they produce for the **C-Band radar wavelength** $\lambda_0 = 5.5 \text{ cm}$.

7.1 One-layered sphere

In this section, the differences in Z_e caused by the application of different EMAs in case of different particle bulk densities is examined at $\lambda_0 = 5.5 \text{ cm}$ (**C-Band**) to provide a qualitative guideline what to expect from what combination of these settings. The focus here is on dry ice particles which are assumed to be one-layered spheres of a homogeneous two-component mixture of ice and air. This particle model should be applicable to graupel and hail particles and in case of Rayleigh approximation, it has to be applied to all kinds of ice particles.

To this end, backscatter cross sections of graupel particles were calculated as a function of particle diameter by the `radar_mielib` subroutine `MIE_DRY_GRAUPEL()` (subsubsection 5.3.1) or, in case of Rayleigh approximation, by subroutine `RAYLEIGH_DRY_GRAUPEL()` (subsubsection 5.3.2). This was done for two different temperatures ($T = -10^\circ\text{C}$, $T = -20^\circ\text{C}$) and for

the mixing rules presented in subsubsection 4.5.4, applied to a two-component mixture. To show the dependence on particle bulk density (important to deduce the volume fractions of ice and air for the EMAs), this parameter is derived alternatively from the four inverse mass-size-relations

$$\frac{D}{D_0} = 0.19091 \left(\frac{x}{x_0} \right)^{0.32258} \quad (\text{"Graupel", standard LM one-moment scheme}) \quad (36)$$

$$\frac{D}{D_0} = 0.11 \left(\frac{x}{x_0} \right)^{0.3} \quad (\text{"Graupel", SB two-moment scheme}) \quad (37)$$

$$\frac{D}{D_0} = 5.12989 \left(\frac{x}{x_0} \right)^{0.5} \quad (\text{"Snow", standard LM one-moment scheme}) \quad (38)$$

$$\frac{D}{D_0} = 1.33398 \left(\frac{x}{x_0} \right)^{0.41667} \quad (\text{"Snow", SB two-moment scheme}) \quad , \quad (39)$$

assuming equivalent spherical particles. x is the particle mass (without the mass of the enclosed air), D its diameter and x_0 and D_0 are constant scaling parameters of 1 kg and 1 m, resp. The general form of the inverse mass-size-relation used throughout this document is

$$\frac{D}{D_0} = a_{geo} \left(\frac{x}{x_0} \right)^{b_{geo}} \quad , \quad (40)$$

with a_{geo} and b_{geo} beeing dimensionless constants.

equation (36) and (38) are taken from the operational one-moment bulk microphysical scheme of the LM, and equation (37) and (39) from the two-moment bulk microphysical scheme of Seifert and Beheng (2006). Figure 10 presents the resulting particle bulk densities as function of size and shows that, with these 4 different relations, nearly the whole range of possible bulk densities occuring in nature is covered.

For the refractive index of ice, the model of Mätzler (1998) (cf. Figure 6 on Page 13) is used in the following.

The results (Figure 11) show that there is no substantial difference at the two assumed temperatures. In addition, all applied mixing rules lead to nearly the same backscattering cross section for a given particle (the variation range of σ_b for different EMAs is less than 3 dB — a factor of two — which is not much). Considerable differences occur for larger particles when Rayleigh scattering is assumed instead of Mie scattering. Most important, the backscattering cross section shows a strong increase with particle bulk density, as shown by the four different used mass-size-relations.

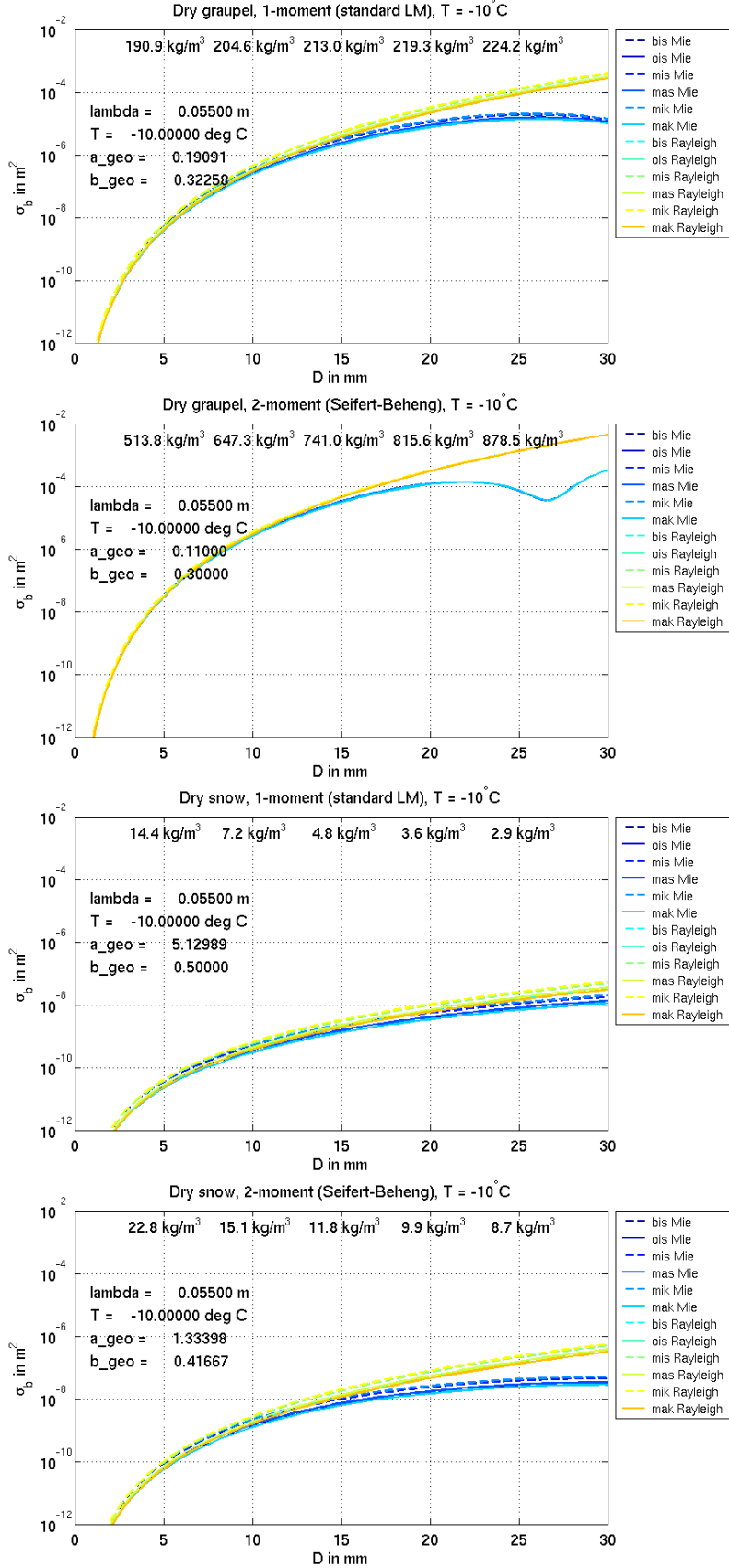


Figure 11: Backscattering cross section σ_b in m^2 as a function of particle diameter, EMA (see legend and explanation in Table 38 in combination with section 5.2.4) for $T = -10^\circ\text{C}$. **Panels from top to bottom:** Graupel with mass-size-relation (36) from the LM standard microphysics scheme, graupel from Seifert and Beheng two-moment scheme (equation (37)), snow from the LM standard scheme (equation (38)), snow from the two-moment scheme (equation (39)).

7.2 Two-layered sphere

Backscattering cross sections for a two-layered sphere (cf. Figure 1 on Page 10) were calculated by using the `radar_mielib` subroutine `MIE_DRYSNOW_TWOSPH()` (subsubsection 5.3.5). Here, an additional important parameter is the ratio between the inner sphere and outer sphere radii. This ratio has to be preset and is a fixed input parameter for subroutine `MIE_DRYSNOW_TWOSPH()`. Without loss of generality, a value of 0.5 is used throughout `radar_mie_lm`, but this can be changed by the user. As mentioned before, this model is applicable to snow particles, as shown by, e.g., Fabry and Szyrmer (1999).

A similar comparison as presented in the last Subsection 7.1 is repeated here for snow particles of two different mass-size-relations as a function of particle diameter, temperature and mixing rule. The inverse mass-size-relations were given earlier in equation (38) and (39) in Subsection 7.1.

For the refractive index of ice, again the model of Mätzler (1998) (cf. Figure 6 on Page 13) is used in the following.

A comment is necessary on the derivation of the particle bulk densities in the inner and outer spherical shells. Note that for snow flakes, it is observed that the bulk density usually decreases with size, reflected by the mass-size-relations found in literature. To explain this behaviour, Fabry and Szyrmer (1999) present an interesting *Gedankenexperiment*: Snow flakes preferably form by aggregation of smaller ice and snow particles. That's why they are called "aggregates" in technical terms. Consider now without loss of generality a population of equally sized snow flakes having equal bulk density. Through collision and sticking, larger flakes are formed. In the extreme case of flakes aggregating around a single "embryonal flake" in dense sphere packing, the resulting flake would be double in diameter with a nearly equal but slightly lower bulk density. In reality, this dense packing will almost never be fully realised and there will always be some voids causing the overall bulk density to be even lower. Generalization to an initial population of differently sized snow flakes, the outcome will always be a decreasing mean bulk density with snow flake diameter.

To model this, the bulk densities of the inner and outer shell of the two-layered spherical particles are calculated in the following way: Given a fixed mass-size-relation representing a decreasing bulk density with diameter, a certain snowflake diameter and an assumed ratio of inner to outer shell diameter (e.g., 0.5), at first the inner core is assigned the density found by applying the inner sphere diameter within the mass-size-relation. Then, given the total mass by applying the outer sphere diameter within the mass-size-relation, the mass of the outer spherical shell is just the difference of total mass minus mass of inner sphere. From this and the preset and fixed ratio of inner to outer sphere radius, the bulk density of the outer shell can be calculated.

From the bulk densities of core and shell, the corresponding volume fractions of ice and air are calculated further. To get m_{eff} of core and shell, the volume fractions are plugged into the different formulas for the EMA approximations presented earlier in this document. Table 38 gives the 6 possible different settings for an ice-air mixture material (cf. subsubsection 5.2.4). With this, backscattering coefficients are calculated as function of size and all implemented combinations of EMA approximations for core and shell ($6 \times 6 = 36$). This was done for both inverse mass-size relations mentioned earlier in this section. In all cases, the temperature was set to -10°C .

Figure 12 shows the results for both mass-size relations in a simplified way (upper panel: relation (38), lower panel: relation (39)). In each figure, the blue "strip" marks the envelope (variation range) of σ_b as function of size and EMA for the two-layered Mie calculation. For

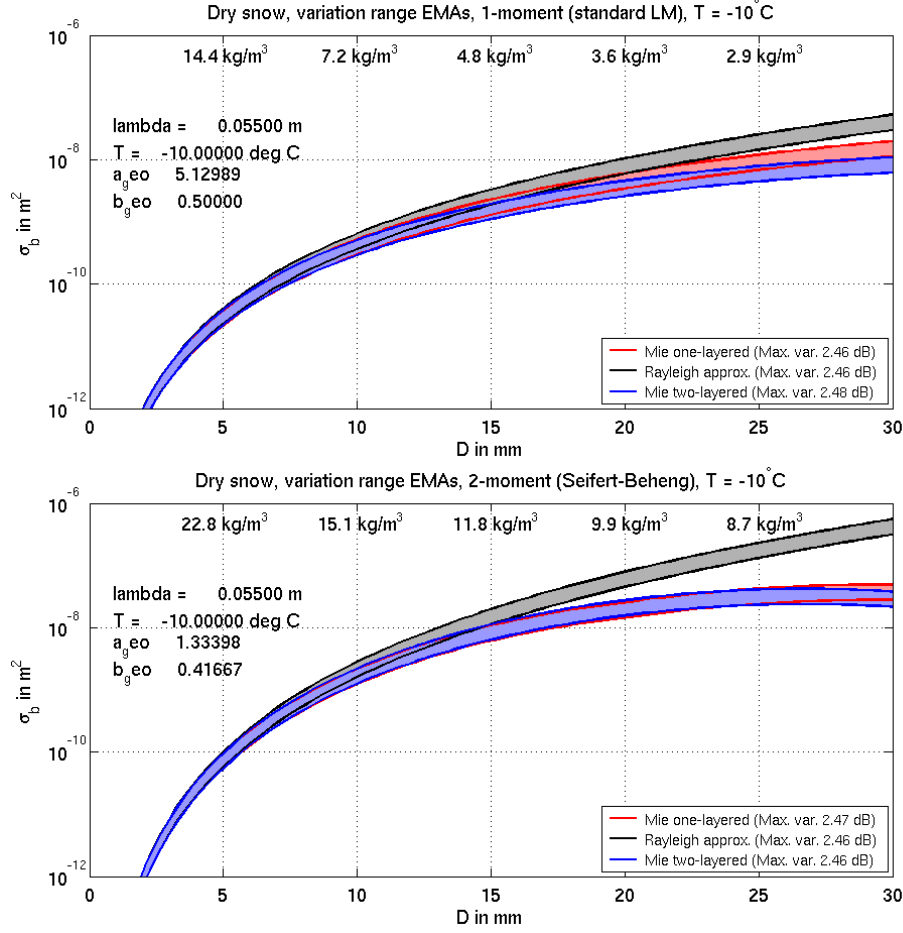


Figure 12: Variation range of Backscattering cross section σ_b for snow in m^2 as a function of particle diameter considering all possible combinations of the implemented EMAs for a two-layered sphere at $T = -10^\circ\text{C}$. See text for explanation. **Upper panel:** Snow with mass-size-relation (38) from the LM standard microphysics scheme, **lower panel:** snow from Seifert and Beheng two-moment scheme (equation (39)).

comparison, the red "strip" gives the corresponding results considering Mie scattering by simple spheres only (6 different EMA approximations), and further applying Rayleigh approximation leads to the grey "strip". It is found that imposing different EMA-approximations leads to only moderate variations of σ_b for a given size. This can be explained by the fact that ice is weak dielectric only and nearly every different choice of an EMA approximation leads to the nearly the same m_{eff} . Moreover, in case of $\lambda_0 = 5.5\text{ cm}$ as considered here, for particles with $D < 15\text{ mm}$ it does not make a large difference if choosing a two-sphere particle model or simple spheres, or if choosing an even simpler Rayleigh approximation. For larger particles, the two-sphere model produces slightly smaller backscattering cross sections than the simple sphere model (larger difference for less dense particles) and the Rayleigh approximation becomes unrealistic.

As a result, considering the large numerical effort, application of Mie scattering for dry snowflakes makes sense in case for large snowflakes whereas a further complication by using the two-layered sphere model seems to be unnecessary in this case.

However, it will be shown in the next section that in case of melting snowflakes, the two-layered sphere model leads to significantly different results compared to simple spheres.

8 Backscattering cross sections for melting ice particles relative to the mass-equivalent water drop

For melting ice particles, the presence of water (a strong dielectric) within the ice structure of melting particles poses a particular problem when it comes to the proper choice of an effective medium approximation. In fact, is there a proper choice at all? The answer to this question strongly depends on the mixture topology of the ice-water-air mixture. Whereas for nearly solid hail it seems quite easy, the structure of melting intermediate- or low-density graupel or snowflakes is more difficult to treat.

Therefore, `radar_mielib` and `radar_mie_lm` provide no definite answer (the one and only solution) but permit the user to choose between many different possibilities to get a feeling for the range of uncertainty of the resulting reflectivity value. However, there are theoretical and experimental results presented in literature providing guidelines which EMA formulation and particle model should work better for certain hydrometeor types. Some basic discussion was presented earlier in the sections describing different EMA approximations. For more detailed informations, the reader is kindly referred to the corresponding literature. A starting point could be, e.g., the book of Bohren and Huffman (1983) and a number of subsequent articles by C. Bohren and coauthors. The literature is so numerous that we omit further citing here.

For LM users, the “hints” and guidelines from literature are reflected by reasonable default parameter values for the corresponding subroutines in `radar_mie_lm`, which can, of course, be changed. And to provide some guideline about what happens to Z_e if the default parameter settings are changed, the following sections provide a detailed sensitivity investigation of the backscattering cross sections of melting hydrometeors considering all possible parameter settings for the most basic particle models implemented into `radar_mielib`.

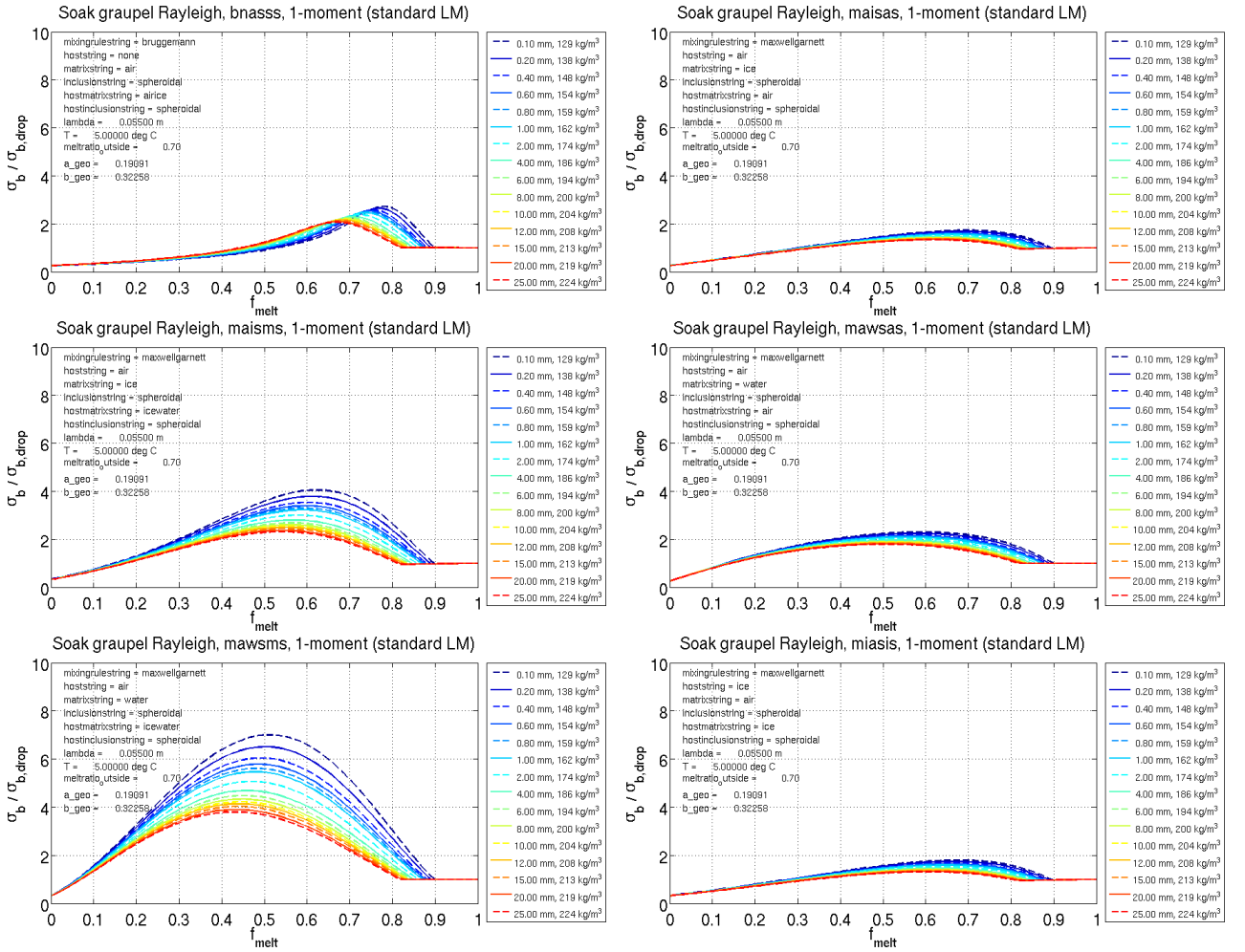
To this end, the same 4 different inverse mass-size relations as in Subsection 7.1 are applied to deduce the mass of the initially unmelted particle which is varied from small to large values. Subsequent variation of the degree of melting f_{melt} and the particle model together with the EMA approximation leads to a very large compilation of results which is presented in the following subsections.

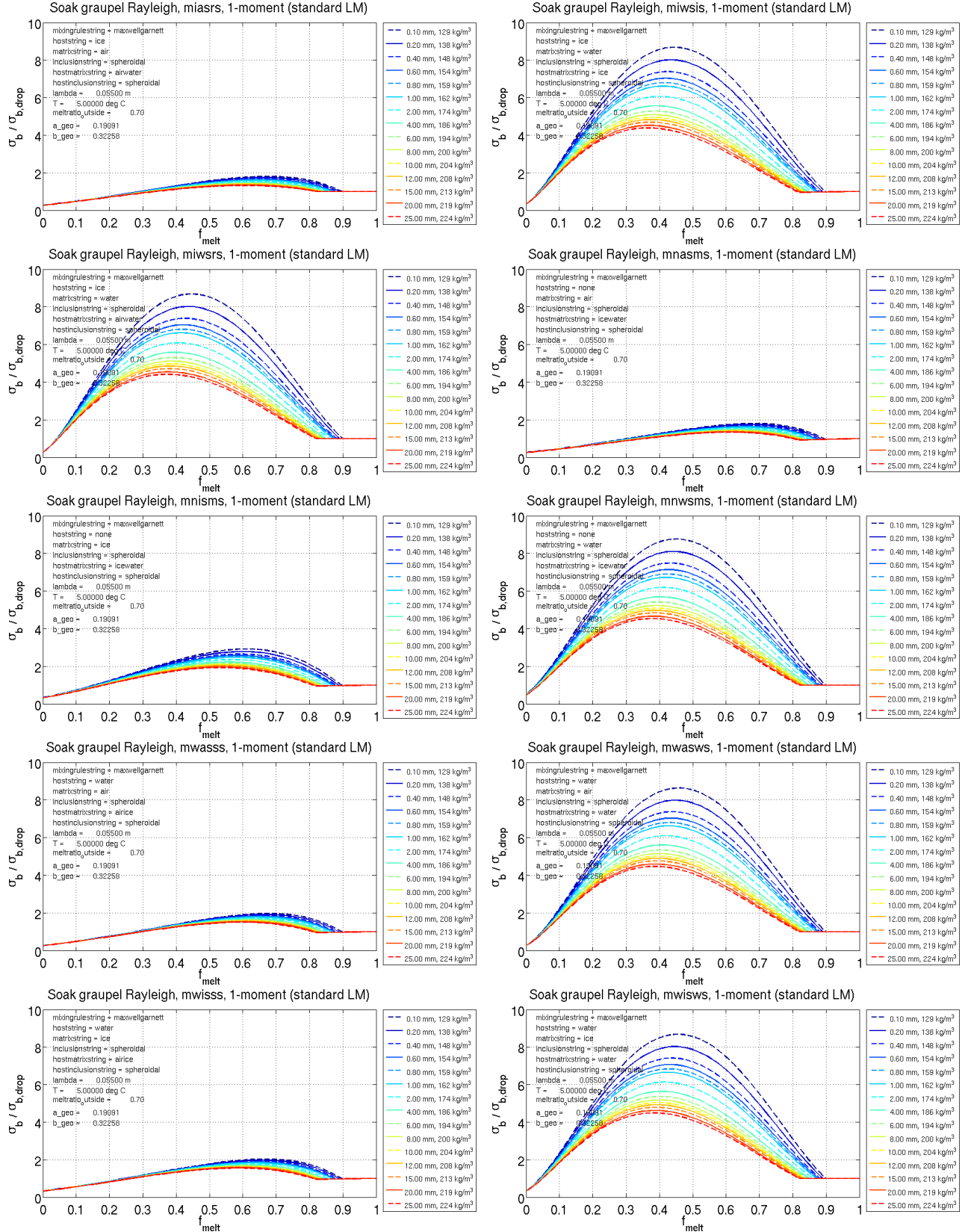
The results apply to a **C-Band radar wavelength of $\lambda_0 = 5.5$ cm and to a temperature of 5°C.**

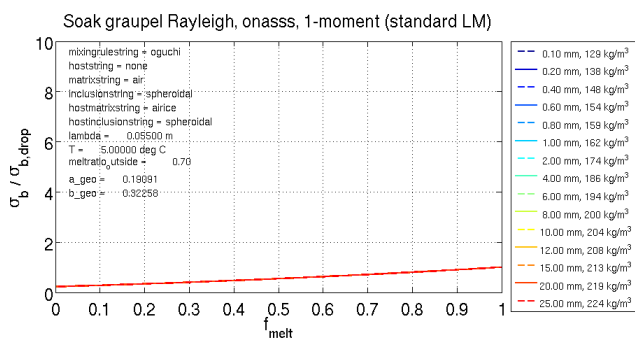
8.1 Rayleigh: soaked wet graupel, LM-scheme

Results are shown for calculations of the backscattering cross section σ_b with subroutine `RAYLEIGH_SOAK_WETGRAUPEL()` (Rayleigh approximation), see subsubsection 5.3.12 on Page 50. The following figures show the ratio of σ_b to the backscattering cross section $\sigma_{b,drop}$ of the resulting water drop, if the particle would be completely melted, as function of f_{melt} and the unmelted particle diameter for different EMA-formulations of the particles effective refractive index m_{eff} . The particle bulk density as function of size is determined by equation (36) on Page 69. A depiction of the resulting bulk density as function of particle size can be found in Figure 10 (black solid line).

Every figure represents one particular EMA-formulation for m_{eff} , which is obtained by using function `get_m_mix_nested()` (subsubsection 5.2.5 on Page 28). The input parameter set for `get_m_mix_nested()` can be found in the text annotation within each graph. For users of the LM, the corresponding setting of the namelist-parameter `ctype_wetgraupel_ray` can be found as 6-character code in the figures title. For explanation of this code, see Table 40. The results of this section apply to the LM for graupel and snow particles in case of application of the standard one-moment bulk microphysical scheme (namelist-parameter `itype_gscp` < 100) together with `itype_refl` = 2.



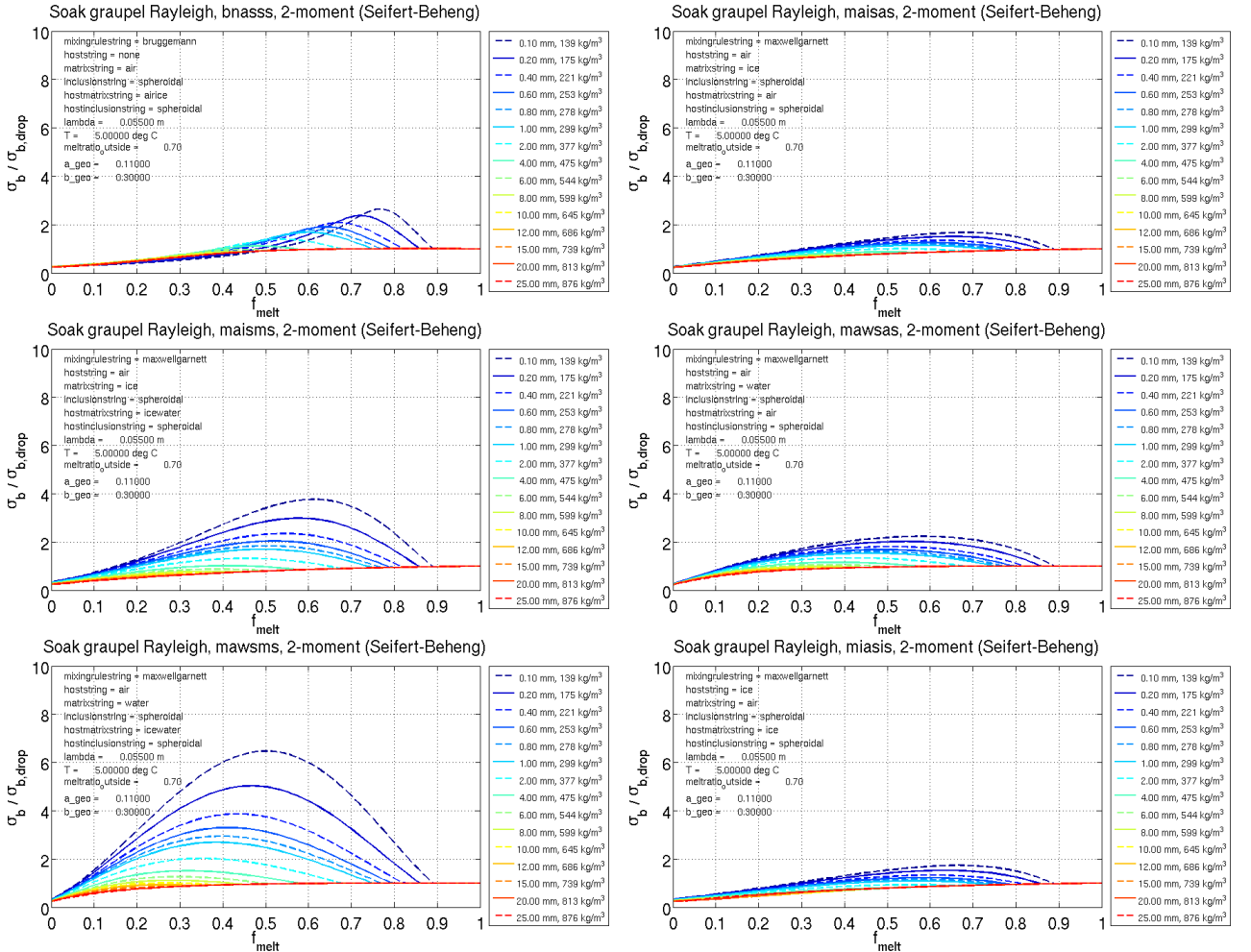


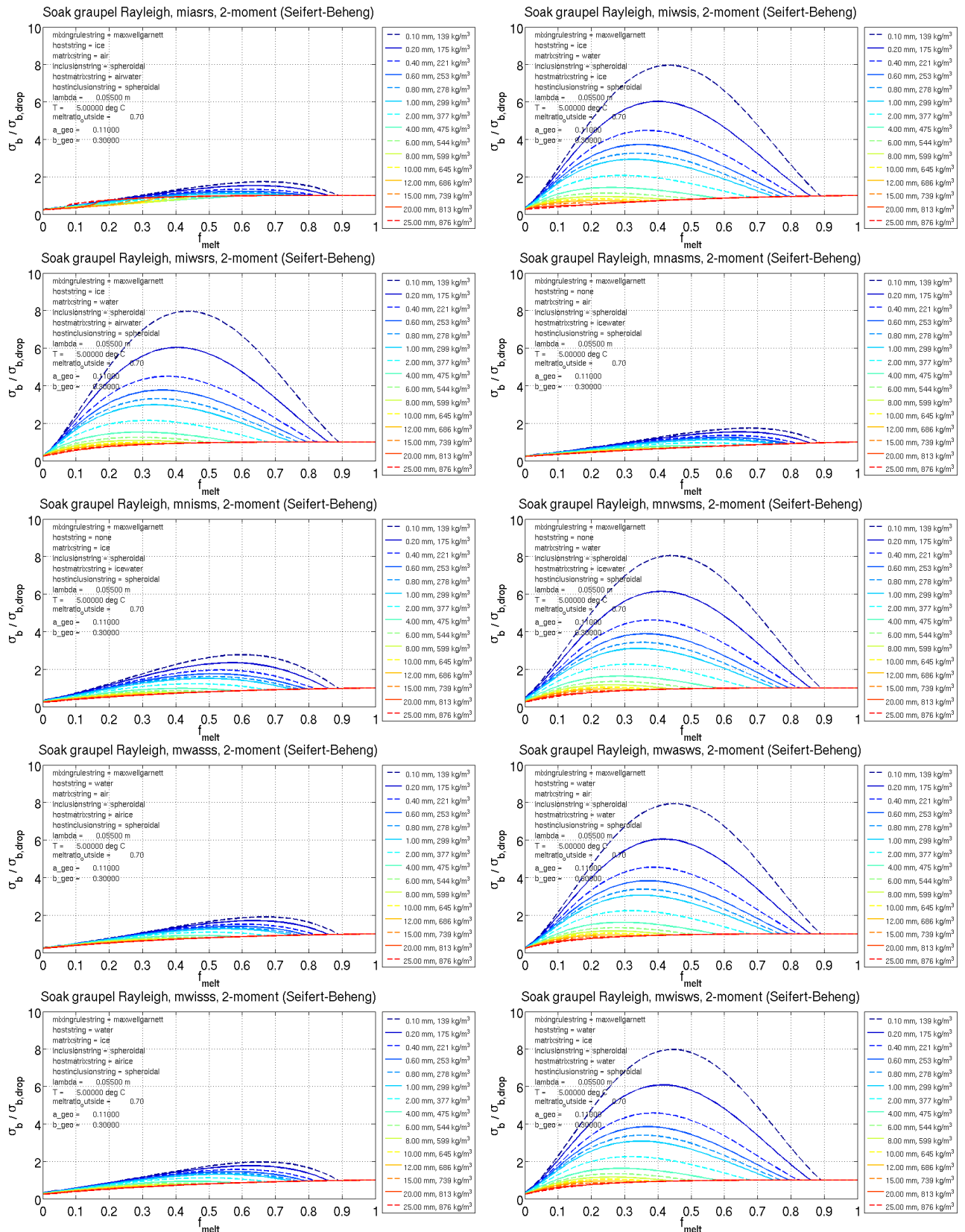


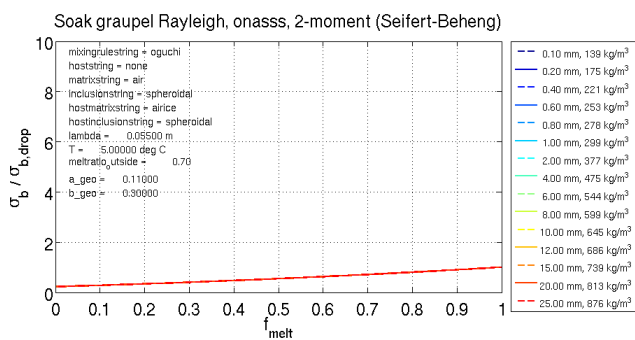
8.2 Rayleigh: soaked wet graupel, Seifert/Beheng-scheme

Similar to Subsection 8.1, results are shown for calculations of the backscattering cross section σ_b with subroutine `RAYLEIGH_SOAK_WETGRAUPEL()` (Rayleigh approximation), see subsection 5.3.12 on Page 50, but this time the particle bulk density as function of size is determined by equation (37) on Page 69. A depiction of the resulting bulk density as function of particle size can be found in Figure 10 (red solid line). The following figures show the ratio of $\sigma_b/\sigma_{b,drop}$ as function of f_{melt} and the unmelted particle diameter for different EMA-formulations of the particles effective refractive index m_{eff} .

Again, every figure represents one particular EMA-formulation for m_{eff} , which is obtained by using function `get_m_mix_nested()` (subsection 5.2.5 on Page 28). The input parameter set for `get_m_mix_nested()` can be found in the text annotation within each graph. For users of the LM, the corresponding setting of the namelist-parameter `ctype_wetgraupel_ray` can be found as 6-character code in the figures title. For explanation of this code, see Table 40. The results of this section apply to the LM for graupel, snow and hail particles in case of application of the Seifert and Beheng (2006) two-moment bulk microphysical scheme (namelist-parameter `itype_gscp` ≥ 100) together with `itype_refl` = 2.



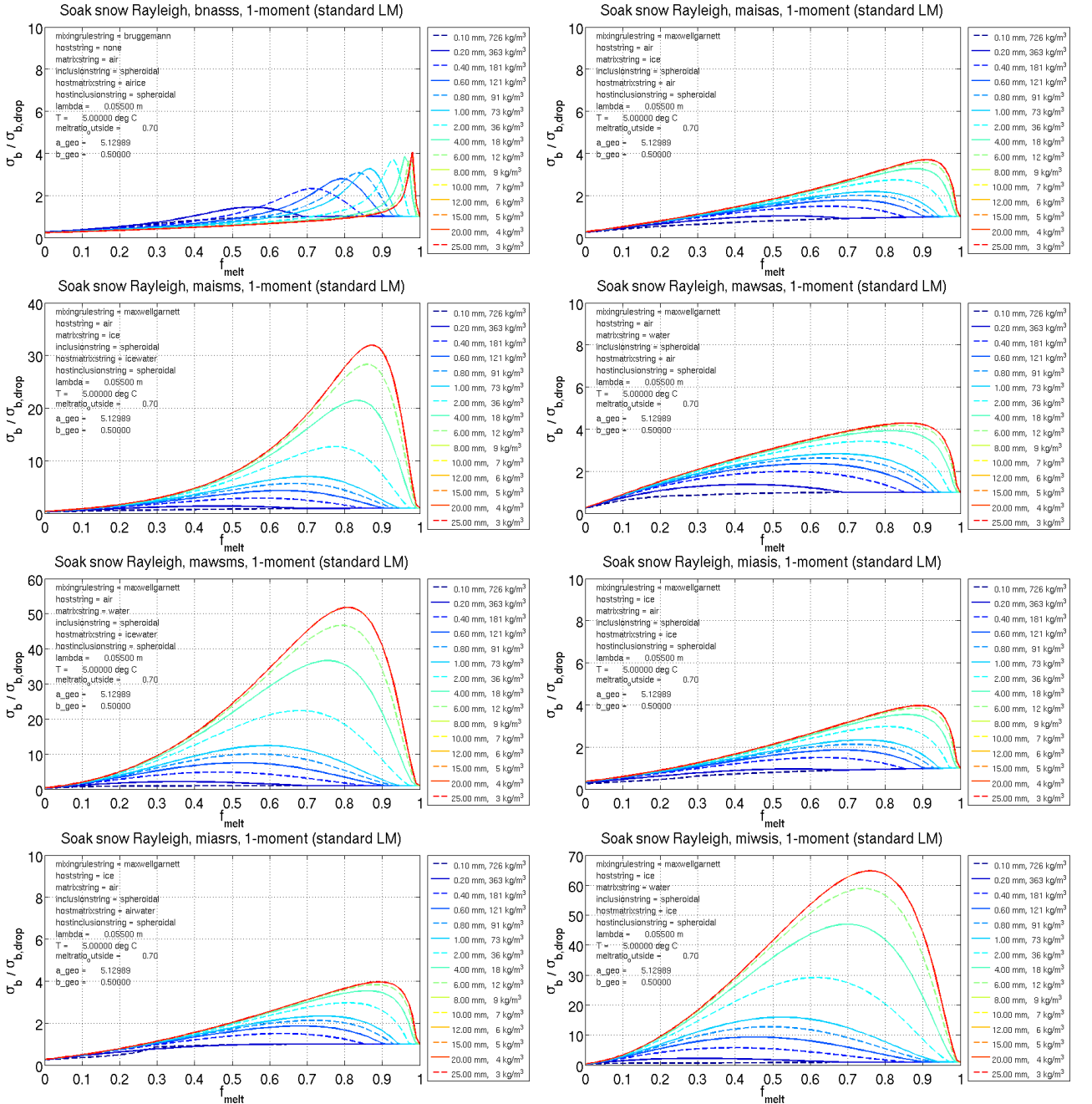


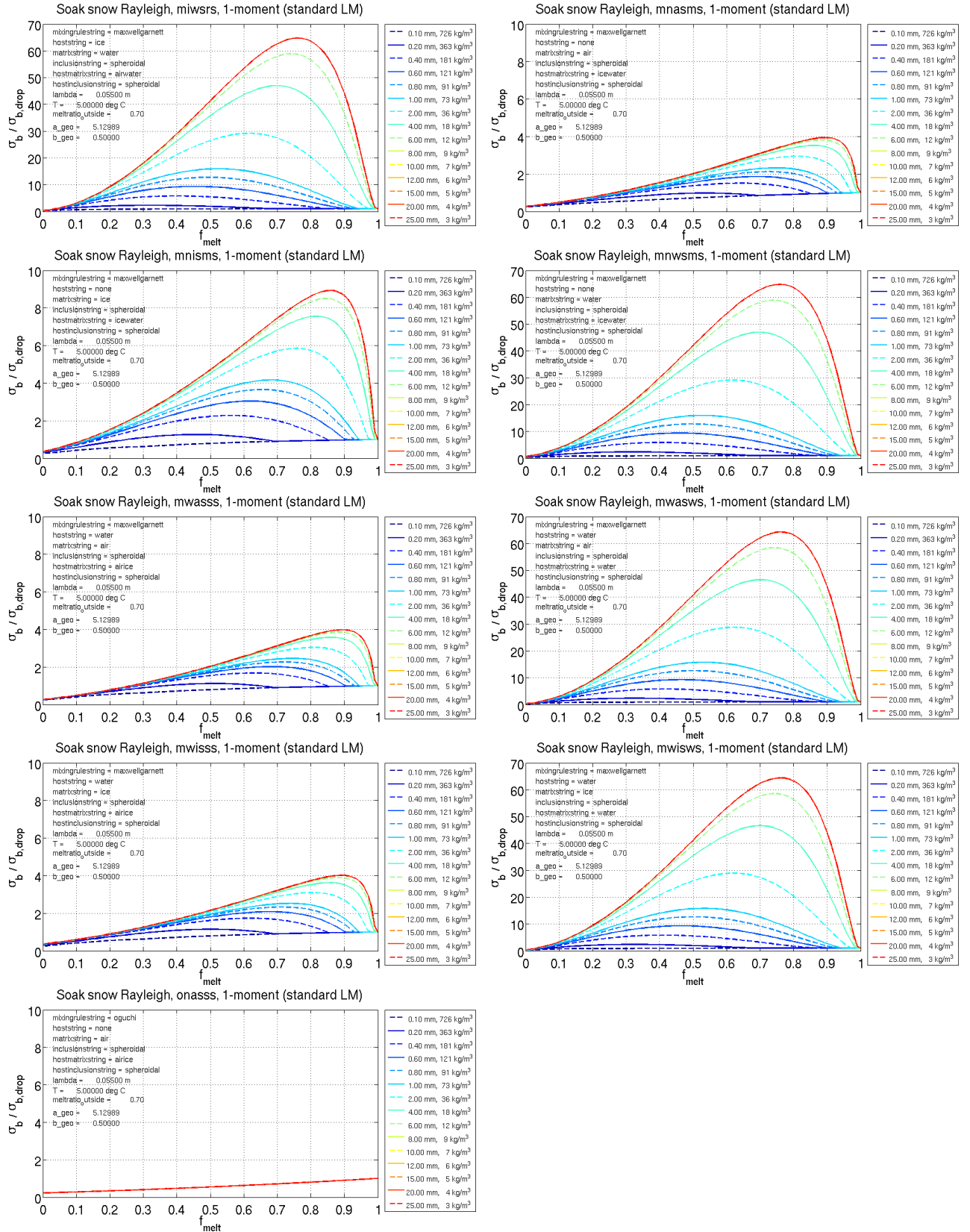


8.3 Rayleigh: soaked wet snow, LM-scheme

Similar to Subsection 8.1, results are shown for calculations of the backscattering cross section σ_b with subroutine `RAYLEIGH_SOAK_WETGRAUPEL()` (Rayleigh approximation), see subsection 5.3.12 on Page 50, but this time the particle bulk density as function of size is determined by equation (38) on Page 69. A depiction of the resulting bulk density as function of particle size can be found in Figure 10 (blue solid line). The following figures show the ratio of $\sigma_b/\sigma_{b,drop}$ as function of f_{melt} and the unmelted particle diameter for different EMA-formulations of the particles effective refractive index m_{eff} .

Again, every figure represents one particular EMA-formulation for m_{eff} , which is obtained by using function `get_m_mix_nested()` (subsection 5.2.5 on Page 28). The input parameter set for `get_m_mix_nested()` can be found in the text annotation within each graph. Although not being implemented into the LM interface functions for snow, the corresponding setting of the namelist-parameter `ctype_wetsnow_ray` (in analogy to `ctype_wetgraupel_ray`) can be found as 6-character code in the figures title. For explanation of this code, see Table 40.

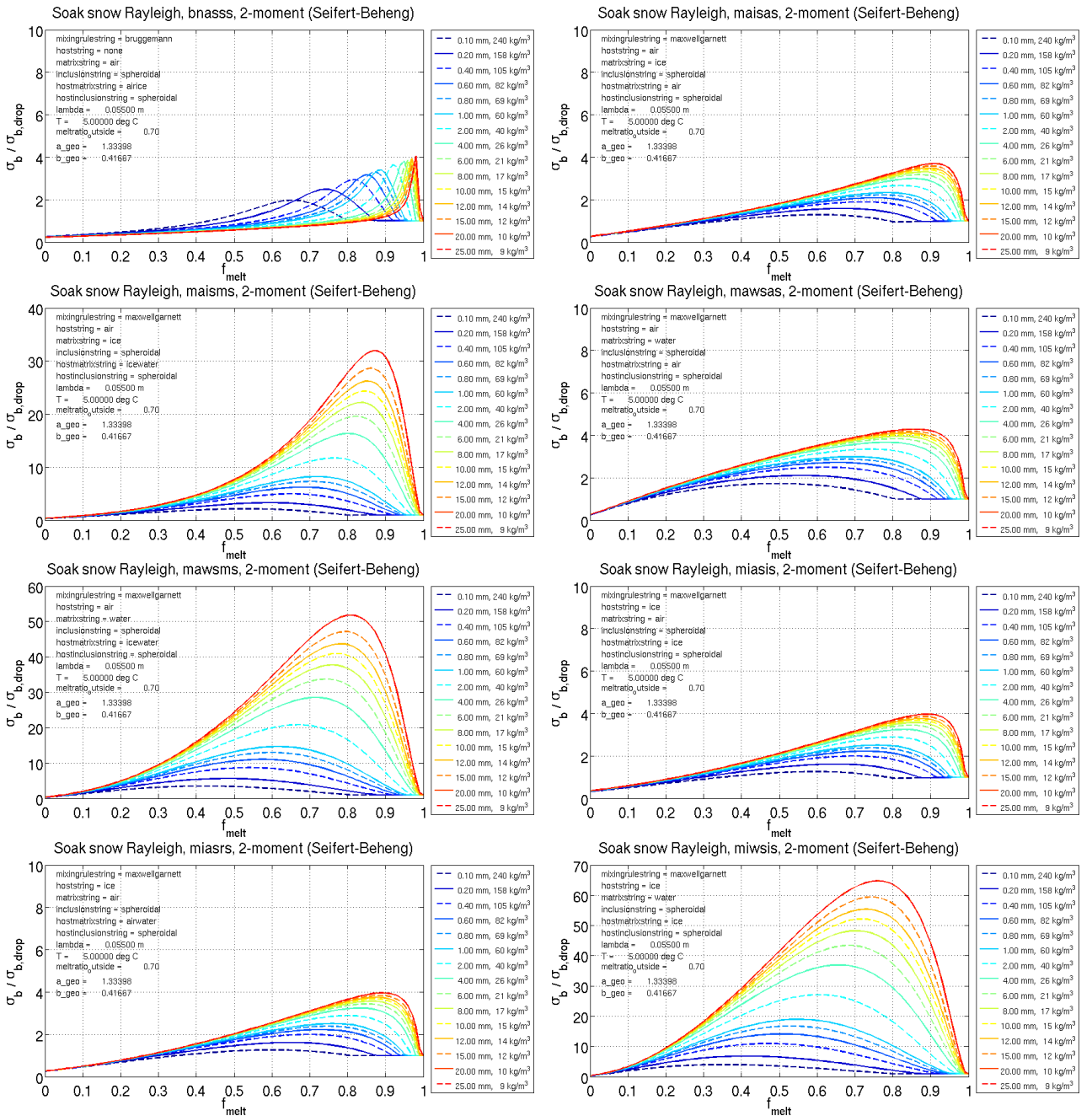


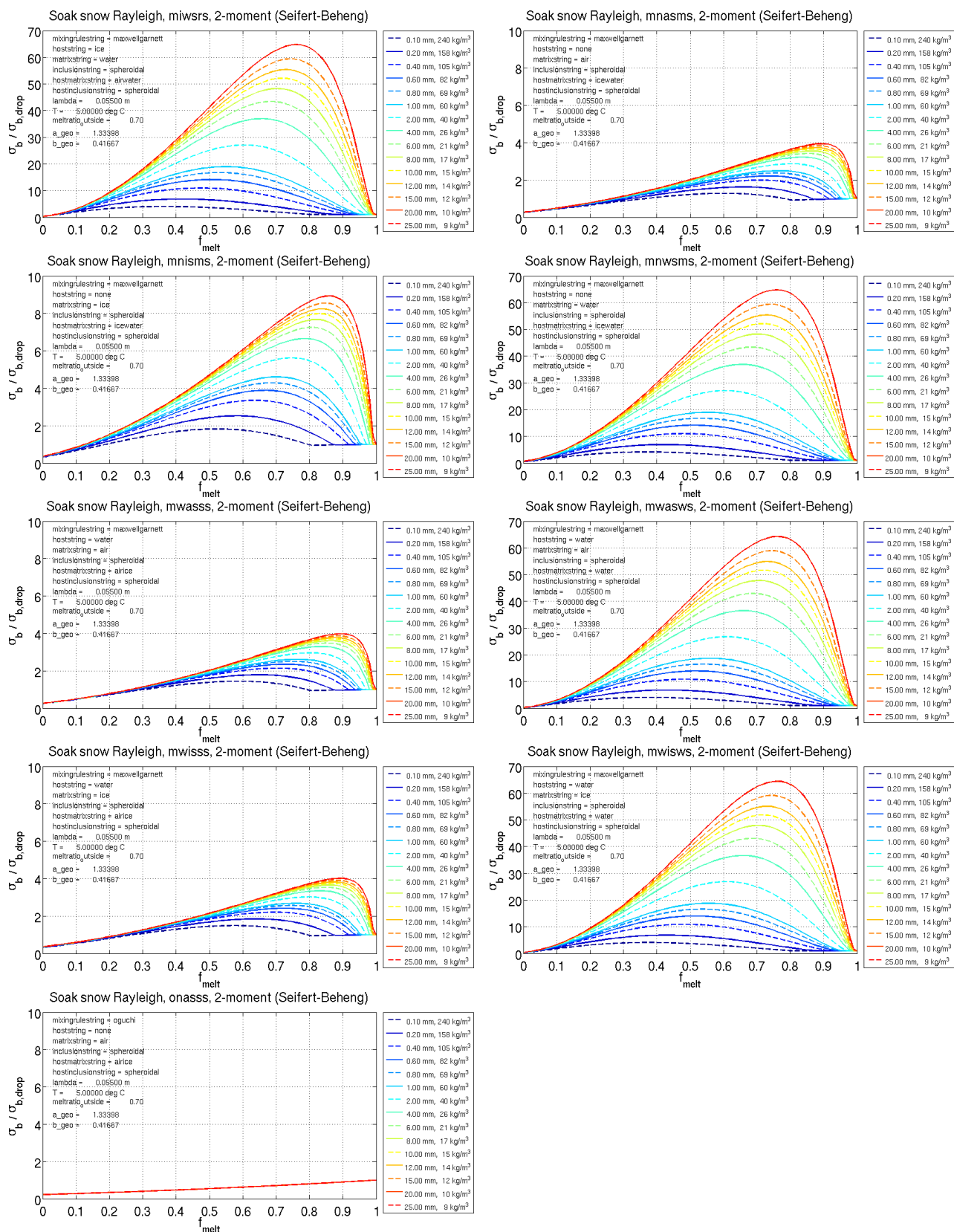


8.4 Rayleigh: soaked wet snow, Seifert/Beheng-scheme

Similar to Subsection 8.1, results are shown for calculations of the backscattering cross section σ_b with subroutine `RAYLEIGH_SOAK_WETGRAUPEL()` (Rayleigh approximation), see subsubsection 5.3.12 on Page 50, but this time the particle bulk density as function of size is determined by equation (39) on Page 69. A depiction of the resulting bulk density as function of particle size can be found in Figure 10 (green solid line). The following figures show the ratio of $\sigma_b/\sigma_{b,drop}$ as function of f_{melt} and the unmelted particle diameter for different EMA-formulations of the particles effective refractive index m_{eff} .

Again, every figure represents one particular EMA-formulation for m_{eff} , which is obtained by using function `get_m_mix_nested()` (subsubsection 5.2.5 on Page 28). The input parameter set for `get_m_mix_nested()` can be found in the text annotation within each graph. Although not being implemented into the LM interface functions for snow, the corresponding setting of the namelist-parameter `ctype_wetsnow_ray` (in analogy to `ctype_wetgraupel_ray`) can be found as 6-character code in the figures title. For explanation of this code, see Table 40.

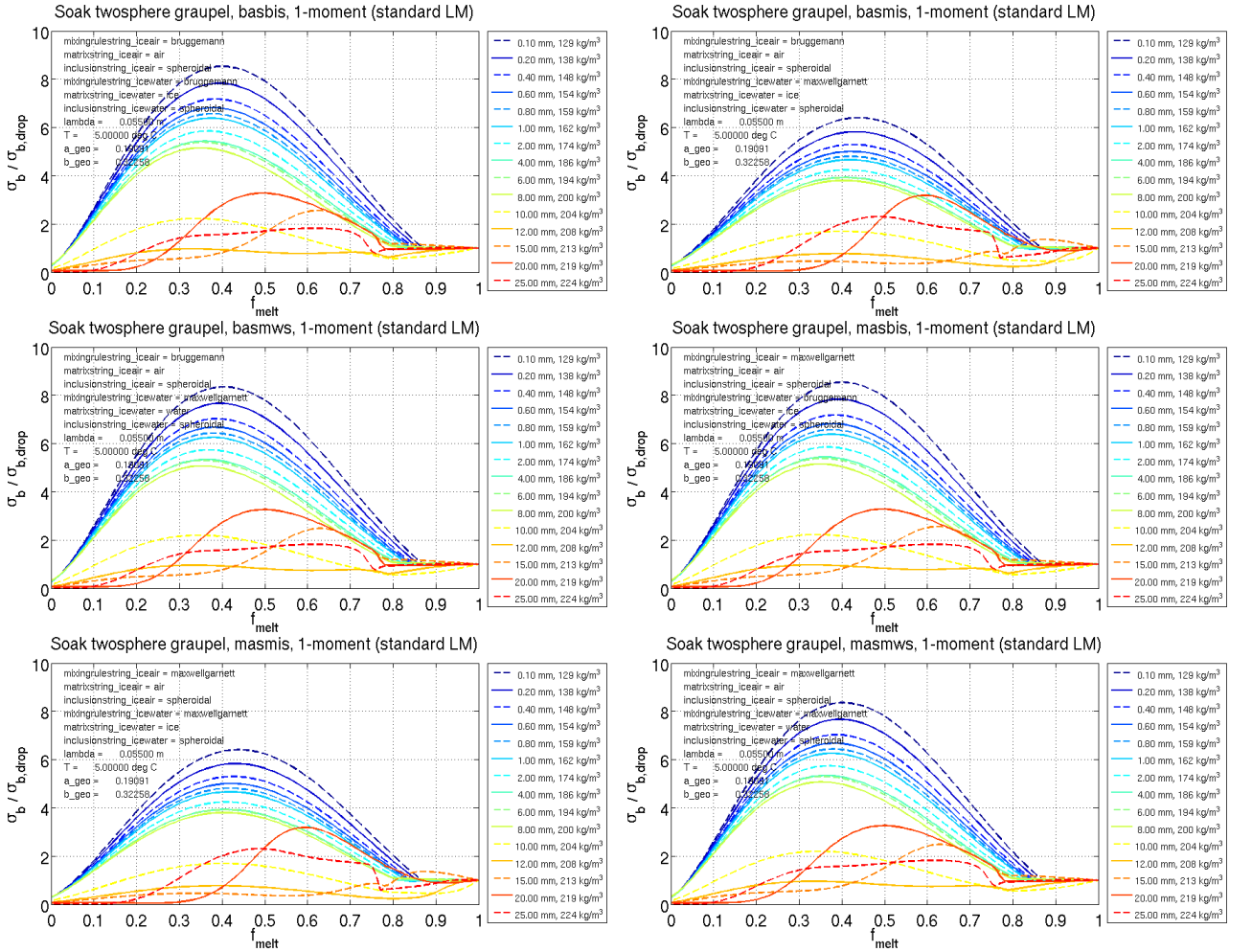


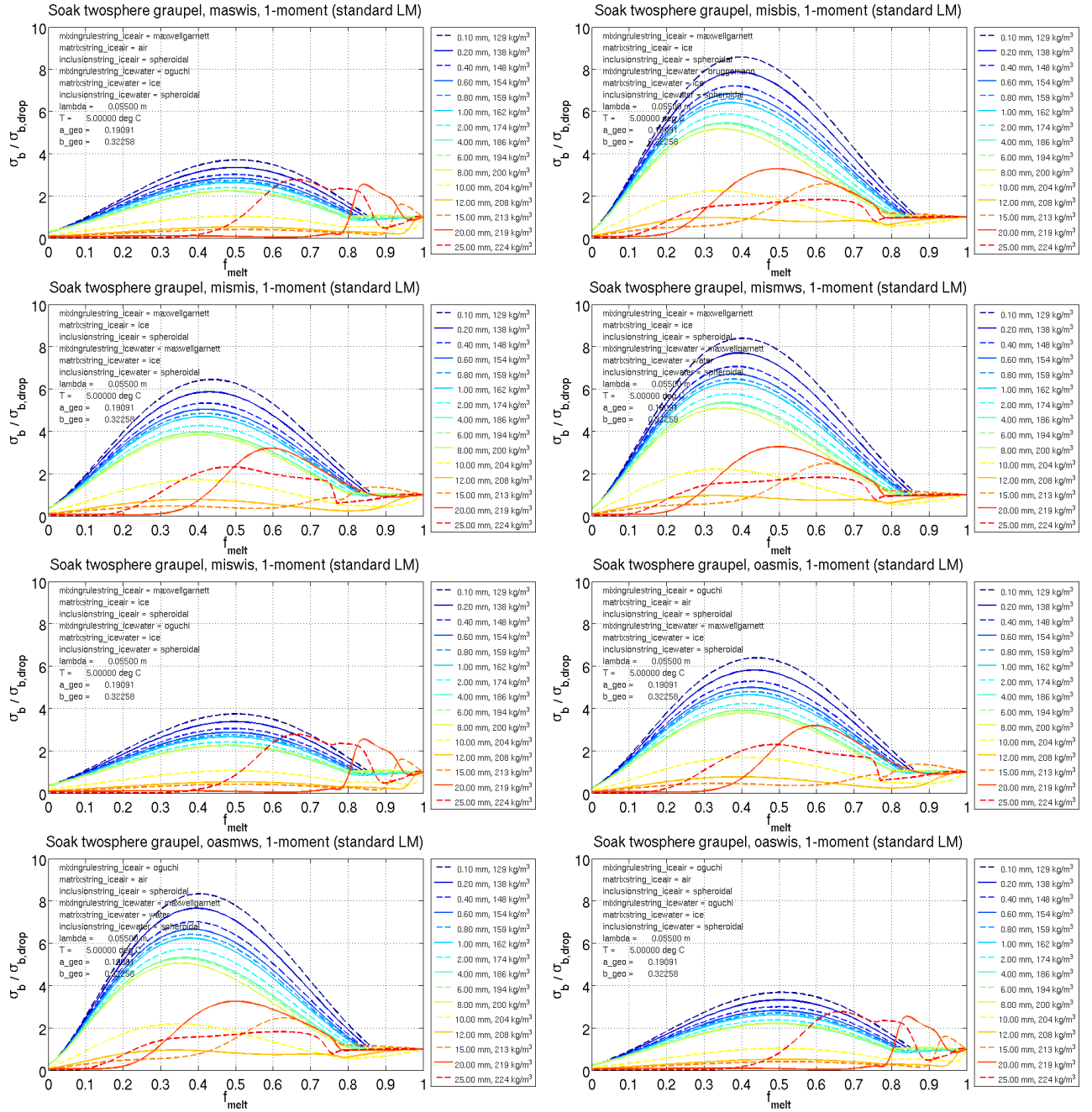


8.5 Mie: soaked twosphere wet graupel, LM-scheme

Similar to Subsection 8.1, results are shown for calculations of the backscattering cross section σ_b with subroutine `MIE_SOAK_TWOSPHERE_WETGRAUPEL()` (Mie scattering, two-layered sphere), see subsubsection 5.3.9 on Page 45. The following figures show the ratio of $\sigma_b/\sigma_{b,drop}$ as function of f_{melt} and the unmelted particle diameter for different EMA-formulations of the particles effective refractive indices m_{eff} of core and shell. The particle bulk density as function of size is determined by equation (36) on Page 69. A depiction of the resulting bulk density as function of particle size can be found in Figure 10 (black solid line).

Again, every figure represents one particular EMA-formulation combination for m_{eff} of core and shell, which both are obtained by using function `get_m_mix()`, applied for two-component mixture materials (subsubsection 5.2.4 on Page 26). The input parameter sets for `get_m_mix()` can be found in the text annotation within each graph, discriminating ice-air core and ice-water shell. For users of the LM, the corresponding setting of the namelist-parameter `ctype_wetgraupel` can be found in the figures title as a combination of two 3-character codes. For explanation of this code, see Table 41. The results of this section apply to the LM for graupel particles in case of application of the standard one-moment bulk microphysical scheme (namelist-parameter `itype_gscp < 100`) together with namelist-parameters `itype_refl = 1` and `igraupel_type = 2`.

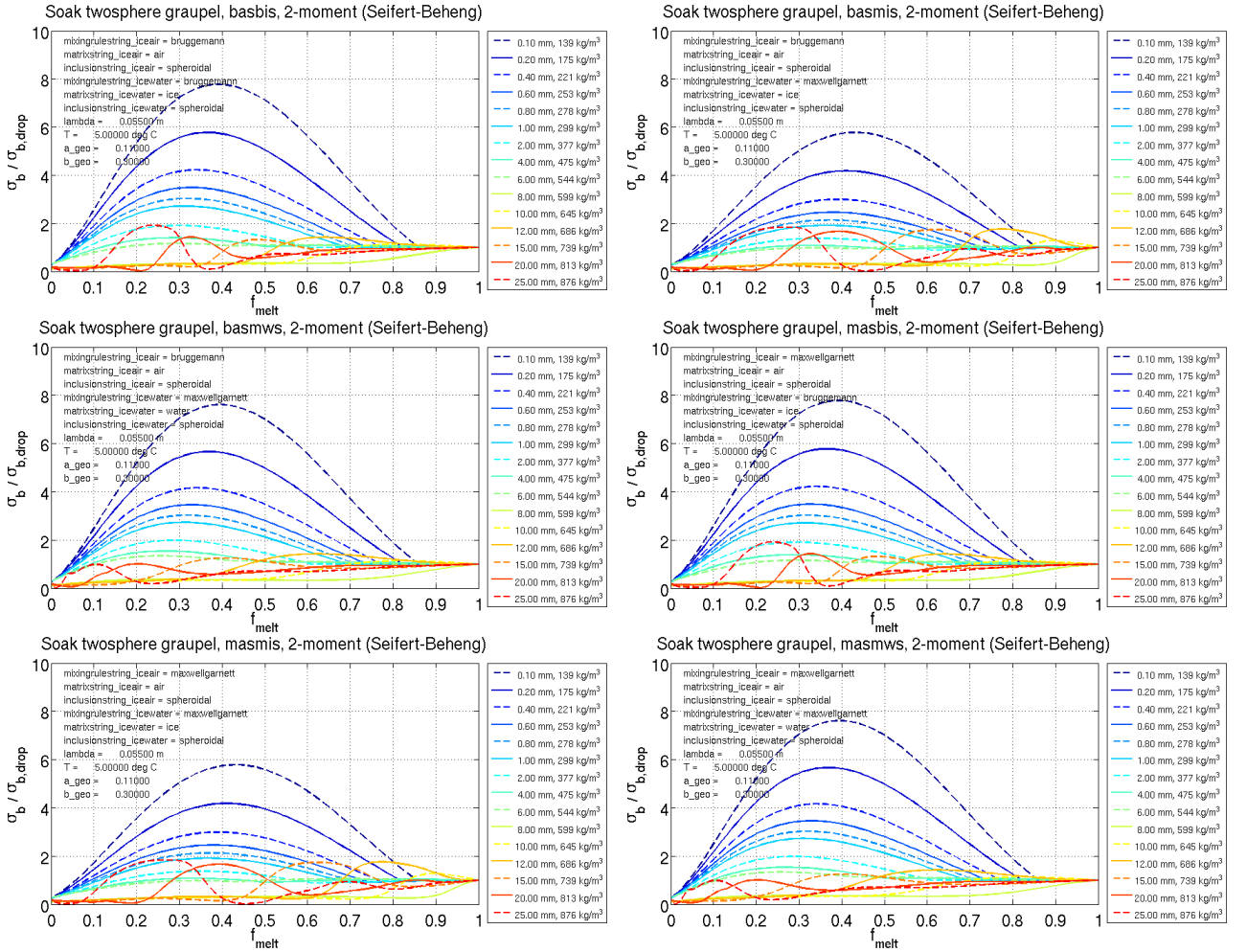


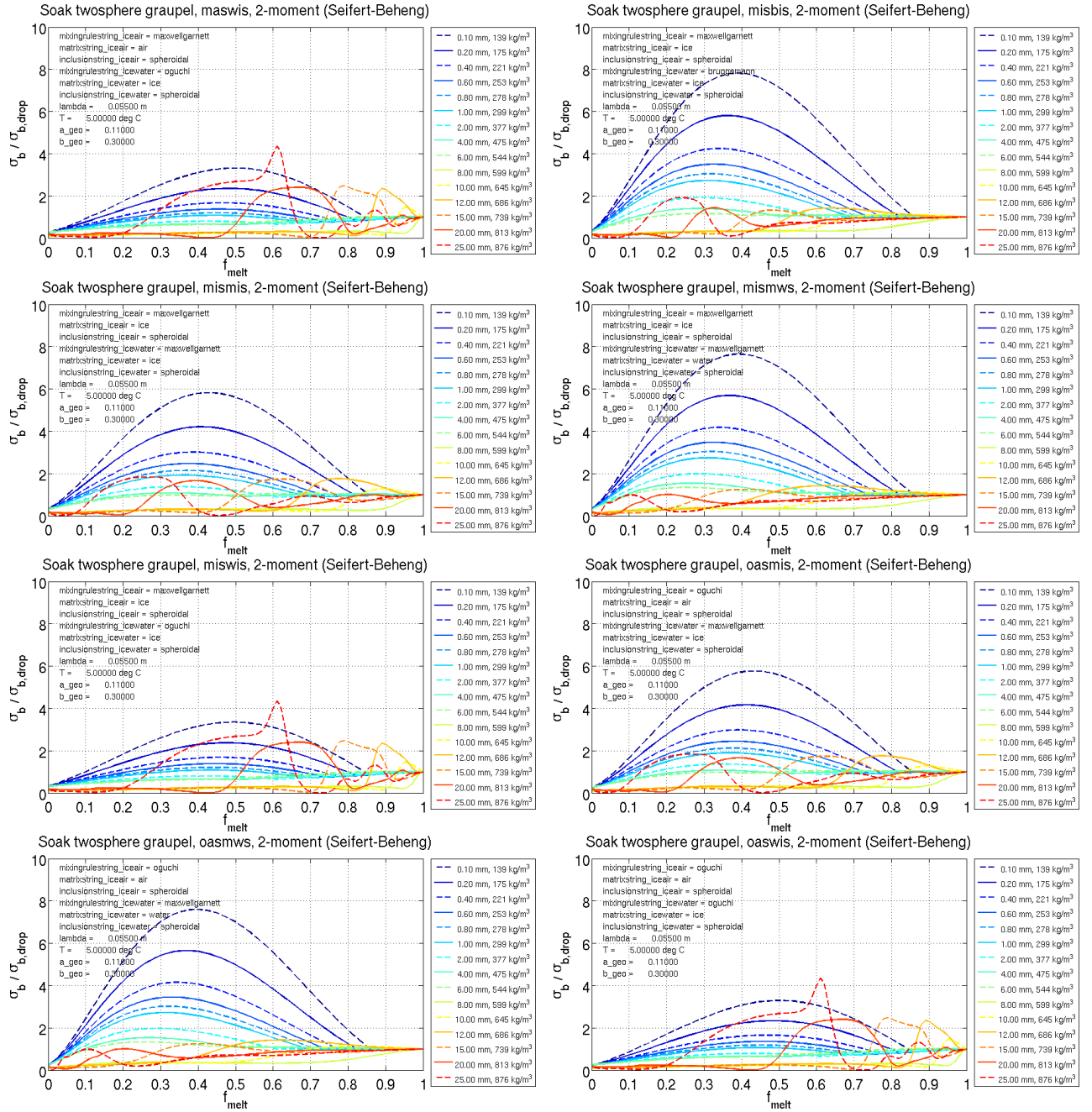


8.6 Mie: soaked twosphere wet graupel, Seifert/Beheng-scheme

Similar to Subsection 8.5, results are shown for calculations of the backscattering cross section σ_b with subroutine `MIE_SOAK_TWOSPHERE_WETGRAUPEL()` (Mie scattering, two-layered sphere), see subsection 5.3.9 on Page 45. But this time, the particle bulk density as function of size is determined by equation (37) on Page 69. A depiction of the resulting bulk density as function of particle size can be found in Figure 10 (red solid line). The following figures show the ratio of $\sigma_b/\sigma_{b,drop}$ as function of f_{melt} and the unmelted particle diameter for different EMA-formulations of the particles effective refractive indices m_{eff} of core and shell.

Again, every figure represents one particular EMA-formulation for m_{eff} of core and shell, which both are obtained by using function `get_m_mix()`, applied for two-component mixture materials (subsection 5.2.4 on Page 26). The input parameter sets for `get_m_mix()` can be found in the text annotation within each graph, discriminating ice-air core and ice-water shell. For users of the LM, the corresponding setting of the namelist-parameter `ctype_wetgraupel` can be found in the figures title as a combination of two 3-character codes. For explanation of this code, see Table 41. The results of this section apply to the LM for graupel particles in case of application of the Seifert and Beheng (2006) two-moment bulk microphysical scheme (namelist-parameter `itype_gscp` ≥ 100) together with namelist-parameters `itype_refl` = 1 and `igraupel_type` = 2.

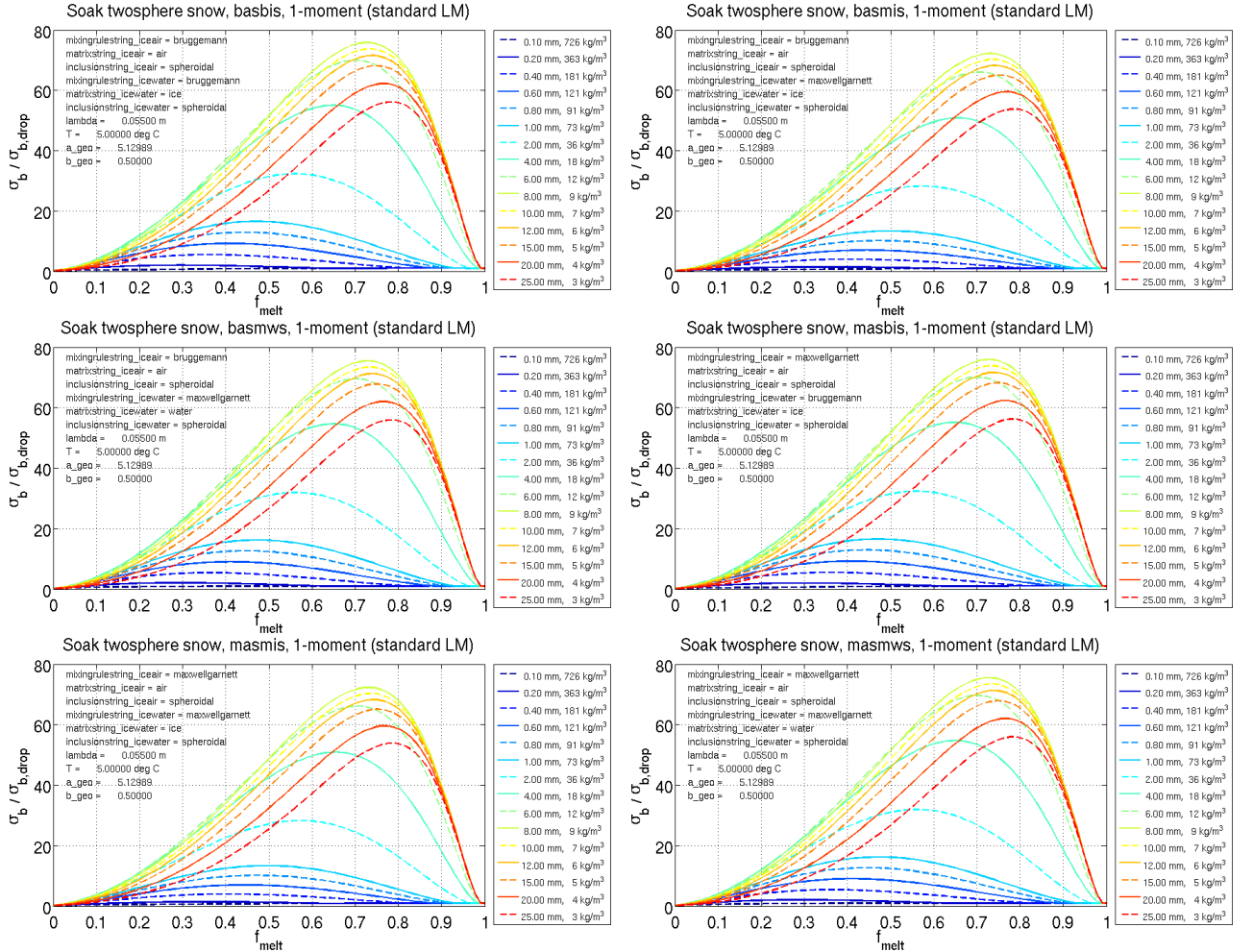


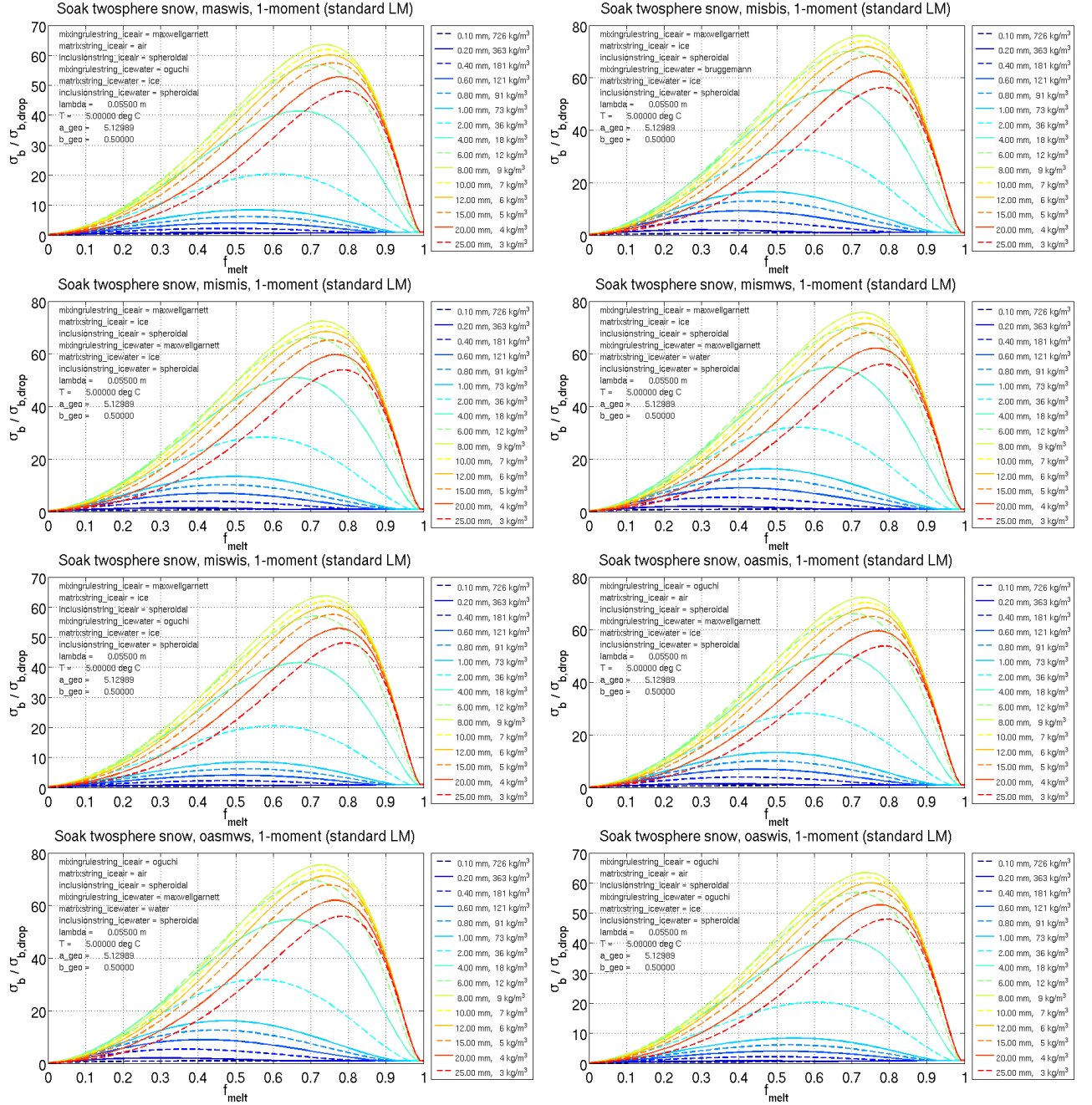


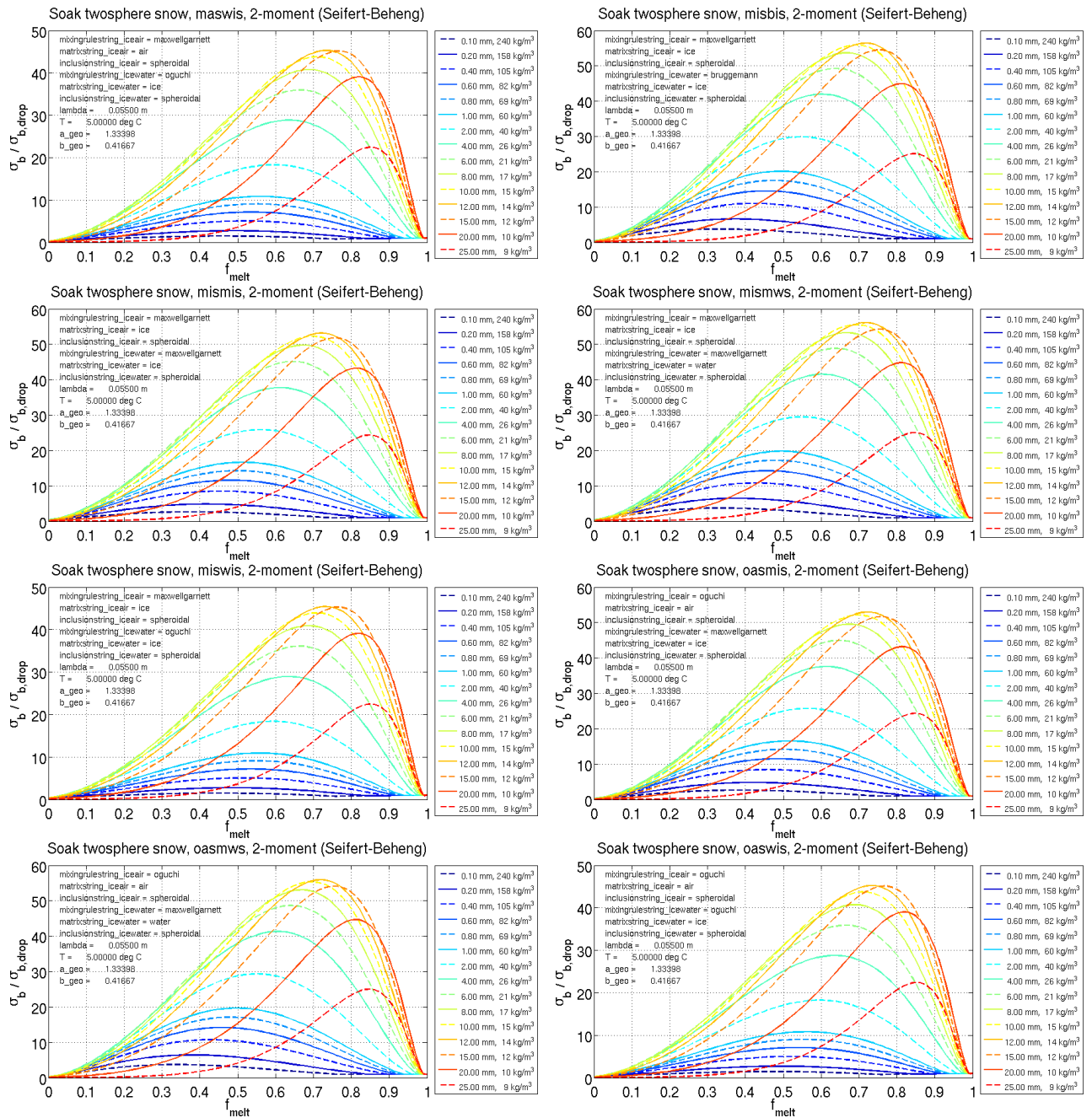
8.7 Mie: soaked twosphere wet snow, LM-scheme

Similar to Subsection 8.5, results are shown for calculations of the backscattering cross section σ_b with subroutine `MIE_SOAK_TWOSPHERE_WETGRAUPEL()` (Mie scattering, two-layered sphere), see subsection 5.3.9 on Page 45. But this time, the particle bulk density as function of size is determined by equation (38) on Page 69. A depiction of the resulting bulk density as function of particle size can be found in Figure 10 (blue solid line). The following figures show the ratio of $\sigma_b/\sigma_{b,drop}$ as function of f_{melt} and the unmelted particle diameter for different EMA-formulations of the particles effective refractive indices m_{eff} of core and shell.

Again, every figure represents one particular EMA-formulation combination for m_{eff} of core and shell, which both are obtained by using function `get_m_mix()`, applied for two-component mixture materials (subsection 5.2.4 on Page 26). The input parameter sets for `get_m_mix()` can be found in the text annotation within each graph, discriminating ice-air core and ice-water shell. Although not being implemented into the LM interface functions for snow, the corresponding setting of the (nonexisting) namelist-parameter `ctype_wetsnow` (in analogy to `ctype_wetgraupe1`) can be found in the figures title as a combination of two 3-character codes. For explanation of this code, see Table 41.



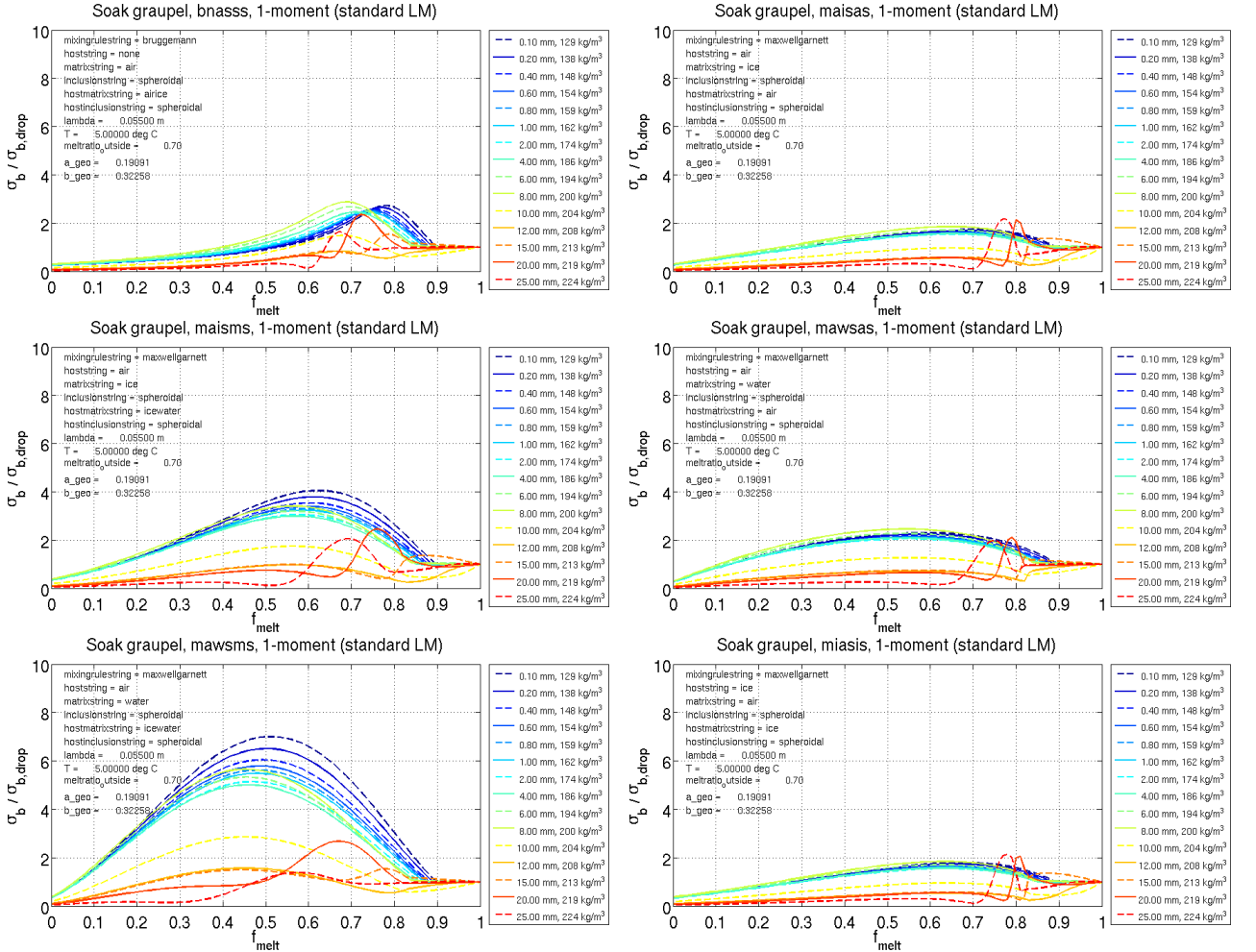


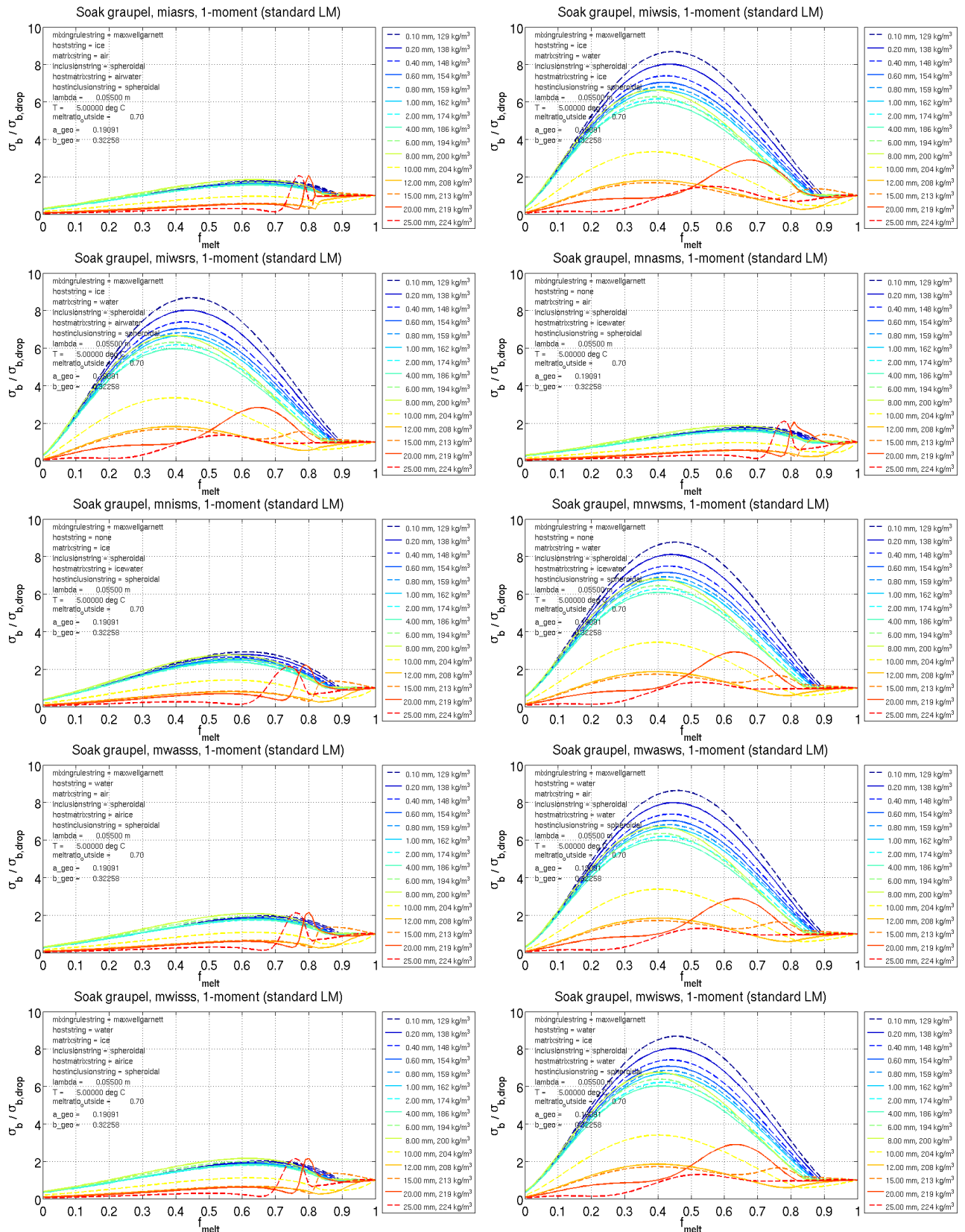


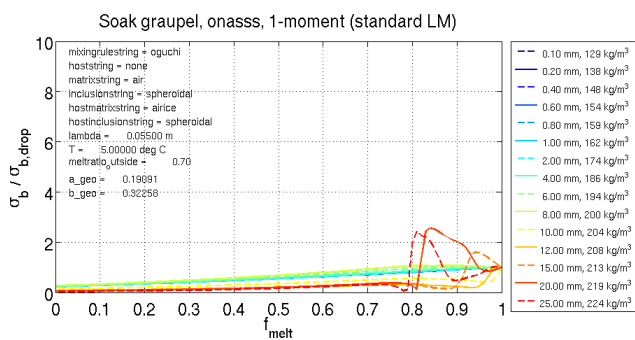
8.9 Mie: soaked wet graupel, LM-scheme

Similar to Subsection 8.1, results are shown for calculations of the backscattering cross section σ_b with subroutine `MIE_SOAK_WETGRAUPEL()` (Mie scattering), see subsubsection 5.3.11 on Page 48. The following figures show the ratio of $\sigma_b/\sigma_{b,drop}$ as function of f_{melt} and the unmelted particle diameter for different EMA-formulations of the particles effective refractive index m_{eff} . The particle bulk density as function of size is determined by equation (36) on Page 69. A depiction of the resulting bulk density as function of particle size can be found in Figure 10 (black solid line).

Again, every figure represents one particular EMA-formulation for m_{eff} , which is obtained by using function `get_m_mix_nested()` (subsubsection 5.2.5 on Page 28). The input parameter set for `get_m_mix_nested()` can be found in the text annotation within each graph. For users of the LM, the corresponding setting of the namelist-parameter `ctype_wetgraupel` can be found as 6-character code in the figures title. For explanation of this code, see Table 40. The results of this section apply to the LM for graupel particles in case of application of the standard LM one-moment bulk microphysical schemes (namelist-parameter `itype_gscp < 100`) together with `itype_refl = 1` and `igraupel_type = 1`.



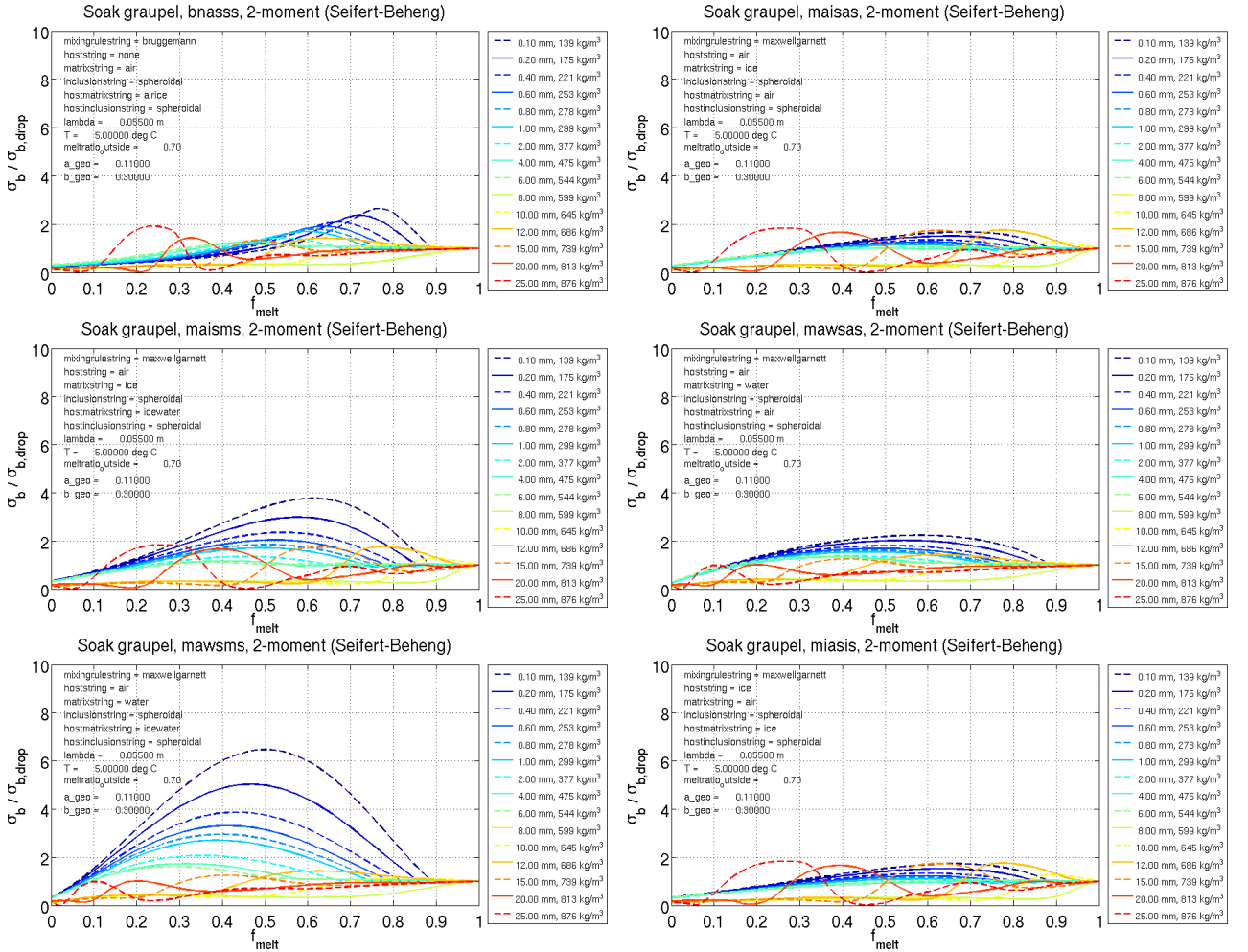


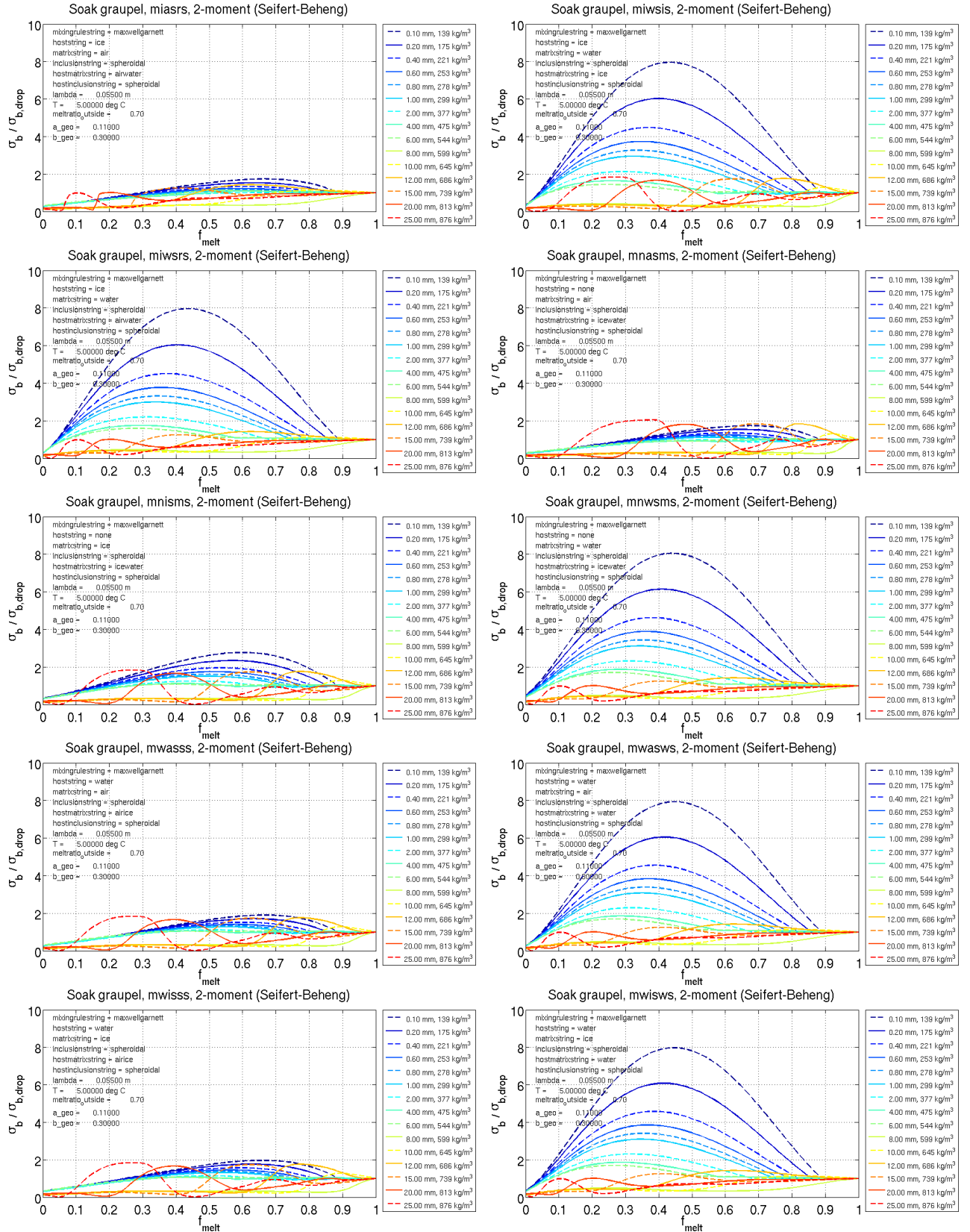


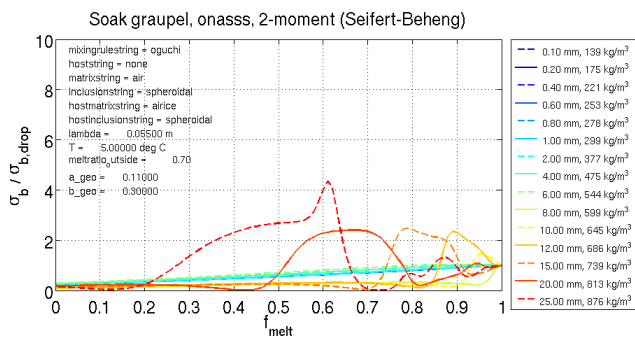
8.10 Mie: soaked wet graupel, Seifert/Beheng-scheme

Similar to Subsection 8.9, results are shown for calculations of the backscattering cross section σ_b with subroutine `MIE_SOAK_WETGRAUPEL()` (Mie scattering), see subsubsection 5.3.11 on Page 48. But this time, the particle bulk density as function of size is determined by equation (37) on Page 69. A depiction of the resulting bulk density as function of particle size can be found in Figure 10 (red solid line). The following figures show the ratio of $\sigma_b/\sigma_{b,drop}$ as function of f_{melt} and the unmelted particle diameter for different EMA-formulations of the particles effective refractive index m_{eff} .

Again, every figure represents one particular EMA-formulation for m_{eff} , which is obtained by using function `get_m_mix_nested()` (subsubsection 5.2.5 on Page 28). The input parameter set for `get_m_mix_nested()` can be found in the text annotation within each graph. For users of the LM, the corresponding setting of the namelist-parameter `ctype_wetgraupel` can be found as 6-character code in the figures title. For explanation of this code, see Table 40. The results of this section apply to the LM for graupel particles in case of application of the Seifert and Beheng (2006) two-moment bulk microphysical scheme (namelist-parameter `itype_gscp` ≥ 100) together with `itype_refl` = 1 and `igraupel_type` = 1.



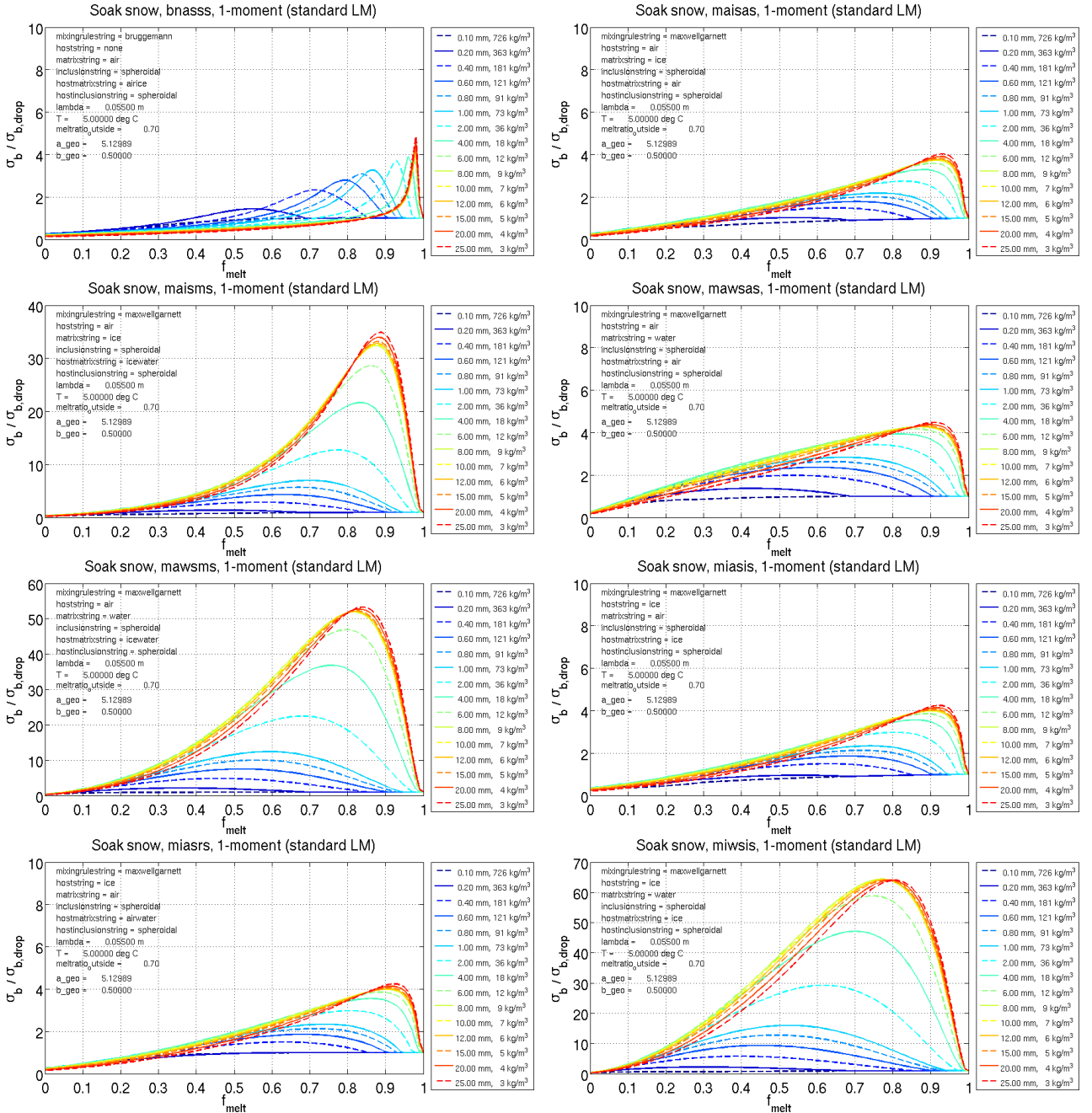


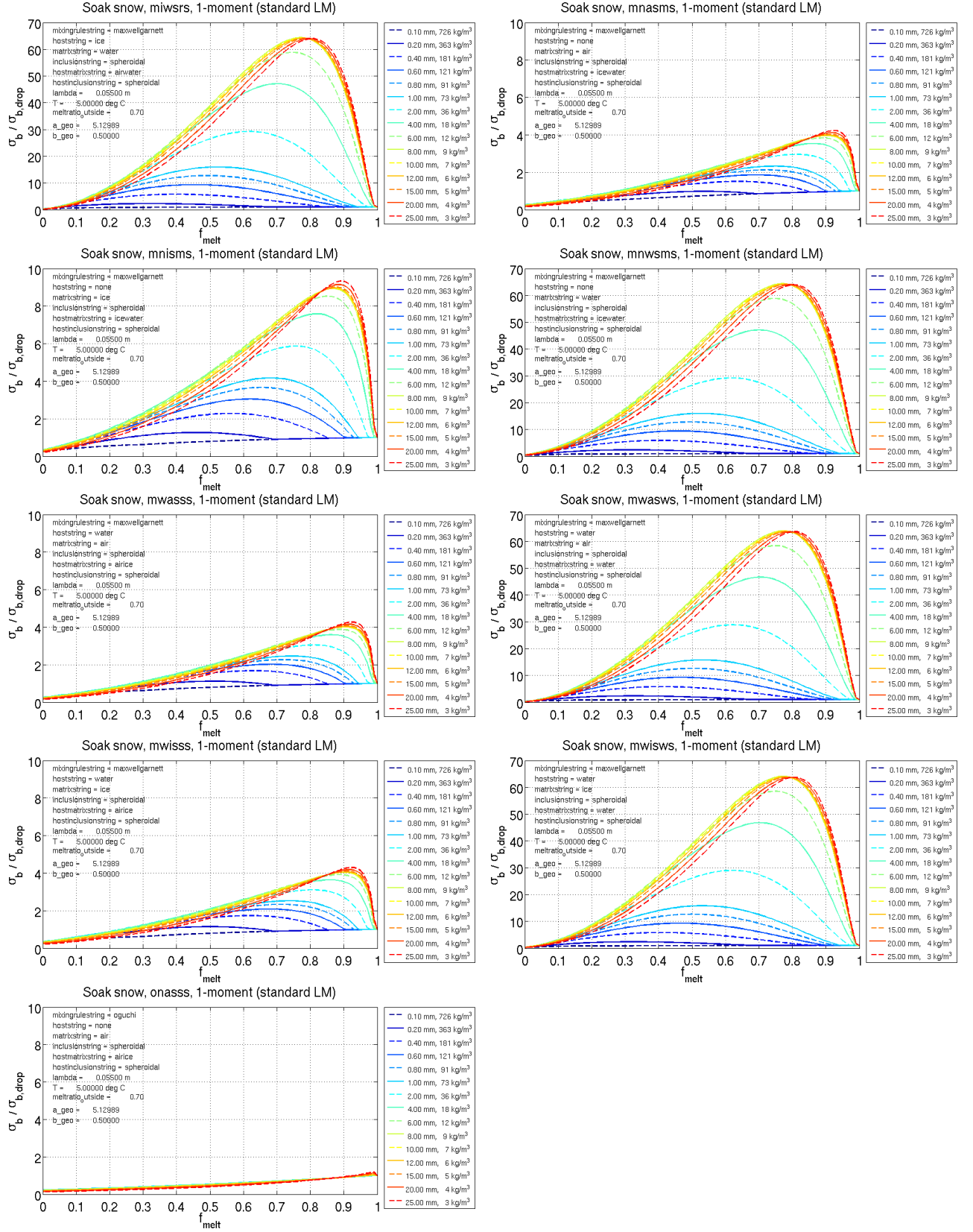


8.11 Mie: soaked wet snow, LM-scheme

Similar to Subsection 8.9, results are shown for calculations of the backscattering cross section σ_b with subroutine `MIE.SOAK_WETGRAUPEL()` (Mie scattering), see subsubsection 5.3.11 on Page 48. But this time, the particle bulk density as function of size is determined by equation (38) on Page 69. A depiction of the resulting bulk density as function of particle size can be found in Figure 10 (blue solid line). The following figures show the ratio of $\sigma_b/\sigma_{b,drop}$ as function of f_{melt} and the unmelted particle diameter for different EMA-formulations of the particles effective refractive index m_{eff} .

Again, every figure represents one particular EMA-formulation for m_{eff} , which is obtained by using function `get_m_mix_nested()` (subsubsection 5.2.5 on Page 28). The input parameter set for `get_m_mix_nested()` can be found in the text annotation within each graph. Although not being implemented into the LM interface functions for snow, the corresponding setting of the (nonexisting) namelist-parameter `ctype_wetsnow` (in analogy to `ctype_wetgraupel`) can be found as 6-character code in the figures title. For explanation of this code, see Table 40.

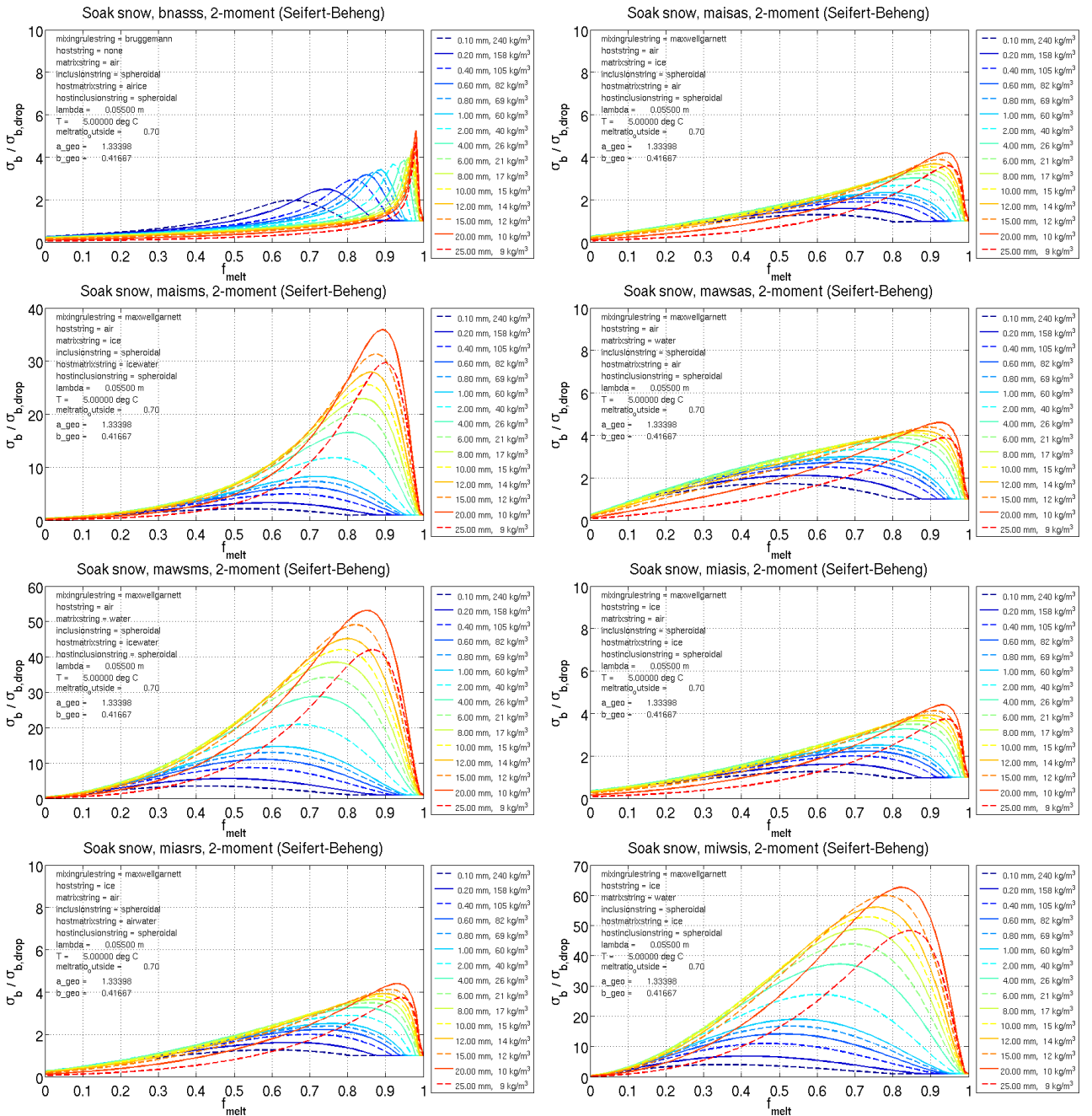


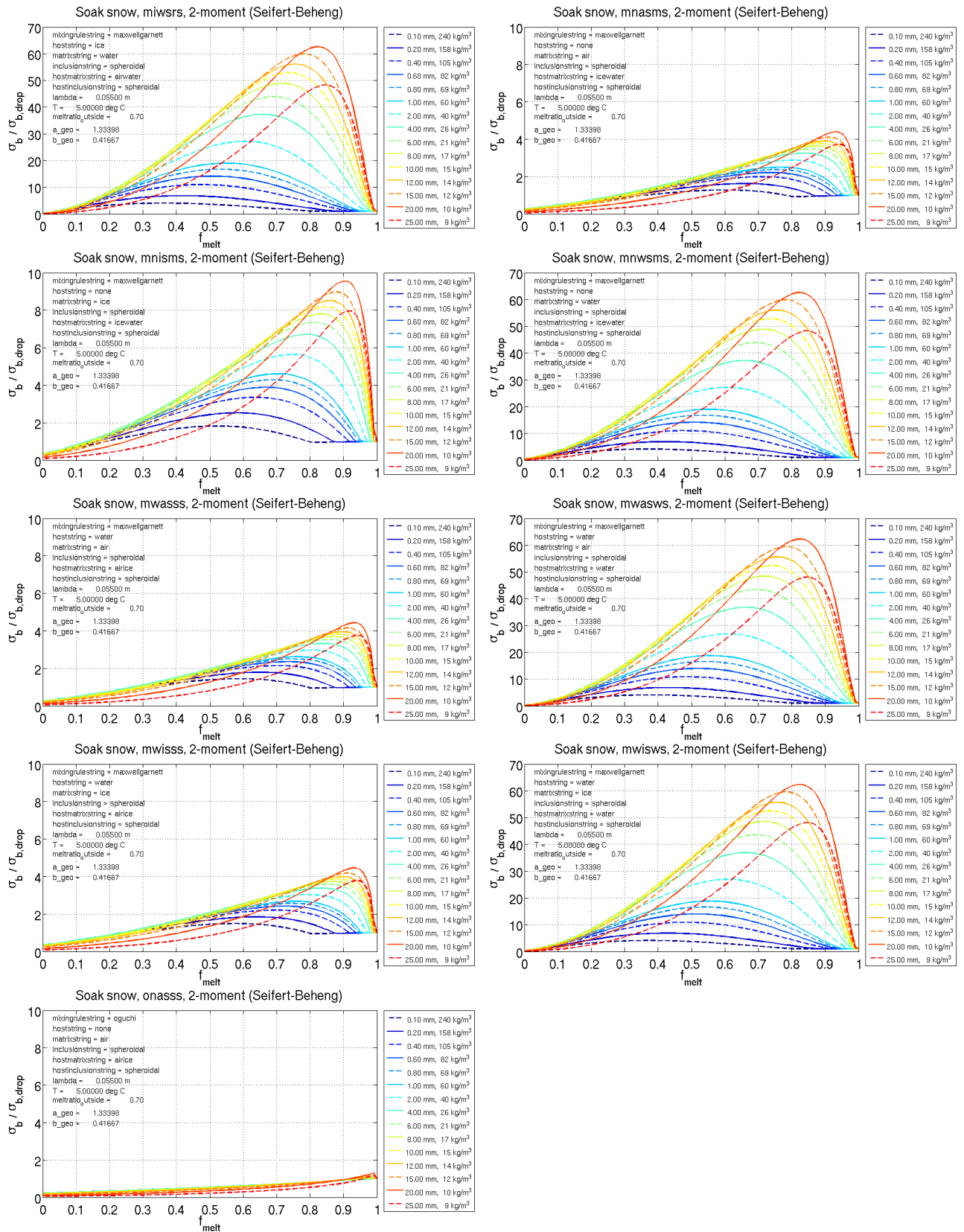


8.12 Mie: soaked wet snow, Seifert/Beheng-scheme

Similar to Subsection 8.9, results are shown for calculations of the backscattering cross section σ_b with subroutine `MIE.SOAK_WETGRAUPEL()` (Mie scattering), see subsubsection 5.3.11 on Page 48. But this time, the particle bulk density as function of size is determined by equation (39) on Page 69. A depiction of the resulting bulk density as function of particle size can be found in Figure 10 (green solid line). The following figures show the ratio of $\sigma_b/\sigma_{b,drop}$ as function of f_{melt} and the unmelted particle diameter for different EMA-formulations of the particles effective refractive index m_{eff} .

Again, every figure represents one particular EMA-formulation for m_{eff} , which is obtained by using function `get_m_mix_nested()` (subsubsection 5.2.5 on Page 28). The input parameter set for `get_m_mix_nested()` can be found in the text annotation within each graph. Although not being implemented into the LM interface functions for snow, the corresponding setting of the (provisional) namelist-parameter `ctype_wetsnow` (in analogy to `ctype_wetgraupel`) can be found as 6-character code in the figures title. For explanation of this code, see Table 40.

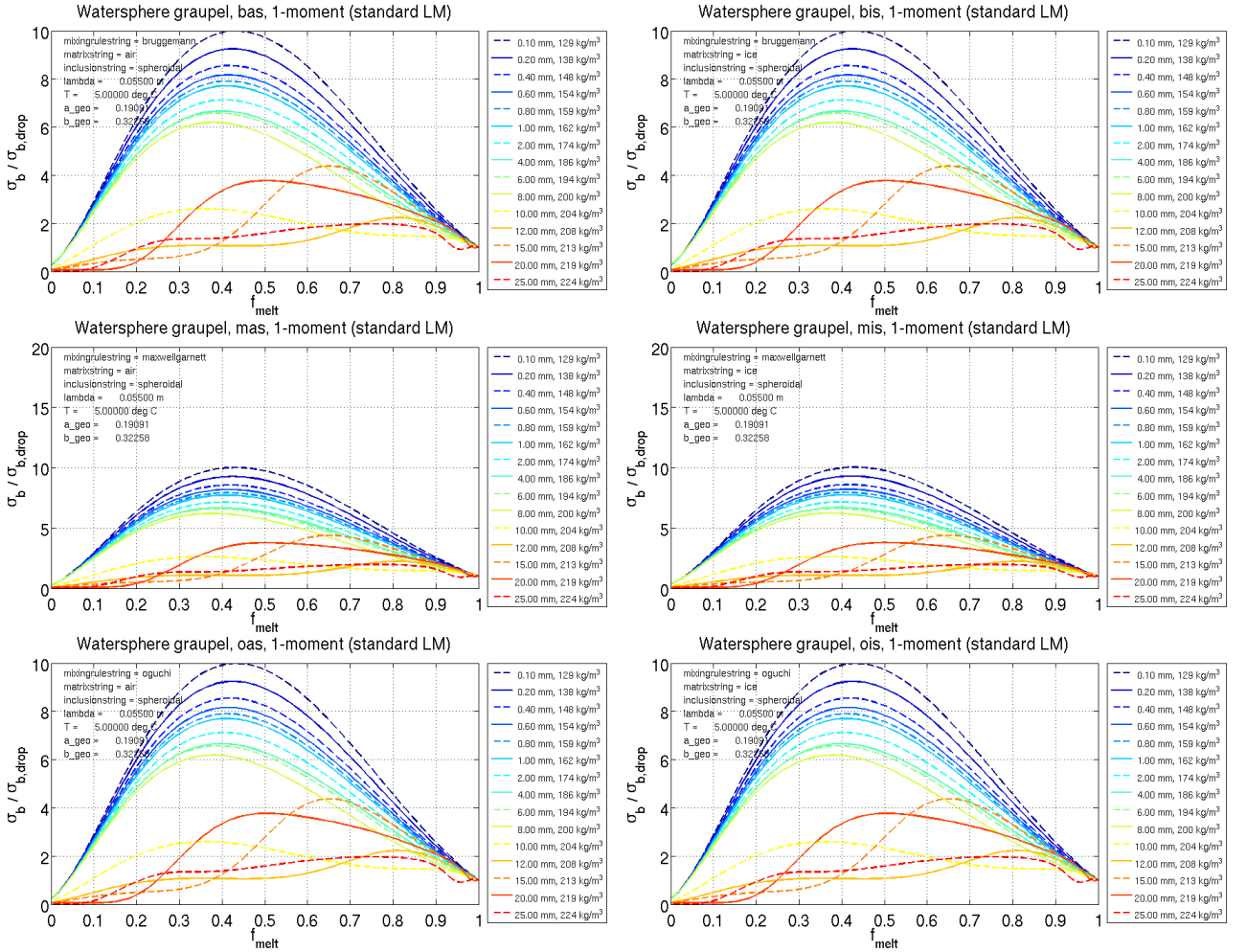




8.13 Mie: watersphere wet graupel, LM-scheme

Similar to Subsection 8.1, results are shown for calculations of the backscattering cross section σ_b with subroutine `MIE_WATERSPHERE_WETGRAUPEL()` (Mie scattering, two-layered sphere), see subsubsection 5.3.8 on Page 43. The following figures show the ratio of $\sigma_b/\sigma_{b,drop}$ as function of f_{melt} and the unmelted particle diameter for different EMA-formulations of the particles core effective refractive index m_{eff} . The particle bulk density as function of size is determined by equation (36) on Page 69. A depiction of the resulting bulk density as function of particle size can be found in Figure 10 (black solid line).

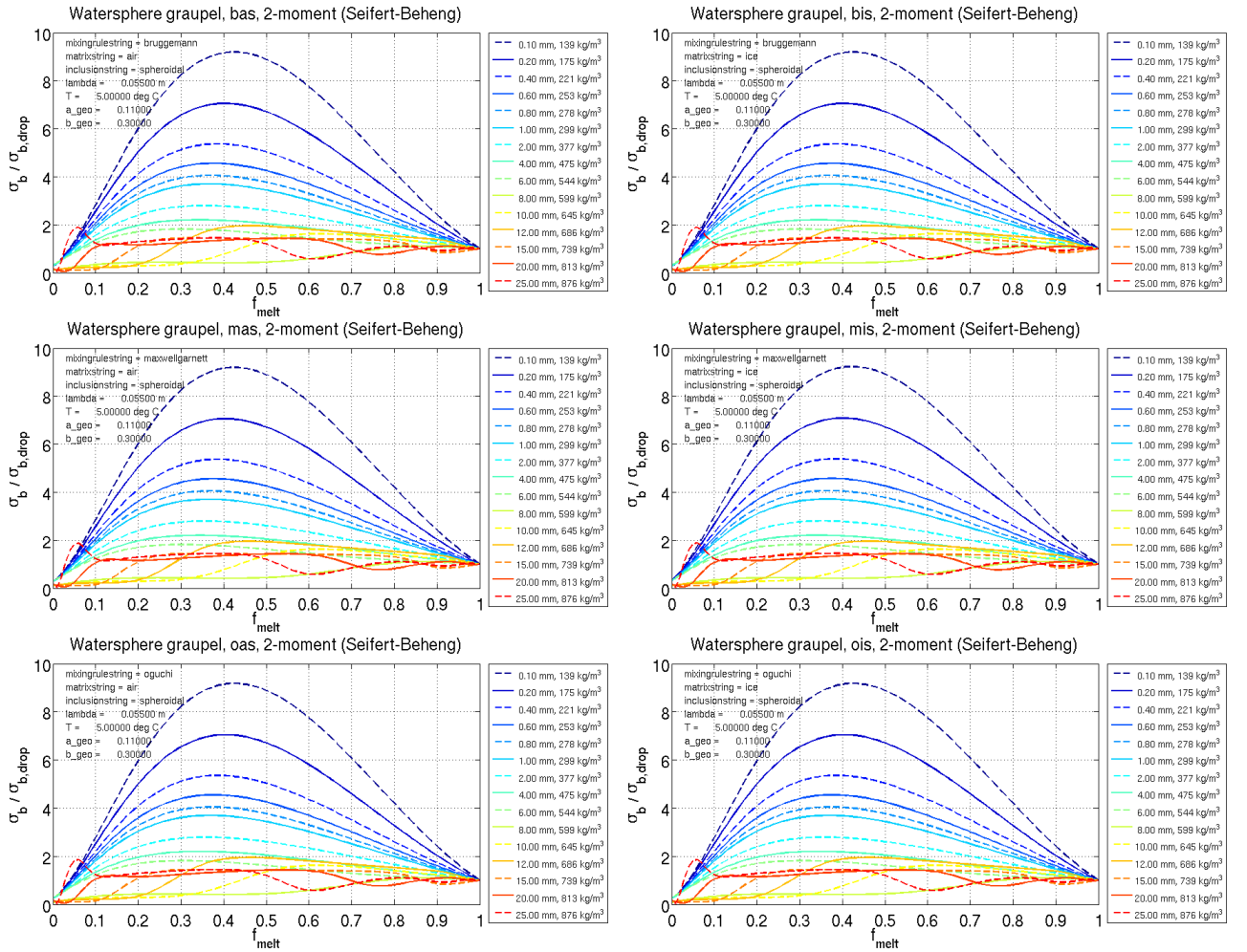
Again, every figure represents one particular EMA-formulation for m_{eff} of the particles ice-air core (the shell is composed of pure water), which is obtained by using function `get_m_mix()` (subsubsection 5.2.4 on Page 26). The input parameter set for `get_m_mix()` can be found in the text annotation within each graph. For users of the LM, the corresponding setting of the namelist-parameter `ctype.wetgraupel` can be found as 3-character code in the figures title. For explanation of this code, see Table 38. The results of this section apply to the LM for graupel particles in case of application of the standard LM one-moment bulk microphysical schemes (namelist-parameter `itype_gscp` < 100) together with `itype_refl` = 1 and `igraupel_type` = 3.



8.14 Mie: watersphere wet graupel, Seifert/Beheng-scheme

Similar to Subsection 8.13, results are shown for calculations of the backscattering cross section σ_b with subroutine `MIE_SOAK_WETGRAUPEL()` (Mie scattering, two-layered sphere), see subsection 5.3.8 on Page 43. But this time, the particle bulk density as function of size is determined by equation (37) on Page 69. A depiction of the resulting bulk density as function of particle size can be found in Figure 10 (red solid line). The following figures show the ratio of $\sigma_b/\sigma_{b,drop}$ as function of f_{melt} and the unmelted particle diameter for different EMA-formulations of the particles core effective refractive index m_{eff} .

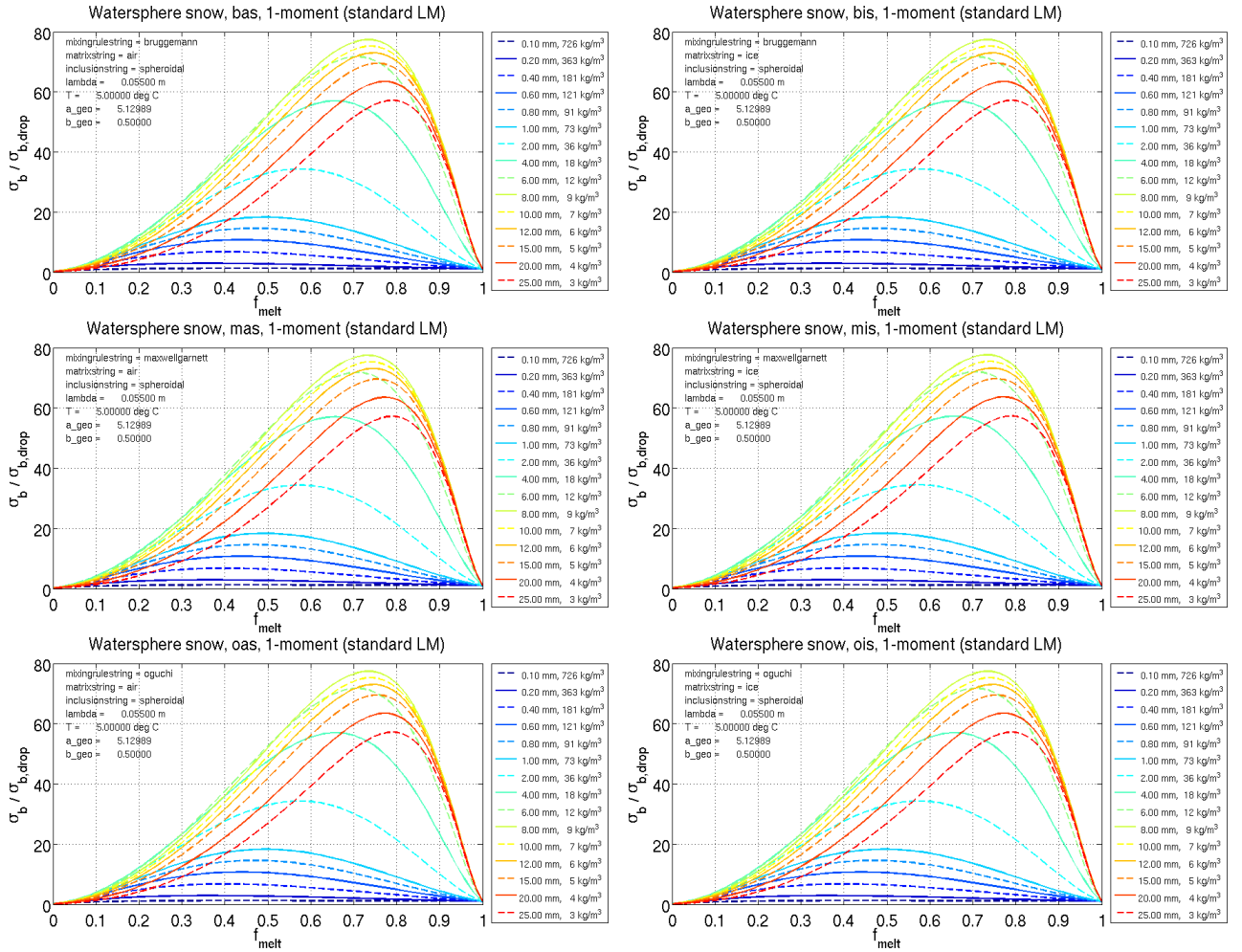
Again, every figure represents one particular EMA-formulation for m_{eff} of the particles ice-air core (the shell is composed of pure water), which is obtained by using function `get_m_mix()` (subsection 5.2.4 on Page 26). The input parameter set for `get_m_mix()` can be found in the text annotation within each graph. For users of the LM, the corresponding setting of the namelist-parameter `ctype_wetgraupel` can be found as 3-character code in the figures title. For explanation of this code, see Table 38. The results of this section apply to the LM for graupel particles in case of application of the Seifert and Beheng (2006) two-moment bulk microphysical scheme (namelist-parameter `itype_gscp` ≥ 100) together with `itype_refl` = 1 and `igraupel_type` = 3.



8.15 Mie: watersphere wet snow, LM-scheme

Similar to Subsection 8.13, results are shown for calculations of the backscattering cross section σ_b with subroutine `MIE_SOAK_WETGRAUPEL()` (Mie scattering, two-layered sphere), see subsubsection 5.3.8 on Page 43. But this time, the particle bulk density as function of size is determined by equation (38) on Page 69. A depiction of the resulting bulk density as function of particle size can be found in Figure 10 (blue solid line). The following figures show the ratio of $\sigma_b/\sigma_{b,drop}$ as function of f_{melt} and the unmelted particle diameter for different EMA-formulations of the particles core effective refractive index m_{eff} .

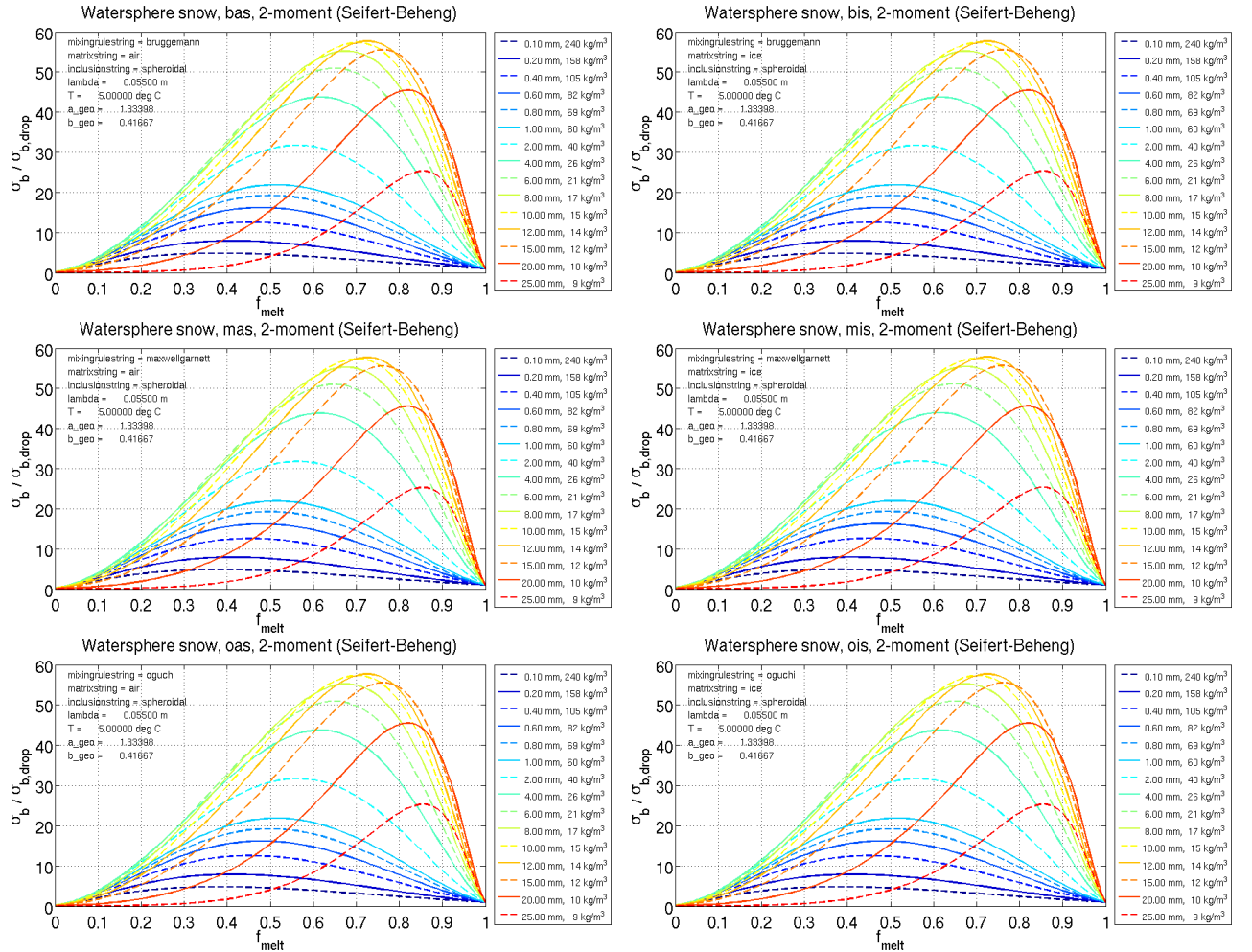
Again, every figure represents one particular EMA-formulation for m_{eff} of the particles ice-air core (the shell is composed of pure water), which is obtained by using function `get_m_mix()` (subsubsection 5.2.4 on Page 26). The input parameter set for `get_m_mix()` can be found in the text annotation within each graph. Although not being implemented into the LM interface functions for snow, the corresponding setting of the (provisional) namelist-parameter `ctype_wetsnow` (in analogy to `ctype_wetgraupele`) can be found as 3-character code in the figures title. For explanation of this code, see Table 38.



8.16 Mie: watersphere wet snow, Seifert/Beheng-scheme

Similar to Subsection 8.13, results are shown for calculations of the backscattering cross section σ_b with subroutine `MIE_SOAK_WETGRAUPEL()` (Mie scattering, two-layered sphere), see subsection 5.3.8 on Page 43. But this time, the particle bulk density as function of size is determined by equation (39) on Page 69. A depiction of the resulting bulk density as function of particle size can be found in Figure 10 (green solid line). The following figures show the ratio of $\sigma_b/\sigma_{b,drop}$ as function of f_{melt} and the unmelted particle diameter for different EMA-formulations of the particles core effective refractive index m_{eff} .

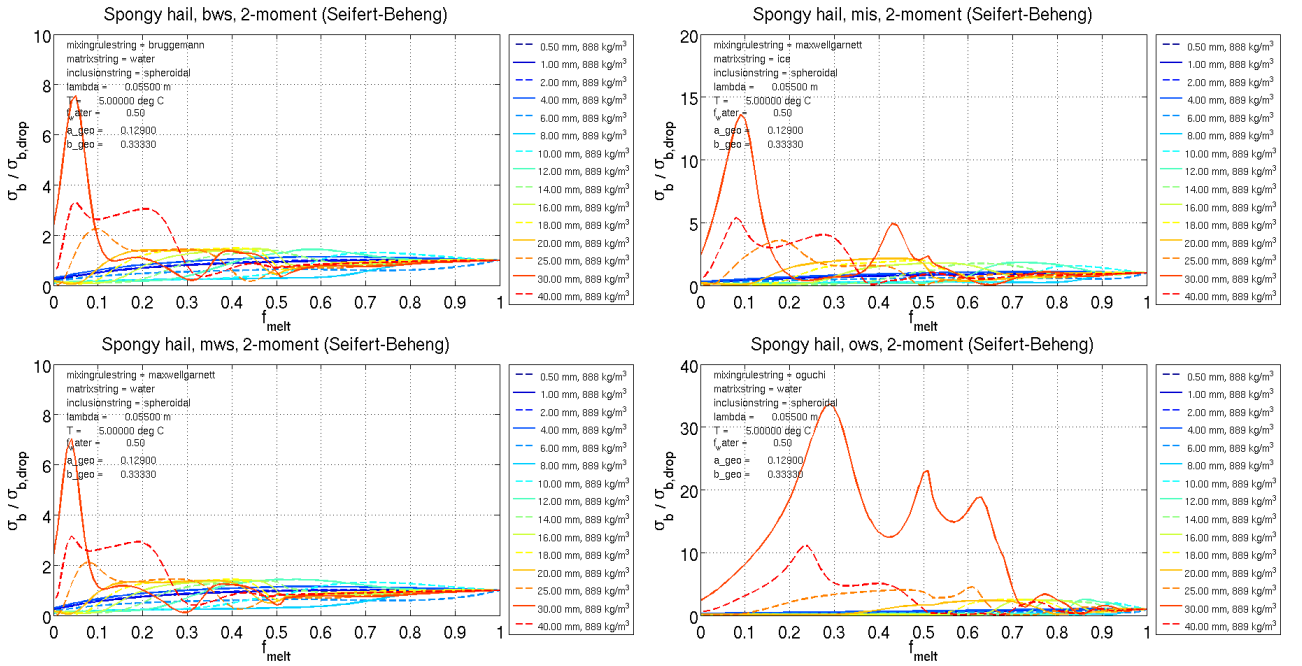
Again, every figure represents one particular EMA-formulation for m_{eff} of the particles ice-air core (the shell is composed of pure water), which is obtained by using function `get_m_mix()` (subsection 5.2.4 on Page 26). The input parameter set for `get_m_mix()` can be found in the text annotation within each graph. Although not being implemented into the LM interface functions for snow, the corresponding setting of the (provisional) namelist-parameter `ctype_wetsnow` (in analogy to `ctype_wetgraupel`) can be found as 3-character code in the figures title. For explanation of this code, see Table 38.



8.17 Mie: spongy wet hail, Seifert/Beheng-scheme

Similar to Subsection 8.1, results are shown for calculations of the backscattering cross section σ_b with subroutine `MIE.SPONGY_WETHAIL()` (Mie scattering, two-layered sphere), see subsubsection 5.3.7 on Page 41. The following figures show the ratio of $\sigma_b/\sigma_{b,drop}$ as function of f_{melt} and the unmelted particle diameter for different EMA-formulations of the particles ice-water shell effective refractive index m_{eff} . The unmelted particle bulk density does not depend on size here and is that of pure ice. The input parameter `f_water` (melt fraction within the ice-water shell) was set to 0.5, independent of size and f_{melt} .

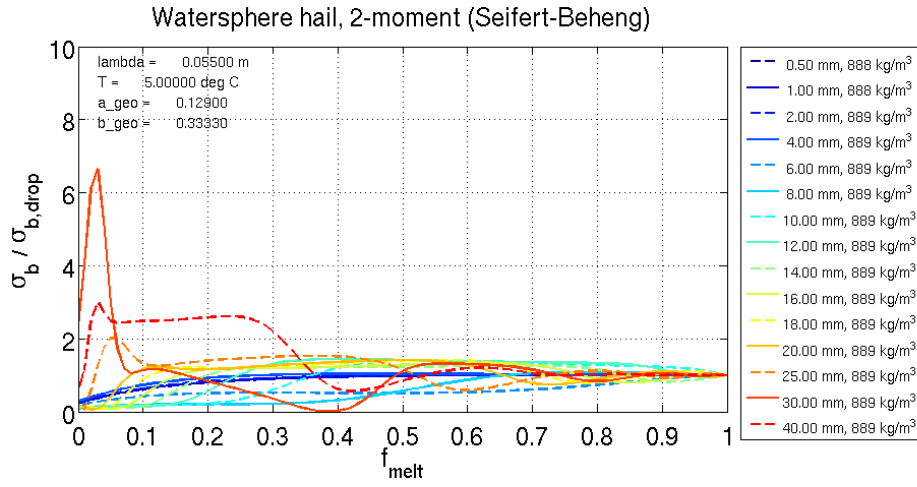
Again, every figure represents one particular EMA-formulation for m_{eff} of the particles ice-water shell (the core is composed of solid ice), which is obtained by using function `get_m_mix()` (subsubsection 5.2.4 on Page 26). The input parameter set for `get_m_mix()` can be found in the text annotation within each graph. For users of the LM, the corresponding setting of the namelist-parameter `ctype_wethail` can be found as 3-character code in the figures title. For explanation of this code, see Table 39. The results of this section apply to the LM for hail particles in case of application of the Seifert and Beheng (2006) two-moment bulk microphysical scheme (namelist-parameter `itype_gscp` ≥ 100) together with `itype_refl` = 1.



8.18 Mie: watersphere wet hail, Seifert/Beheng-scheme

Similar to Subsection 8.17, results are shown for calculations of the backscattering cross section σ_b with subroutine `MIE_WATERSPHERE_WETHAIL()` (Mie scattering, two-layered sphere), see subsubsection 5.3.6 on Page 40. The following figure shows the ratio of $\sigma_b/\sigma_{b,drop}$ as function of f_{melt} and the unmelted particle diameter. Since the core is composed of pure ice and the shell is assumed to be water, no effective medium approximation for m_{eff} of mixture materials is needed here. Therefore, only one figure is sufficient in the following.

`MIE_WATERSPHERE_WETHAIL()` is not implemented into the interface subroutines for the LM, but would be a possible choice in case of application of the Seifert and Beheng (2006) two-moment bulk microphysical scheme (namelist-parameter `itype_gscp` ≥ 100), together with `itype_refl` = 1.

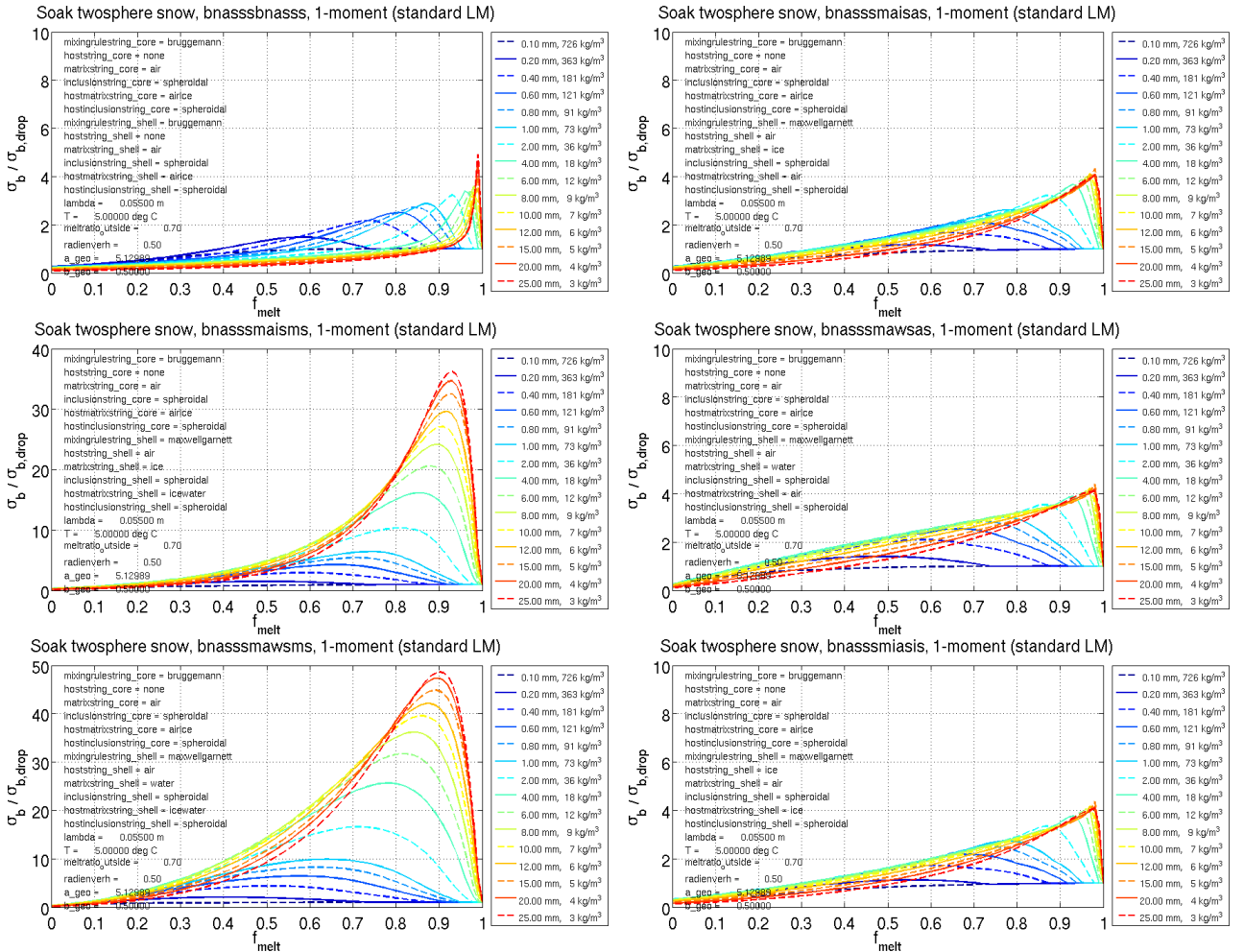


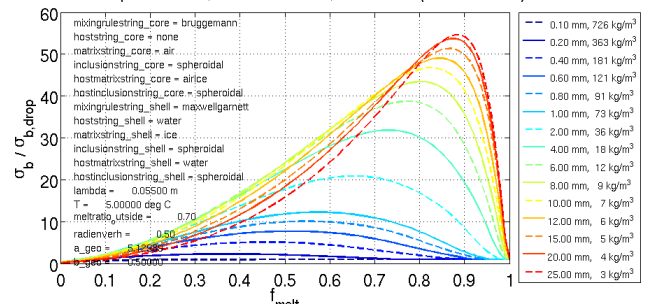
8.19 Mie: twosphere soaked wet snow, LM-scheme

Similar to Subsection 8.1, results are shown for calculations of the backscattering cross section σ_b with subroutine `MIE_WETSNOW_TWOSPHERE()` (Mie scattering, two-layered sphere), see subsubsection 5.3.13 on Page 51. The following figures show the ratio of $\sigma_b/\sigma_{b,drop}$ as function of f_{melt} and the unmelted particle diameter for different EMA-formulations of the particles core and shell effective refractive indices m_{eff} . The particle bulk density as function of size is determined by equation (38) on Page 69. A depiction of the resulting bulk density as function of particle size can be found in Figure 10 (blue solid line).

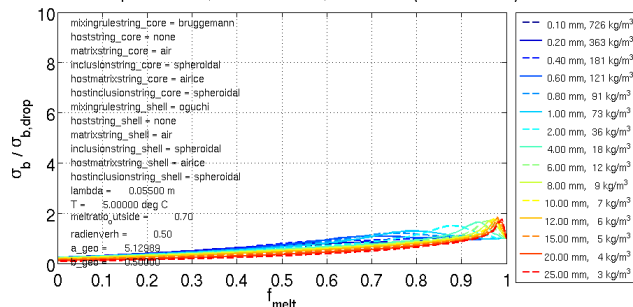
The input parameter `meltingratio_outside` (see subsubsection 5.3.13 on Page 51) is set to 0.7, and `radienverh` (inner to outer sphere radius) is set to 0.5, independent of size and f_{melt} .

Again, every figure represents one particular EMA-formulation for m_{eff} of the particles ice-water-air core and ice-water-air shell, which both are obtained by using function `get_m_mix_nested()` (subsubsection 5.2.5 on Page 28). The input parameter sets of `get_m_mix_nested()` for core and shell can be found in the text annotation within each graph. For users of the LM, the corresponding setting of the namelist-parameter `ctype_wetsnow` can be found as 12-character code in the figures title. For explanation of the two 6-character parts of this code, see Table 40. The first 6-character sequence corresponds to the core material, the second 6-character sequence to the shell material. The results of this section apply to the LM for snow particles in case of application of the standard LM one-moment bulk microphysical schemes (namelist-parameter `itype_gscp` < 100) together with `itype_refl` = 1.

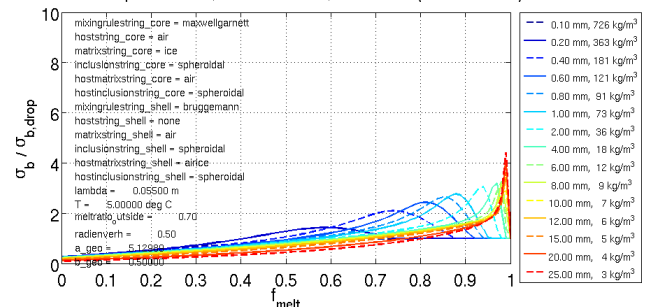




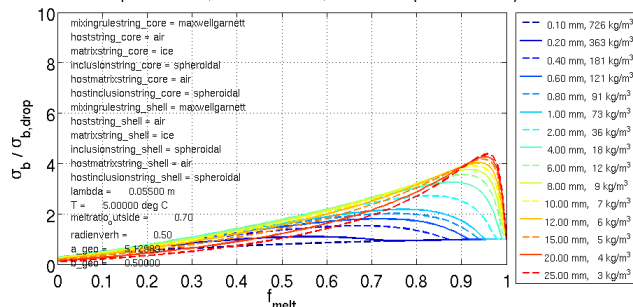
Soak twosphere snow, bnasssonasss, 1-moment (standard LM)



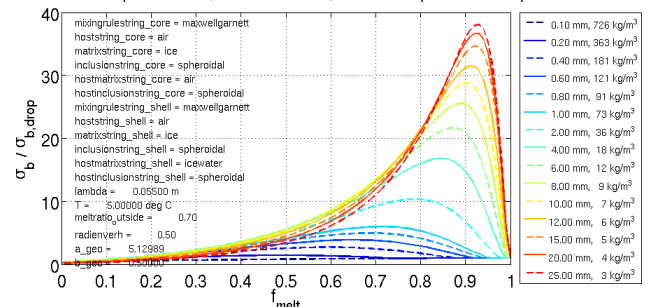
Soak twosphere snow, maisasbnasss, 1-moment (standard LM)



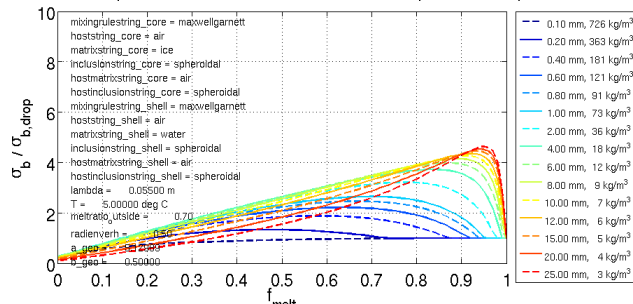
Soak twosphere snow, maisasmaisas, 1-moment (standard LM)



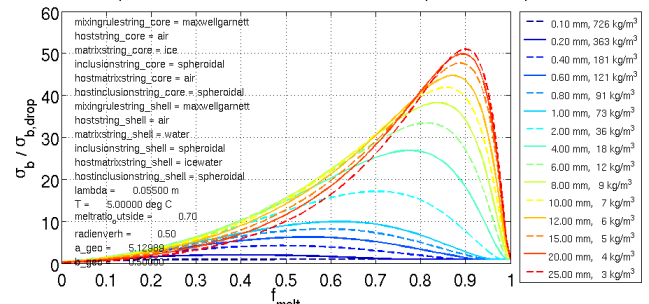
Soak twosphere snow, maisasmaisms, 1-moment (standard LM)



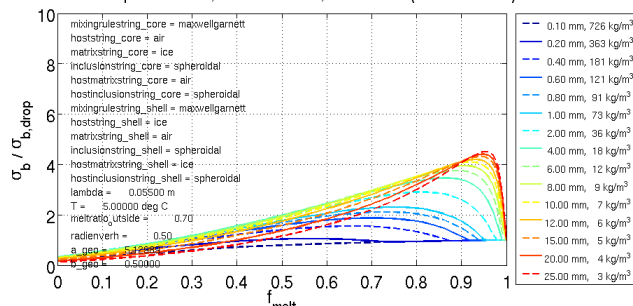
Soak twosphere snow, maisasmawsas, 1-moment (standard LM)



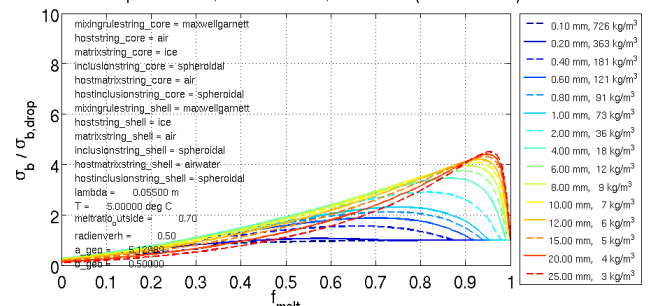
Soak twosphere snow, maisasmawsms, 1-moment (standard LM)



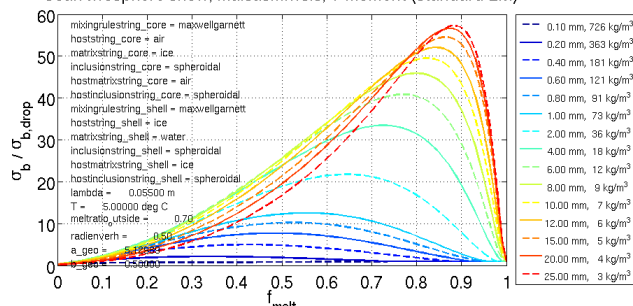
Soak twosphere snow, maisasmiasis, 1-moment (standard LM)



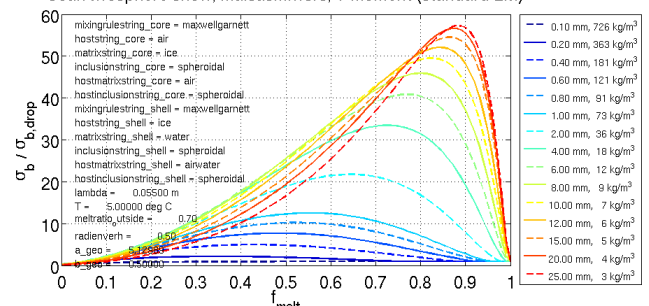
Soak twosphere snow, maisasmiasrs, 1-moment (standard LM)



Soak twosphere snow, maisasmis, 1-moment (standard LM)



Soak twosphere snow, maisasmisrs, 1-moment (standard LM)



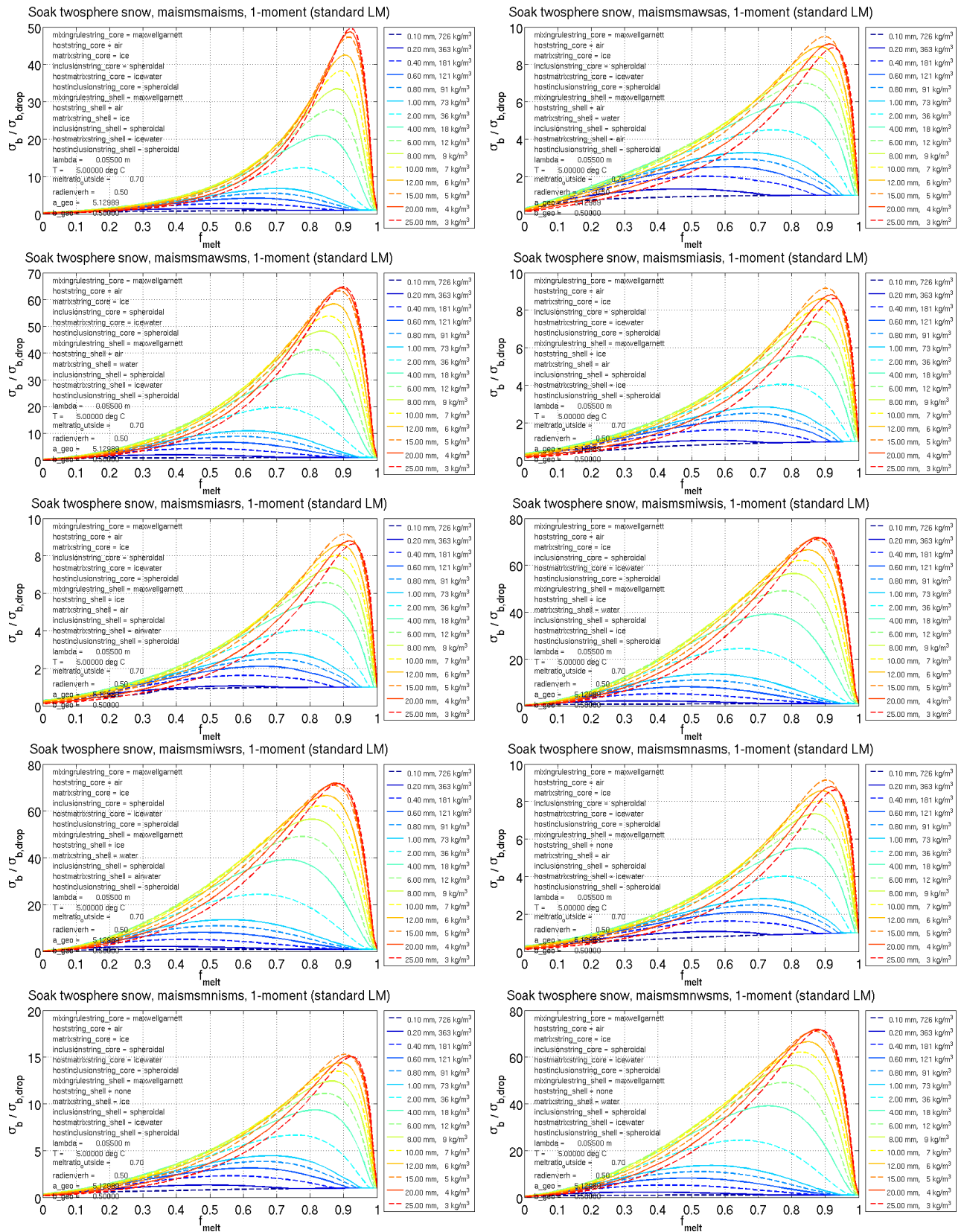
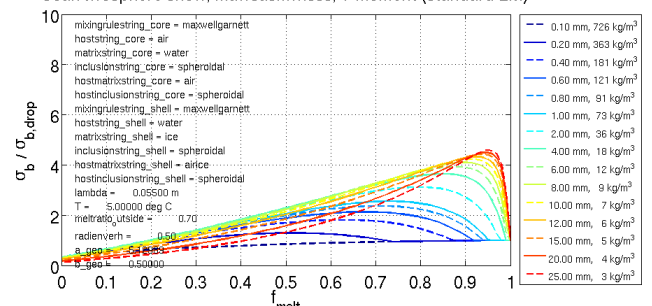


Figure 1 is a line graph showing the normalized standard deviation of the drop diameter, σ_b / σ_{drop} , as a function of the normalized time, t / t_{max} . The y-axis ranges from 0 to 60, and the x-axis ranges from 0 to 1. The legend lists 16 different cases, including combinations of core and shell materials and densities. The curves show that the standard deviation generally increases over time, peaking around $t / t_{max} = 0.9$, and then decreases. The peak values vary significantly depending on the material properties, with some cases reaching over 50.

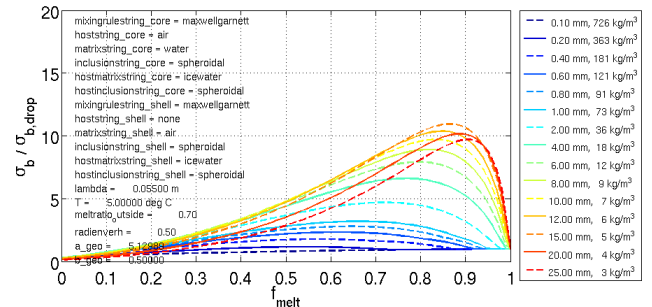
Case	Core Material	Shell Material	Density (kg/m^3)
1	mixingrulestring_core = maxwellgarnett	hoststring_core = air	0.10 mm, 726 kg/m^3
2	mixingrulestring_core = maxwellgarnett	hoststring_core = water	0.20 mm, 363 kg/m^3
3	inclusionstring_core = spheroidal	hoststring_core = air	0.40 mm, 181 kg/m^3
4	inclusionstring_core = spheroidal	hoststring_core = water	0.60 mm, 121 kg/m^3
5	mixingrulestring_shell = maxwellgarnett	hoststring_shell = air	0.80 mm, 91 kg/m^3
6	mixingrulestring_shell = maxwellgarnett	hoststring_shell = water	1.00 mm, 73 kg/m^3
7	inclusionstring_shell = spheroidal	hoststring_shell = air	2.00 mm, 36 kg/m^3
8	inclusionstring_shell = spheroidal	hoststring_shell = water	4.00 mm, 18 kg/m^3
9	mixingrulestring_shell = maxwellgarnett	hoststring_shell = air	6.00 mm, 12 kg/m^3
10	mixingrulestring_shell = maxwellgarnett	hoststring_shell = water	8.00 mm, 9 kg/m^3
11	inclusionstring_shell = spheroidal	hoststring_shell = air	10.00 mm, 7 kg/m^3
12	inclusionstring_shell = spheroidal	hoststring_shell = water	12.00 mm, 6 kg/m^3
13	mixingrulestring_shell = maxwellgarnett	hoststring_shell = air	15.00 mm, 5 kg/m^3
14	mixingrulestring_shell = maxwellgarnett	hoststring_shell = water	20.00 mm, 4 kg/m^3
15	inclusionstring_shell = spheroidal	hoststring_shell = air	25.00 mm, 3 kg/m^3
16	inclusionstring_shell = spheroidal	hoststring_shell = water	30.00 mm, 2 kg/m^3

Parameters for all cases:

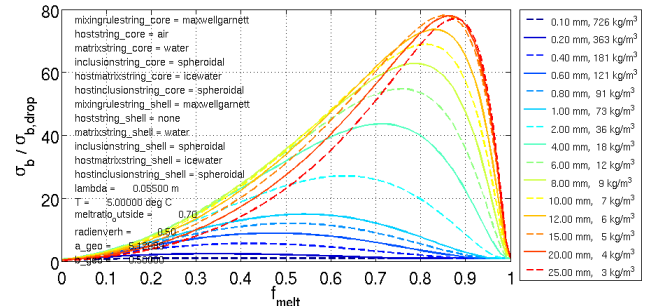
- $\lambda_{beta} = 0.06505 \text{ m}$
- $T = 5.00000 \text{ deg C}$
- $m_{relratio_ubside} = 0.70$
- $\text{radienverb} = 0.50$
- $\text{a_geo} = 5.12898$
- $\text{a_geo} = 14.5000$



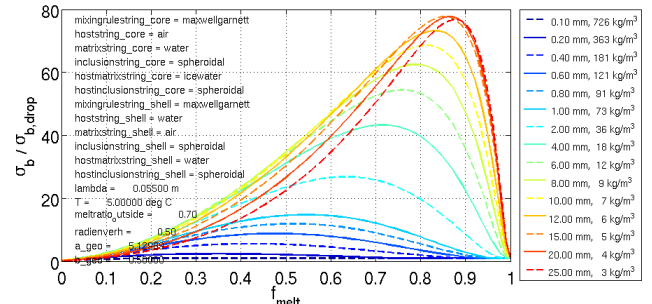
Soak twosphere snow, mawsmmnasms, 1-moment (standard LM)



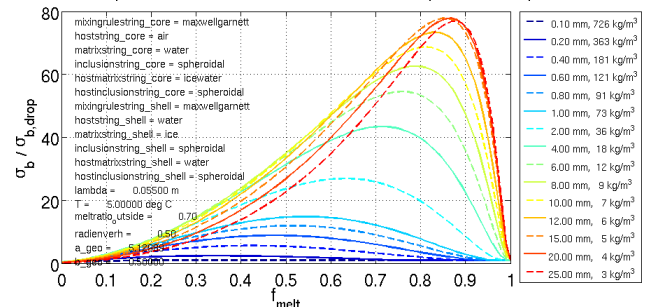
Soak twosphere snow, mawsmnwsms, 1-moment (standard LM)



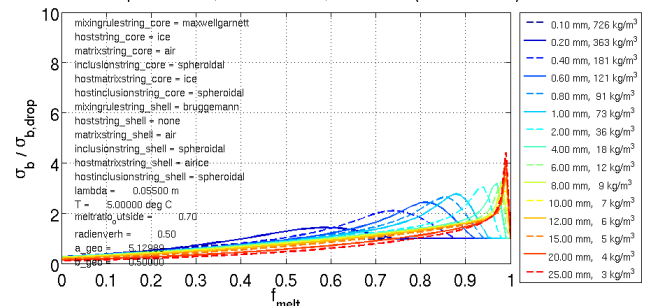
Soak twosphere snow, mawsmmswasws, 1-moment (standard LM)



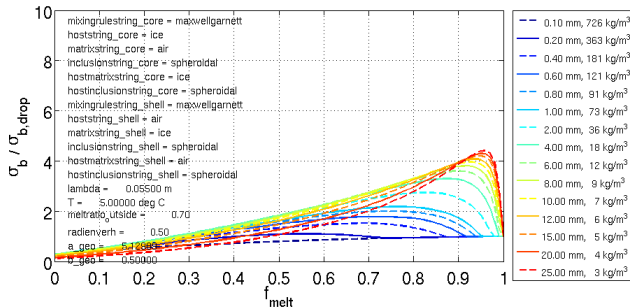
Soak twosphere snow, mawsmismwisws, 1-moment (standard LM)



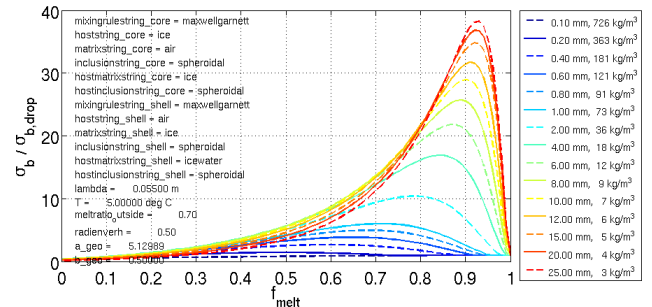
Soak twosphere snow, miasisbnasss, 1-moment (standard LM)



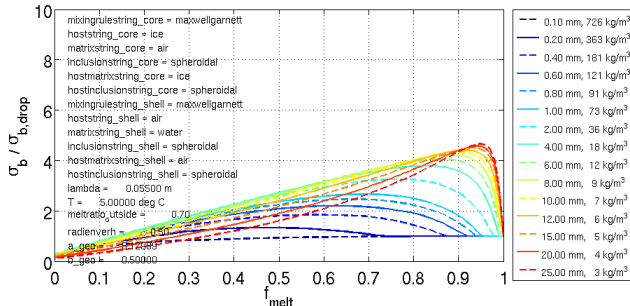
Soak twosphere snow, miasismaisas, 1-moment (standard LM)



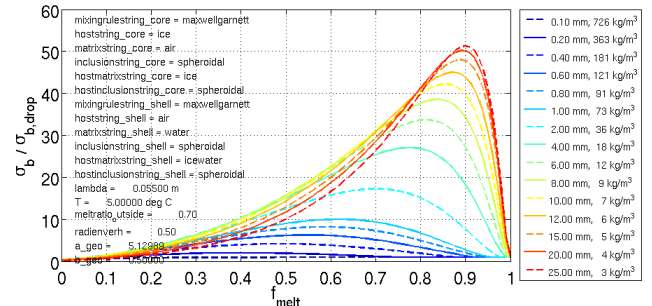
Soak twosphere snow, miasismaisms, 1-moment (standard LM)



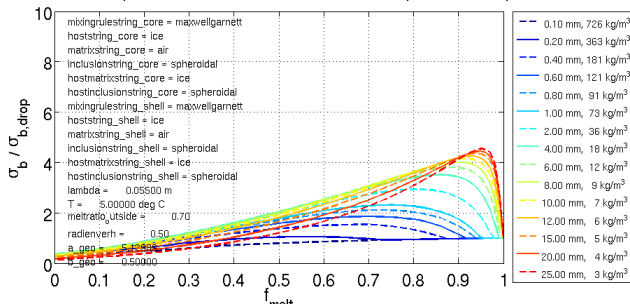
Soak twosphere snow, miasismawsas, 1-moment (standard LM)



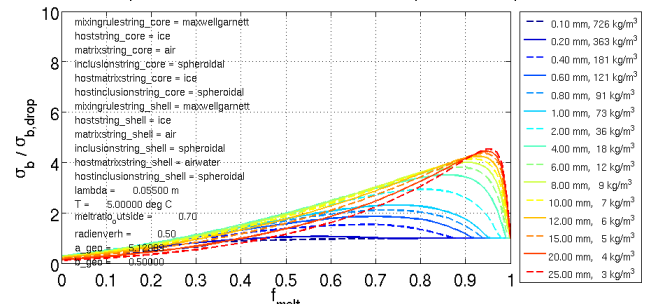
Soak twosphere snow, miasismawsms, 1-moment (standard LM)



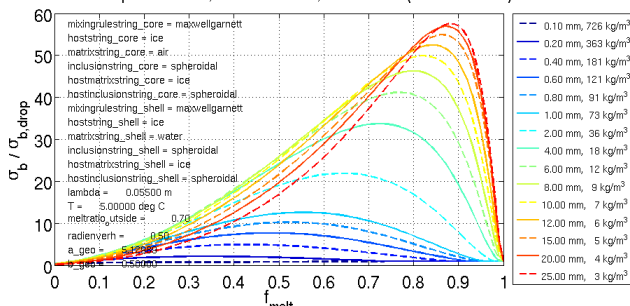
Soak twosphere snow, miasismiasis, 1-moment (standard LM)



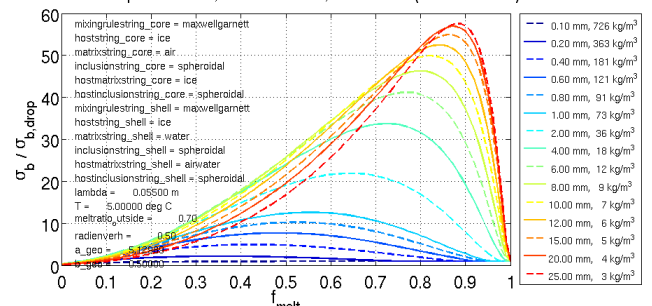
Soak twosphere snow, miasismiasrs, 1-moment (standard LM)



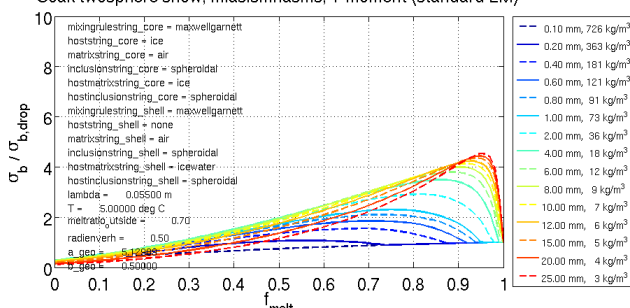
Soak twosphere snow, miasismiwsis, 1-moment (standard LM)



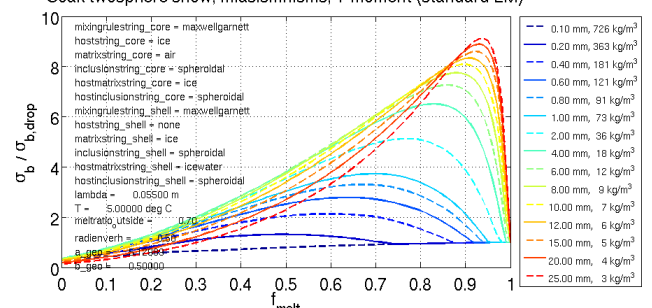
Soak twosphere snow, miasismiwsrs, 1-moment (standard LM)

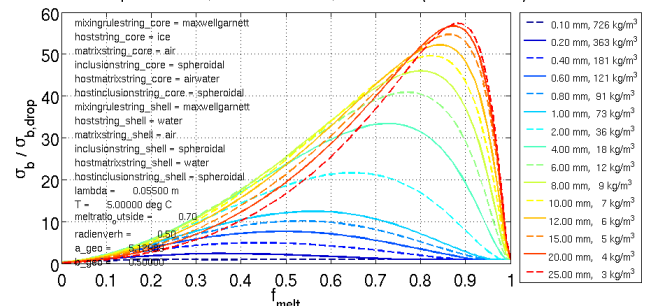


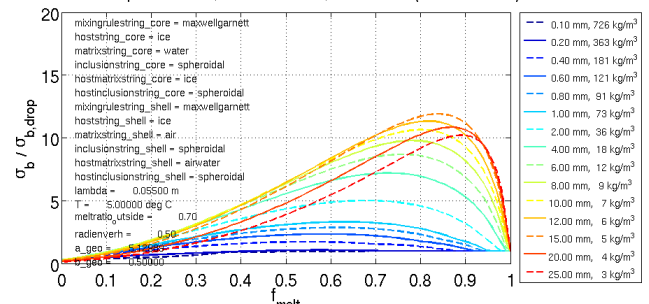
Soak twosphere snow, miasismnasms, 1-moment (standard LM)

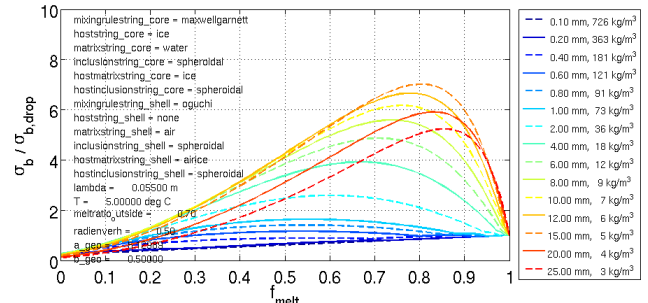


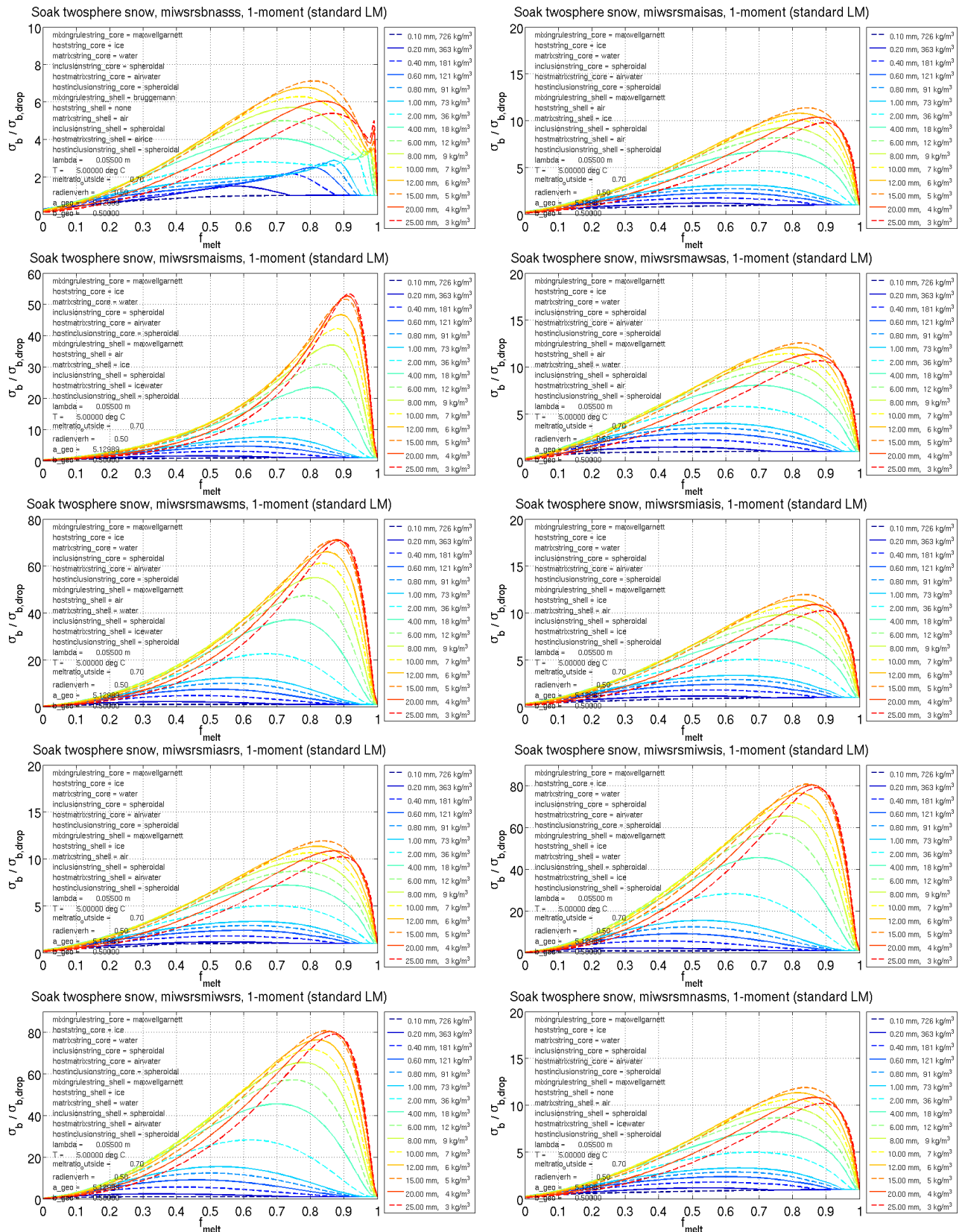
Soak twosphere snow, miasismnisms, 1-moment (standard LM)



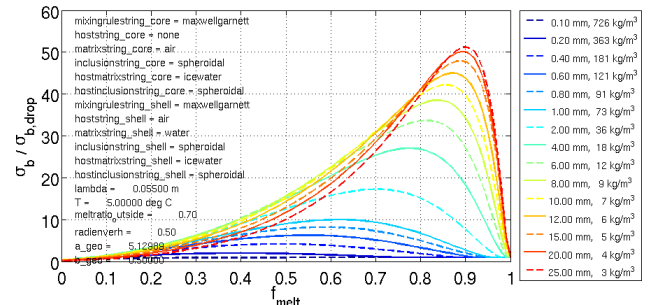




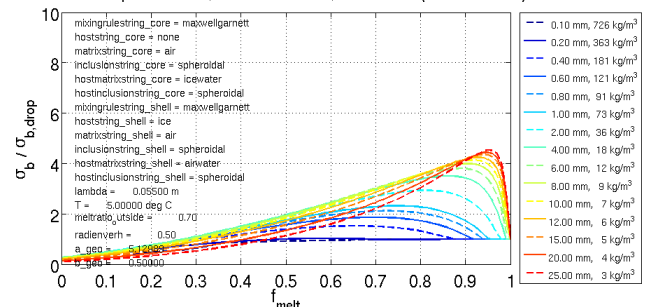




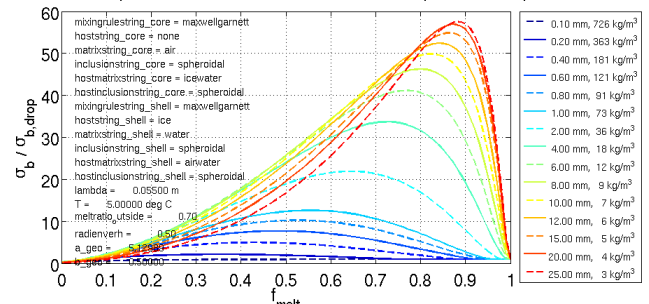
Soak twosphere snow, mnasmsmawsms, 1-moment (standard LM)



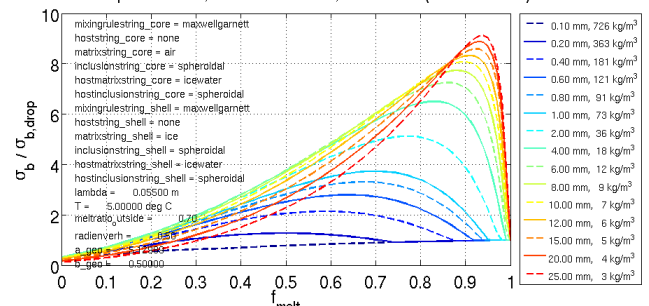
Soak twosphere snow, mnasmsmiasrs, 1-moment (standard LM)



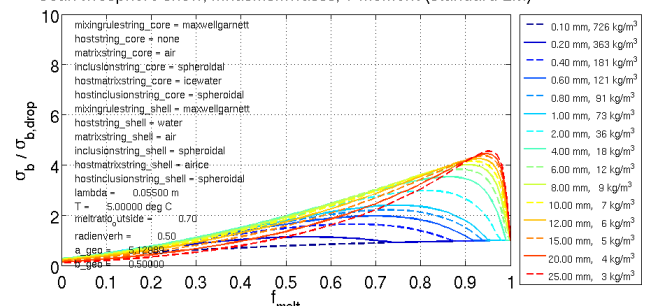
Soak twosphere snow, mnasmsmiwsrs, 1-moment (standard LM)

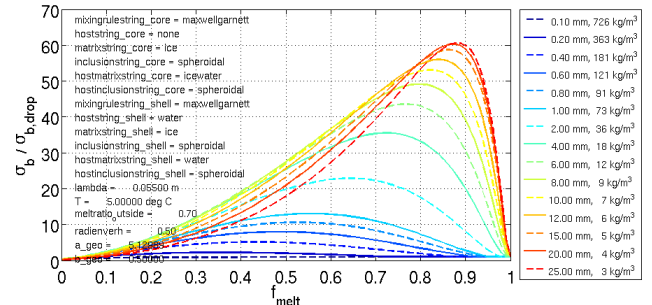


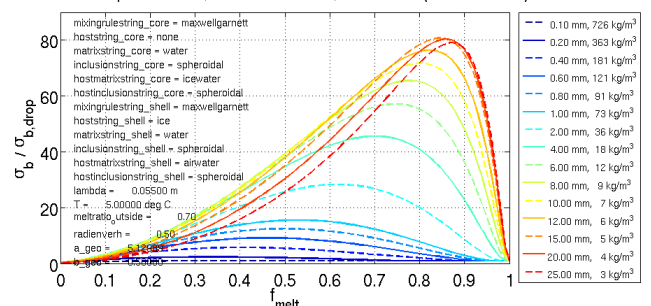
Soak twosphere snow, mnasmsmnisms, 1-moment (standard LM)



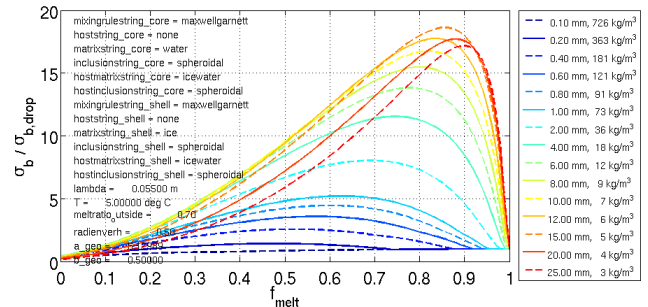
Soak twosphere snow, mnasmsmwasss, 1-moment (standard LM)



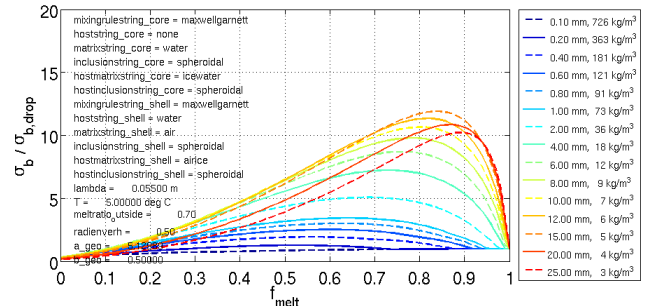




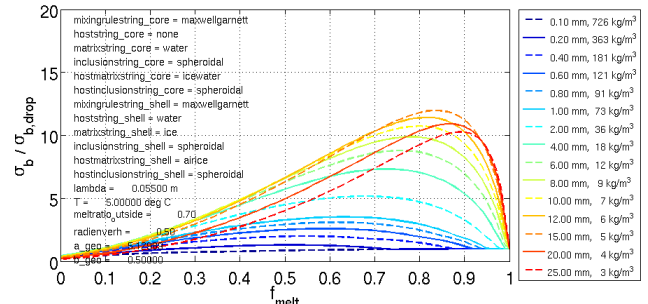
Soak twosphere snow, mnwsmsmnisms, 1-moment (standard LM)



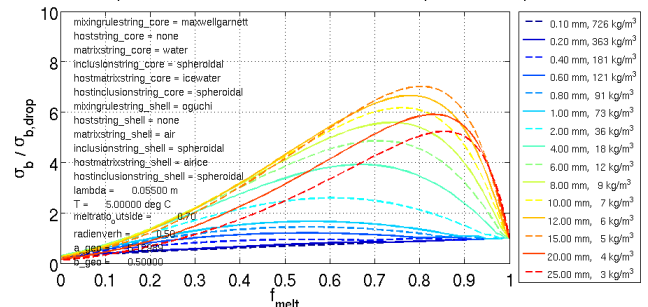
Soak twosphere snow, mnwsmsmwasss, 1-moment (standard LM)



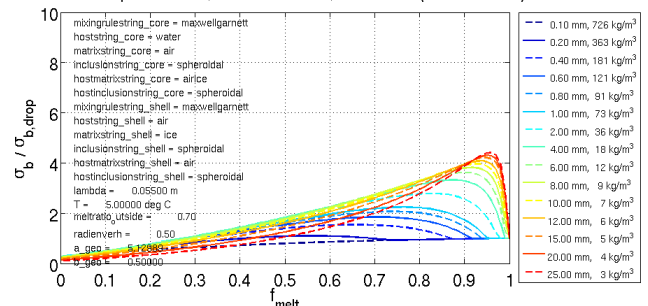
Soak twosphere snow, mnwsmmwisss, 1-moment (standard LM)

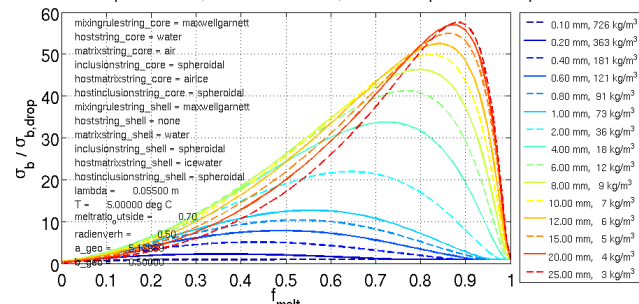


Soak twosphere snow, mnwsmsonasss, 1-moment (standard LM)

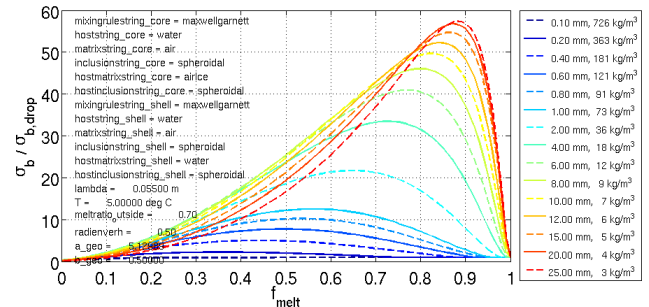


Soak twosphere snow, mwassssmaisas, 1-moment (standard LM)

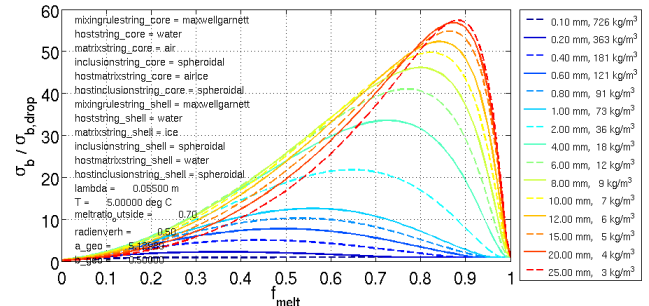




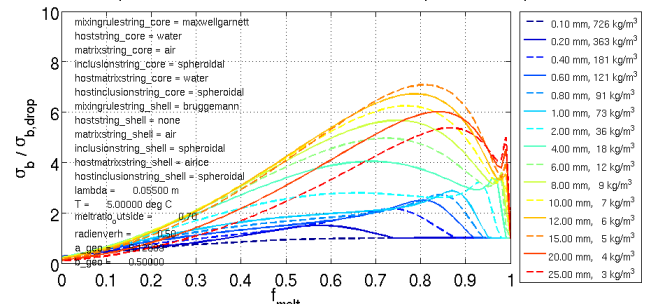
Soak twosphere snow, mwasssmwasws, 1-moment (standard LM)



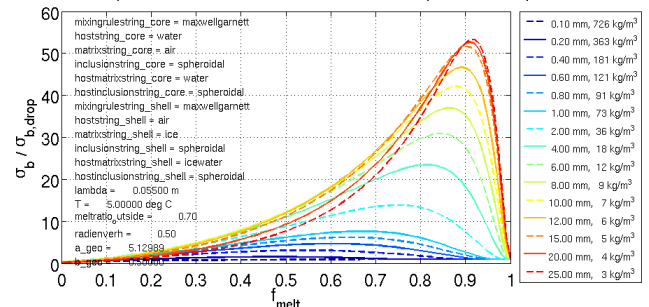
Soak twosphere snow, mwasssmwisws, 1-moment (standard LM)



Soak twosphere snow, mwaswsbnasss, 1-moment (standard LM)



Soak twosphere snow, mwaswsmaisms, 1-moment (standard LM)



Soak twosphere snow, mwaswsmawsms, 1-moment (standard LM)

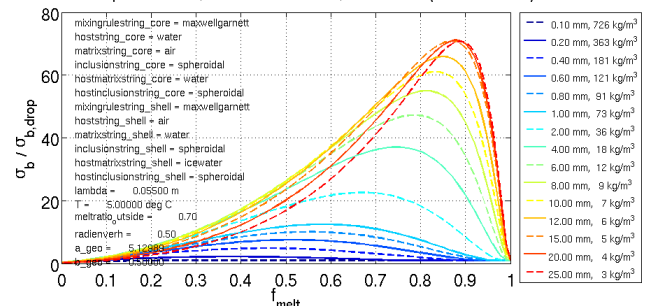


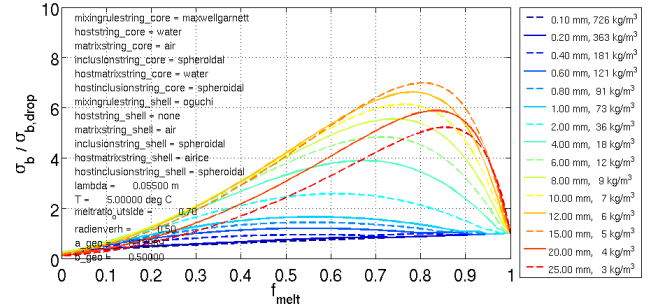
Figure 1 is a line graph showing the normalized standard deviation of the normalized standard deviation, σ_b / σ_{drop} , as a function of the normalized standard deviation of the normalized standard deviation, σ_b / σ_{drop} . The x-axis ranges from 0 to 1, and the y-axis ranges from 0 to 20. The graph displays multiple curves for different parameter values, including mixingrulestring_core, hoststring_core, matrixstring_core, inclusionstring_core, hostmatrixstring_core, hostinclusionstring_core, mixingrulestring_shell, hoststring_shell, matrixstring_shell, inclusionstring_shell, hostmatrixstring_shell, hostinclusionstring_shell, lambda_beta, T, a_geo, radiienv, and a_geo. The curves show a peak around $\sigma_b / \sigma_{drop} = 0.7$, with the peak height increasing as the parameter values increase. A legend on the right lists the parameter values for each curve.

Parameter	Value
mixingrulestring_core	maywellgarnett
hoststring_core	water
matrixstring_core	air
inclusionstring_core	spheroidal
hostmatrixstring_core	water
hostinclusionstring_core	spheroidal
mixingrulestring_shell	maywellgarnett
hoststring_shell	water
matrixstring_shell	ice
inclusionstring_shell	spheroidal
hostmatrixstring_shell	airice
hostinclusionstring_shell	spheroidal
lambda_beta	0.08500 m
T	-15.00000 deg C
radiienv	0.50
a_geo	0.50000

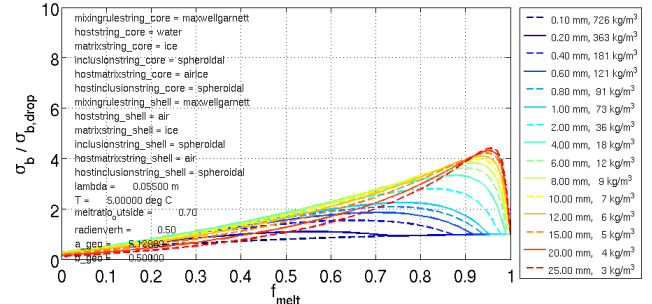
Legend (Right):

- 0.10 mm, 726 kg/m³
- 0.20 mm, 363 kg/m³
- 0.40 mm, 181 kg/m³
- 0.60 mm, 121 kg/m³
- 0.80 mm, 91 kg/m³
- 1.00 mm, 73 kg/m³
- 2.00 mm, 36 kg/m³
- 4.00 mm, 18 kg/m³
- 6.00 mm, 12 kg/m³
- 8.00 mm, 9 kg/m³
- 10.00 mm, 7 kg/m³
- 12.00 mm, 6 kg/m³
- 14.00 mm, 5 kg/m³
- 16.00 mm, 4 kg/m³
- 18.00 mm, 3 kg/m³
- 20.00 mm, 2 kg/m³
- 22.00 mm, 1 kg/m³
- 24.00 mm, 0.5 kg/m³
- 26.00 mm, 0.2 kg/m³

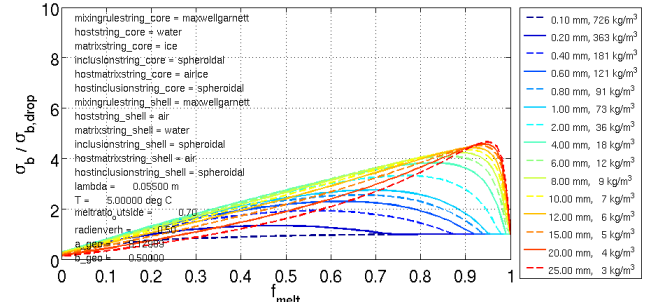
Soak twosphere snow, mwaswsonasss, 1-moment (standard LM)



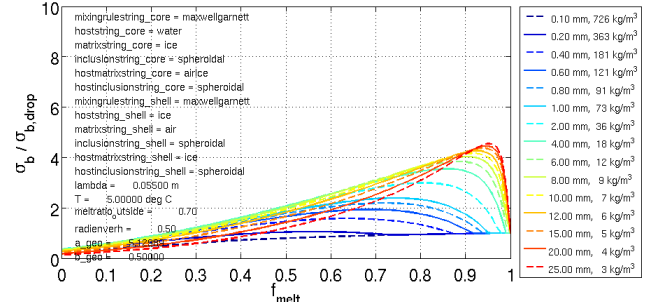
Soak twosphere snow, mwissssmaisas, 1-moment (standard LM)



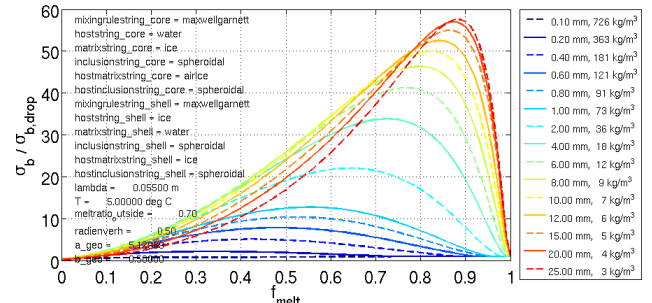
Soak twosphere snow, mwisssmawsas, 1-moment (standard LM)

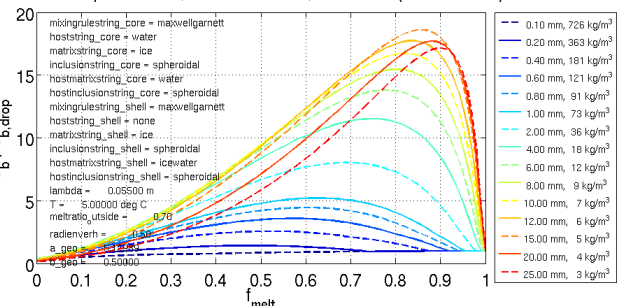


Soak twosphere snow, mwisssmiasis, 1-moment (standard LM)

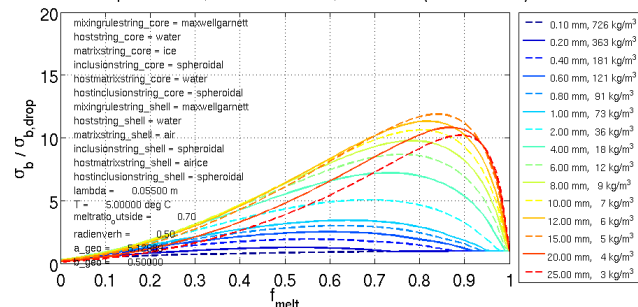


Soak twosphere snow, mwisssmiwsis, 1-moment (standard LM)

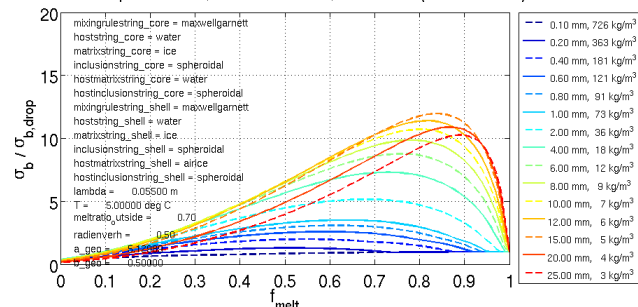




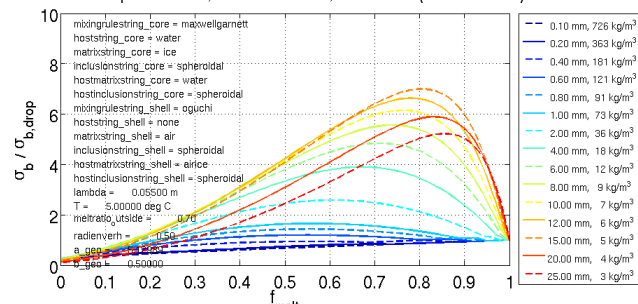
Soak twosphere snow, mwiswsmwasss, 1-moment (standard LM)



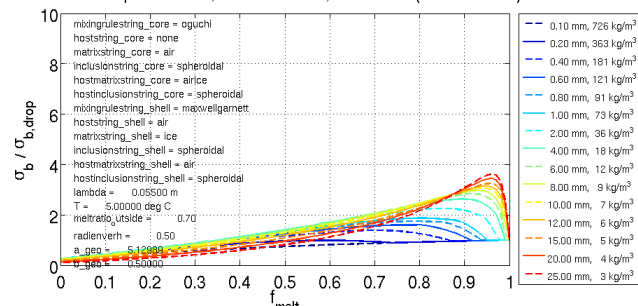
Soak twosphere snow, mwiswsmwisss, 1-moment (standard LM)



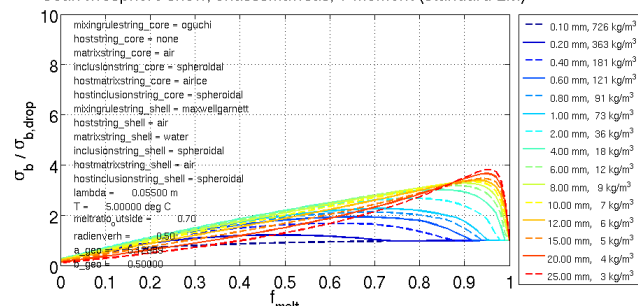
Soak twosphere snow, mwiswsonasss, 1-moment (standard LM)



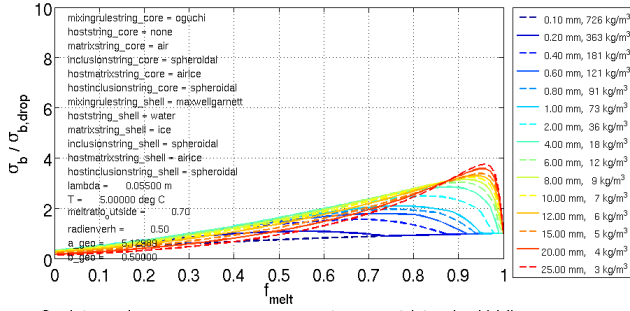
Soak twosphere snow, onasssmasias, 1-moment (standard LM)



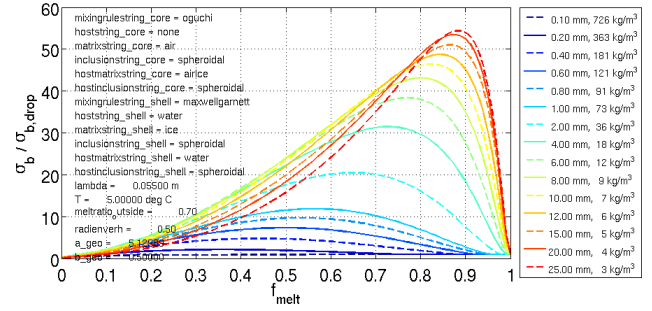
Soak twosphere snow, onasssmawsas, 1-moment (standard LM)



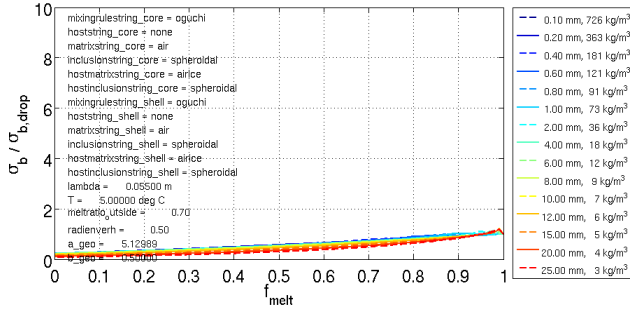
Soak twosphere snow, onasssmwisws, 1-moment (standard LM)



Soak twosphere snow, onasssmwisws, 1-moment (standard LM)



Soak twosphere snow, onasssonasss, 1-moment (standard LM)

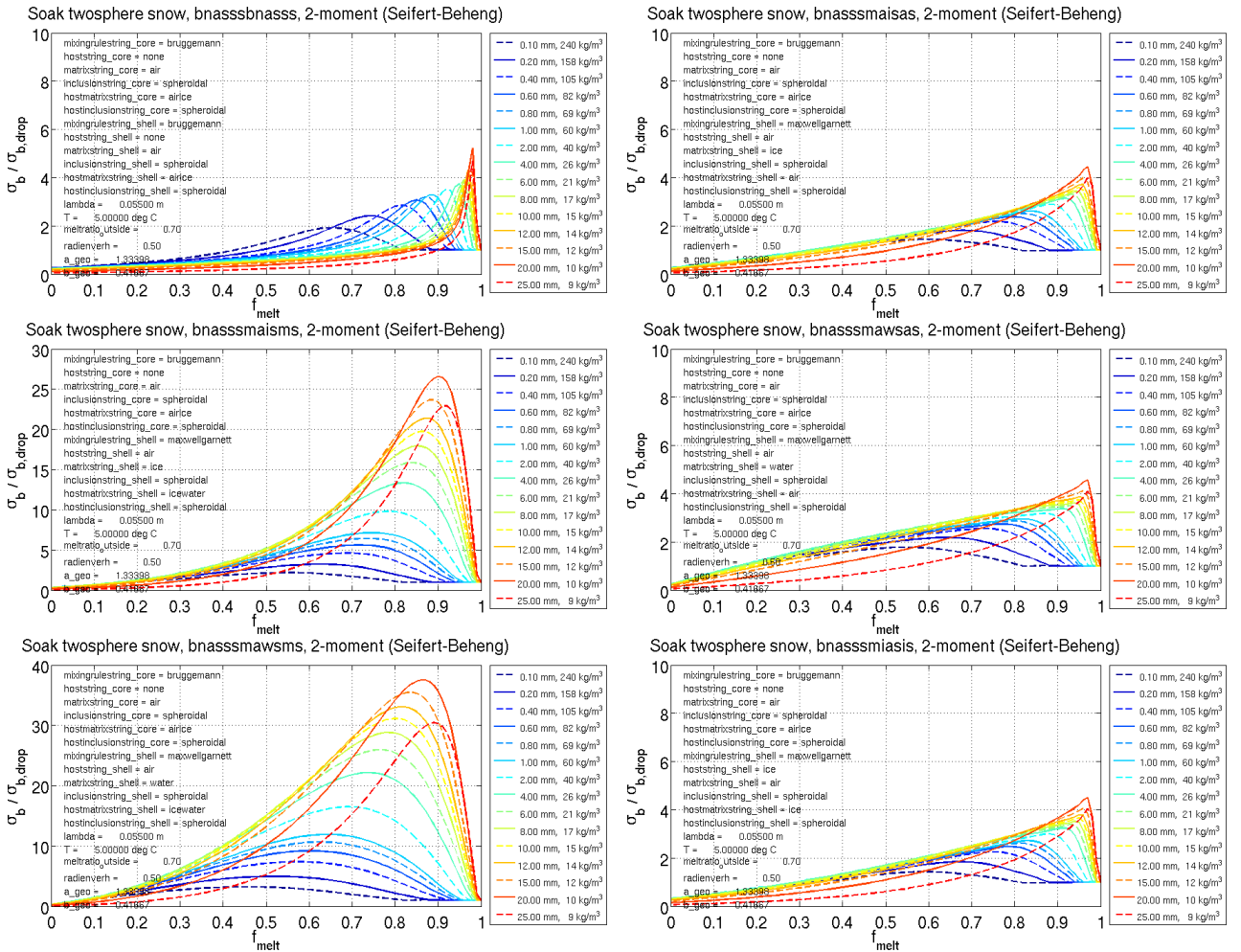


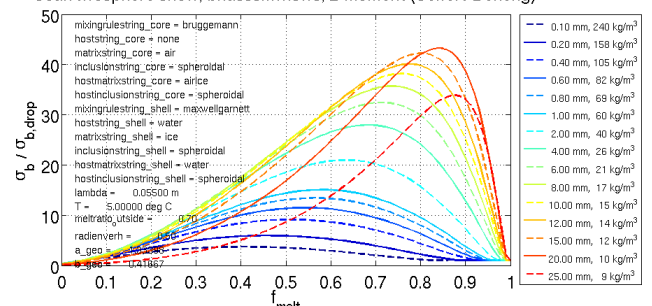
8.20 Mie: twosphere soaked wet snow, Seifert/Beheng-scheme

Similar to Subsection 8.19, results are shown for calculations of the backscattering cross section σ_b with subroutine `MIE_WETSNOW_TWOSPHERE()` (Mie scattering, two-layered sphere), see subsubsection 5.3.13 on Page 51. But this time, the particle bulk density as function of size is determined by equation (39) on Page 69. A depiction of the resulting bulk density as function of particle size can be found in Figure 10 (green solid line). The following figures show the ratio of $\sigma_b/\sigma_{b,drop}$ as function of f_{melt} and the unmelted particle diameter for different EMA-formulations of the particles core and shell effective refractive indices m_{eff} .

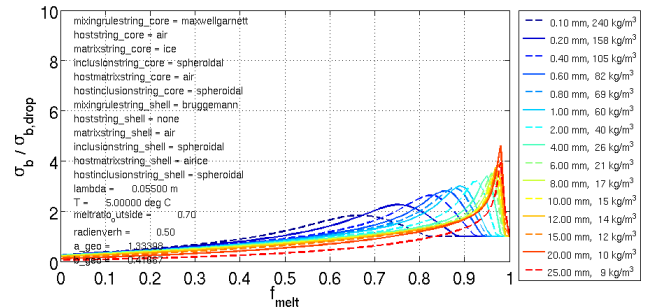
The input parameter `meltingratio_outside` (see subsubsection 5.3.13 on Page 51) is set to 0.7, and `radienverh` (inner to outer sphere radius) is set to 0.5, independent of size and f_{melt} .

Again, every figure represents one particular EMA-formulation for m_{eff} of the particles ice-water-air core and ice-water-air shell, which both are obtained by using function `get_m_mix_nested()` (subsubsection 5.2.5 on Page 28). The input parameter sets of `get_m_mix_nested()` for core and shell can be found in the text annotation within each graph. For users of the LM, the corresponding setting of the namelist-parameter `ctype_wetsnow` can be found as 12-character code in the figures title. For explanation of the two 6-character parts of this code, see Table 40. The first 6-character sequence corresponds to the core material, the second 6-character sequence to the shell material. The results of this section apply to the LM for snow particles in case of application of the Seifert and Beheng (2006) two-moment bulk microphysical scheme (namelist-parameter `itype_gscp` ≥ 100) together with `itype_refl` = 1.

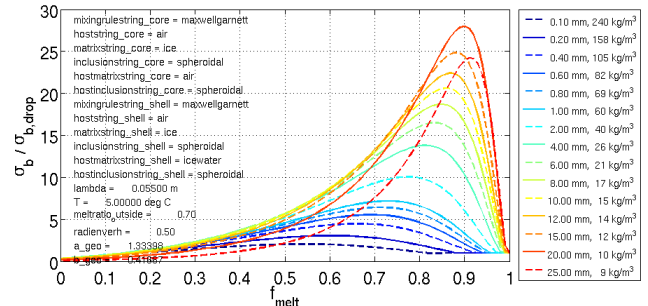




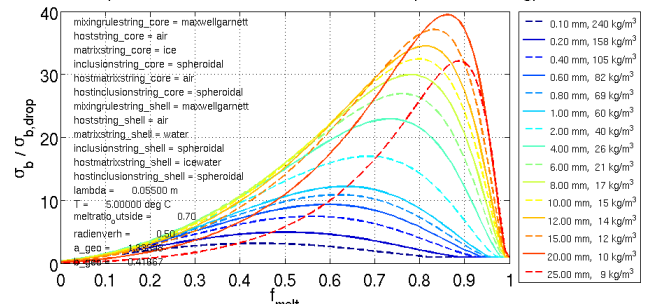
Soak twosphere snow, maisasbnasss, 2-moment (Seifert-Beheng)



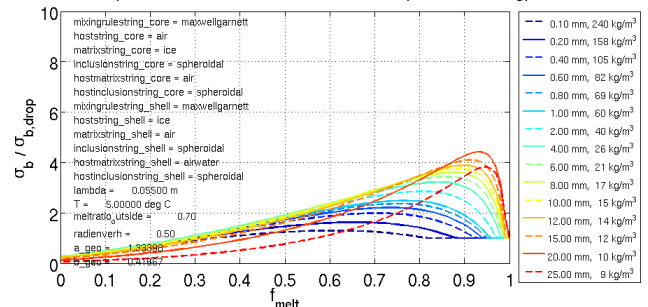
Soak twosphere snow, maisasmaisms, 2-moment (Seifert-Beheng)



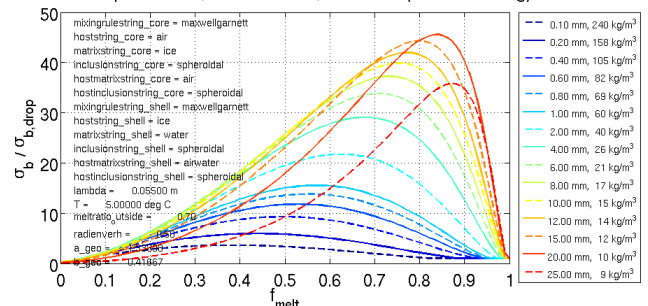
Soak twosphere snow, maisasmawsms, 2-moment (Seifert-Beheng)



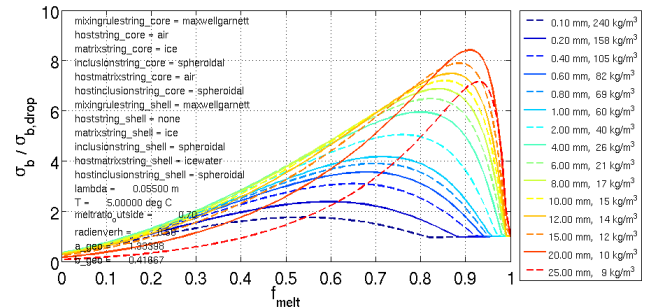
Soak twosphere snow, maisasmiasrs, 2-moment (Seifert-Beheng)



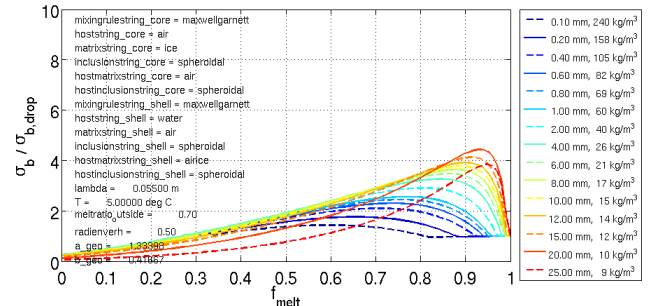
Soak twosphere snow, maisasmiwsrs, 2-moment (Seifert-Beheng)



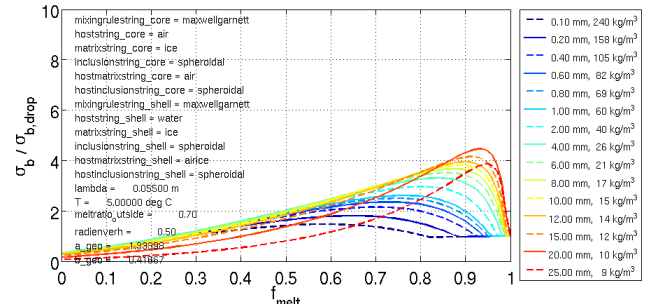
Soak twosphere snow, maisasmnisms, 2-moment (Seifert-Beheng)



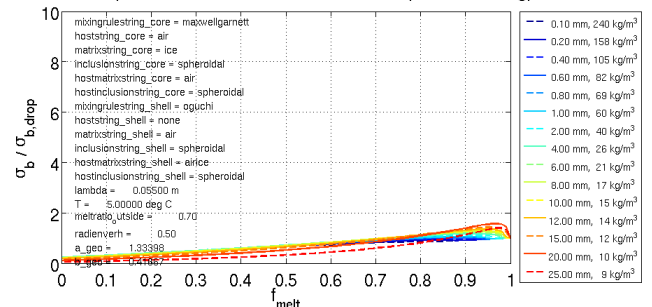
Soak twosphere snow, maisasmwasss, 2-moment (Seifert-Beheng)



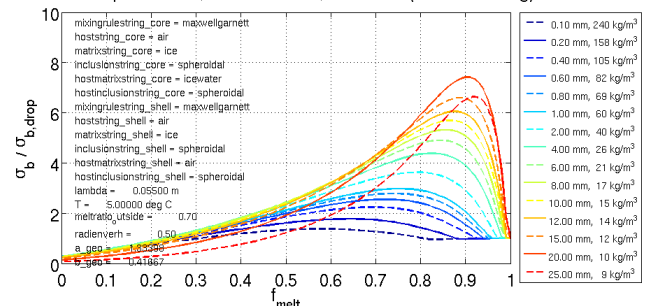
Soak twosphere snow, maisasmwss, 2-moment (Seifert-Beheng)

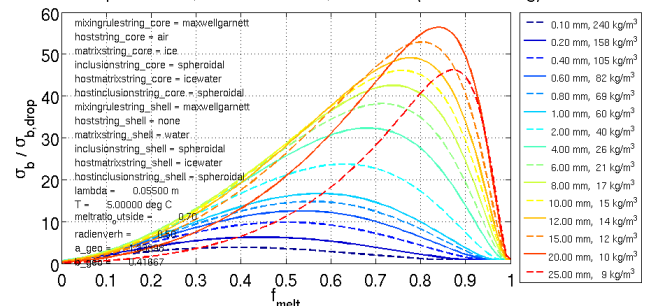


Soak twosphere snow, maisasonasss, 2-moment (Seifert-Beheng)

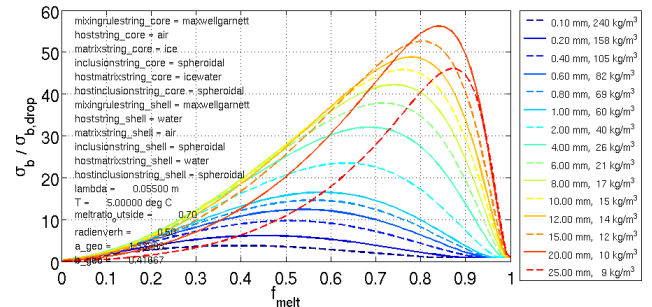


Soak twosphere snow, maismsmaisas, 2-moment (Seifert-Beheng)

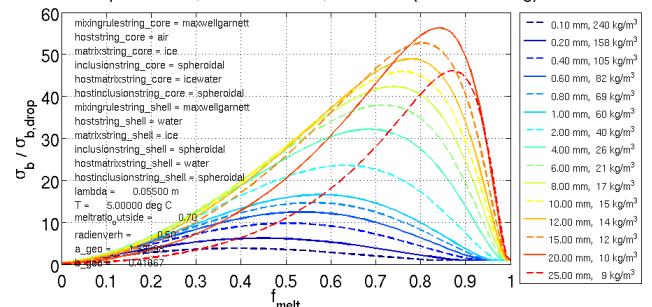




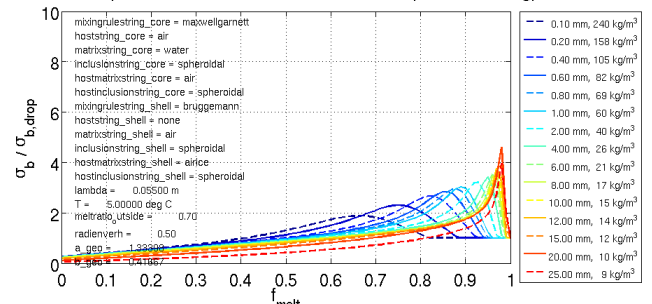
Soak twosphere snow, maismsmwasws, 2-moment (Seifert-Beheng)



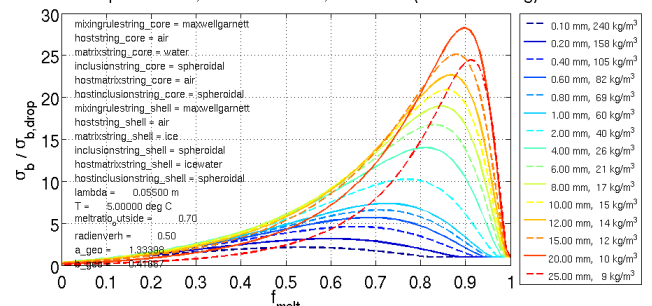
Soak twosphere snow, maismsmwisws, 2-moment (Seifert-Beheng)



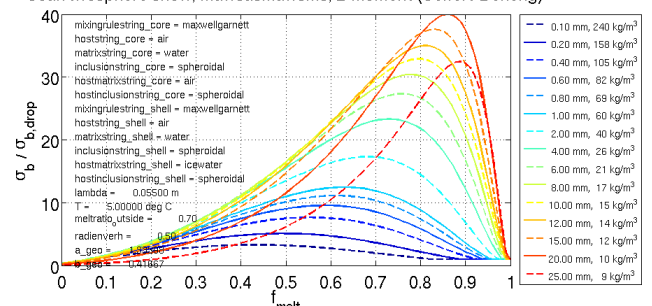
Soak twosphere snow, mawsasbnasss, 2-moment (Seifert-Beheng)



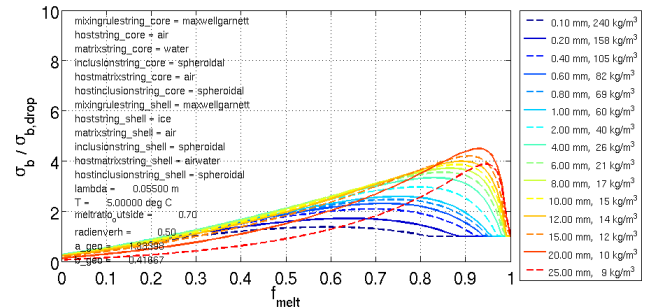
Soak twosphere snow, mawsasmaisms, 2-moment (Seifert-Beheng)



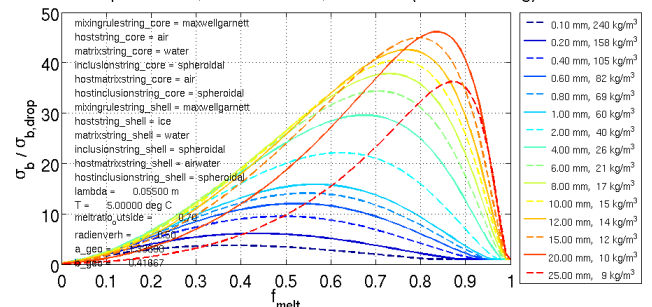
Soak twosphere snow, mawsasmawsms, 2-moment (Seifert-Beheng)



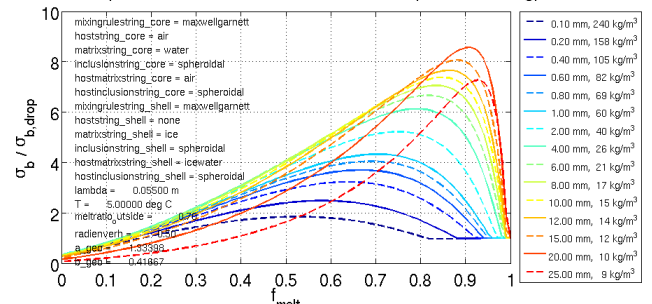
Soak twosphere snow, mawsasmiasrs, 2-moment (Seifert-Beheng)



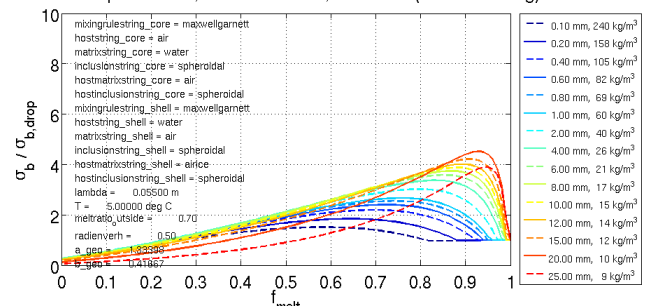
Soak twosphere snow, mawsasmiwsrs, 2-moment (Seifert-Beheng)



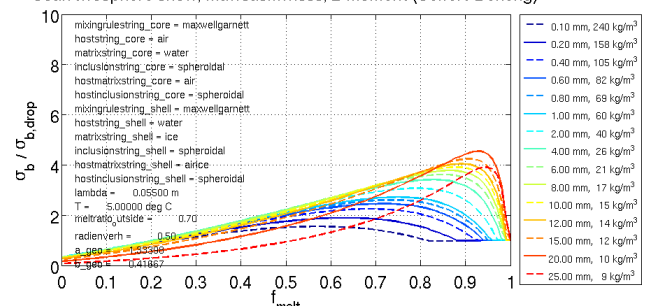
Soak twosphere snow, mawsasmnisms, 2-moment (Seifert-Beheng)



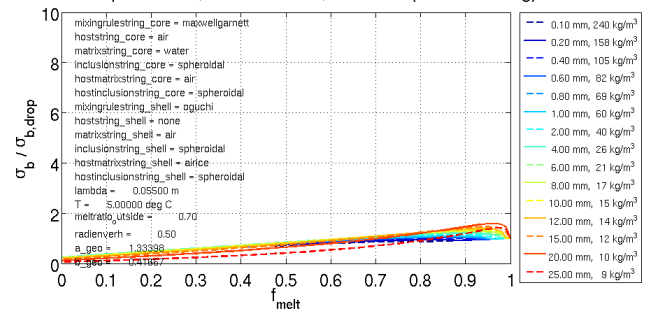
Soak twosphere snow, mawsasmwasss, 2-moment (Seifert-Beheng)



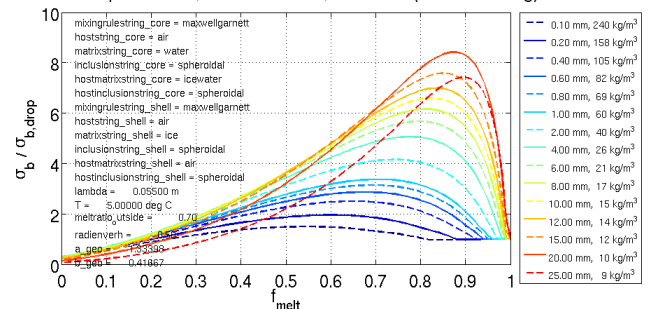
Soak twosphere snow, mawsasmwisss, 2-moment (Seifert-Beheng)



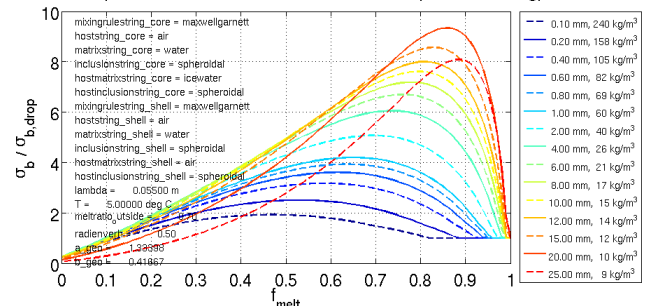
Soak twosphere snow, mawsasonasss, 2-moment (Seifert-Beheng)



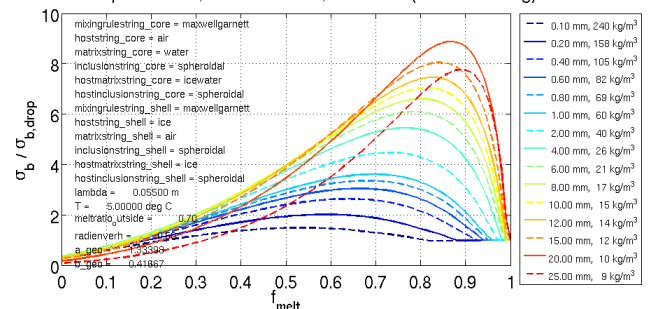
Soak twosphere snow, mawsmmaisas, 2-moment (Seifert-Beheng)



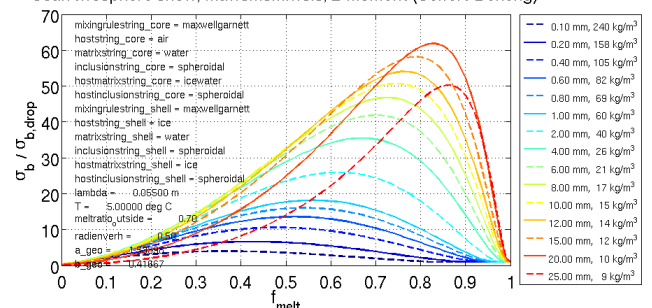
Soak twosphere snow, mawsmasmawsas, 2-moment (Seifert-Beheng)



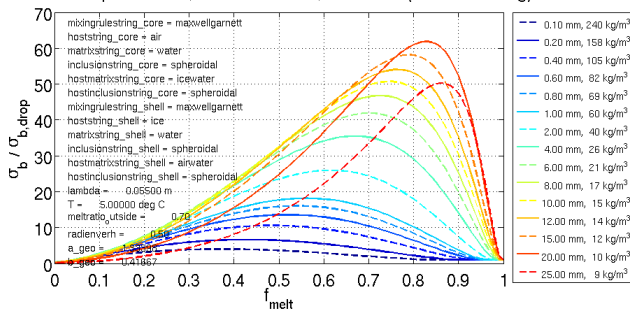
Soak twosphere snow, mawmsmiasis, 2-moment (Seifert-Beheng)



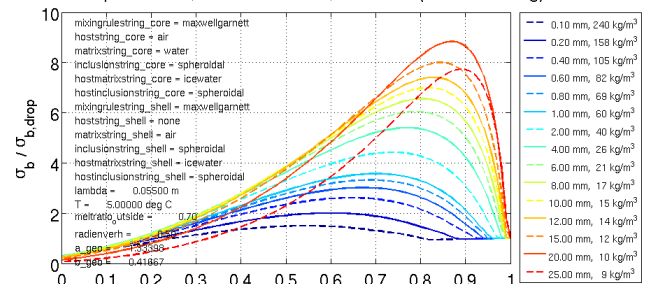
Soak twosphere snow, mawsmismiwsis, 2-moment (Seifert-Beheng)



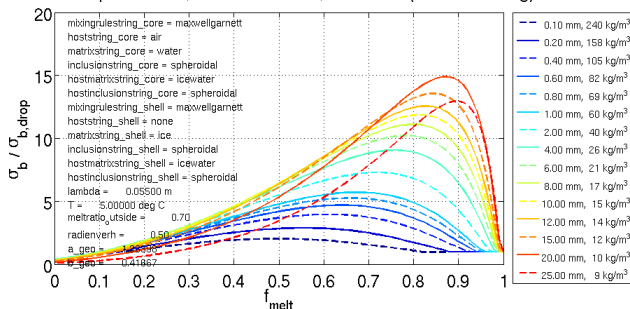
Soak twosphere snow, mawmsmiwsrs, 2-moment (Seifert-Beheng)



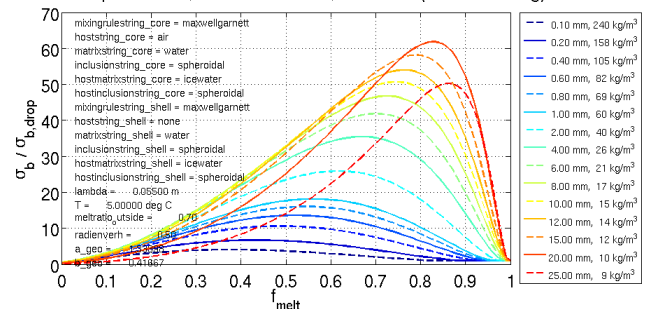
Soak twosphere snow, mawsmmnasms, 2-moment (Seifert-Beheng)



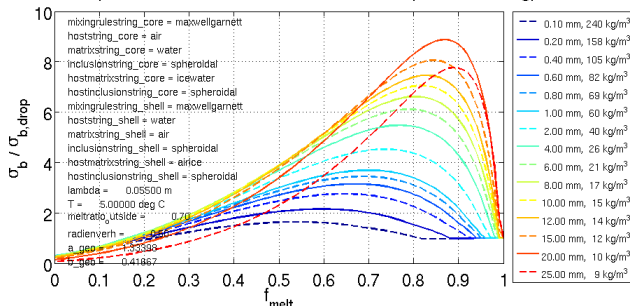
Soak twosphere snow, mawsmismisms, 2-moment (Seifert-Beheng)



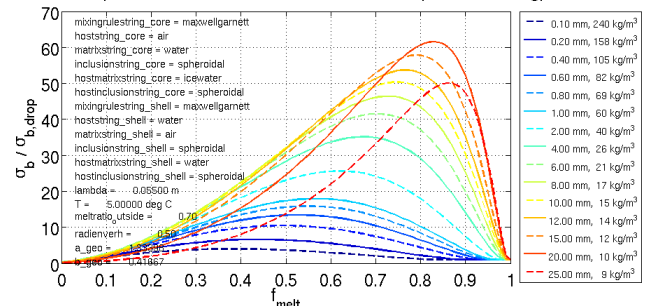
Soak twosphere snow, mawsmmsnwsms, 2-moment (Seifert-Beheng)



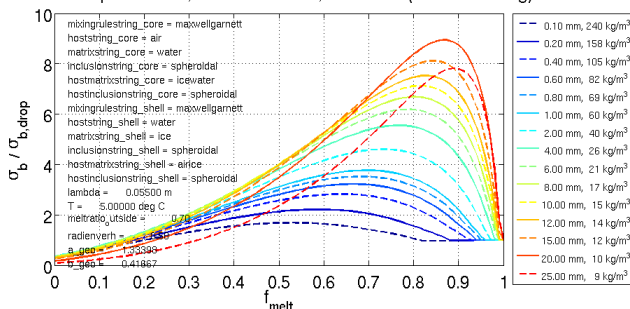
Soak twosphere snow, mawsmmwasss, 2-moment (Seifert-Beheng)



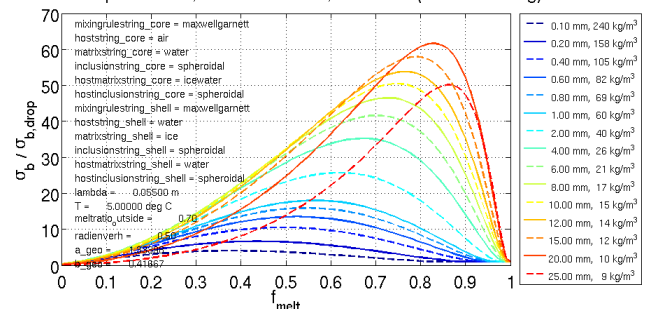
Soak twosphere snow, mawsmmswasws, 2-moment (Seifert-Beheng)



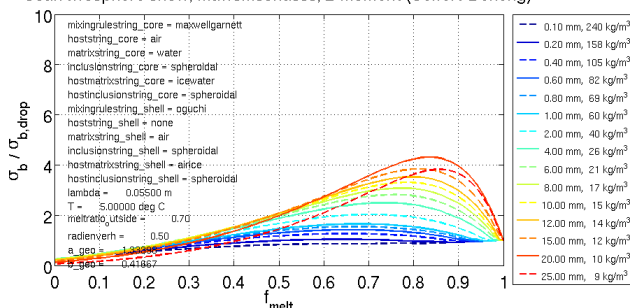
Soak twosphere snow, mawsmismwiss, 2-moment (Seifert-Beheng)



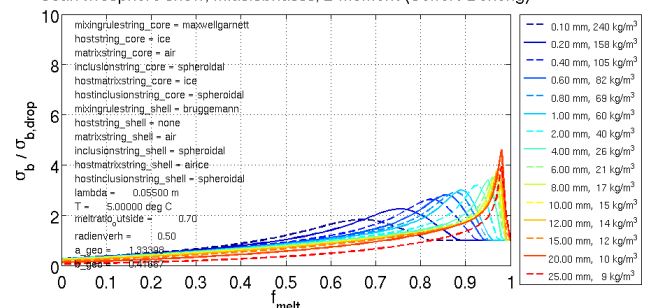
Soak twosphere snow, mawsmismwisws, 2-moment (Seifert-Beheng)

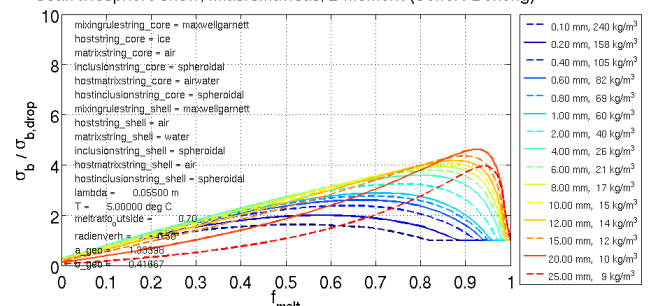
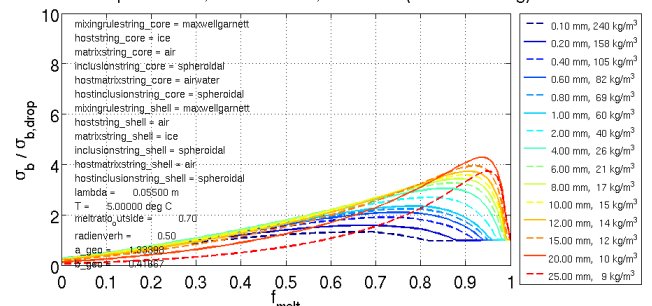
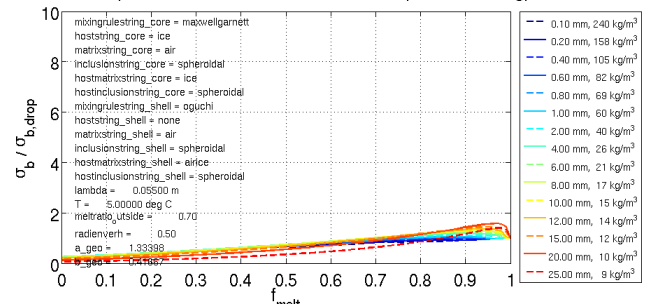
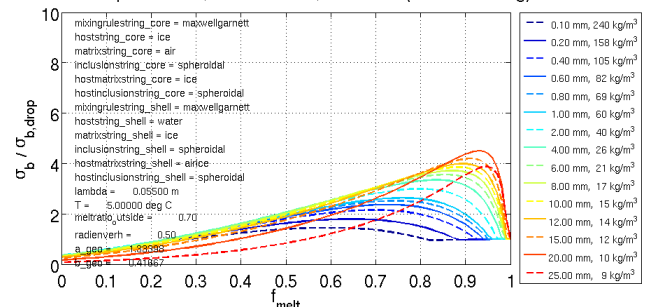
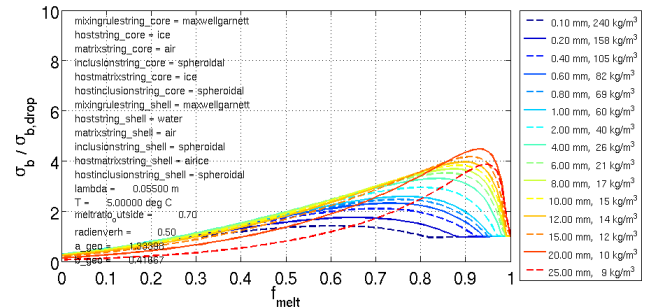


Soak twosphere snow, mawsmsonasss, 2-moment (Seifert-Beheng)

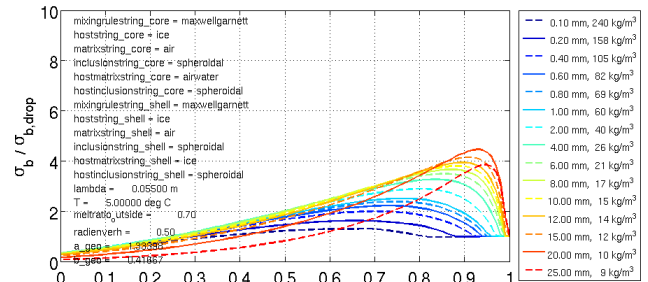


Soak twosphere snow, miasisbnasss, 2-moment (Seifert-Beheng)

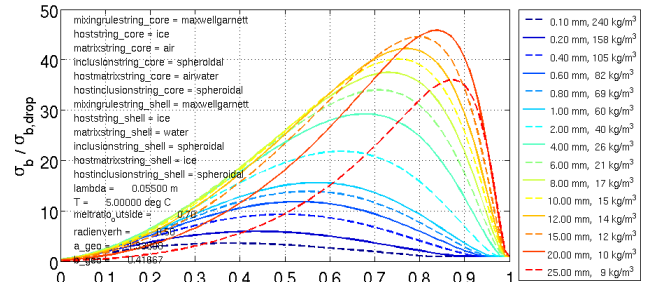




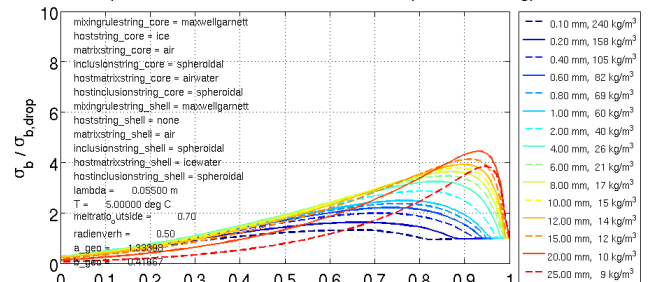
Soak twosphere snow, miasrmsiasis, 2-moment (Seifert-Beheng)



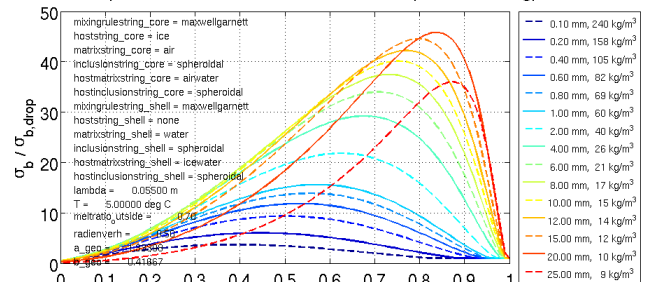
Soak twosphere snow, miasrsmiwsis, 2-moment (Seifert-Beheng)



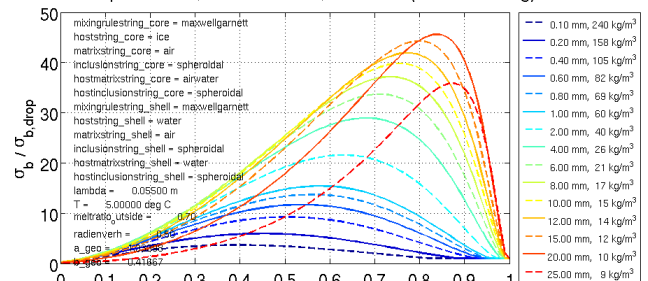
Soak twosphere snow, miasrsmnasms, 2-moment (Seifert-Beheng)



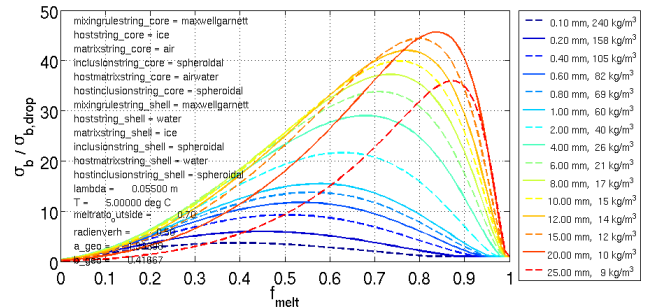
Soak twosphere snow, miasrmsnmwsms, 2-moment (Seifert-Beheng)



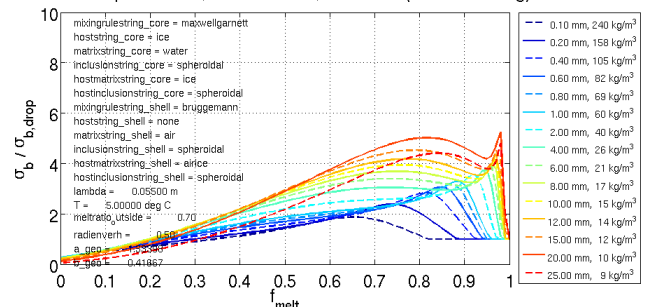
Soak twosphere snow, miasrsmwasws, 2-moment (Seifert-Beheng)



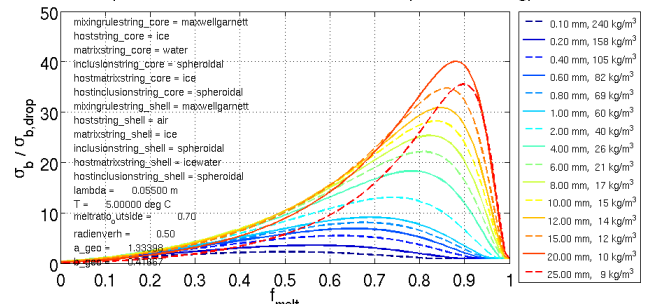
Soak twosphere snow, miasrmswisws, 2-moment (Seifert-Beheng)



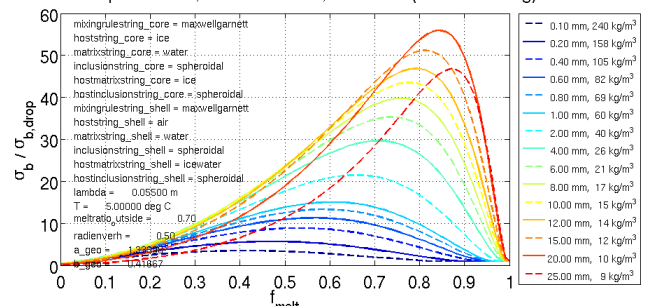
Soak twosphere snow, miwsisbnasss, 2-moment (Seifert-Beheng)



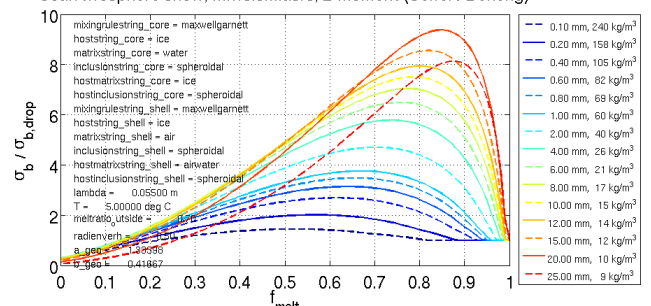
Soak twosphere snow, miwsismaisms, 2-moment (Seifert-Beheng)



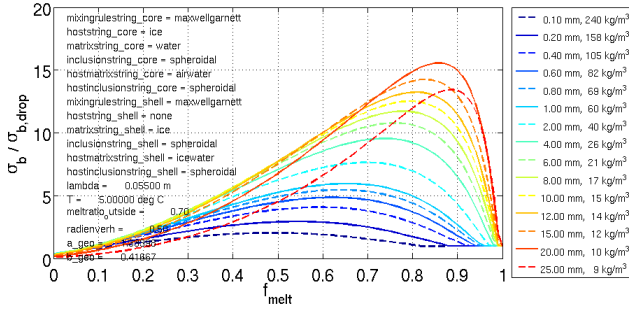
Soak twosphere snow, miwsismawsms, 2-moment (Seifert-Beheng)



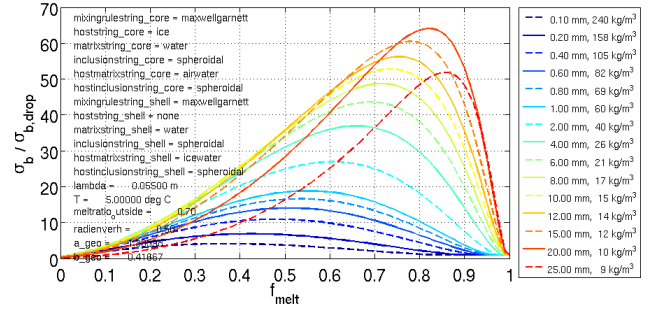
Soak twosphere snow, miwsismiasrs, 2-moment (Seifert-Beheng)



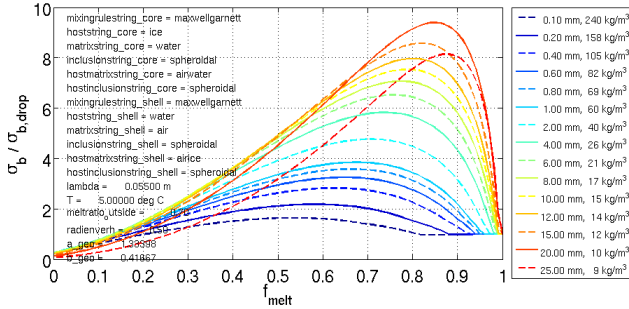
Soak twosphere snow, miwrsrsmnisms, 2-moment (Seifert-Beheng)



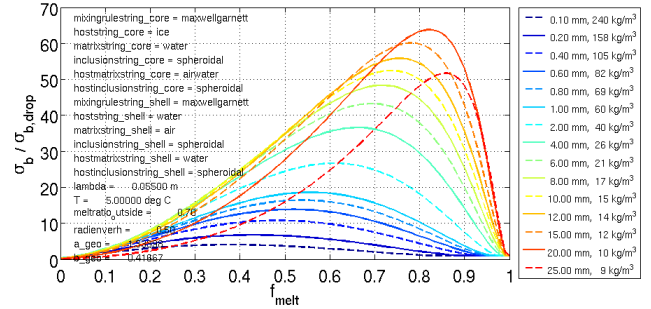
Soak twosphere snow, miwrsrsmnwsms, 2-moment (Seifert-Beheng)



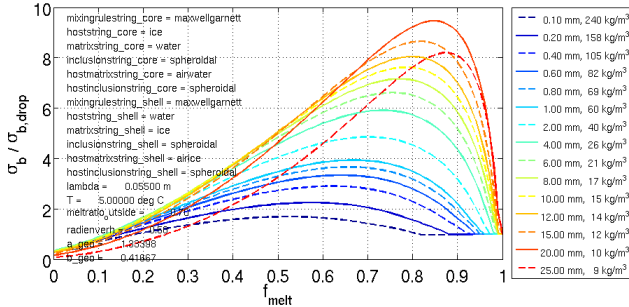
Soak twosphere snow, miwrsrsmwasss, 2-moment (Seifert-Beheng)



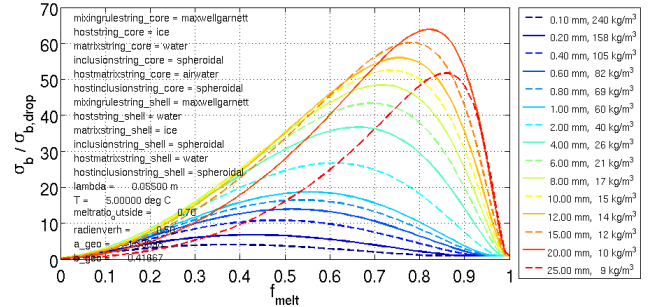
Soak twosphere snow, miwrsrsmwasws, 2-moment (Seifert-Beheng)



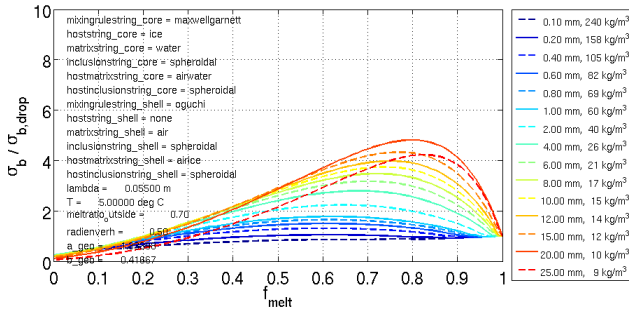
Soak twosphere snow, miwrsrsmwisss, 2-moment (Seifert-Beheng)



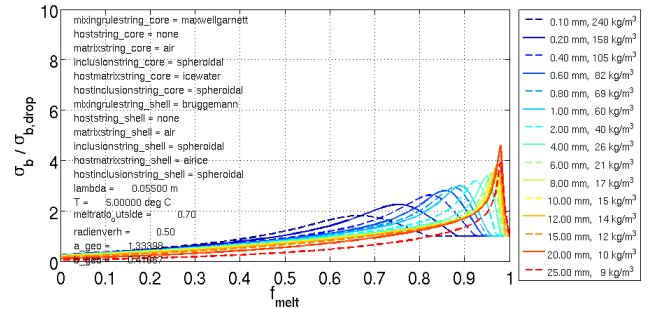
Soak twosphere snow, miwrsrsmwisws, 2-moment (Seifert-Beheng)



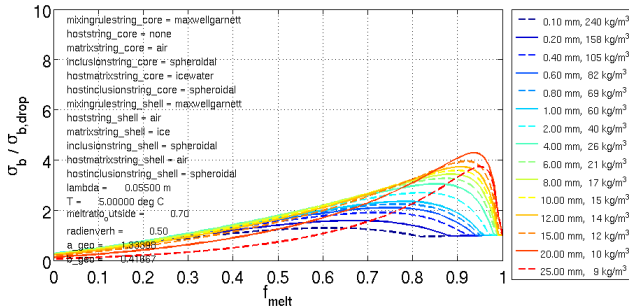
Soak twosphere snow, miwrsrsonasss, 2-moment (Seifert-Beheng)



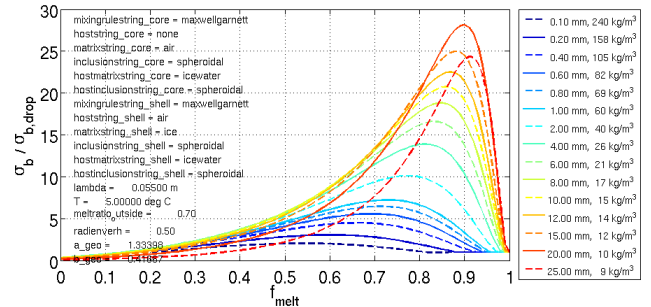
Soak twosphere snow, mnasmsbnasss, 2-moment (Seifert-Beheng)



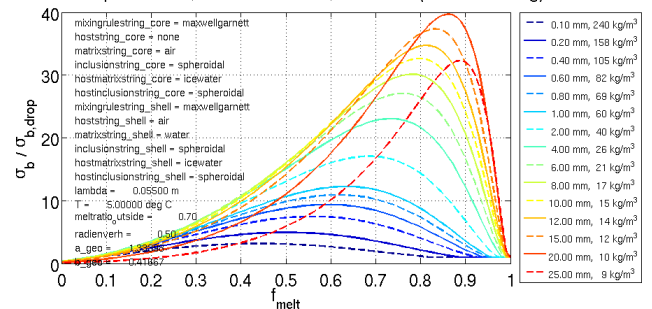
Soak twosphere snow, mnasmsmaiss, 2-moment (Seifert-Beheng)



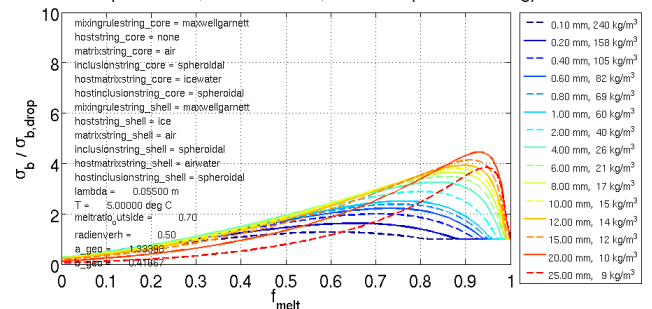
Soak twosphere snow, mnasmsmaisms, 2-moment (Seifert-Beheng)



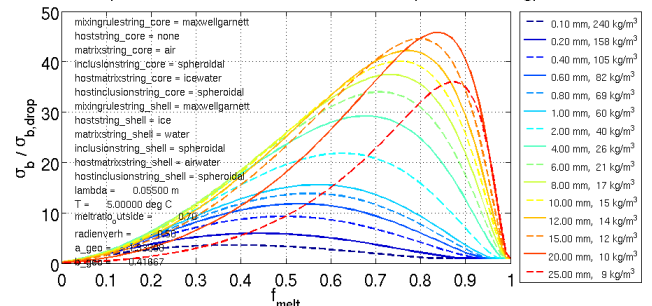
Soak twosphere snow, mnasmsmawsms, 2-moment (Seifert-Beheng)



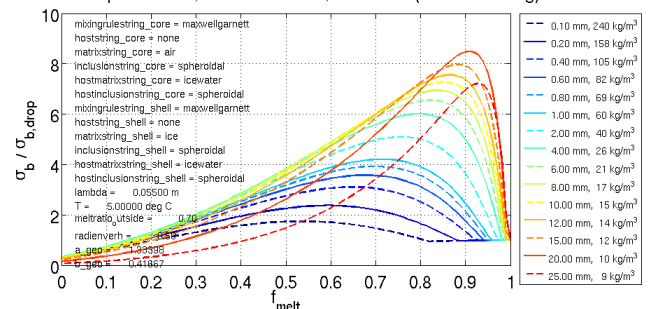
Soak twosphere snow, mnasmsmiasrs, 2-moment (Seifert-Beheng)



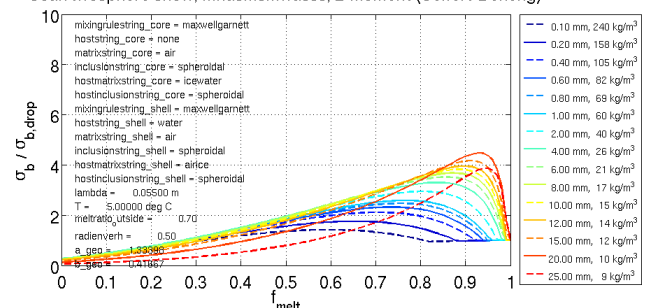
Soak twosphere snow, mnasmsmiwsrs, 2-moment (Seifert-Beheng)



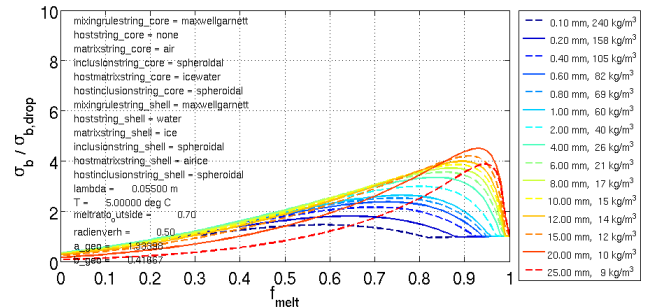
Soak twosphere snow, mnasmsmnisms, 2-moment (Seifert-Beheng)



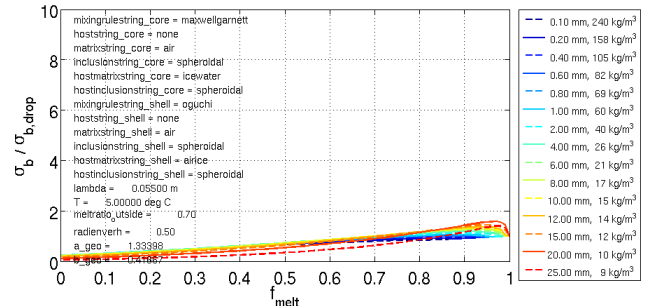
Soak twosphere snow, mnasmsmwasss, 2-moment (Seifert-Beheng)



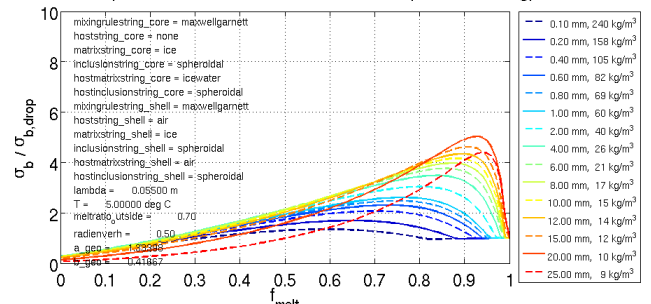
Soak twosphere snow, mnasmsmwisss, 2-moment (Seifert-Beheng)



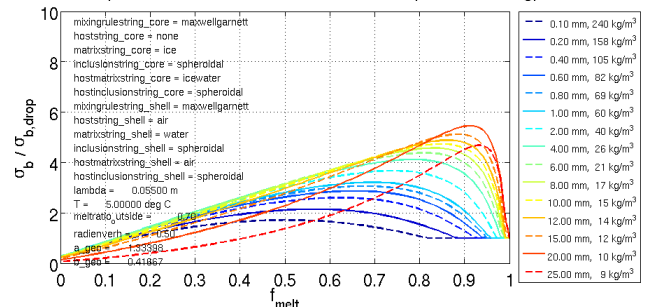
Soak twosphere snow, mnasmsonasss, 2-moment (Seifert-Beheng)



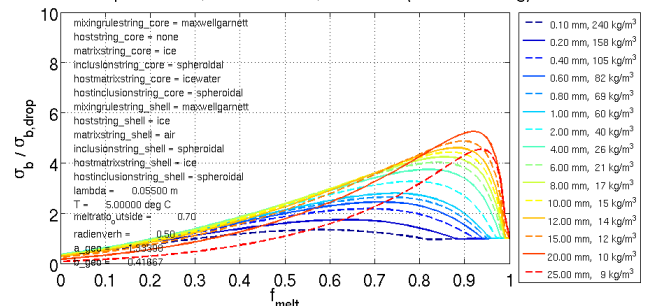
Soak twosphere snow, mnismsmaisas, 2-moment (Seifert-Beheng)



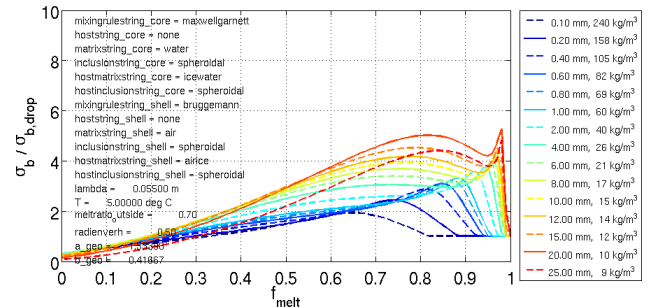
Soak twosphere snow, mnismsmawsas, 2-moment (Seifert-Beheng)



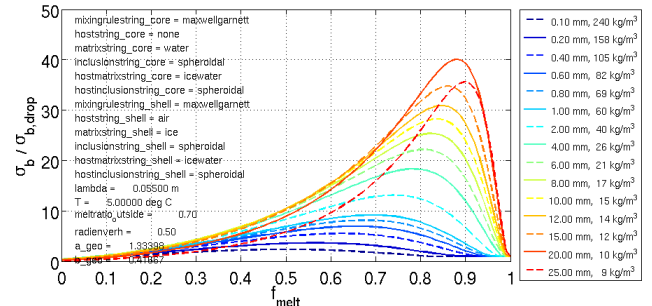
Soak twosphere snow, mnismsmiasis, 2-moment (Seifert-Beheng)



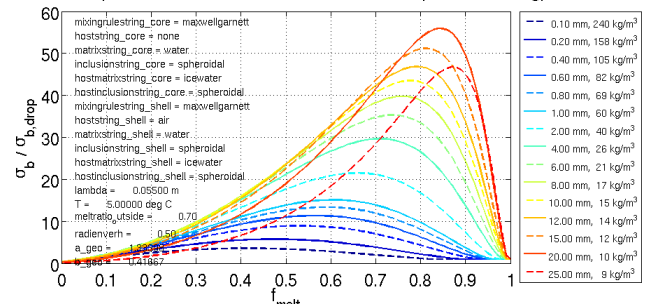
Soak twosphere snow, mnwsmsbnasss, 2-moment (Seifert-Beheng)



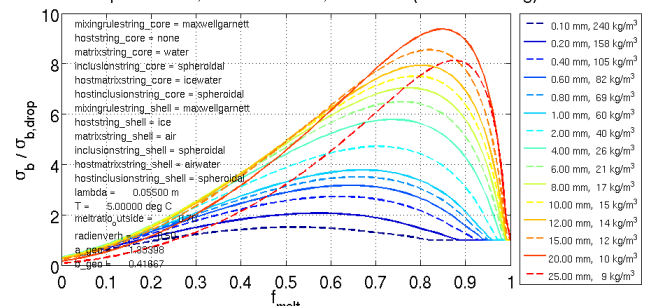
Soak twosphere snow, mnwsmismaisms, 2-moment (Seifert-Beheng)



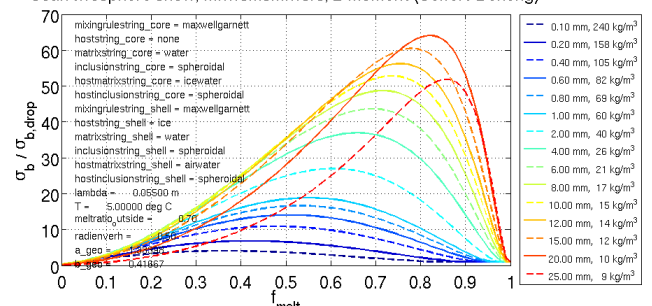
Soak twosphere snow, mnwsmmsmawsms, 2-moment (Seifert-Beheng)



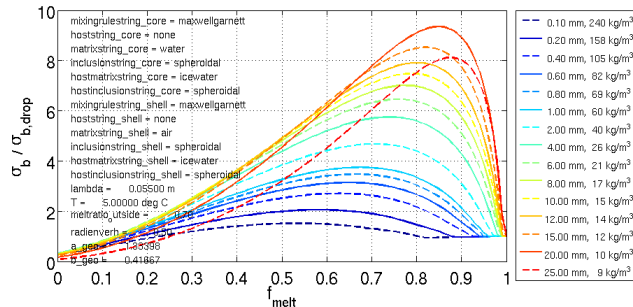
Soak twosphere snow, mnwsmmsiasrs, 2-moment (Seifert-Beheng)



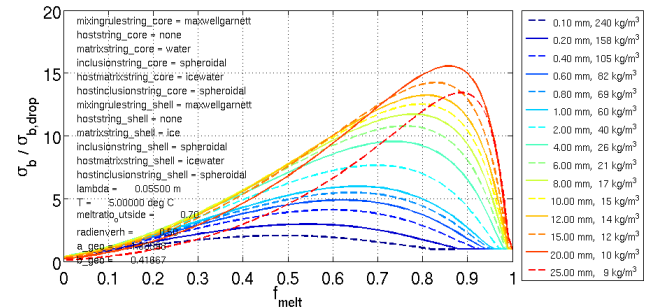
Soak twosphere snow, mnwsmmsiwsrs, 2-moment (Seifert-Beheng)



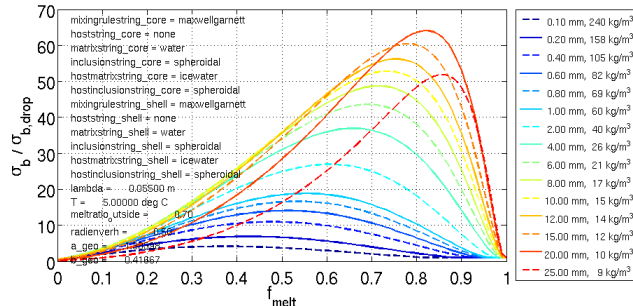
Soak twosphere snow, mnwsmmnasms, 2-moment (Seifert-Beheng)



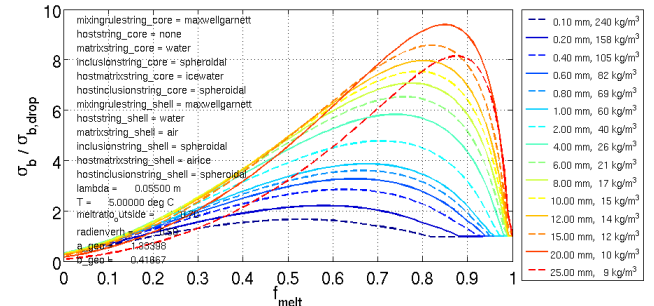
Soak twosphere snow, mnwsmnisms, 2-moment (Seifert-Beheng)



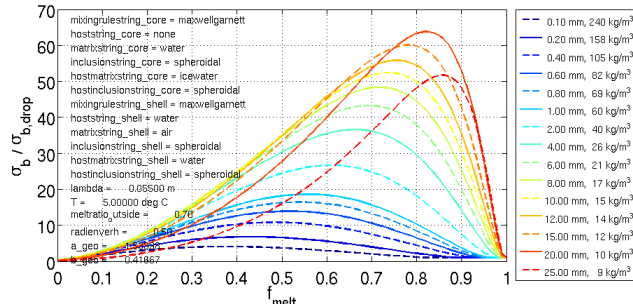
Soak twosphere snow, mnwsmsmnwsms, 2-moment (Seifert-Beheng)



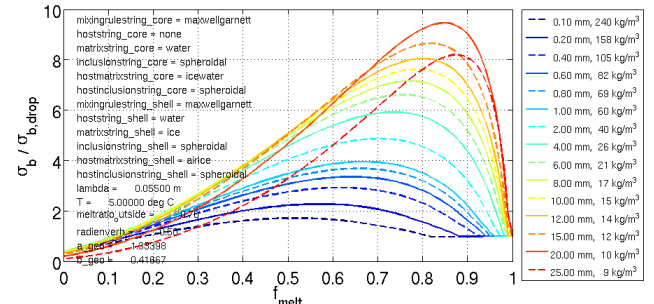
Soak twosphere snow, mnwsmmwasss, 2-moment (Seifert-Beheng)



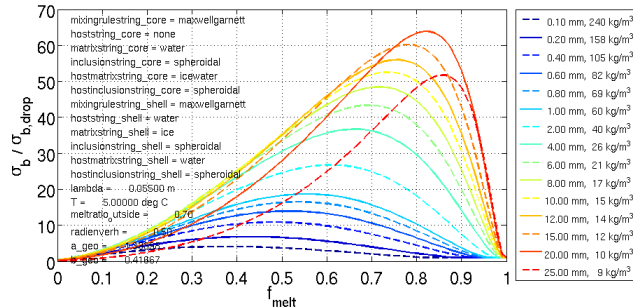
Soak twosphere snow, mnwsmmswasws, 2-moment (Seifert-Beheng)



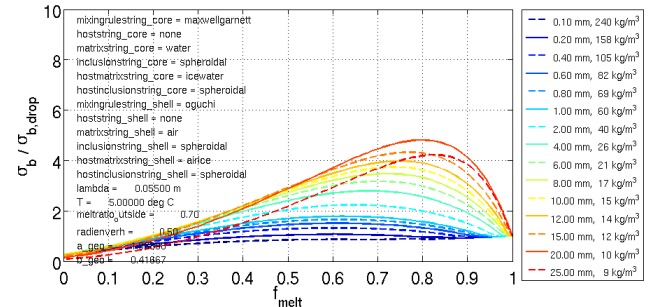
Soak twosphere snow, mnwsmmwisss, 2-moment (Seifert-Beheng)



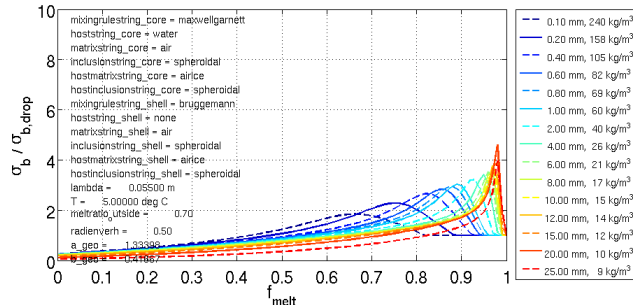
Soak twosphere snow, mnwsmmwisws, 2-moment (Seifert-Beheng)



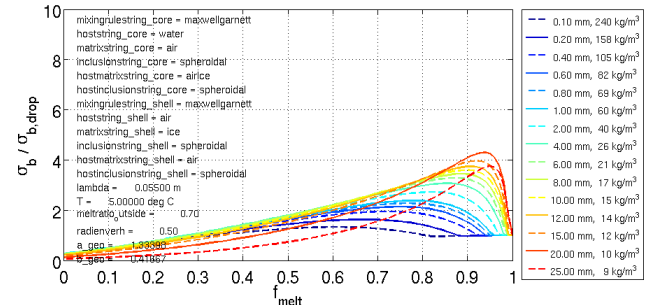
Soak twosphere snow, mnwsmsonasss, 2-moment (Seifert-Beheng)

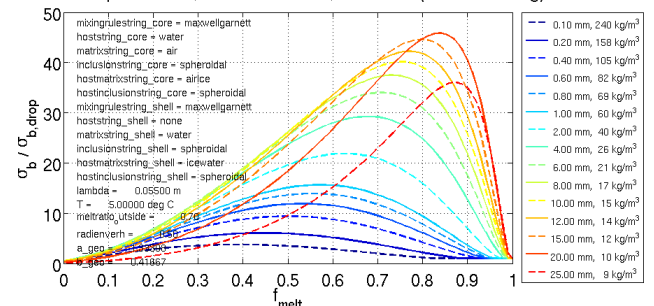


Soak twosphere snow, mwasssbnasss, 2-moment (Seifert-Beheng)

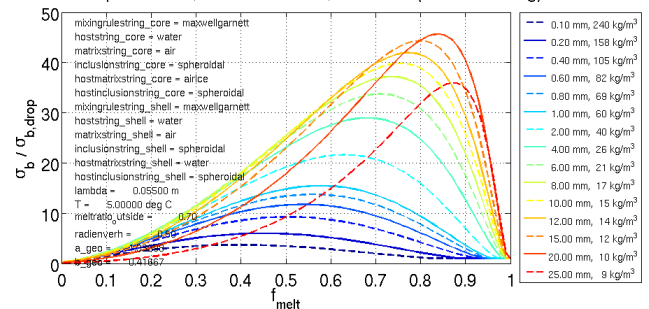


Soak twosphere snow, mwassssmaisas, 2-moment (Seifert-Beheng)

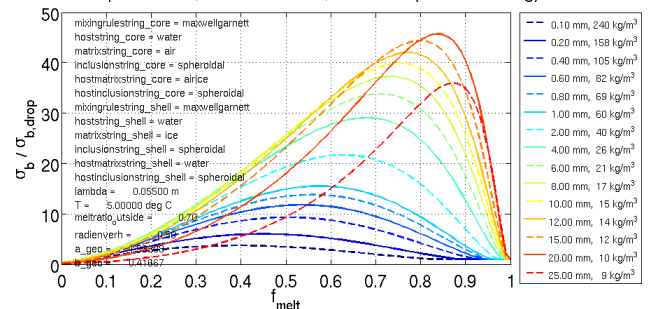




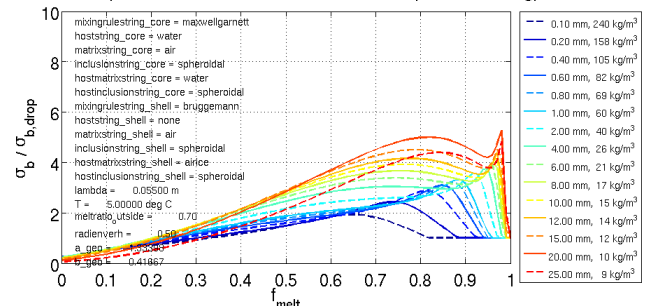
Soak twosphere snow, mwasssmwasws, 2-moment (Seifert-Beheng)



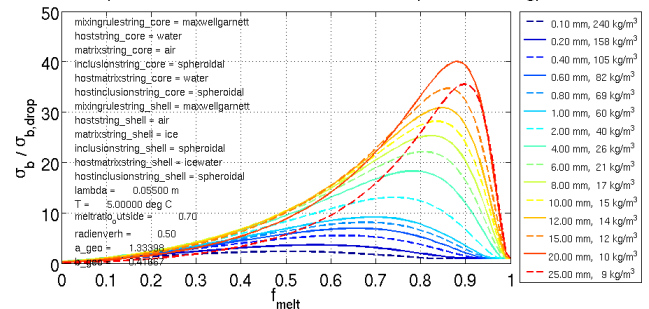
Soak twosphere snow, mwasssmwisws, 2-moment (Seifert-Beheng)



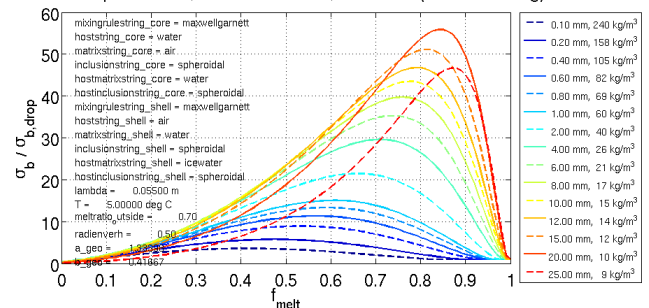
Soak twosphere snow, mwaswsbnasss, 2-moment (Seifert-Beheng)



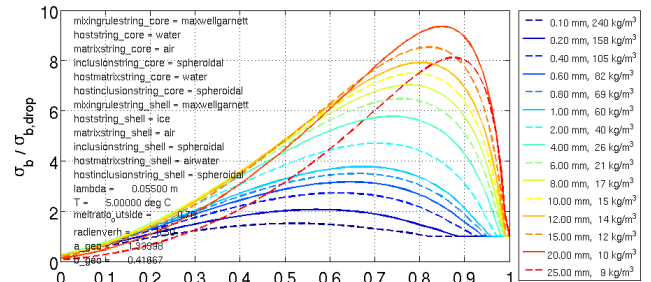
Soak twosphere snow, mwaswsmaisms, 2-moment (Seifert-Beheng)



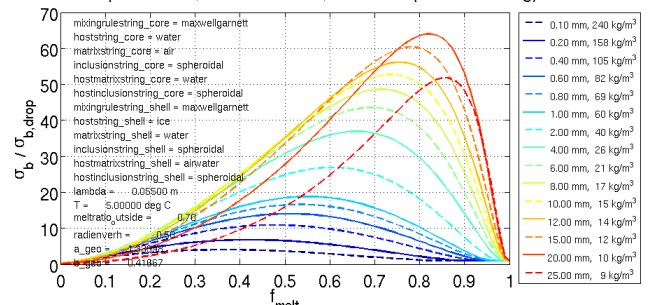
Soak twosphere snow, mwaswsmawms, 2-moment (Seifert-Beheng)



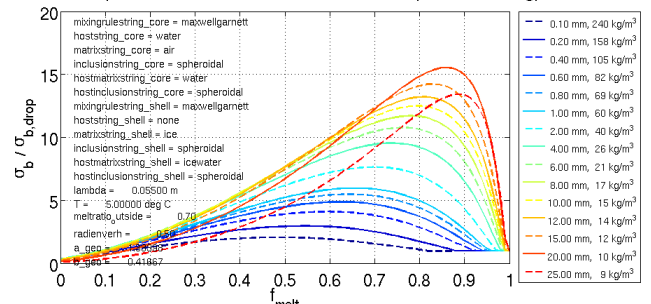
Soak twosphere snow, mwaswsdiasrs, 2-moment (Seifert-Beheng)



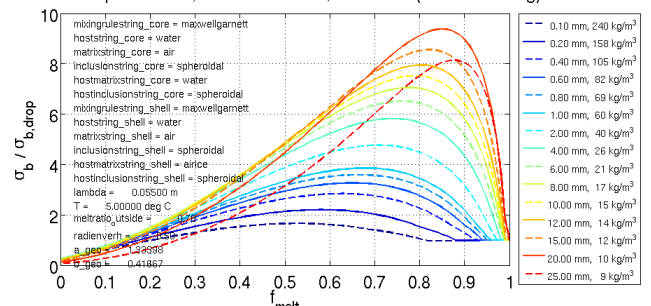
Soak twosphere snow, mwaswsmiwsrs, 2-moment (Seifert-Beheng)



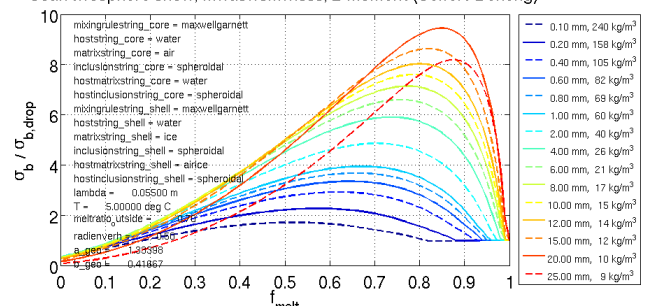
Soak twosphere snow, mwaswsmnisms, 2-moment (Seifert-Beheng)



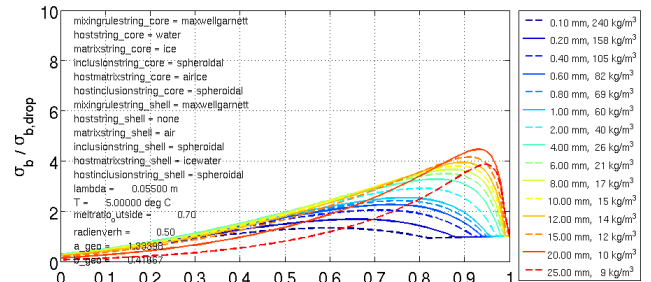
Soak twosphere snow, mwaswsmwasss, 2-moment (Seifert-Beheng)



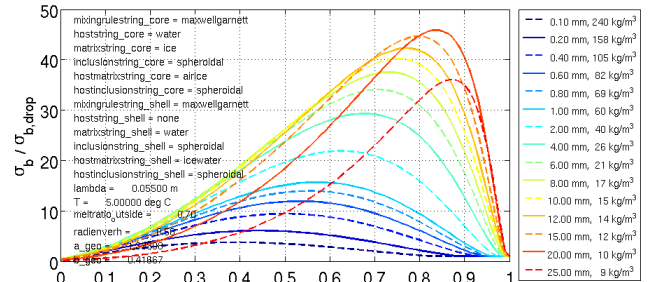
Soak twosphere snow, mwaswsmwisss, 2-moment (Seifert-Beheng)



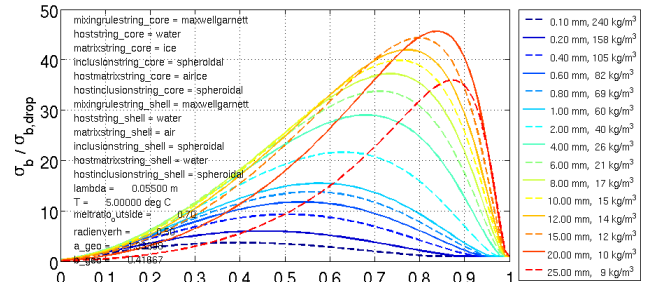
Soak twosphere snow, mwisssmnasms, 2-moment (Seifert-Beheng)



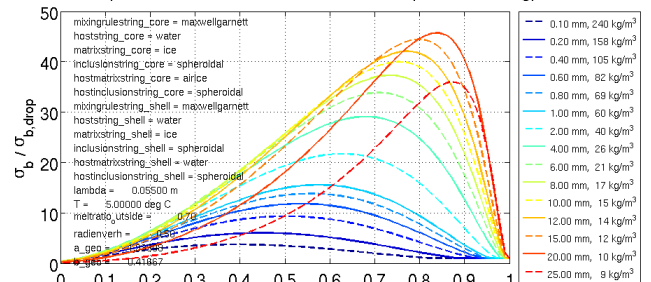
Soak twosphere snow, mwisssmnwsm, 2-moment (Seifert-Bheng)



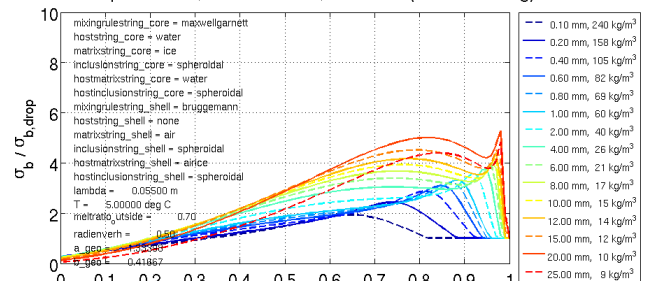
Soak twosphere snow, mwisssmwasws, 2-moment (Seifert-Beheng)

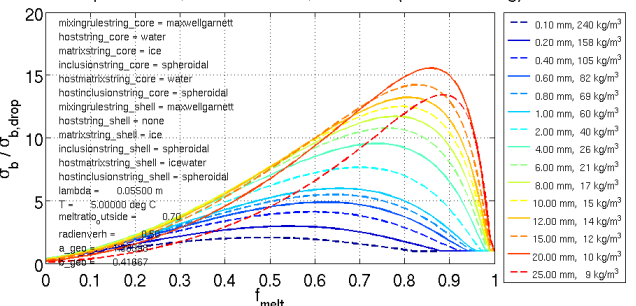


Soak twosphere snow, mwisssmwisws, 2-moment (Seifert-Beheng)

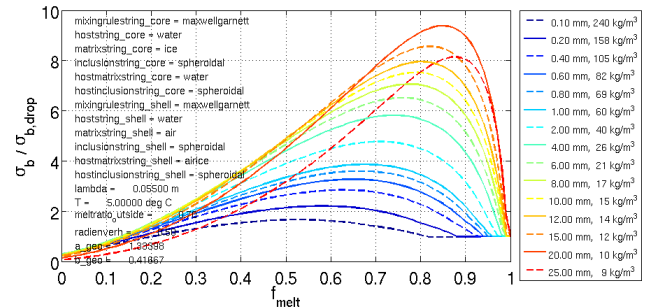


Soak twosphere snow, mwiswsbnasss, 2-moment (Seifert-Beheng)

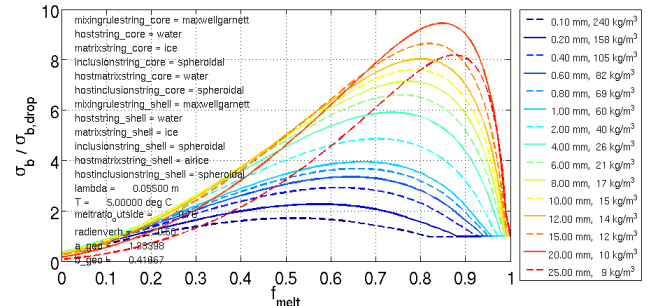




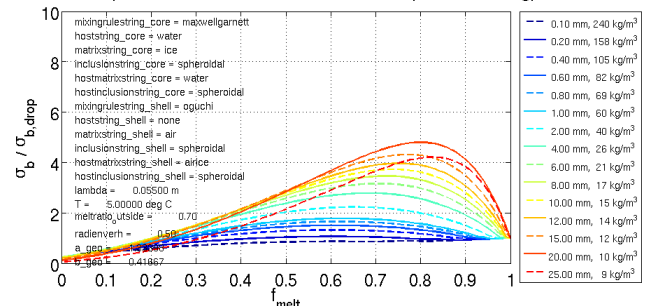
Soak twosphere snow, mwiswsmwasss, 2-moment (Seifert-Beheng)



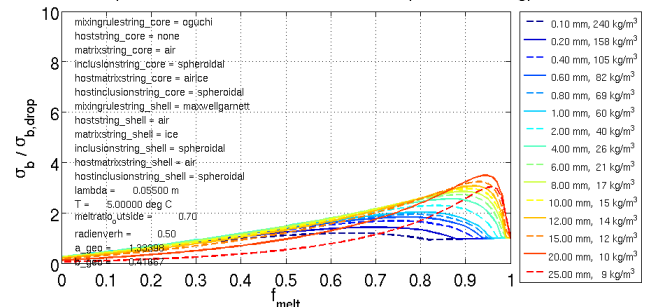
Soak twosphere snow, mwiswsmwisss, 2-moment (Seifert-Beheng)



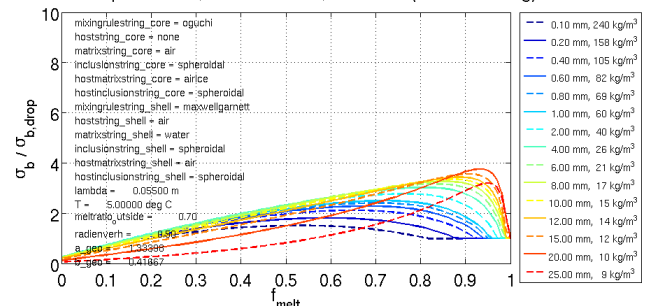
Soak twosphere snow, mwiswsonasss, 2-moment (Seifert-Beheng)



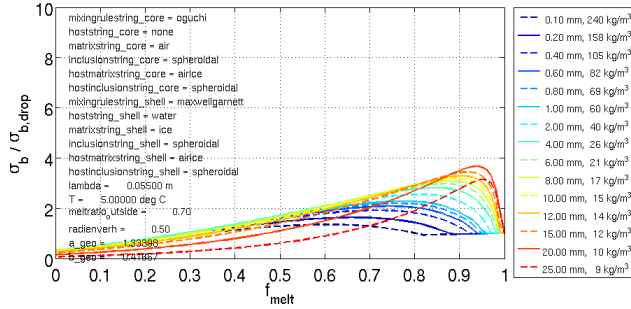
Soak twosphere snow, onasssmaisas, 2-moment (Seifert-Beheng)



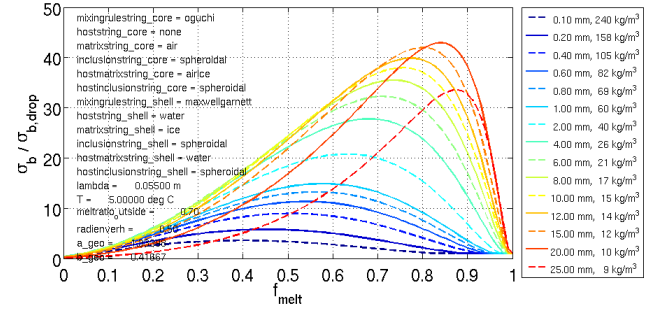
Soak twosphere snow, onasssmawsas, 2-moment (Seifert-Beheng)



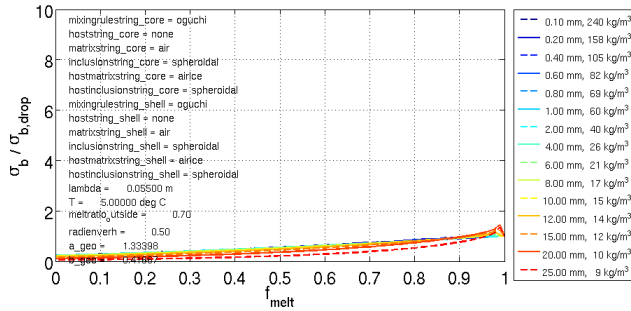
Soak twosphere snow, onasssmwisss, 2-moment (Seifert-Beheng)



Soak twosphere snow, onasssmwisws, 2-moment (Seifert-Beheng)



Soak twosphere snow, onasssonasss, 2-moment (Seifert-Beheng)



9 Index of the Figures of Section 8

9.1 Rayleigh: soaked wet graupel, LM-scheme

bnasss	74	miasrs	75	mwasss	75
maisas	74	miwsis	75	mwasws	75
maisms	74	miwsrs	75	mwisss	75
mawsas	74	mnasms	75	mwisws	75
mawsms	74	mnisms	75	onasss	76
miasis	74	mnwsms	75		

9.2 Rayleigh: soaked wet graupel, Seifert/Beheng-scheme

bnasss	77	miasrs	78	mwasss	78
maisas	77	miwsis	78	mwasws	78
maisms	77	miwsrs	78	mwisss	78
mawsas	77	mnasms	78	mwisws	78
mawsms	77	mnisms	78	onasss	79
miasis	77	mnwsms	78		

9.3 Rayleigh: soaked wet snow, LM-scheme

bnasss	80	miasrs	80	mwasss	81
maisas	80	miwsis	80	mwasws	81
maisms	80	miwsrs	81	mwisss	81
mawsas	80	mnasms	81	mwisws	81
mawsms	80	mnisms	81	onasss	81
miasis	80	mnwsms	81		

9.4 Rayleigh: soaked wet snow, Seifert/Beheng-scheme

bnasss	82	miasrs	82	mwasss	83
maisas	82	miwsis	82	mwasws	83
maisms	82	miwsrs	83	mwisss	83
mawsas	82	mnasms	83	mwisws	83
mawsms	82	mnisms	83	onasss	83
miasis	82	mnwsms	83		

9.5 Mie: soaked twosphere wet graupel, LM-scheme

basbis	84	masmws	84	miswis	85
basmis	84	maswis	85	oasmis	85
basmws	84	misbis	85	oasmws	85
masbis	84	mismis	85	oaswis	85
masmis	84	mismws	85		

9.6 Mie: soaked twosphere wet graupel, Seifert/Beheng-scheme

basbis	86	masmws	86	miswis	87
basmis	86	maswis	87	oasmis	87
basmws	86	misbis	87	oasmws	87
masbis	86	mismis	87	oaswis	87
masmis	86	mismws	87		

9.7 Mie: soaked twosphere wet snow, LM-scheme

basbis	88	masmws	88	miswis	89
basmis	88	maswis	89	oasmis	89
basmws	88	misbis	89	oasmws	89
masbis	88	mismis	89	oaswis	89
masmis	88	mismws	89		

9.8 Mie: soaked twosphere wet snow, Seifert/Beheng-scheme

basbis	90	masmws	90	miswis	91
basmis	90	maswis	91	oasmis	91
basmws	90	misbis	91	oasmws	91
masbis	90	mismis	91	oaswis	91
masmis	90	mismws	91		

9.9 Mie: soaked wet graupel, LM-scheme

bnasss	92	miasrs	93	mwasss	93
maisas	92	miwsis	93	mwasws	93
maisms	92	miwsrs	93	mwisss	93
mawsas	92	mnasms	93	mwisws	93
mawsms	92	mnisms	93	onasss	94
miasis	92	mnwsms	93		

9.10 Mie: soaked wet graupel, Seifert/Beheng-scheme

bnasss	95	miasrs	96	mwasss	96
maisas	95	miwsis	96	mwasws	96
maisms	95	miwsrs	96	mwisss	96
mawsas	95	mnasms	96	mwisws	96
mawsms	95	mnisms	96	onasss	97
miasis	95	mnwsms	96		

9.11 Mie: soaked wet snow, LM-scheme

bnasss	98	miasrs	98	mwasss	99
maisas	98	miwsis	98	mwasws	99
maisms	98	miwsrs	99	mwisss	99
mawsas	98	mnasms	99	mwisws	99
mawsms	98	mnisms	99	onasss	99
miasis	98	mnwsms	99		

9.12 Mie: soaked wet snow, Seifert/Beheng-scheme

bnasss	100	miasrs	100	mwasss	101
maisas	100	miwsis	100	mwasws	101
maisms	100	miwsrs	101	mwisss	101
mawsas	100	mnasms	101	mwisws	101
mawsms	100	mnisms	101	onasss	101
miasis	100	mnwsms	101		

9.13 Mie: watersphere wet graupel, LM-scheme

bas	102	mis	102	ois	102
bis	102	oas	102		
mas	102				

9.14 Mie: watersphere wet graupel, Seifert/Beheng-scheme

bas	103	mis	103	ois	103
bis	103	oas	103		
mas	103				

9.15 Mie: watersphere wet snow, LM-scheme

bas	104	mis	104	ois	104
bis	104	oas	104		
mas	104				

9.16 Mie: watersphere wet snow, Seifert/Beheng-scheme

bas	105	mis	105	ois	105
bis	105	oas	105		
mas	105				

9.17 Mie: spongy wet hail, Seifert/Beheng-scheme

bws	106	mws	106	ows	106
mis	106				

9.18 Mie: watersphere wet hail, Seifert/Beheng-scheme

figure	107
--------	-----

9.19 Mie: twosphere soaked wet snow, LM-scheme

bnasssbnasss	108	maismsmawsms	112	mawmsmiwrs	116
bnasssmaisas	108	maismsmiasis	112	mawmsmnnasms	116
bnasssmaisms	108	maismsmiasrs	112	mawmsmnnisms	116
bnasssmawsas	108	maismsmiwsis	112	mawmsmnnwsms	116
bnasssmawsms	108	maismsmiwrs	112	mawmsmwasss	116
bnasssmiasis	108	maismsmnnasms	112	mawmsmwawas	116
bnasssmiasrs	109	maismsmnnisms	112	mawmsmwawss	116
bnasssmiwsis	109	maismsmnnwsms	112	mawmsmwawss	116
bnasssmiwrs	109	maismsmwasss	113	mawmsmsonasss	116
bnasssmnnasms	109	maismsmwasws	113	miasisbnasss	116
bnasssmnnisms	109	maismsmwawss	113	miasismaisas	117
bnasssmnnwsms	109	maismsmwiws	113	miasismaisms	117
bnasssmwasss	109	maismsonasss	113	miasismawsas	117
bnasssmwasws	109	mawsasbnasss	113	miasismawsms	117
bnasssmwawss	109	mawsasmaisas	113	miasismiasis	117
bnasssmwiws	109	mawsasmaisms	113	miasismiasrs	117
bnasssonasss	110	mawsasmawsas	113	miasismiwsis	117
maisasbnasss	110	mawsasmawsms	113	miasismiwrss	117
maisasmaisas	110	mawsasmiasis	114	miasismnnasms	117
maisasmaisms	110	mawsasmiasrs	114	miasismnnisms	117
maisasmawsas	110	mawsasmiwsis	114	miasismnnwsms	118
maisasmawsms	110	mawsasmiwrs	114	miasismwasss	118
maisasmiasis	110	mawsasmnnasms	114	miasismwasws	118
maisasmiasrs	110	mawsasmnnisms	114	miasismwawss	118
maisasmiwsis	110	mawsasmnnwsms	114	miasismwiws	118
maisasmiwrs	110	mawsasmwasss	114	miasismwiws	118
maisasmnnasms	111	mawsasmwasws	114	miasisonasss	118
maisasmnnisms	111	mawsasmwawss	114	miasrsbnasss	118
maisasmnnwsms	111	mawsasmwiws	115	miasrsmaisas	118
maisasmwasss	111	mawsasonasss	115	miasrsmaisms	118
maisasmwasws	111	mawmsbnasss	115	miasrsmawsas	118
maisasmwawss	111	mawmsmaisas	115	miasrsmawsms	119
maisasmwiws	111	mawmsmaisms	115	miasrsmiasis	119
maisasonasss	111	mawmsmawsas	115	miasrsmiasrs	119
maismsbnasss	111	mawmsmawsms	115	miasrsmiwsis	119
maismsmaisas	111	mawmsmiasis	115	miasrsmnnasms	119
maismsmaisms	112	mawmsmiasrs	115	miasrsmnnisms	119
maismsmawsas	112	mawmsmiwsis	115	miasrsmnnwsms	119

miasrsmwasss	119	mnasmsmwasss	124	mwasssmwasss	130
miasrsmwasws	119	mnasmsmwasws	125	mwasssmwasws	130
miasrsmwisss	120	mnasmsmwisss	125	mwasssmwisss	130
miasrsmwisws	120	mnasmsmwisws	125	mwasssmwisws	130
miasrsonasss	120	mnasmsonasss	125	mwasssonasss	130
miwsisbnasss	120	mnismsbnasss	125	mwaswsbnasss	130
miwsismaisas	120	mnismsmaisas	125	mwaswsmaisas	130
miwsismaisms	120	mnismsmaisms	125	mwaswsmaisms	130
miwsismawsas	120	mnismsmawsas	125	mwaswsmawsas	130
miwsismawsms	120	mnismsmawsms	125	mwaswsmawsms	130
miwsismiasis	120	mnismsmiasis	125	mwaswsmiasis	131
miwsismiasrs	120	mnismsmiasrs	126	mwaswsmiasrs	131
miwsismiwsis	121	mnismsmiwsis	126	mwaswsmiwsis	131
miwsismiwsrs	121	mnismsmiwsrs	126	mwaswsmiwsrs	131
miwsismnasms	121	mnismsmnasms	126	mwaswsmnasms	131
miwsismnisms	121	mnismsmnisms	126	mwaswsmnisms	131
miwsismnwsm	121	mnismsmnwsm	126	mwaswsmnwsm	131
miwsismwasss	121	mnismsmwasss	126	mwaswsmwasss	131
miwsismwasws	121	mnismsmwasws	126	mwaswsmwasws	131
miwsismwisss	121	mnismsmwisss	126	mwaswsmwisss	131
miwsismwisws	121	mnismsmwisws	126	mwaswsmwisws	132
miwsisonasss	121	mnismsonasss	127	mwaswsonasss	132
miwsrsbnasss	122	mnwsmsbnasss	127	mwisssbnasss	132
miwsrsmisas	122	mnwsmsmaisas	127	mwisssmaisas	132
miwsrsmiaisms	122	mnwsmsmaisms	127	mwisssmaisms	132
miwsrsmawsas	122	mnwsmsmawsas	127	mwisssmawsas	132
miwsrsmawsms	122	mnwsmsmawsms	127	mwisssmawsms	132
miwsrsmiasis	122	mnwsmsmiasis	127	mwisssmiasis	132
miwsrsmiasrs	122	mnwsmsmiasrs	127	mwisssmiasrs	132
miwsrsmiwsis	122	mnwsmsmiwsis	127	mwisssmiwsis	132
miwsrsmiwsrs	122	mnwsmsmiwsrs	127	mwisssmiwsrs	133
miwsrsmnasms	122	mnwsmsmnasms	128	mwisssmnasms	133
miwsrsmnisms	123	mnwsmsmnisms	128	mwisssmnisms	133
miwsrsmnwsm	123	mnwsmsmnwsm	128	mwisssmnwsm	133
miwsrsmwasss	123	mnwsmsmwasss	128	mwisssmwasss	133
miwsrsmwasws	123	mnwsmsmwasws	128	mwisssmwasws	133
miwsrsmwisss	123	mnwsmsmwisss	128	mwisssmwisss	133
miwsrsmwisws	123	mnwsmsmwisws	128	mwisssmwisws	133
miwsrsonasss	123	mnwsmsonasss	128	mwisssonasss	133
mnasmsbnasss	123	mwasssbnasss	128	mwiswsbnasss	133
mnasmsmaisas	123	mwasssmaisas	128	mwiswsmaisas	134
mnasmsmaisms	123	mwasssmaisms	129	mwiswsmaisms	134
mnasmsmawsas	124	mwasssmawsas	129	mwiswsmawsas	134
mnasmsmawsms	124	mwasssmawsms	129	mwiswsmawsms	134
mnasmsmiasis	124	mwasssmiasis	129	mwiswsmiasis	134
mnasmsmiasrs	124	mwasssmiasrs	129	mwiswsmiasrs	134
mnasmsmiwsis	124	mwasssmiwsis	129	mwiswsmiwsis	134
mnasmsmiwsrs	124	mwasssmiwsrs	129	mwiswsmiwsrs	134
mnasmsmnasms	124	mwasssmnasms	129	mwiswsmnasms	134
mnasmsmnisms	124	mwasssmnisms	129	mwiswsmnisms	134
mnasmsmnwsm	124	mwasssmnwsm	129	mwiswsmnwsm	135

mwiswsmwasss	135	onasssmawsas	135	onasssmnwsms	136
mwiswsmwasws	135	onasssmawsms	136	onasssmwasss	136
mwiswsmwisss	135	onasssmiasis	136	onasssmwasws	136
mwiswsmwisws	135	onasssmiasrs	136	onasssmwisss	137
mwiswsonasss	135	onasssmiwsis	136	onasssmwisws	137
onasssbnasss	135	onasssmiwsrs	136	onasssonasss	137
onasssmaisas	135	onasssmnasms	136		
onasssmaisms	135	onasssmnisms	136		

9.20 Mie: twosphere soaked wet snow, Seifert/Beheng-scheme

bnasssbnasss	138	maismsmiasis	142	mawmsmnmisms	146
bnasssmaisas	138	maismsmiasrs	142	mawmsmnmwsms	146
bnasssmaisms	138	maismsmiwsis	142	mawmsmnmwasss	146
bnasssmawsas	138	maismsmiwsrs	142	mawmsmnmwasws	146
bnasssmawsms	138	maismsmnasms	142	mawmsmnmwisss	146
bnasssmiasis	138	maismsmnisms	142	mawmsmnmwisws	146
bnasssmiasrs	139	maismsmnwsms	142	mawmsnasss	146
bnasssmiwsis	139	maismsmwasss	143	miasisbnasss	146
bnasssmiwsrs	139	maismsmwasws	143	miasismaisas	147
bnasssmnasms	139	maismsmwisss	143	miasismaisms	147
bnasssmnisms	139	maismsmwisws	143	miasismawsas	147
bnasssmnwsms	139	maismsonasss	143	miasismawsms	147
bnasssmwasss	139	mawsasbnasss	143	miasismiasis	147
bnasssmwasws	139	mawsasmaisas	143	miasismiasrs	147
bnasssmwisss	139	mawsasmaisms	143	miasismiwsis	147
bnasssmwisws	139	mawsasmawsas	143	miasismiwsrs	147
bnasssonasss	140	mawsasmawsms	143	miasismnasms	147
maisasbnasss	140	mawsasmiasis	144	miasismnisms	147
maisasmaisas	140	mawsasmiasrs	144	miasismnwsms	148
maisasmaisms	140	mawsasmiwsis	144	miasismwasss	148
maisasmawsas	140	mawsasmiwsrs	144	miasismwasws	148
maisasmawsms	140	mawsasmnasms	144	miasismwisss	148
maisasmiiasis	140	mawsasmnisms	144	miasismwisws	148
maisasmiarsrs	140	mawsasmnwsms	144	miasisonasss	148
maisasmiwsis	140	mawsasmwasss	144	miasrsbnasss	148
maisasmiwsrs	140	mawsasmwasws	144	miasrsmaixas	148
maisasmnasms	141	mawsasmwisss	144	miasrsmאים	148
maisasmnisms	141	mawsasmwisws	145	miasrsmawsas	148
maisasnmnwsms	141	mawsasonasss	145	miasrsmawsms	149
maisasnmwasss	141	mawmsbnasss	145	miasrsmiasis	149
maisasnmwasws	141	mawmsmaisas	145	miasrsmiasrs	149
maisasnmwisss	141	mawmsmaisms	145	miasrsmiwsis	149
maisasnmwisws	141	mawmsmawsas	145	miasrsmiwsrs	149
maiasonasss	141	mawmsmawsms	145	miasrsmnasms	149
maismsbasss	141	mawmsmiasis	145	miasrsmnisms	149
maismsmaixas	141	mawmsmiasrs	145	miasrsmnwsms	149
maismsmawsas	142	mawmsmiwsis	145	miasrsmwasss	149
maismsmawsms	142	mawmsmiwsrs	146	miasrsmwasws	149
		mawmsmnasms	146	miasrsmwisss	150

miasrsmwisws	150	mnasmsmwisws	155	mwasssmwisws	160
miasrsonasss	150	mnasmsonasss	155	mwasssonasss	160
miwsisbnasss	150	mnismsbnasss	155	mwaswsbnasss	160
miwsismaisas	150	mnismsmaisas	155	mwaswsmaisas	160
miwsismaisms	150	mnismsmaisms	155	mwaswsmaisms	160
miwsismawsas	150	mnismsmawsas	155	mwaswsmawsas	160
miwsismawsms	150	mnismsmawsms	155	mwaswsmawsms	160
miwsismiasis	150	mnismsmiasis	155	mwaswsmiasis	161
miwsismiasrs	150	mnismsmiasrs	156	mwaswsmiasrs	161
miwsismiwsis	151	mnismsmiwsis	156	mwaswsmiwsis	161
miwsismiwsrs	151	mnismsmiwsrs	156	mwaswsmiwsrs	161
miwsismnasms	151	mnismsmnasms	156	mwaswsmnasms	161
miwsismnisms	151	mnismsmnisms	156	mwaswsmnisms	161
miwsismnwsms	151	mnismsmnwsms	156	mwaswsmnwsms	161
miwsismwasss	151	mnismsmwasss	156	mwaswsmwasss	161
miwsismwasws	151	mnismsmwasws	156	mwaswsmwasws	161
miwsismwiss	151	mnismsmwiss	156	mwaswsmwiss	161
miwsismwisws	151	mnismsmwisws	156	mwaswsmwisws	162
miwsisonasss	151	mnismsonasss	157	mwaswsonasss	162
miwsrsbnasss	152	mnwsmsbnasss	157	mwissbnasss	162
miwsrsmaixas	152	mnwsmsmaisas	157	mwissmaisas	162
miwsrsmאים	152	mnwsmsmaisms	157	mwissmaisms	162
miwsrsmawsas	152	mnwsmsmawsas	157	mwissmawsas	162
miwsrsmawsms	152	mnwsmsmawsms	157	mwissmawsms	162
miwsrsmiasis	152	mnwsmsmiasis	157	mwissmiasis	162
miwsrsmiasrs	152	mnwsmsmiasrs	157	mwissmiasrs	162
miwsrsmiwsis	152	mnwsmsmiwsis	157	mwissmiwsis	162
miwsrsmiwsrs	152	mnwsmsmiwsrs	157	mwissmiwsrs	163
miwsrsmnasms	152	mnwsmsmnasms	158	mwissmnasms	163
miwsrsmnisms	153	mnwsmsmnisms	158	mwissmnisms	163
miwsrsmnwsms	153	mnwsmsmnwsms	158	mwissmnwsms	163
miwsrsmwasss	153	mnwsmsmwasss	158	mwissmwasss	163
miwsrsmwasws	153	mnwsmsmwasws	158	mwissmwasws	163
miwsrsmwiss	153	mnwsmsmwiss	158	mwissmwiss	163
miwsrsmwisws	153	mnwsmsmwisws	158	mwissmwisws	163
miwsrsonasss	153	mnwsmsonasss	158	mwisssonasss	163
mnasmsbnasss	153	mwassbnasss	158	mwiswsbnasss	163
mnasmsmaisas	153	mwassmaisas	158	mwiswsmaisas	164
mnasmsmaisms	153	mwassmaisms	159	mwiswsmaisms	164
mnasmsmawsas	154	mwassmawsas	159	mwiswsmawsas	164
mnasmsmawsms	154	mwassmawsms	159	mwiswsmawsms	164
mnasmsmiasis	154	mwassmiasis	159	mwiswsmiasis	164
mnasmsmiasrs	154	mwassmiasrs	159	mwiswsmiasrs	164
mnasmsmiwsis	154	mwasssmiwsis	159	mwiswsmiwsis	164
mnasmsmiwsrs	154	mwasssmiwsrs	159	mwiswsmiwsrs	164
mnasmsmnasms	154	mwasssmnasms	159	mwiswsmnasms	164
mnasmsmnisms	154	mwasssmnisms	159	mwiswsmnisms	164
mnasmsmnwsms	154	mwasssmnwsms	159	mwiswsmnwsms	165
mnasmsmwasss	154	mwasssmwasss	160	mwiswsmwasss	165
mnasmsmwasws	155	mwasssmwasws	160	mwiswsmwasws	165
mnasmsmwiss	155	mwasssmwiss	160	mwiswsmwiss	165

mwiswsmwisws	165	onasssmiasis	166	onasssmwasss	166
mwiswsonasss	165	onasssmiasrs	166	onasssmwasws	166
onasssbnasss	165	onasssmiwsis	166	onasssmwisss	167
onasssmaisas	165	onasssmiwsrs	166	onasssmwisws	167
onasssmaisms	165	onasssmnasms	166	onasssonasss	167
onasssmawsas	165	onasssmnisms	166		
onasssmawsms	166	onasssmnwsms	166		

References

- Battan, L. J., *Radar Observations of the Atmosphere*, The University of Chicago Press, Chicago, 1973.
- Bohren, C. F. and L. J. Battan, 1982: Radar backscattering of microwaves by spongy ice spheres, *J. Atmos. Sci.*, **39**, 2623–2628.
- Bohren, C. F. and D. R. Huffman, *Absorption and Scattering of Light by Small Particles*, John Wiley and Sons, Inc., 1983.
- Bruggemann, D. A. G., 1935: Berechnung verschiedener physikalischer Konstanten von heterogenen Substanzen. I. Dielektrizitätskonstanten und Leitfähigkeiten der Mischkörper aus isotropen Substanzen, *Ann. Phys.*, **24**, 636–679.
- Chýlek, P. and V. Srivastava, 1983: Dielectric constant of a composite inhomogeneous medium, *Phys. Rev. B*, **27**(8), 5098–5106.
- Debye, P., *Polar Molecules*, New York (The Chemical Catalogue), 1929.
- Deirmendjian, D., *Electromagnetic Scattering on Spherical Polydispersions*, American Elsevier Publishing Company, New York, 1969.
- Fabry, F. and W. Szyrmer, 1999: Modeling of the melting layer. Part II: Electromagnetic, *J. Atmos. Sci.*, **56**, 3593–3600.
- Joss, J. and A. N. Aufdermaur, 1965: Experimental determination of the radar cross sections of artificial hailstones containing water, *J. Appl. Meteor.*, **4**, 723–726.
- Kerker, M., *The Scattering of Light and Other Electromagnetic Radiation*, Academic Press, New York, San Francisco, London, 1969.
- Lichtenecker, A., 1926: Die Dielektrizitätskonstante natürlicher und künstlicher Mischkörper, *Phys. Z.*, **27**, 115–158.
- Liebe, H. J., G. A. Hufford and T. Manabe, 1991: A model for the complex permittivity of water at frequencies below 1 THz, *Int. J. Infrared Millim. Waves*, **12**, 659–675.
- Mätzler, C., Microwave properties of ice and snow, in: B. Schmitt et al. (editor), *Solar System Ices*, volume 227 of *Astrophysics and Space Science Library*, Kluwer Academic Publishers, Dordrecht, 1998, pp. 241–257.
- Maxwell Garnett, J. C., 1904: Colors in metal glasses and in metallic films, *Phil. Trans. Roy. Soc. London*, **A203**, 385–420.
- Oguchi, T., 1983: Electromagnetic wave propagation and scattering in rain and other hydrometeors, *Proc. IEEE*, **71**(9), 1029–1078.
- Press, W. H., S. A. Teukolsky, W. T. Vetterling and B. P. Flannery, *Numerical Recipes in Fortran 77: The Art of Scientific Computing*, Cambridge University Press, 2001, 2. edition.
- Ray, P. S., 1972: Broadband complex refractive indices of ice and water, *Appl. Opt.*, **11**, 1836–1844.
- Segelstein, D. J., 1981: *The Complex Refractive Index of Water*, Master's thesis, Department of Physics, University of Missouri, Kansas City.

- Seifert, A. and K. D. Beheng, 2006: A two-moment cloud microphysics parameterization for mixed-phase clouds. Part I: Model description, *Meteorol. Atmos. Phys.*, **92**, 45–66.
- Stroud, D., 1975: Generalized effective-medium approach to the conductivity of an inhomogeneous material, *Phys. Rev. B*, **12**(8), 3368–3373.
- Warren, S. G., 1984: Optical constants of ice from the ultraviolet to the microwave, *Appl. Opt.*, **23**(8), 1206–1225.
- Wiener, O., 1912: Die Theorie des Mischkörpers für das Feld der stationären Strömung. Erste Abhandlung. Die Mittelwertsätze für Kraft, Polarisation und Energie, *32. Band der Abhandlungen der mathematisch-physikalischen Klasse der Königl. Sächsischen Gesellschaft der Wissenschaften*, (509–604).
- Zhang, S. and J. Jin, *Computation of Special Functions*, John Wiley and sons, 1996.

List of COSMO Newsletters and Technical Reports

(available for download from the COSMO Website: www.cosmo-model.org)

COSMO Newsletters

- No. 1: February 2001.
- No. 2: February 2002.
- No. 3: February 2003.
- No. 4: February 2004.
- No. 5: April 2005.
- No. 6: July 2006.
- No. 7: April 2008; Proceedings from the 8th COSMO General Meeting in Bucharest, 2006.
- No. 8: September 2008; Proceedings from the 9th COSMO General Meeting in Athens, 2007.
- No. 9: December 2008.
- No. 10: March 2010.
- No. 11: April 2011.
- No. 12: April 2012.
- No. 13: April 2013.
- No. 14: April 2014.
- No. 15: July 2015.

COSMO Technical Reports

- No. 1: Dmitrii Mironov and Matthias Raschendorfer (2001):
Evaluation of Empirical Parameters of the New LM Surface-Layer Parameterization Scheme. Results from Numerical Experiments Including the Soil Moisture Analysis.
- No. 2: Reinhold Schrodin and Erdmann Heise (2001):
The Multi-Layer Version of the DWD Soil Model TERRA_LM.
- No. 3: Günther Doms (2001):
A Scheme for Monotonic Numerical Diffusion in the LM.
- No. 4: Hans-Joachim Herzog, Ursula Schubert, Gerd Vogel, Adelheid Fiedler and Roswitha Kirchner (2002):
LLM - the High-Resolving Nonhydrostatic Simulation Model in the DWD-Project LIT-FASS.
Part I: Modelling Technique and Simulation Method.

- No. 5: Jean-Marie Bettems (2002):
EUCOS Impact Study Using the Limited-Area Non-Hydrostatic NWP Model in Operational Use at MeteoSwiss.
- No. 6: Heinz-Werner Bitzer and Jürgen Steppeler (2004):
Documentation of the Z-Coordinate Dynamical Core of LM.
- No. 7: Hans-Joachim Herzog, Almut Gassmann (2005):
Lorenz- and Charney-Phillips vertical grid experimentation using a compressible non-hydrostatic toy-model relevant to the fast-mode part of the 'Lokal-Modell'.
- No. 8: Chiara Marsigli, Andrea Montani, Tiziana Paccagnella, Davide Sacchetti, André Walser, Marco Arpagaus, Thomas Schumann (2005):
Evaluation of the Performance of the COSMO-LEPS System.
- No. 9: Erdmann Heise, Bodo Ritter, Reinhold Schrodin (2006):
Operational Implementation of the Multilayer Soil Model.
- No. 10: M.D. Tsyrlunikov (2007):
Is the particle filtering approach appropriate for meso-scale data assimilation ?
- No. 11: Dmitrii V. Mironov (2008):
Parameterization of Lakes in Numerical Weather Prediction. Description of a Lake Model.
- No. 12: Adriano Raspanti (2009):
COSMO Priority Project "VERification System Unified Survey" (VERSUS): Final Report.
- No. 13: Chiara Marsigli (2009):
COSMO Priority Project "Short Range Ensemble Prediction System" (SREPS): Final Report.
- No. 14: Michael Baldauf (2009):
COSMO Priority Project "Further Developments of the Runge-Kutta Time Integration Scheme" (RK): Final Report.
- No. 15: Silke Dierer (2009):
COSMO Priority Project "Tackle deficiencies in quantitative precipitation forecast" (QPF): Final Report.
- No. 16: Pierre Eckert (2009):
COSMO Priority Project "INTERP": Final Report.
- No. 17: D. Leuenberger, M. Stoll and A. Roches (2010):
Description of some convective indices implemented in the COSMO model.
- No. 18: Daniel Leuenberger (2010):
Statistical analysis of high-resolution COSMO Ensemble forecasts in view of Data Assimilation.
- No. 19: A. Montani, D. Cesari, C. Marsigli, T. Paccagnella (2010):
Seven years of activity in the field of mesoscale ensemble forecasting by the COSMO-LEPS system: main achievements and open challenges.
- No. 20: A. Roches, O. Fuhrer (2012):
Tracer module in the COSMO model.

- No. 21: Michael Baldauf (2013):
A new fast-waves solver for the Runge-Kutta dynamical core.
- No. 22: C. Marsigli, T. Diomede, A. Montani, T. Paccagnella, P. Louka, F. Gofa, A. Corigliano (2013):
The CONSENS Priority Project.
- No. 23: M. Baldauf, O. Fuhrer, M. J. Kurowski, G. de Morsier, M. Müllner, Z. P. Piotrowski, B. Rosa, P. L. Vitagliano, D. Wójcik, M. Ziemiański (2013):
The COSMO Priority Project 'Conservative Dynamical Core' Final Report.
- No. 24: A. K. Miltenberger, A. Roches, S. Pfahl, H. Wernli (2014):
Online Trajectory Module in COSMO: a short user guide.
- No. 25: P. Khain, I. Carmona, A. Voudouri, E. Avgoustoglou, J.-M. Bettems, F. Grazzini (2015):
The Proof of the Parameters Calibration Method: CALMO Progress Report.
- No. 26: D. Mironov, E. Machulskaya, B. Szintai, M. Raschendorfer, V. Perov, M. Chumakov, E. Avgoustoglou (2015):
The COSMO Priority Project 'UTCS' Final Report.
- No. 27: J.-M. Bettems (2015):
The COSMO Priority Project 'COLOBOC': Final Report.

COSMO Technical Reports

Issues of the COSMO Technical Reports series are published by the *CO*nsortium for *S*mall-scale *MO*delling at non-regular intervals. COSMO is a European group for numerical weather prediction with participating meteorological services from Germany (DWD, AWGeophys), Greece (HNMS), Italy (USAM, ARPA-SIMC, ARPA Piemonte), Switzerland (MeteoSwiss), Poland (IMGW), Romania (NMA) and Russia (RHM). The general goal is to develop, improve and maintain a non-hydrostatic limited area modelling system to be used for both operational and research applications by the members of COSMO. This system is initially based on the COSMO-Model (previously known as LM) of DWD with its corresponding data assimilation system.

The Technical Reports are intended

- for scientific contributions and a documentation of research activities,
- to present and discuss results obtained from the model system,
- to present and discuss verification results and interpretation methods,
- for a documentation of technical changes to the model system,
- to give an overview of new components of the model system.

The purpose of these reports is to communicate results, changes and progress related to the LM model system relatively fast within the COSMO consortium, and also to inform other NWP groups on our current research activities. In this way the discussion on a specific topic can be stimulated at an early stage. In order to publish a report very soon after the completion of the manuscript, we have decided to omit a thorough reviewing procedure and only a rough check is done by the editors and a third reviewer. We apologize for typographical and other errors or inconsistencies which may still be present.

At present, the Technical Reports are available for download from the COSMO web site (www.cosmo-model.org). If required, the member meteorological centres can produce hard-copies by their own for distribution within their service. All members of the consortium will be informed about new issues by email.

For any comments and questions, please contact the editor:

Massimo Milelli

Massimo.Milelli@arpa.piemonte.it